2017

A 360◦ comprehensive study of quantitative pricing of options, ranging from theory and computation to model calibration and empirical studies

Xin-Jiang He
University of Wollongong

A 360° comprehensive study of quantitative pricing of options, ranging from theory and computation to model calibration and empirical studies

A thesis submitted in fulfilment of the requirements for the award of the degree

Doctor of Philosophy

from

University of Wollongong

by

Xin-Jiang He

B.Sc. (Donghua University)

School of Mathematics and Applied Statistics

Certification

I, Xin-Jiang He, declare that this thesis, submitted in partial fulfilment of the requirements for the award of Doctor of Philosophy, in the School of Mathematics and Applied Statistics, University of Wollongong, is wholly my own work unless otherwise referenced or acknowledged. The document has not been submitted for qualifications at any other academic institution.

Xin-Jiang He

July 28, 2017

Acknowledgements

First and foremost, I would like to express my sincere gratitude and appreciation to my principal supervisor, Prof. Song-Ping Zhu, for his insightful supervision and continuous support. It is fortunate and a great honor for me to be one of his Ph.D. students. I, in particular, appreciate all his contributions of time and ideas, especially the proper guidance and encouragement of independent thinking, to make my Ph.D. studies fruitful. His suggestions on both my research and career have been priceless, and his high standard as well as rigorous altitude towards research has exceptionally inspired and led me to grow from a raw beginner to an academic researcher. I am indebted to him more than he knows.

My deep appreciation also goes to my co-supervisor, Dr. Xiaoping Lu, for her continuous help and warm care throughout my Ph.D. studies. I am also thankful for Dr. Wenting Chen to be an excellent example as a successful early career researcher, which keeps driving me to work hard and pursue my dreams. I wish to thank all the fellow students in School of Mathematics and Applied Statistics, especially Mr. Guiyuan Ma, Mr. Xiangchen Zeng, Ms. Sha Lin and Ms. Ziwei Ke, who have made my studies in University of Wollongong full of fun. I am also extremely grateful for the financial support of International Postgraduate Tuition Award and University Postgraduate Award from the University of Wollongong, which enables me to chase up my dream of being an academic researcher.

Finally, I would like to thank my parents for educating me to be hard-working and disciplined in my work, and always be confident to myself. I would also like to thank them for their endless support, understanding and love.

Abstract

Classified by different purposes and contributions, this thesis is divided into three parts. In specific, Part 1 focuses on different option pricing models with analytical pricing formula for European options, and three topics covered by the first part are 1) a new closed-form pricing formula is obtained under a skew Brownian motion; 2) an analytical approximation formula is derived when regime-switching is introduced into the Heston model; and 3) a modified Black-Scholes option pricing formula is presented when the underlying price is bounded. Part 2 is devoted to solving option pricing problems with different solution techniques, including analytical approximation, series solution techniques, integral equation approaches and numerical methods. Part 3 considers calibration problems of the Heston model, the Stein-Stein model and the local regime-Switching model with real market data.

Preface

Financial derivatives have become increasingly popular among investors as well as academic researchers recently. Among these, options are one kind of the most basic and important instruments for investment and hedging risk, which results in the high demand for the accuracy of option valuation. There are mainly four kinds of options traded in open exchange markets, including European options, American options, Asian options and barrier options. Although Black & Scholes [19] made a breakthrough by deriving a closed-form analytical pricing formula for European options with the underlying log-price following a normal distribution, some of its simplified assumptions made to achieve analytical tractability are inappropriate and may lead to large pricing errors. Therefore, how to price options efficiently and accurately remains one of the major challenges today. This thesis contributes to the literature significantly by pricing options under different models and making model comparison with real market data.

Classified by different purposes and contributions, this thesis is divided into three parts, with Part 1 focusing on different option pricing models with analytical pricing formula for European options, Part 2 using different solution techniques for option pricing problems, and Part 3 presenting the results of two specific issues in model calibration. There are various issues in Financial Mathematics, most of which are covered in this thesis. In specific, in terms of exercise style, we have not only worked on European options, but also dealt with American options. Moreover, in terms of theory and practice, empirical studies for the assessment of the performance of different models in real markets are an important part of this thesis, apart from providing theoretical derivation of option prices. Furthermore, in terms of option pricing approaches, analytical methods and numerical methods, as two main categories, are both involved in this thesis. In addition, in terms of specific tools, the PDE (partial differential equation) approach solving PDEs governing option prices, and the Monte-Carlo simulation approach directly simulating the dynamics of the underlying price, as two of main ones, are both made use of here. In summary, these three parts are based on twelve papers published in or submitted to various top-ranking journals.

Three different kinds of models and their option pricing problems are considered in Part 1, which contains Chapter 2, Chapter 3, Chapter 4. In the first chapter of this part, we consider a modified Black-Scholes model with the standard Brownian motion being replaced by a particular process constructed with a special type of skew Brownian motions. In particular, the adopted stochastic process for the dynamics of the underlying asset is the sum of a standard Brownian motion and a reflected Brownian motion that are independent of each other. The motivation for such a modification originates from observations of the non-normal distribution of asset log-price in the financial markets [153, 188, 191], which are at odds with one of the fundamental assumptions in the Black-Scholes pricing theory. Although Corns & Satchell [51] have worked on this model, the results they obtained are incorrect. In this chapter, not only do we identify precisely where the errors in [51] are, but also present a new closed-form pricing formula based on a newly-proposed equivalent martingale measure, called "endogenous risk neutral measure" which reflects that only endogenous risks can and should be fully hedged, as a result of no unique risk neutral measure for incomplete markets. The newly derived option pricing formula takes the Black-Scholes formula as a special case and it does not add any significantly extra burden in terms of numerical computations involved in calculating option values, compared with those involved in invoking the Black-Scholes formula. Amazingly, the simple analytic form of the Black-Scholes formula is preserved by the new formula and an elegant financial interpretation can also be given under the new martingale measure. In Chapter 3, we propose a new hybrid model with the volatility of volatility in the Heston model following a Markov chain, the adoption of which is motivated by the empirical evidence of the existence of regime-switching in real markets. An analytical approximation formula for pricing European options is obtained with the perturbation method, based on the derived coupled PDE (partial differential equation) system that governs the European option price. It should be noted that the newly derived formula is fast and easy to implement with only normal distribution function involved, and numerical experiments confirm that our formula could provide quite accurate option prices, especially for relatively short-tenor ones. Finally, empirical studies are carried out to show the superiority of our model based on S&P 500 returns and options with the time to expiry less than one month. On the other hand, a modified Black-Scholes (B-S) model is proposed in Chapter 4, based on a revised assumption that the range of the underlying asset varies within a finite zone,

rather than being allowed to vary in a semi-infinite zone as presented in the classical B-S theory. This is motivated by the fact that the underlying price of any option can never reach infinity in reality; a trader may use our new formula to adjust the option price that he/she is willing to long or short. To develop this modified option pricing formula, we assume that a trader has a view on the realistic price range of a particular asset and the log-returns follow a truncated normal distribution within this price range. Finally, empirical studies are carried out to compare the pricing performance of our model and that of the Black-Scholes model with real market data.

Part 2 is devoted to solving option pricing problems with different solution techniques, i.e., approximation techniques, series solution approaches, integral equation approaches, and numerical methods, and Chapter 5-8 are included in this part. In particular, we will firstly consider two relevant problems related to pricing European options with the discrete dividend under the classic Black-Scholes framework in Chapter 5. For the case when a discrete dividend payment being proportional to the underlying asset value, we reveal the fundamental reasons, from both mathematical and financial viewpoints, why the option price is independent of the dividend payment date. When the amount of the discrete dividend is fixed, we provide a closed-form approximation formula for European option prices, with only one-dimensional integrals involved. This formula is a general one since it can not only be applied when there is only a single dividend, but also be suitable for the case of multiple dividends. Then a closed-form pricing formula in the form of an infinite series for European call options is derived in Chapter 6 for the Heston stochastic volatility model under a chosen martingale measure. Given that markets with the stochastic volatility are incomplete, there exists a number of equivalent martingale measures and consequently investors face a problem of making a choice of appropriate measure when they price options. The one we adopt here is the so-called minimal entropy martingale measure shown to be related to the expected utility maximization theory [91] and the financial rationality for choosing this measure will be further illustrated in this chapter. A great advantage of our newly-derived pricing formula is that the convergence of the solution in series form can be proved theoretically; such a proof of the convergence is also complemented by some numerical examples to demonstrate the speed of convergence. For the case that the time to expiry exceeds the derived radius, we further work on this model and present a modified formula for European options as well as a set of complete

convergence proofs for the solution that would cover the entire time horizon of a European option contact are presented under the Heston model with minimal entropy martingale measure. Afterwards, a new integral equation to solve the American put price as well as its optimal exercise price is successfully derived in Chapter 7. Unlike all previously derived integral equations for pricing American options, there are two distinguishable advantages of ours; the first is that it is without any discontinuity and in a form of one-dimensional integral, which means that it has a great advantage in terms of substantially increasing the speed with which values of an American option can be numerically computed, while another is that singularities associated with the optimal exercise boundary at the expiry time are elegantly avoided; the computational accuracy and efficiency can thus be further enhanced. We first derive a new free boundary problem for the first order derivative of the American put price with respect to the time to expiry, and then we apply a novel approach to transform a linear PDE containing an unknown free boundary into a nonlinear PDE with the fixed boundary. Finally, the accuracy and efficiency of the newly derived integral equation formulation for pricing American options are demonstrated through results of numerical experiments. Finally, the main content of Chapter 8 is to propose appropriate numerical approaches for option pricing. In particular, we propose a new numerical approach for option pricing with the combination of the Monte Carlo simulation and the ADI (alternating direction implicit) method. Our motivation originates from the fact that option traders may be particularly interested in the influence of a small change of variables in a certain region on option prices, while they are indifferent to option prices outside this region since short-term options are dominated in real markets and most of the underlying will not dramatically change within a short amount of time. In this situation, it will waste a lot of time with classical numerical approaches as a large discretization is needed to obtain accurate results. In contrast, our approach uses the Monte Carlo simulation to generate boundary conditions of the interested region, and then option prices inside this region will be obtained with the ADI method, the advantage of which is that we do not have to calculate option prices that we do not need. Numerical experiments are carried out to show the accuracy as well as the efficiency of this newly proposed approach.

The final part of this thesis consists of Chapter 9, Chapter 10, Chapter 11 and Chapter 12, in which we also consider two distinct issues under the framework of model calibration. The first issue is to propose different forms of the existing models that may bring certain

advantages when these models are calibrated with real market data. We work on the Heston model and the correlated Stein-Stein model in Chapter 9 and Chapter 10 respectively since they are the two of the most popular stochastic volatility models. We present an alternative form of the Heston model that preserves an essential advantage of the Heston model, its analytic tractability, by imposing the necessary and sufficient conditions for the existence of a solution in affine form, while it is in a different form so that it offers certain advantages in parameter determination. To demonstrate this, we conducted some empirical studies, exploring if this new form does have certain advantages over the original version under certain market conditions. Moreover, we propose an alternative form of the correlated Stein-Stein option pricing model that preserves its analytic tractability, which is one of its essential advantages. It is in a different form so that it could offer certain advantages in parameter determination over the original form. We have also conducted some empirical studies, the results of which show that under certain market conditions, our new form could provide better performance than the original Stein-Stein form.

The second issue of the final part is to develop new algorithms to calibrate local regime-switching models, and there is only little results regarding this problem in the literature. Actually, local regime-switching models are a natural consequence of combining the concept of a local volatility model with that of a regime-switching model. However, even though Elliott et al. [85] have derived a Dupire formula for a local regime-switching model, its calibration still remains a challenge, primarily due to the fact that the derived volatility function for each state involves all the state price variables whereas only one market price is available for model calibration, and a direct implementation of Elliott et al.'s formula may not yield stable results. In Chapter 11, a "closed" system for option pricing and data extraction under the classical regime-switching model is proposed with a special approach, splitting one market price into two "market-implied state prices". The success of our approach hinges on the recovery of the two local volatility functions being transformed into an optimal control problem, which is solved through the Tikhonov regularization. In addition, an efficient algorithm is proposed to obtain the optimal solution by iteration. Our numerical experiments show that different shapes of local volatility functions can be accurately recovered with the newly-proposed algorithm. Furthermore, a new algorithm of calibrating local regime-switching models with market observed option prices is established in Chapter 12. It should be noticed that the technique we adopt

here is distinct from that used in Chapter 11 since we calibrate the local regime-switching model directly instead of using the Dupire formula in local regime-switching models. This new algorithm is also very efficient and accurate, which is demonstrated with designed numerical experiments, and thus it has the potential to be implemented in real markets.

Contents

List of Figures

List of Tables

Chapter 1

Introduction and Background

1.1 Option derivatives

Financial derivatives are becoming increasingly popular among investors for speculation and hedging purposes, and they are different financial contracts that depends on the price of the underlying asset. Among these, options have attracted a lot of attention and their trading volumes have experienced a rapid growth ever since the establishment of Chicago Board Options Exchange in 1973. Now, options are written on different kinds of underlying assets and traded on various exchanges as well as in the over-the-counter market. Actually, there are two basic types of options, i.e., vanilla and exotic options. The former are a normal kind of options with standardized terms while without no special feature, while the latter is more complex than the former with several triggers related to the determination of payoff functions. These two categories will be elaborately illustrated in the following two subsections.

1.1.1 Vanilla options

Vanilla options can usually be divided into two sub-categories according to the types of transaction, i.e., call and put options. The former and the latter give the holder the rights to buy and sell the underlying asset for a specified strike price at a certain date respectively, while the writer has the obligation to accept the choices that the holder makes. Form this, one can clearly find that the option writer could suffer a large amount of loss when the underlying price goes against the expectation of the writer. As a result, the option writer should be compensated with the option premium, which needs to be determined so that

it could satisfy the demand of the writer and the holder of the option.

Another popular classification for vanilla options is according to different inner mechanics associated with exercisable dates. Those can only be exercised at expiry is called European options, while its counterpart American options can be exercised at any time before maturity. From the definition, one can easily find that the holder of an American option has more rights than that of a corresponding European option, which implies that an American option is more valuable than its European counterpart. Moreover, it is usually much more difficult to value an American options since the optimal exercise boundary and the option price need to be determined simultaneously.

1.1.2 Exotic options

Other types of options are the so-called exotic options, whose payoff functions are more complicated than those of vanilla options. Most of exotic options are traded in the over-the-counter market, and they are created by financial engineers for some specific reasons. For example, some of them are created for hedging purposes, while some of others are designed to reflect the potential changes of the underlying price.

One kind of the most popular exotic options is barrier options, whose payoff depends not only on the underlying price at expiry, but also on whether the underlying price has reached a certain level during the lifetime of the contract. They are very attractive since they are less valuable than the corresponding regular options. There are two types of barrier options, knock-in and knock-out options, which is classified by the different existing requirements. In particular, a knock-out option will become worthless when the underlying price reaches the certain level, while a knock-in option starts to exist if and only if the underlying price reaches a barrier.

Other useful exotic options include Asian options, lookback options and so on. Specifically, Asian options are defined with the payoff depending on the average of the underlying price during the life of the option contracts, and their prices are less expensive than those of regular options. On the other hand, the payoff of lookback options is related to the maximum or minimum underlying price reached during the lifetime of the option, which means that lookback option prices are always higher than regular option prices.

1.2 Literature review

1.2.1 European option pricing

As we all know that European options are the most basic option types, the accurate pricing of European options is becoming really demanding. As a result, considerable research interests have been devoted into this area, aiming at finding appropriate models and approaches to accurately determine European option prices.

The development of the option valuing problem can be dated back to 1900, when Bachelier [9] priced options under the assumption that the stock price follow a normal distribution in his PhD thesis. However, it has been pointed out by Merton [177] that this assumption is inappropriate since it would lead to negative stock and option prices. More than 70 years later, Black & Scholes [19] made a breakthrough by proposing that the underlying price follow a log-normal distribution and derived a simple and analytical formula for European option prices. This model is so popular that it is still widely adopted in real markets. However, it should be pointed out that although the continuous dividend can be easily incorporated into the Black-Scholes model with the property of analytical tractability preserved [177], pricing options written on the underlying with discretely paid dividend, which is usually the case in real markets, is usually harder than the case with continuous dividend payment, simply because the latter does not involve any jump conditions in a PDE pricing system. In fact, there exists no closed-form solution when the dividend is paid discretely with fixed-amount, which makes it very time-consuming to value option contracts in this case and contradicts to the recent trend of algorithmic trading. Recently, Zhu & He [238] derived an accurate approximation formula for pricing European options with fixed-amount dividend payments, which can somewhat facilitate the application of the Black-Scholes model with discrete dividends, and its details are provided in Chapter 5.

Despite the popularity of the Black-Scholes model that is easy and efficient to be implemented in real markets, some of its simplified assumptions made to achieve analytical tractability are not consistent with real market observations. For example, the distribution of the underlying returns is actually asymmetric and process the features such as skewness [188] and fat-tails [191]. Another typical example is that the implied volatility extracted from the market option prices usually exhibit a "smile" curve [73], which violates the

constant volatility assumption. As a result, finding new models for the underlying price by relaxing some of the assumptions made in Black-Scholes model has attracted a lot of attention, and various models are established to obtain more accurate option prices.

In the literature, there are mainly two kinds of option pricing models, i.e. structural models and non-structural models. The difference between the two categories is that the former provide the dynamics of the underlying price at every moment for a given period of time horizon, while the latter only specify the probability density function of the underlying at maturity conditional upon the filtration at the current time without completely describing the fine details of the stochastic process themselves at each moment. Although the former is much more popular than the latter, non-structural models are also meaningful since they process some nice properties, and a typical one is that different characteristics of the asset returns and the volatility term structure that structural models failed to describe properly can be captured with more flexible distributions.

Modifications to the Black-Scholes model with structural approaches can be divided into two sub-categories; one is to replace the standard Brownian motion with other stochastic volatility processes, and another is to add non-constant volatility to the Black-Scholes model. Regarding the former approach, Lévy processes are really popular since they have independent and stationary increments as the Brownian motion. As a special kind of Lévy models, jump-diffusion models are considered by some authors. For instance, Merton [178] proposed a model with jumps of log-returns following a Guassian distribution, while Kou [158] adopted another one with the jump size following an asymmetric double exponential distribution. Another type of Lévy processes that are widely adopted in option pricing models is the so-called infinite activity lévy process where the Brownian component is omitted. Three well-known examples are Variance-Gamma model proposed by Madan [173], Normal Inverse Gaussian process used by Rydberg [196], and CGMY model proposed by Carr, et al. [29]. Of course, apart from the Lévy processes, there are also other stochastic processes used to replace the Brownian motion, such as the fractional Brownian motion used by Necula [185] to capture the long range dependence in asset price [225]. Recently, a particular kind of skew Brownian motions is adopted in Zhu & He [242], in which a new martingale measure is proposed and a closed-form pricing formula for European options is derived. This issue forms the main context of Chapter 2.

On the other hand, relaxing the constant volatility assumption in the Black-Scholes

model has also attracted a lot of attention. One of the most natural methods is to make the volatility a deterministic function of underlying price and time, which is named as the local volatility model. This model was proposed by Dupire [75] and Derman & Kani [67], and the local volatility function can be theoretically determined by the Dupire formula. However, the Dupire formula can not be directly implemented since it may not yield stable results due to the denominator being directly affected by the second-order derivative of option prices [105]. In this sense, Egger & Engl [78] and Jiang et al. [144] proposed different algorithms to accurately recover the local volatility function for the Black-Scholes model. Although the theory on the local Black-Scholes model seems to be very comprehensive, it is not very popular among market traders and academic researchers since many empirical studies suggest the "smile dynamics" are poorly captured by the local volatility model (e.g., Hagan et. al [102]). Therefore, another kind of non-constant volatility models called stochastic volatility models, in which the volatility is made another random variable described by another stochastic process, receive much more attention. Johnson [146] is believed to be the first to study the continuous-time stochastic volatility model in 1979. Later on, numerical methods were employed by Johnson & Shanno[147], Scott [204], and Wiggins [224] to price European options as it is very difficult to find closed-form pricing formulae with a newly added source of randomness. In particular, Johnson & Shanno and Scott adopted the Monte Carlo simulation techniques to simulate SDE (stochastic differential equation) directly while Wiggins proposed a finite difference method to solve the involved PDE (partial differential equation) governing the option price. However, it should be pointed out that it is really difficult to apply a model without closed-form pricing formula to real markets since this could make the time-consuming model calibration process even much more stressed. This has stimulated further research interest into finding appropriate models with analytical formulae. One well-known example is the Hull-White model [127], where the volatility is assumed to follow a log-normal distribution, and a power series solution is obtained for European option prices. Although this is a positive progress compared with those without closed-form formulae, the assumption of zero correlation made between the underlying price and the volatility process is inappropriate since it violates the so-called "leverage effects" that the underlying price and the volatility should be negatively correlated [11]. Another well-known model is presented by Stein & Stein [213] several years later, who assumed that the volatility follow an Ornstein-Uhlenbeck process

[93] and derived a closed-form pricing formula. However, apart from the assumption of no correlation between the underlying price and volatility, this model can not prevent the volatility from going negative, which was also not satisfactory. Fortunately, Heston [117] made a great contribution in 1993, who proposed that the volatility process follow a CIR model correlated with the underlying process and derived a closed-form pricing formula for European options with the inverse Fourier transform technique. The popularity of this model can be attributed to two main reasons; one is that the CIR model used for the volatility process satisfies a wide range of basic properties that shown by real market data, such as the apparent non-negative property and the mean-reverting property [14], and another, which is more important, is that the possession of closed-form pricing formula can provide some obvious advantages. Specifically, with closed-form solutions, computational accuracy could certainly be guaranteed while there would exist systematical errors when numerical solutions must be resorted to for models that no closed-form solutions are associated with. Moreover, closed-form solution can ensure the efficiency in the calculation of option prices, which can largely facilitate its application in real markets since model parameters always need to be determined with real market data so that it could function properly. Despite the popularity of the Heston model, it should be addressed that there exist different martingale measures in the Heston model since the introduction of the stochastic volatility makes the market become incomplete. Thus, the price formula derived in Heston's original paper [117] is only one fair price with his chosen measure under this model, and there are also other meaningful choices of different martingale measures. In fact, the minimal entropy martingale measure is a reasonable choice since this specific equivalent martingale measure can be connected with the principle of maximum expected utility, and He & Zhu [114] derived a closed-form pricing formula in a series form for European options in the Heston stochastic volatility model with the minimal entropy martingale measure with a radius of convergence. Zhu & He [239] went further and provided a set of converged pricing formulae that can cover the entire time horizon. This will be elaborately discussed in Chapter 6.

Except local and stochastic volatility models, there is also another kind of non-constant volatility models, called regime-switching models. This particular model gains much popularity recently since a lot of empirical evidence strongly demonstrate the existence of regime switching in the underlying price [86, 104], and many authors have worked on this

kind of models. For example, a closed-form pricing formula for European options has been derived by Zhu et al. [244] under the regime-switching Black-Scholes model. Moreover, regime-switching has already been combined with stochastic volatility models, a typical example of which is the model proposed by Elliott & Lian [81] with the constant long-term mean in the original Heston model being regime-switching. Most recently, He & Zhu [111] proposed a new stochastic volatility model, where the volatility of volatility in the Heston model follows a Markov chain so that it can jump between different states, and derived a simple and analytical pricing formula for short-tenor European options, which forms the main content of Chapter 3.

Non-structural models, which are briefly introduced above, are also one available approach to model the underlying price such that various characteristics of the underlying price distribution exhibited by real market data can be captured. Generalized beta distribution of the second kind and Burr-3 distribution was adopted by Bookstaber & McDonald [174] and Sherrick et al. [207] respectively to replace the log-normal distribution to provide appropriate skewness and kurtosis. Moreover, Savickas [197] suggested that Weibull distribution should be adopted to model the underlying price when pricing options since its negative skewness of this particular distribution matches well with what is exhibited by real market data, while Fabozzi [87] provided empirical evidence for using generalized gamma distribution. Furthermore, several option pricing models are based on the series expansion of the underlying price distribution to correct the higher moments of the Black-Scholes model. For example, Jarrow and Rudd [143] used the generalized Edgeworth expansion of a log-normal distribution, while Corrado & Su [53] adopted the Gram-Charlier series expansion of a normal distribution. However, all the pricing models in the existing literature assume that the underlying price is unbounded above, i.e., the price range from zero to infinity, which is inappropriate since there is no way that any underlying price could reach infinity in reality. As a result, Zhu & He [241] recently proposed that the underlying price follow a truncated normal distribution and derived an analytical formula for European options with empirical studies demonstrating its superiority over the Black-Scholes model, the details of which are presented in Chapter 4.

1.2.2 American option pricing

It should be pointed out that pricing American options is a much more intriguing problem [125, 171], the main reason of which is the inherent characteristic of an American option that it can be exercised at any time before the expiry time. This additional right for the holder of an American option over that of a European counterpart has cast the American option pricing problem into a free boundary problem that the optimal exercise boundary, in addition to the American option price, needs to be determined. Mathematically, the existence of the optimal exercise boundary has made the problem of pricing American options highly nonlinear since the domain of the solution becomes unknown in advance and varies with time, which forms the main difficulty in finding the prices of American options.

In the literature, various numerical approaches have been proposed for the valuation problem of American options. Typical examples include finite difference method [179, 227], finite element method [4, 121], Monte Carlo method [171], the binomial tree method [237] and the radial basis function method [122]. However, as the main disadvantage of numerical approaches is always the efficiency problem, analytical methods are preferred among market practitioners. Although closed-form analytical formula can hardly be found for American option prices, Zhu [232] recently made a breakthrough in the pricing of American options by deriving an exact and explicit formula. Unfortunately, despite this formula is of great significance theoretically, it is not computational appealing since it involves the calculation of infinite series, which means it can take a considerable amount of time to evaluate.

An alternative method for the pricing of American options included in the category of analytical approaches is the integral equation method. The essence of this particular method is to cast the differential equation into an integral equation, and the solution of the integral equation will satisfy the original differential equation. McKean [175] seems to be the first to derive an integral equation for American option prices with the technique of incomplete Fourier transform. Despite the advantage of this particular integral equation that it only involves two one-dimensional integrals, there are two main drawbacks for this representation that can not be ignored; one is that the presence of the derivative of the optimal exercise boundary can create numerical difficulties because of the infinite slope of the optimal exercise boundary at maturity [37], and another is that the value of

the integral equation at the optimal exercise boundary only equals to half of its original value due to the fact that the inverted Fourier transform of a discontinuous function will converge to the midpoint of the discontinuity [69], and this may cause problems when conducting numerical experiments. Another approach was proposed by Jamshidian [141], who transformed the homogeneous Black-Scholes equation into an inhomogeneous one, and derived a different integral equation for American option prices. This particular formulation does have some advantages over that of McKean, a typical example of which is that Jamshidian's formulation does not involve the derivative of the optimal exercise boundary. However, the integral equation contains a two-dimensional integral equation, which is very computational intensive. One of the most famous integral equations for American option prices is derived by Kim [154] with the compound option approach. Although Kim contributed the literature a lot as his formulation is financial meaningful and able to show that the value of an American option equals to that of the corresponding European option and an early exercise premium, one of its main drawbacks is still the time cost to find the solution since two-dimensional integrals should be evaluated every time we try to find the unknown free boundary. Recently, Zhu et al. [245] present a new integral equation for American put option prices under the Black-Scholes model with two obvious advantages over the existing formulae; one is that it does not suffer from the problem of discontinuity, and another is that this integral equation only involves a one-dimensional integral, which implies that the realization of it is far less time-intensive than those involving two-dimensional integrals. This forms the main context of Chapter 7.

1.2.3 Numerical algorithms

It should be pointed out here that it is often very difficult to analytically evaluate even European options. As a result, numerical methods must be resorted to in most cases when option pricing.

In the literature, a number of different numerical approached have been proposed and adopted to efficiently price options. One of the most basic ones is the so-called binomial tree approach [54], in which option prices are evaluated backwards from the expiry time to the current time, and it is very easy and straightforward to be implemented. Although this method can clearly reflect the construction of the replicating portfolio, it can cause

some biases since the underlying price actually does not discretely change within a two-valued framework. As another basic approach, the Monte-Carlo simulation technique, which directly simulates the dynamics of the underlying price, is also quite popular and has a lot of application in derivative pricing [23, 171, 200]. However, this approach suffers from the insufficiency problem due to the requirement of large number of generations [129]. Being different from the two methods introduced above, both of which directly simulate the underlying price process, the finite difference method, which seeks the discretization of the differential operators, can be certainly employed if a PDE (partial different equation) system governing option price is derived. This method is firstly applied to option pricing by Schwartz [199] and Brennan & Schwartz [24], and it has been widely used by a number of other authors [50, 128]. Of course, there are some other well-known numerical approaches that have already been used in option pricing problems, such as the ADI (alternating direction implicit) approach [138] and the finite element method [121].

Unfortunately, it will take a large amount of time for all the existing numerical approaches to deal with a common situation, where option traders will probably only be interested in a relatively small region around the current value of the underlying price, and want to accurately figure out the influence of a small change in this region on option prices as a result of short-term options being dominated in real markets and the probability for a dramatic change in the underlying price being quite low. This is because the operating domain should be truncated in these numerical algorithms as the underlying price ranges from zero to infinity and a large enough boundary for the underlying price and the volatility should be chosen respectively so that the boundary condition at the truncated domain can be a good approximation of that at infinity, which means that we will have to discretize the whole operating domain if we employ traditional numerical approaches, and thus alternative ways should be found. Recently, Zhu & He [240] proposed a new numerical approach with a combination of the Monte-Carlo simulation technique and the ADI method, in which we artificially generate boundary conditions for the interested region so that we can avoid being restricted to work on a very large domain, and option prices inside this region can be efficiently obtained through the ADI method with the generated boundary condition. This issue will be presented in Chapter 8.

1.2.4 Model calibration

Model calibration with model parameters determined by real market data is always an important process for any mathematical models to function properly in real markets. During this process, we need to find an "optimal" set of parameters such that the "distance" between the calculated and market option prices is minimized. In this sense, this problem is actually an optimization problem, which could be solved with various approaches presented in the literature.

One of the popular methods is to adopt the non-linear least squared method, which is easy and fast to implement. However, the minimizing problem is not well-posed since the minimizing functional is not necessarily convex and with the existence of several local minima, local optimization methods may not succeed in finding the global minimum. As a result, the obtained results could be very sensitive to the input prices as well as the starting point of the local minimization algorithms, which implies the uniqueness and stability issues remain unsolved. In order to obtain a unique solution in a stable manner, we need to introduce a regularization method. A useful and widely adopted regularization criterion is to introduce the relative entropy between the pricing measure and the physical measure into the minimizing functional [18, 48, 49]. Another popular regularization method is the Tikhonov regularization [216], which has been adopted to develop algorithms for calibrating the local Black-Scholes model in [36, 56, 144] and stochastic volatility models [58]. However, to the best of our knowledge, the calibration of local regime-switching models has never been considered in the literature before, and He & Zhu [112, 115] proposed two new algorithms for calibrating local regime-switching based on the Tikhonov regularization, which is provided in Chapter 11-12.

As local optimization approaches would usually result in a local minimum being taken as a global one, it is very natural for us to consider the global optimization techniques so that the global minimum could be identified in an efficient way. In fact, there are a number of different global optimization algorithms. For instance, the method of Markov Chain Monte Carlo (MCMC) has been applied in the area of option pricing model calibration by many authors [6, 145], while the maximum likelihood method is also very popular among researchers as well as market practitioners [3, 131]. Another well-known global optimization algorithm is the so-called genetic algorithm [46] with several nice features. Actually, it is developed based on the idea of natural selection with stochastic factors

introduced to skip over local optima when searching for a satisfactory result. Moreover, it randomly selects a number of different initial guesses to explore the entire solution space so that this algorithm is not sensitive to the starting point. Also, a so-called "mutation" step in the optimization process allows the algorithm to avoid local minima by preventing parameters from being restricted to a small region. It is even pointed out by Bajpai & Kumar [10] that genetic algorithms are one of the best global optimization methods and can provide high quality solutions since they are intrinsically parallel and can explore the solution space in multiple directions at the same time. There already have been the application of genetic algorithms in finance. For example, the term structure of interest rates was estimated with a genetic algorithm by Gimeno & Nave [97], while Grace [99] and Cont & Ben Hamida [47] have adopted it in the area of option pricing. Most recently, a genetic algorithm is adopted by He & Zhu [113, 116] to check whether an alternative form of the Heston model and the Stein-Stein model would make any difference when model calibration is conducted. Chapter 9-10 of this thesis are based on these two papers.

1.3 Mathematical background

1.3.1 Fundamental pricing theorems

In this subsection, we introduce the fundamental pricing framework of how to obtain the fair price of a financial derivative. Before we start, we need to define the probability space $(\Omega, \mathcal{F}_t, P)$, where Ω is the sample space, $\mathcal{F}_t$ represents the filtration that contains the information of the underlying price before time t, and P denotes the probability measure.

It should be noticed that one of the most important concepts in pricing financial derivatives is the equivalent martingale measure or risk-neutral measure (denoted by Q) that all derivatives should be valued under the risk-neutral measure to ensure the non-existence of arbitrage opportunities. If we assume the constant risk-free interest rate be r, it requires that under the the risk-neutral measure, the discounted asset price $e^{-rt}S_t$ be a martingale, which implies that the underlying price S_t should satisfy the following two properties, i.e.,

$$\begin{aligned} E^Q[|S_t|] &< \infty, \\ E^Q[e^{-rT}S_T|\mathcal{F}_t] &= e^{-rt}S_t. \end{aligned} \tag{1.1}$$

In fact, two fundamental theorems of asset pricing [106, 107] have already been developed to show the relationship among market completeness, the risk-neutral measure and the existence of arbitrage opportunities, and they are provided in the following.

Theorem 1 (First fundamental theorem of asset pricing)**.** *A financial market is arbitrage free if and only if there exists at least one risk-neutral measure.*

Theorem 2 (Second fundamental theorem of asset pricing)**.** *A financial market is complete if and only if there exists a unique risk-neutral measure.*

Obviously, the first fundamental theorem of asset pricing establishes the equivalence between market arbitrage-freeness and the existence of the risk-neutral measure, while the second fundamental theorem of asset pricing presents the equivalence of market completeness and the uniqueness of risk-neutral measures. It is not difficult to deduce that when the market becomes incomplete, there can exist different risk-neutral measures, in which case the choice among different risk-neutral measures is also very important and should be financially meaningful as this may have a huge influence on the accuracy of calculated fair prices.

1.3.2 Stochastic calculus

Having figured out the appropriate probability measure that should be used for asset pricing, two important mathematical tools to calculate derivative prices should be introduced.

Itô's lemma

Itô's lemma is the identity to calculate the differential of a deterministic function of a stochastic process and serves as the chain rule for random processes. This identity can be derived by expanding the function with the Taylor series expansion up to the second derivative and keeping the terms up to first order in the time increment and the second order in the Brownian motion. The details of Itô's lemma are provided in the following theorem.

Theorem 3 (Itô's lemma)**.** *If a stochastic process S_t follows the SDE (stochastic differential equation) presented below*

$$dS = \mu(S,t)dt + \sigma(S,t)dW_t, \tag{1.2}$$

with W_t being a standard Brownian motion, then for any twice differentiable function f, the differential of $f(S)$ can be derived as

$$df = (\frac{1}{2}\sigma^2\frac{d^2f}{dS^2} + \mu\frac{df}{dS})dt + \sigma\frac{df}{dS}dW_t. \tag{1.3}$$

Connections between SDE and PDE

Another important tool to deal with the pricing problem of financial derivatives is the relationship between the SDE of the underlying price and the PDE governing the derivative prices, which is established in Feynman-Kac theorem by relating the expectation of final payoff with the PDE. As a result, the content of Feynman-Kac theorem is illustrated in the following theorem.

Theorem 4 (Feynman-Kac theorem)**.** *If the underlying price S_t follows Equation (1.2) with the coefficient $\mu(S,t)$ and $\sigma^2(S,t)$ satisfying the Lipschitz condition*

$$\begin{aligned} P^Q[\int_0^t |\mu(S_z,z)|dz < \infty] &= 1, \forall 0 \le t \le \infty, \\ P^Q[\int_0^t \sigma^2(S_z,z)dz < \infty] &= 1, \forall 0 \le t \le \infty, \end{aligned} \tag{1.4}$$

and $f(S,t) \in C^2(R) \times [0,\infty]$ satisfy the following PDE system

$$\begin{aligned} &\frac{\partial f}{\partial t} + \frac{1}{2}\sigma^2(S,t)\frac{\partial^2 f}{\partial S^2} + \mu(S,t)\frac{\partial f}{\partial S} - g(S,t)f + h(S,t) = 0, \\ &f(S,T) = \phi(S), \end{aligned} \tag{1.5}$$

then the solution $f(S,t)$ to the above PDE system admits the stochastic representation

$$f(S,t) = E^Q[\int_t^T e^{-\int_t^\tau g(S,z)dz}h(S,\tau)d\tau + e^{-\int_t^T g(S,z)dz}\phi(S)|\mathcal{F}_t]. \tag{1.6}$$

1.3.3 Fourier transform and characteristic function

Fourier transform is one of classical and useful methods to solve ODEs and PDEs. It is often used to transform the target problem in the original space into a new problem in the Fourier space, which can be solved more easily, and then the original solution can be obtained with inverse Fourier transform, either analytically or numerically. For any

smooth function $f(x)$, the Fourier transform and its inversion are defined as follows.

$$\begin{aligned} F[f(x)] &= \int_{-\infty}^{+\infty} e^{-i\phi x} f(x) dx, \\ F^{-1}[f(\phi)] &= \frac{1}{2\pi} \int_{-\infty}^{+\infty} e^{i\phi x} f(\phi) d\phi, \end{aligned} \tag{1.7}$$

where $i = \sqrt{-1}$.

With the knowledge of the Fourier transform, we are now ready to introduce the characteristic function, which is the Fourier transform of the probability density function of a real-valued random variable, a key concept in probability theory. If we let S be a random variable and denote $p(x)$ as the density function of S, its characteristic function is defined as

$$f(\phi) = E^Q[e^{i\phi S}] = \int_{-\infty}^{+\infty} e^{-i\phi x} p(x) dx. \tag{1.8}$$

It should be noticed that the characteristic function of a random variable completely defines its probability distribution, and it provides an alternative method to deal with the problems related to the random variable, apart from directly working on the density or distribution function. Moreover, since the characteristic function itself can fully describe a random variable, the relationship among its density, distribution function and itself should be figured out first, which is given with the inverse Fourier transform as

$$\begin{aligned} p(x) &= \frac{1}{2\pi} \int_{-\infty}^{+\infty} e^{i\phi x} f(\phi) d\phi, \\ P(x) &= P(S \leq x) = \frac{1}{2} - \frac{1}{\pi} \int_{0}^{+\infty} Re[\frac{e^{i\phi x} f(\phi)}{i\phi}] \phi, \end{aligned} \tag{1.9}$$

where $P(x)$ is the distribution function of the random variable S.

One of the most basic reasons for the popularity of the characteristic function in mathematical finance is that the transition density of a stochastic process is usually very difficult to find while it is relatively easy to derive its characteristic function. Therefore, the characteristic function is a useful tool in deriving analytical solutions for financial derivative prices. For example, Heston [117] derived a closed-form pricing formula for European options in a stochastic volatility model, based on the derived analytical characteristic function of the underlying price.

1.3.4 Perturbation method

As we all know that it is very difficult to derive closed-form pricing formula for financial derivatives, approximation methods have also received a lot of attention. One of the most popular methods used for option pricing problems is the perturbation theory. This technique is applicable if the target problem can not be analytically solved, but can be formulated by adding a "small" term to the mathematical description of the exactly solvable problem.

In order to apply the perturbation theory, a small parameter ϵ should be introduced so that the desired solution A can be expressed as $A = \sum_{n=0}^{\infty} A_n \epsilon^n$ with A_0 being the leading term. Substituting this particular expression into the original system could yield a series of simplified solvable problems governing A_n. An Nth order approximated solution can be obtained by truncating the series by $N+1$ terms as $A \approx \sum_{n=0}^{N} A_n \epsilon^n$ if it is accurate to the order of $O(\epsilon^{N+1})$ for the entire domain. This is called regular perturbation method.

However, if a problem contains a small parameter that can not be approximated by setting the parameter to zero, the solution based on regular perturbation method would only be accurate on some sub-domains instead of the entire domain, and the approximation is no longer accurate in some small areas, called boundary layers, of other sub-domains. This implies that regular perturbation method is not suitable for this case, and singular perturbation method should be adopted, in which three main steps should be taken to reach the final solution. In the first place, for the region outside the boundary layer, we need to expand the target solution in the original small parameter, similar to the regular perturbation method. The obtained solution is called the outer solution. Secondly, rescale the original system by making the transformation of original variables, and then construct an expansion in the boundary layer and substitute it into the new system to obtain the inner solution. Finally, match the inner and outer solution to obtain a uniform expansion that is accurate for the entire domain.

1.3.5 Model calibration

Once a model has been proposed with the pricing formula for options, model calibration needs to be conducted before it can be applied in real markets. There are two main steps in calibrating mathematical models, which will be clearly discussed in the following.

The first step is called data filtering [11, 41] since there could be some sample noise in the raw data. Four widely used filters in the literature are mainly focused. Firstly, only Wednesday options data is used in the stage of parameter estimation for two reasons; one is that Wednesday is least likely to be a holiday in a week and also less likely to be affected by day-of-the-week effect, and another is that the process of model calibration is very time-consuming, which makes it possible to study a longer time series if we choose one day a week. Secondly, options with small time to expiry (such as less than 7 days) should be discarded since they usually possess less time value and less information about the future dynamics of the firm. Also, options with very large time to maturity (such as more than 120 days) should also be excluded as they are unpopular because of the high premium. Thirdly, very deep in-the-money and very deep out-of-money options should not be considered since they are not active in the market and may have liquidity-related biases. Fourthly, options with very low premiums (such as \$1/8) should be removed as these prices are rather volatile.

Once we have obtained the filtered data, we can proceed to the next step, i.e., parameter estimation. In order to determine the model parameters, one common approach is to find the set of "optimal" parameters that minimizes the "distance" between market and model prices. There are different kinds of definitions for the distance, among which the percentage mean squared error (PMSE) is very popular to measure the relative difference between market and model prices. If we denote C^{Market} as the market price of an option contract, let C^{Model} be the corresponding calculated model price with a particular set of parameters, and assume N be the total number of observations selected in a single estimation, the PMSE can be defined as

$$PMSE = \frac{1}{N}\sum_{i=1}^{N}[\frac{C^{Market} - C^{Model}}{C^{Model}}]^2. \tag{1.10}$$

As the main disadvantage of chossing PMSE is that a cheap option could place an abnormally high amount of weight, another choice of the objective function is the dollar mean squared errors defined as

$$MSE = \frac{1}{N}\sum_{i=1}^{N}[C^{Market} - C^{Model}]^2. \tag{1.11}$$

With the chosen objective function and the optimization algorithm, model parameters can

be finally obtained.

1.4 Option pricing models

It is widely acknowledged that a good option pricing model should provide accurate results that close to real market prices. Although the well-known Black-Scholes model has attracted a lot of attention among researchers and market practitioners since the closed-form pricing formula under this particular model is easy to implement, its simplified assumptions, such as the constant volatility assumption, made to achieve the analytical tractability are inappropriate and are at odds with market observations. Therefore, a number of modifications to the Black-Scholes model with non-constant volatility have been proposed. In this section, we will present an overview of these option pricing models.

1.4.1 The Black-Scholes model

The Black-Scholes model introduced by Black & Scholes in 1973 is one of the most elegant and fundamental option pricing models, which provides a good approximation for the underlying price models. In this model, the underlying price S_t is assumed to follow the log-normal distribution, which is specified as

$$dS_t = \mu S_t dt + \sigma S_t dW, \tag{1.12}$$

where μ is the drift term, σ is the constant volatility, and W_t is a standard Brownian motion. There are several important assumptions under this model that should be mentioned. Firstly, the bank pays continuously compounded risk-free interest rate r. Secondly, the financial market to be worked on is perfect, which means that the market trading is continuous and there is no transaction costs. Thirdly, short selling is permitted and all securities are perfectly divisible. Most importantly, there exist no arbitrage opportunities, and all derivatives can be perfectly hedged with the underlying price and bank deposit. Under these assumptions, we can derive the PDE governing the European option prices. Specifically, if we denote $V(S,t)$ as the price of European options, we can construct a portfolio longing an option and shorting Δ shares of the underlying, which means that the

value of this particular portfolio is

$$\Pi = V(S,t) - \Delta S. \tag{1.13}$$

Then, according to the Itô's lemma, the derivative of the portfolio price can be derived as

$$\begin{aligned} d\Pi &= dV(S,t) + \delta dS, \\ &= (\frac{\partial V}{\partial t} + \mu S\frac{\partial V}{\partial S} + \frac{1}{2}\sigma^2 S^2\frac{\partial^2 V}{\partial S^2} - \mu\Delta S)dt + (\frac{\partial V}{\partial S} - \Delta)\sigma S dB_t. \end{aligned} \tag{1.14}$$

With the strategy of dynamic hedging, the stochastic part of the above equation should be eliminated, which implies that $\Delta = \dfrac{\partial V}{\partial S}$, and can yield

$$d\Pi = (\frac{\partial V}{\partial t} + \frac{1}{2}\sigma^2 S^2\frac{\partial^2 V}{\partial S^2})dt. \tag{1.15}$$

On the other hand, the portfolio becomes risk-free since there is no stochastic source, and we can obtain

$$d\Pi = r\Pi dt = r(V - \frac{\partial V}{\partial S}S)dt. \tag{1.16}$$

Clearly, combining Equation (1.15) and (1.16), we can finally obtain the PDE for the European options, which is also called the Black-Scholes equation

$$\frac{\partial V}{\partial t} + \frac{1}{2}\sigma^2 S^2\frac{\partial^2 V}{\partial S^2} + rS\frac{\partial V}{\partial S} - rV = 0. \tag{1.17}$$

The boundary conditions and the terminal condition should be specified so that we can derive the pricing formula with the complete PDE system. We will use the European call option $C(S,t)$ as an example and the corresponding European put option price $P(S,t)$ can be derived with the so-called put-call parity

$$C(S,t) - P(S,t) = S - e^{-r(T-t)}K, \tag{1.18}$$

if K is assumed to be the strike price.

According to the definition of the European call option, we can easily obtain the

terminal condition given by the final payoff at maturity as

$$C(S,T) = \max(S-K,0). \tag{1.19}$$

When the underlying price approaches zero, the call option becomes deep out-of-money, which implies that the option value is close to zero

$$C(0,t) = 0. \tag{1.20}$$

In contrast, when the underlying price approaches infinity, the call option is deeply in-the-money, and its price increases with the same speed as the underlying price, which can be expressed as

$$\lim_{S\to\infty} C(S,t) \sim S. \tag{1.21}$$

With the terminal and boundary conditions specified above, the complete PDE system governing the European call option price has been established. If we denote $k = \dfrac{2r}{\sigma^2}$ and make the transformation of

$$x = \ln\frac{S}{K}, \tau = \frac{\sigma^2}{2}(T-t), U(x,\tau) = \frac{e^{\frac{(k-1)x}{2}+\frac{(k+1)^2\tau}{4}}}{K}C(S,t), \tag{1.22}$$

the PDE system becomes

$$\frac{\partial U}{\partial \tau} = \frac{\partial^2 U}{\partial S^2}, \tag{1.23}$$

with the initial condition

$$U(x,0) = \max(e^{\frac{(k+1)x}{2}} - e^{\frac{(k-1)x}{2}}, 0), \tag{1.24}$$

and the boundary conditions

$$\begin{aligned} &\lim_{x\to-\infty} U(x,\tau) = 0, \\ &\lim_{x\to+\infty} U(x,\tau) \sim e^{\frac{(k+1)x}{2}}. \end{aligned} \tag{1.25}$$

Obviously, this PDE system is a heat equation with an initial condition, which can be solved with the theory of fundamental solution. As a result, we can finally obtain the European call option pricing formula under the Black-Scholes model in the original variables

$$C(S,t) = SN(d_1) - Ke^{-r(T-t)}N(d_2), \tag{1.26}$$

where $N(\cdot)$ represents the standard normal distribution function. d_1 and d_2 are defined as

$$\begin{aligned} d_1 &= \frac{\ln \frac{S}{K} + (r + \frac{1}{2}\sigma^2)(T-t)}{\sigma\sqrt{T-t}}, \\ d_2 &= d_1 - \sigma\sqrt{T-t}. \end{aligned} \tag{1.27}$$

However, as illustrated before, the constant volatility assumption in the Black-Scholes model is inappropriate due to the existence of "volatility smile" exhibited by the implied volatility. This has prompted several alternative kinds of models for the underlying prices, which are discussed in the following three subsections.

1.4.2 Local volatility models

One of the most well-known approaches is proposed by Dupire [75] and Rubinstein [195], who made volatility a deterministic function of the underlying price and time instead of being a constant as the Black-Scholes model. In particular, the underlying asset price S_t in the local Black-Scholes model under the risk-neutral measure is specified as

$$\frac{dS}{S} = rdt + \sigma(S,t)dW_t. \tag{1.28}$$

Here we assume that European option prices denoted by $V(K,T,;S,t)$ in real markets are continuous with respect the strike price K and the maturity time T. In other words the data of European option prices with any strike price K and maturity time T are available. In order to work out the relationship between the local volatility function $\sigma(K,T)$ and the market option price $V(K,T,;S,t)$, we adopt the risk-neutral pricing rule and obtain

$$V(K,T,;S_0,0) = e^{-rT}\int_K^\infty (S-K)p(S_0,0;S,T)dS, \tag{1.29}$$

where $p(S_0,0;S,T)$ is the transition probability and the current time is assumed to be zero for simplicity. Differentiating Equation (1.29) once and twice with respect to K can respectively yield

$$\frac{\partial V}{\partial K} = e^{-rT}\int_K^\infty p(S,T;S_0,0)dS, \tag{1.30}$$

and

$$\frac{\partial^2 V}{\partial K^2} = e^{-rT} p(K, T; S_0, 0), \tag{1.31}$$

Also, we can obtain another identity by differentiating Equation (1.29) once with respect to T

$$\frac{\partial V}{\partial T} = -rV + e^{-rT} \int_K^\infty \frac{\partial p(S, T; S_0, 0)}{\partial T} (S - K) dS. \tag{1.32}$$

On the other hand, according to the forward Kolmogorov equation, the transition probability for the underlying price process (1.28) should satisfy

$$\frac{\partial p}{\partial T} = \frac{\partial^2}{\partial S^2}[\frac{1}{2}\sigma^2(S, T)S^2 p] - \frac{\partial}{\partial S}[rSp]. \tag{1.33}$$

Then, substituting Equation (1.33) into (1.32) can yield

$$\begin{aligned} \frac{\partial V}{\partial T} &= -rV + e^{-rT} \int_K^\infty \{\frac{\partial^2}{\partial S^2}[\frac{1}{2}\sigma^2(S, T)S^2 p] - \frac{\partial}{\partial S}[rSp]\}(S - K) dS, \\ &= \frac{K^2}{2}\sigma^2(K, T)\frac{\partial^2 V}{\partial K^2} - rK\frac{\partial V}{\partial K}, \end{aligned} \tag{1.34}$$

the last step of which is obtained based on the integration by parts and the substitution of Equation (1.30) into (1.31). Therefore, rearranging the above equation can yield the corresponding local volatility function $\sigma(K, T)$ with the following well-known Dupire formula

$$\sigma^2(K, T) = \sqrt{\frac{\frac{\partial V}{\partial T} + rK\frac{\partial V}{\partial K}}{\frac{K^2}{2}\frac{\partial^2 V}{\partial K^2}}}. \tag{1.35}$$

Although it seems very straightforward to obtain the local volatility function if we implement the Dupire formula with market data, there exist several problems associated with the local volatility models. First of all, it is very difficult to obtain the accurate local volatility function since the market option data is not continuous and often not enough. Secondly, direct implementation of the Dupire formula may not yield stable and accurate results since the denominator is directly affected by the second-order derivative of option prices, and it would sometimes even become negative due to the existence of noise in market option data. Most importantly, it has been pointed out that the smile dynamics are poorly captured by local volatility models, which implies that local volatility models fail to provide accurate results for options.

1.4.3 Stochastic volatility models

Another natural approach to modify the constant volatility assumption of the Black-Scholes model is to make the volatility another random variable described by a stochastic process, which is conceptually different from the local volatility model. This assumption is financially meaningful as many empirical studies have shown that the estimated volatility of the underlying price tends to change randomly, and the fat-tail property exhibited by the underlying returns can be simulated by some stochastic volatility models.

In fact, a number of stochastic volatility models have been proposed in the literature, such the Hull-White model [127] and the Stein-Stein model [213]. Among these, one of the most famous models is the Heston model [117], in which the volatility process follows the CIR model with some fundamental properties being consistent with real market observation, such as the non-negative property and the mean-reverting property. Most importantly, a closed-form pricing formula can be derived under the Heston model, which can contribute to the great efficiency and accuracy when pricing options and calibrating models.

In the Heston model, the underlying price S_t is assumed to follow the geometric Brownian motion specified as

$$dS_t = \mu S_t dt + \sqrt{v_t} S_t dW_t, \tag{1.36}$$

where μ is the drift term and W_t is a standard Brownian motion. v_t is governed by the mean-reverting process

$$dv_t = k(\theta - v_t)dt + \sigma\sqrt{v_t} dB_t, \tag{1.37}$$

where k is the mean-reversion speed, θ denotes the long-term mean, and σ represents the volatility of volatility. B_t is another standard Brownian motion correlated with W_t with correlation ρ. In order to find the PDE governing European option prices $C(S, v, t)$, we can again adopt the hedging strategy. It should be pointed out that unlike the Black-Scholes model, where there is only one stochastic source, two sources of randomness present in the stochastic volatility models. Therefore, the constructed portfolio π should contain not only the target option $C(S, v, t)$ and the $-\Delta_1$ shares of stock, but also $-\Delta_2$ shares of another option $U(S, v, t)$, which means

$$\Pi = C - \Delta_1 S - \Delta_2 U. \tag{1.38}$$

According to the Itô's lemma, the change of the portfolio value can be obtained as

$$d\Pi = dC - \Delta_1 dS - \Delta_2 dU, \tag{1.39}$$

where

$$\begin{aligned}
dC &= A_C dt + \sqrt{v} S \frac{\partial C}{\partial S} dW_t + \sigma \sqrt{v} \frac{\partial C}{\partial v} dB_t, \\
dU &= A_U dt + \sqrt{v} S \frac{\partial U}{\partial S} dW_t + \sigma \sqrt{v} \frac{\partial U}{\partial v} dB_t, \\
A_C &= \frac{\partial C}{\partial t} + \mu S \frac{\partial C}{\partial S} + k(\theta - v) \frac{\partial C}{\partial v} + \frac{1}{2} v S^2 \frac{\partial^2 C}{\partial S^2} + \frac{1}{2} \sigma^2 v \frac{\partial^2 C}{\partial v^2}, \\
A_U &= \frac{\partial U}{\partial t} + \mu S \frac{\partial U}{\partial S} + k(\theta - v) \frac{\partial U}{\partial v} + \frac{1}{2} v S^2 \frac{\partial^2 U}{\partial S^2} + \frac{1}{2} \sigma^2 v \frac{\partial^2 U}{\partial v^2}.
\end{aligned}$$

As a result, rearranging Equation (1.39) can yield

$$d\Pi = a dW_t + b dB_t + c dt, \tag{1.40}$$

with a, b and c defined as

$$\begin{aligned}
a &= \sqrt{v} S [\frac{\partial C}{\partial S} - \Delta_1 - \Delta_2 \frac{\partial U}{\partial S}], \\
b &= \sigma \sqrt{v} [\frac{\partial C}{\partial v} - \Delta_2 \frac{\partial U}{\partial v}], \\
c &= A_C - \Delta_1 \mu S - \Delta_2 A_U.
\end{aligned}$$

By adopting the strategy of dynamic hedging, we need to eliminate the term dW_t and dB_t, i.e.,

$$\begin{aligned}
\Delta_1 &= \frac{\partial C}{\partial S} - \Delta_2 \frac{\partial U}{\partial S}, \\
\Delta_2 &= \frac{\partial C}{\partial v} / \frac{\partial U}{\partial v}.
\end{aligned} \tag{1.41}$$

On the other hand, since this portfolio becomes risk-free now, the following equation should hold according to the arbitrage-free condition

$$d\Pi = r\Pi dt = r(C - \Delta_1 S - \Delta_2 U), \tag{1.42}$$

which implies that

$$cdt = r(C - \Delta_1 S - \Delta_2 U). \tag{1.43}$$

The above equation can be further simplified as

$$\begin{aligned}[\frac{\partial C}{\partial t} + rS\frac{\partial C}{\partial S} + k(\theta - v)\frac{\partial C}{\partial v} + \frac{1}{2}vS^2\frac{\partial^2 C}{\partial S^2} + \frac{1}{2}\sigma^2 v\frac{\partial^2 C}{\partial v^2} - rC]/\frac{\partial C}{\partial v} = \\ [\frac{\partial U}{\partial t} + rS\frac{\partial U}{\partial S} + k(\theta - v)\frac{\partial U}{\partial v} + \frac{1}{2}vS^2\frac{\partial^2 U}{\partial S^2} + \frac{1}{2}\sigma^2 v\frac{\partial^2 U}{\partial v^2} - rU]/\frac{\partial U}{\partial v}.\end{aligned} \tag{1.44}$$

The left hand side of Equation (1.44) is only a function of C, while its right hand side is a function of U. Obviously, Equation (1.44) will hold only if both sides equal to a function with variables S, v and t. Therefore, if we denote $\lambda(S, v, t)$ as the function, we can obtain the PDE governing the target option price

$$\frac{\partial C}{\partial t} + rS\frac{\partial C}{\partial S} + k(\theta - v)\frac{\partial C}{\partial v} + \frac{1}{2}vS^2\frac{\partial^2 C}{\partial S^2} + \frac{1}{2}\sigma^2 v\frac{\partial^2 C}{\partial v^2} - rC = \lambda(S, v, t)\frac{\partial C}{\partial v}. \tag{1.45}$$

From this, one can clearly find the European option prices under the Heston model depend on the choice of $\lambda(S, v, t)$, which is called the market price of volatility risk, and there are certainly different choices due to the arbitrariness of the function $\lambda(S, v, t)$. The results are consistent with the argument that markets with stochastic volatility is incomplete and there exists different risk-neutral measures. In fact, the pricing formula derived in the Heston's original paper [117] is based on the assumption that $\lambda(S, v, t) = \lambda S$. However, different fair prices of options can be obtained if we choose other risk-neutral measures, such as the minimal entropy martingale measure.

1.4.4 Regime-Switching models

Recently, a new kind of non-constant volatility models has attracted a lot of attention among researchers and market practitioners since a lot of empirical evidence strongly demonstrates the existence of regime switching in the underlying price [86, 104]. One of the most basic models in this category is the regime-switching Black-Scholes model with the constant volatility in the original Black-Scholes model replaced by the volatility controlled by a Markov chain jumping among different states.

In particular, the regime-switching Black-Scholes model with S being the underlying

price under the risk-neutral measure is specified as

$$\frac{dS}{S} = rdt + \sigma_{X_t} dW_t, \tag{1.46}$$

where r and σ_{X_t} represent the risk-free interest rate and the volatility respectively, and W_t is a standard Brownian motion. X_t is a Markov chain independent of W_t, and it is defined[1] as

$$X_t = \begin{cases} 1, & \text{when the economy is believed to be in State 1,} \\ 2, & \text{when the economy is believed to be in State 2,} \end{cases}$$

where the transition between the two states follows a Poisson process as

$$P(t_{ij} > t) = e^{-\lambda_{ij} t}, i, j = 1, 2, \ i \neq j.$$

Here λ_{ij} is the transition rate from State i to j, and t_{ij} is the time spent in State i before transferring to State j.

It should be noted that under the regime-switching models, option prices become a price vector, each element of which corresponds to each initial state of the volatility. As a result, we can denote the European option price vector as

$$\widetilde{U}(S, t) = (U(S, t, e_1), U(S, t, e_2))', \tag{1.47}$$

where v' denotes the transpose of the vector v. Moreover, according to the discussion in [83], the state space of X_t is taken to be the set of unit vectors $\{e_1, e_2\}$ with $e_1 = (1, 0)'$ and $e_2 = (0, 1)'$. In this case, for a given initial state X_t, the corresponding European option price can be calculated as

$$U(S, t, X_t) =< \widetilde{U}(S, t), X_t >, \tag{1.48}$$

where $< \cdot, \cdot >$ denotes the inner product of two vectors. From this, the change of the European option price can be derived as

$$dU = d < \widetilde{U}, X_t >=< d\widetilde{U}, X_t > + < \widetilde{U}, dX_t >, \tag{1.49}$$

[1]For illustration purpose, we use the two-state Markov chain as an example here.

the right hand side of which can be further calculated with the Itô's lemma as

$$< d\widetilde{U}, X_t >= dU(S,t,X_t) = \frac{\partial U}{\partial t}dt + \frac{\partial U}{\partial S}dS + \frac{1}{2}\frac{\partial^2 U}{\partial S^2}(dS)^2 + < \widetilde{U}, dX_t > . \tag{1.50}$$

Considering the fact that the martingale representation of the Markov chain [83] is

$$X_t = X_0 + \int_0^t AX_s ds + M_t, \tag{1.51}$$

with M_t being a martingale, we can obtain the change of the Markov chain

$$dX_t = AX_t dt + dM_t. \tag{1.52}$$

Furthermore, the discounted option price $e^{-rt}U$ should be a martingale in order to obtain the arbitrage-free price, which can yield the coupled PDE system governing the European option price

$$\begin{aligned} \frac{\partial U_1}{\partial t} &+ \frac{1}{2}\sigma_1^2 S^2 \frac{\partial^2 U_1}{\partial S^2} + rS\frac{\partial U_1}{\partial S} - rU_1 = \lambda_{12}(U_1 - U_2), \\ \frac{\partial U_2}{\partial t} &+ \frac{1}{2}\sigma_2^2 S^2 \frac{\partial^2 U_2}{\partial S^2} + rS\frac{\partial U_2}{\partial S} - rU_2 = \lambda_{21}(U_2 - U_1). \end{aligned} \tag{1.53}$$

Clearly, the coupled PDE system should be solved simultaneously to obtain the European option price under the regime-switching models, though we may only need one state price.

1.5 Structure of the thesis

In this thesis, we comprehensively study the area of option pricing, ranging from theory and computation to model calibration and empirical studies. This thesis is organized into three parts, with the first part working on different option pricing models with analytical pricing formula for European options, the second part dealing with option pricing problems with different solution techniques, and the third part focusing on several issues related to model calibration. Each part is further divided into several chapters with each chapter discussing one relevant issue.

Part 1 consists of three chapters, Chapter 2-4, in which three different option pricing models are considered. In Chapter 2, upon identifying two errors in a key reference [51], a new closed-form formula for pricing European options is derived under a particular skew

Brownian motion, which is constructed by a linear combination of a standard Brownian motion and a standard reflected Brownian motion. By adopting such a stochastic process for the underlying price, we aim to introduce the non-normality property to reflect skewed and leptokurtic returns exhibited by real market data. Numerical experiments are also carried out to show the quantitative impacts of different parameters on the option prices. Another key contribution of this Chapter is the proposal of a new equivalent martingale measure called "endogenous risk neutral measure". This is based on the fact that in incomplete markets, the risk associated with the underlying could be split into two parts; an endogenous part that measures the risks within the financial system which is somewhat controllable as they are mainly due to management and people's interaction with each other, and an exogenous part that refers to the risks caused by external factors, over which we have no control.

In Chapter 3, we propose a new stochastic volatility model with the constant volatility of volatility in the Heston model following a Markov chain so that it could jump between different states. Our motivation for adopting this particular model is that a lot of empirical evidence has demonstrated the existence of regime-switching. Furthermore, we present an analytical approximation formula with the perturbation method, which is rather simple with only normal distribution function involved and is suitable for options with short tenors. In order to show the performance of our newly proposed model in real markets, we have also conducted empirical studies to make the comparison of our model and the well-known Heston model with S&P 500 returns and short-tenor options. Results confirm that our model generally outperforms the Heston model, and thus it could be used as an alternative to the Heston model for some markets.

Different from the two models in Chapter 2 and 3, the model we adopt in Chapter 4 is one kind of non-structural models so that some particular characteristics of the underlying returns can be captured. In specific, we assume that the log-returns of the underlying follow a truncated normal distribution. The motivation for us to propose such a new model is that all the pricing models in the existing literature assume that the underlying price is unbounded above, which is not consistent with reality as there is no way that any underlying price could reach infinity. The price range of the underlying price under this model can be determine based on traders' own view of what a reasonable price range of the underlying should be before the option expires. Moreover, the Black-Scholes model is

a special case of our model since the truncated normal distribution could degenerate to the normal distribution when the lower and upper bound approach negative and positive infinity respectively. We also derive a closed-form pricing formula for European options, which does not bring any significantly extra burden compared with the B-S formula as far as the computational efficiency is concerned with numerical experiments showing various properties of the new formula.

In Part 2, different solution techniques are adopted to solve option pricing models. This part contains four chapter, i.e., Chapter 5-8. Specifically, in Chapter 5, we consider the problem of pricing European options under the Black-Scholes model with fixed-amount dividends. It should be noted that unlike the case that the dividends are continuously compounded or proportional to the underlying price, where closed-form pricing formula can be easily found, analytical pricing formula for fixed-amount dividends has never been discovered in the literature, which makes it hard to be implemented in real markets since the calibration process is time consuming and the calculation of option prices with numerical methods can cost much more time. We therefore derive a general closed-form approximation formula for all the cases of the single and multiple dividends to value European options with the Taylor series approximation technique. Our formula can certainly facilitate the application in real markets since no matter how many times the underlying pay its dividends before the expiry of the option, the formula is always the sum of one-dimensional integrals, the implementation of which is very efficient. Furthermore, numerical experiments are subsequently carried out to show the accuracy of the newly derived formula.

In Chapter 6, we derive a new closed-form pricing formula in series form for European options under the Heston model with the minimal entropy martingale measure. It should be pointed out that the introduction of stochastic volatility has made the market incomplete and there exist different equivalent martingale measures, which makes it financially important to choose an appropriate risk-neutral measure. The minimal entropy martingale measure is a reasonable choice since choosing it is equivalent to attaining the maximum expected utility [91]. Although the pricing problem becomes much more complicated than the results presented in the original Heston model since there exist variable coefficients in the PDE system governing European option prices as a result of the time-dependent drift term in the volatility process introduced by the particular risk-neutral measure, we

still manage to obtain an analytical pricing formula expressed as an infinite series. We are also able to provide a lower bound for the radius of convergence such that the series solution would converge if the time to maturity is less than the lower bound, which makes our solution even more attractive. In addition, numerical results are provided to show the speed of convergence of the series solution, and the accuracy of the formula is further demonstrated by the comparison of the prices calculated with our formula and those obtained through finite difference method and Monte Carlo simulation. Finally, we provide a slightly modified pricing formula for European options constructed with a set of different formulae that hold for different time range so that the entire time horizon can be covered by converged solution.

In Chapter 7, we present a new integral equation for American put option prices under the Black-Scholes model. There are several steps to take before we reach the new integral equation. Firstly, we present a new free boundary problem with a new PDE system governing the first order derivative of the American put price with respect to the time to maturity. Upon noticing the fact that the free boundary is a monotonic decreasing function of the time to expiry, we apply a novel approach that one of the variables, the time to expiry, in the new PDE is replaced by the free boundary. In this way, a linear PDE containing an unknown free boundary is transformed into a nonlinear PDE with the fixed boundary. After applying the Fourier transform to this particular nonlinear PDE, an analytical solution in the Fourier space is successfully derived. However, our approach should not be regarded as successful if we can not obtain the analytical inversion of the solution since the numerical inversion of a function in the Fourier space is not simple and often time-intensive. Fortunately, we finally manage to derive a simple and elegant integral equation after applying the inverse Fourier transform. Numerical experiments are also carried out to confirm the accuracy of the newly derived integral equation by comparing the results calculated with our formula and those obtained from other approaches in the existing literature.

In Chapter 8, we propose a new numerical algorithm for option pricing combining Monte-Carlo simulation and the ADI method, in which we artificially generate boundary conditions with Monte-Carlo simulation and then the option pricing problem inside the boundaries are solved with the ADI method. With this new method, we can avoid being restricted to work on a very large domain since the semi-infinite domain of the underlying

price (as well as the volatility) needs to be truncated, and usually we need to choose a large enough boundary so that the boundary condition at the truncated domain can be a good approximation of that at infinity. Numerical experiments are subsequently carried out to show the accuracy as well as efficiency of the new approach.

The last part of this thesis focuses on the problem of calibrating different models, and in particular focus on two different issues. This part is further divided into four chapters, i.e., Chapter 9-12. The first issue we work on is to propose alternative forms of the existing models that can provide better performance than the original versions in real markets. Our work seems to be meaningless since the form is actually equivalent to the original version if one could determine all model parameters analytically. However, the calibration of a model in reality is so complicated that model parameters always need to be determined numerically with an optimization algorithm. In the latter case, one would never be able to obtain the "optimized" set of parameters, but probably would have to settle near it. In Chapter 9, we propose an alternative form of the well-known Heston model by proving and imposing the necessary and sufficient conditions on a general stochastic volatility model to ensure the existence of a solution in an affine form. This alternative form can offer certain advantages in parameter determination, which is demonstrated with an empirical study with S&P 500 returns and options. Results show that our form generally outperforms the original Heston version for the case tested so far and it could be used as an alternative to the Heston version for some markets.

In Chapter 10, to further demonstrate the results in Chapter 9 that different forms of one model can provide different performance in real markets, we propose an alternative form of the Stein-Stein model, which is another famous stochastic volatility model with a closed-form pricing formula for European options. After we have successfully derived the analytical formula under the new form, we also make empirical comparison of our form and the original Stein-Stein version based on the S&P 500 Index returns and options to show the superiority of this new form.

The second issue of this part is how to calibrate local regime-switching models. Actually, there are few empirical studies on regime-switching option pricing models, the calibration of which still remains a challenge; one is that the calibration market price for a single option is available in real markets while two corresponding state prices are needed, and another is that an efficient algorithm needs to be developed to recover the

two local volatility functions. In Chapter 11, we propose a new "closed" system on how to price options in real markets with classical regime-switching models, based on which one market price is split into two market-implied state prices through two reasonable equations. With the obtained two sets of market-implied state prices, we proceed to design an efficient algorithm to recover local volatility functions with the Dupire formula for the local regime-switching models through the Tikhonov regularization approach. We have also conducted numerical tests, the results of which clearly show that our algorithm can recover volatility functions of different shapes.

In Chapter 12, we propose a new algorithm to directly calibrate local regime-switching models without using the Dupire formula for the local regime-switching models under the new "closed" system established in Chapter 11. The calibration problem is firstly transformed into an inverse problem, which is further formed as a minimization problem. By applying the Tikhonov Regularization, two necessary conditions are derived to obtain the optimal solution with a designed numerical algorithm. One of the most important differences between the two algorithms in Chapter 11 and 12 is that the variational derivative involved in the necessary conditions is obtained directly as the numerical solution of certain PDEs by introducing the Dirac delta function here, while it is dealt with in Chapter 11 with the Dupire formula.

Part I

Option pricing models

Chapter 2

A new closed-form formula for pricing European options under a skew Brownian motion

2.1 Introduction

An option is a financial derivative which gives the holder of a call the right to buy and the holder of a put to sell the underlying asset for a strike price in the future. European options can only be exercised on the expiration date while American options can be exercised any time before its maturity. In this chapter, we consider the problem of pricing European call options with the underlying asset being assumed to follow a stochastic process driven by the sum of a standard Brownian motion and a reflected Brownian motion that are independent of each other. The corresponding pricing formula for European put options can be easily derived since the call-put parity still holds under skew Brownian motions.

In 1973, a great breakthrough in option pricing was first achieved by Black & Scholes [19] who assumed that the log-returns followed a normal distribution and obtained a closed-form option pricing formula. However, there are some drawbacks in the B-S (Black-Scholes) model because of some unrealistic assumptions made to achieve analytical simplicity and tractability. Firstly, the normality of the log-return model can not capture the features like skewness [188], fat-tails [191] and time-dependence [153] that appear in the real market data. Secondly, the assumption of constant volatility in the well-known B-S model proved to be an over simplification as a result of the observed "volatility smile"

from market data [73]. These two major drawbacks among some other minor ones, have prompted research in searching for modification of B-S model.

In the literature, many attempts have been made to modify the B-S model related to distributional assumptions. Among them, Lévy processes are really popular since they have independent and stationary increments as the Brownian motion. First kind is the jump-diffusion models with Guassian jumps. Merton [178] proposed a model whose jumps in the log-returns have a Guassian distribution and Kou [158] adopted another one with the jump size having an asymmetric double exponential distribution. Another one is infinite activity lévy process where the Brownian component is omitted. Madan [173] introduced the Variance-Gamma model which is a time-changed Brownian motion. Others in this category include Normal Inverse Gaussian process used by Rydberg [196], CGMY model proposed by Carr, et al. [29] and Generalized hyperbolic model adopted by Eberlein [77]. Also, fractional Brownian motion was used to replace Brownian motion by Necula [185] for the long range dependence in asset price [225]. Other modifications are to incorporate time-dependent volatility including deterministic local volatility and stochastic volatility. The former one is adopted by Dupire [74] and the latter one includes the well-known Hull & White model [127] and Heston model [117].

A stochastic process considered in this chapter in option pricing is constructed with a skew Brownian motion. By "skew", we mean that the distribution of the underlying asset log-price is no longer symmetric and is instead a skew-normal distribution. Skew Brownian motion was firstly introduced by Itô & McKean [139] and indeed it is indexed by a skew parameter $\alpha \in [0, 1]$, and its excursion from zero has the probability α to be positive and $1 - \alpha$ to be negative. Need to say that a series of studies has been done regarding skew Brownian motions. For instance, Harrison & Shepp [108] connected the skew Brownian motion to a particular stochastic equation and showed it was a unique solution to that equation under certain conditions. Another example is given by Lejay [166], who summarized several ways to construct skew Brownian motions and also introduced their extensions and potential applications.

Recently, several authors have adopted skew Brownian motions and skew-normal distributions in financial modeling. For example, skew-normal distribution was applied to portfolio selection by Adcock & Shutes [2] while Vernic [218] proposed skew-normal distribution as an alternative to classic distributions for risk measurement and capital allocation.

Moreover, it has been pointed out by Eling et al. [80] that the Azzalini skew-normal distribution [8], which is the probability density of the adopted skew Brownian motion in this chapter, has a number of advantages compared with common measures of skewness. Nilsen & Sayit [186] even went further and provided their opinion that skew Brownian motions were able to describe the bounces and sinks of financial firms in distress. Furthermore, Decamps, et al. [65], Corns & Satchell [51] and Gairat & Shcherbakov [92] used them in derivative pricing. In particular, Decamps and Gairat & Shcherbakov built a relationship between discontinuous local volatility models and skew Brownian motions, which can be used in option pricing. In terms of option pricing by adopting skew Brownian motions directly in asset modeling, Corns & Satchell [51] were the first to derive a pricing formula for European options. Unfortunately, the results they provided are completely wrong, which will be proven later in this chapter.

In our chapter, we choose a typical type of skew Brownian motions, constructed by a linear combination of a standard Brownian motion and a standard reflected Brownian motion, whose density function is a skew-normal distribution. By adopting the particular skew Brownian motion in option pricing, the non-normality property is introduced in the distribution of log-returns, which is skewed and leptokurtic observed in real market. We will firstly show the results in the paper of Corns & Satchell [51] are incorrect and then use the martingale approach to derive the new formula for the price of European call option. In the process of developing this new pricing formula, another key contribution of this chapter emerged: for pricing financial derivatives in any incomplete markets, if the risk associated with the underlying could be split into two parts, an endogenous part that measures the risks within the financial system which is somewhat controllable as they are mainly due to management and people's interaction with each other, and an exogenous part that refers to the risks caused by external factors, over which we have no control, then a risk neutral martingale measure called "endogenous risk neutral measure" could be adopted. It is based on this new concept that our pricing formula was derived.

The rest of the chapter is organized as follows. In Section 2.2, we will point out and confirm two errors contained in [51], which leads to a totally wrong pricing formula. In Section 2.3, We will first briefly introduce this particular class of skew Brownian motions we adopt. The real challenge is to find a new equivalent martingale measure, based on which we are able to derive a closed-form analytical solution for pricing European options

under the skew Brownian motion constructed by the sum of a standard Brownian motion and a reflected Brownian motion that are independent of each other. In Section 2.4, numerical examples and some useful discussions are presented. Concluding remarks are given in the last section.

2.2 Incorrectness of a key pricing formula

As pointed out in the previous section, Corns & Satchell [51] option pricing formula was a key pricing formula in closed form with the adoption of skew Brownian in the assumptions of underlying dynamics. Unfortunately, there are two key errors in their formula. To demonstrate that the errors are not simple typos and the correction needs a careful choice of a new risk-neutral measure, two lemmas need to be introduced first in this Section.

Lemma 2.2.1. *Let X be a random variable with its probability density function*

$$f_X(x) = \frac{2}{\sigma x}\phi\big(\frac{\ln x - u}{\sigma}\big)\Phi\big(\lambda\frac{\ln x - u}{\sigma}\big), \tag{2.1}$$

where ϕ and Φ represent the standard normal density and distribution functions, respectively. Then if $Y = \ln X$, Y has the probability density function

$$f_Y(y) = \frac{2}{\sigma}\phi\big(\frac{y - u}{\sigma}\big)\Phi\big(\lambda\frac{y - u}{\sigma}\big). \tag{2.2}$$

Proof.

$$F_Y(y) = P(Y \le y) = P(\ln X \le y) = P(X \le e^y) = F_X(e^y),$$

from which we can derive

$$f_Y(y) = e^y f_X(e^y) = \frac{2}{\sigma}\phi\big(\frac{y - u}{\sigma}\big)\Phi\big(\lambda\frac{y - u}{\sigma}\big).$$

□

Lemma 2.2.2. *Let Z be a random variable with its density function*

$$f_Z(z) = \frac{2}{\sigma}\phi\big(\frac{z - u}{\sigma}\big)\Phi\big(\lambda\frac{z - u}{\sigma}\big),$$

where ϕ and Φ represent the standard normal density and distribution functions, respec-

tively. Then, $E(z) = \sigma\delta\sqrt{\frac{2}{\pi}} + u$.

Proof. The moment generating function of Z can be calculated as before:

$$\begin{aligned} M_Z(\theta) = E(e^{\theta z}) &= \int_{-\infty}^{\infty} \frac{2}{\sigma} e^{\theta z} \phi(\frac{z-u}{\sigma}) \Phi(\lambda \frac{z-u}{\sigma})\, dz, \\ &= \frac{2}{\sigma\sqrt{2\pi}} e^{u\theta + 0.5\theta^2\sigma^2} \int_{-\infty}^{\infty} e^{-\frac{(z-u-\theta\sigma^2)^2}{2\sigma^2}} \Phi(\lambda \frac{z-u}{\sigma}) dz, \\ &= \frac{2}{\sigma\sqrt{2\pi}} e^{u\theta + 0.5\theta^2\sigma^2} \int_{-\infty}^{\infty} e^{-\frac{y^2}{2\sigma^2}} \Phi(\lambda \frac{y}{\sigma} + \lambda\theta\sigma) dy, \\ &= 2e^{u\theta + 0.5\theta^2\sigma^2} \Phi(\frac{\lambda\theta\sigma}{\sqrt{1+\lambda^2}}). \end{aligned}$$

The last step is according to Lemma 2 in [8]. Moreover, if we set $\delta = \frac{\lambda}{\sqrt{1+\lambda^2}}$, we then have

$$\frac{\partial(E(e^{\theta z}))}{\partial\theta} = \frac{\partial(2e^{u\theta + 0.5\theta^2\sigma^2}\Phi(\delta\theta\sigma))}{\partial\theta},$$

which can be simplified to

$$E(ze^{\theta z}) = 2e^{u\theta + 0.5\theta^2\sigma^2}(u + \theta\sigma^2)\Phi(\delta\theta\sigma) + 2e^{u\theta + 0.5\theta^2\sigma^2}\phi(\delta\theta\sigma)\delta\sigma. \tag{2.3}$$

Setting $\theta = 0$ in Equation (2.3) leads to the desired result

$$E(z) = \sigma\delta\sqrt{\frac{2}{\pi}} + u. \tag{2.4}$$

□

Let S_t denote the underlying asset price at time t and $f(S_T \mid S_t)$ be the probability density function of S_T conditional upon the S_t for $t < T$ as defined in [51]. The expression $f(S_T \mid S_t)$, which is used in option pricing, is wrongly derived from the expression of S_t, which is proven by contradiction.

On one hand, according to [51],

$$f(S_T \mid S_t) = \frac{2}{\sigma S_T\sqrt{T-t}} \phi(y)\Phi(\lambda y), \tag{2.5}$$

where $y = \frac{\ln S_T - \ln S_t - (r - 0.5\sigma^2)(T-t) + \ln[2\Phi(\delta\sigma\sqrt{T-t})]}{\sigma\sqrt{T-t}}$, which implies $\ln S_T = \sigma\sqrt{T-t}y + \ln S_t + (r - 0.5\sigma^2)(T-t) - \ln[2\Phi(\delta\sigma\sqrt{T-t})]$. From Lemma 5.2.1, we know

that

$$f(\ln S_T \mid S_t) = \frac{2}{\sigma\sqrt{T-t}}\phi(y)\Phi(\lambda y),$$

by which we can calculate

$$\begin{aligned} E(\ln S_T \mid S_t) &= \int_{-\infty}^{\infty} \ln S_T f(\ln S_T \mid S_t)\, d(\ln S_T), \\ &= \int_{-\infty}^{\infty} 2\phi(y)\Phi(\lambda y)[\sigma\sqrt{T-t}y + \ln S_t + (r-0.5\sigma^2)(T-t) - \ln(2\Phi(\delta\sigma\sqrt{T-t}))]dy, \\ &= \ln S_t + (r-0.5\sigma^2)(T-t) - \ln[2\Phi(\delta\sigma\sqrt{T-t})] + \sigma\sqrt{T-t}\int_{-\infty}^{\infty} 2y\phi(y)\Phi(\lambda y)dy, \\ &= \ln S_t + (r-0.5\sigma^2)(T-t) - \ln[2\Phi(\delta\sigma\sqrt{T-t})] + \delta\sigma\sqrt{\frac{2(T-t)}{\pi}}. \end{aligned} \tag{2.6}$$

The last step results from Lemma 5.2.2.

On the other hand, according to Equation (12) in [51]

$$S_t = S_0 e^{(r-0.5\sigma^2)t - \ln[2\Phi(\delta\sigma\sqrt{t})] + \sigma\bar{X}_t}, \tag{2.7}$$

where $\bar{X}_t$ is a $\mathbb{Q}$ skew Brownian motion. So we can obtain the following two equations,

$$\begin{aligned} \ln S_t &= \ln S_0 + (r-0.5\sigma^2)t - \ln[2\Phi(\delta\sigma\sqrt{t})] + \sigma\bar{X}_t, \\ \ln S_T &= \ln S_0 + (r-0.5\sigma^2)T - \ln[2\Phi(\delta\sigma\sqrt{T})] + \sigma\bar{X}_T. \end{aligned}$$

Then combining these two equations yields

$$\ln S_T - \ln S_t = (r-0.5\sigma^2)(T-t) - \{\ln[2\Phi(\delta\sigma\sqrt{T})] - \ln[2\Phi(\delta\sigma\sqrt{t})]\} + \sigma(\bar{X}_T - \bar{X}_t),$$

which leads to another expression of $E(\ln S_T \mid S_t)$ given below,

$$E(\ln S_T \mid S_t) = \ln S_t + (r-0.5\sigma^2)(T-t) - \{\ln[2\Phi(\delta\sigma\sqrt{T})] - \ln[2\Phi(\delta\sigma\sqrt{t})]\} + E[\sigma(\bar{X}_T - \bar{X}_t) \mid S_t]. \tag{2.8}$$

Subtracting Equation (2.8) from Equation (2.6) on both sides respectively and getting expectation from the both sides of the resulted equation, the following should be valid.

$$E[\sigma(\bar{X}_T - \bar{X}_t)] = \ln[2\Phi(\delta\sigma\sqrt{T})] - \ln[2\Phi(\delta\sigma\sqrt{t})] - \ln[2\Phi(\delta\sigma\sqrt{T-t})] + \sigma\delta\sqrt{\frac{2}{\pi}}(\sqrt{T-t}).$$

According to Lemma 5.2.2, $E[\sigma(\bar{X}_T - \bar{X}_t)] = \sigma\delta\sqrt{\frac{2}{\pi}}(\sqrt{T} - \sqrt{t})$. Thereby, we finally arrive at

$$\sigma\delta\sqrt{\frac{2}{\pi}}(\sqrt{T} - \sqrt{t} - \sqrt{T-t}) = \ln[2\Phi(\delta\sigma\sqrt{T})] - \ln[2\Phi(\delta\sigma\sqrt{t})] - \ln[2\Phi(\delta\sigma\sqrt{T-t})], \quad (2.9)$$

which should hold if (2.5) was correct.

To prove an equation correct, we have to show it holds for every set of parameters. On the other hand, to prove an equation wrong, all we need to do is to show that is does not hold for a single set of parameters. Here, we can demonstrate that Equation (2.9) does not hold as we can easily find not only one, but a set of continuous points in the parameter space such that the difference between the two sides of Equation (2.9) is far from zero.

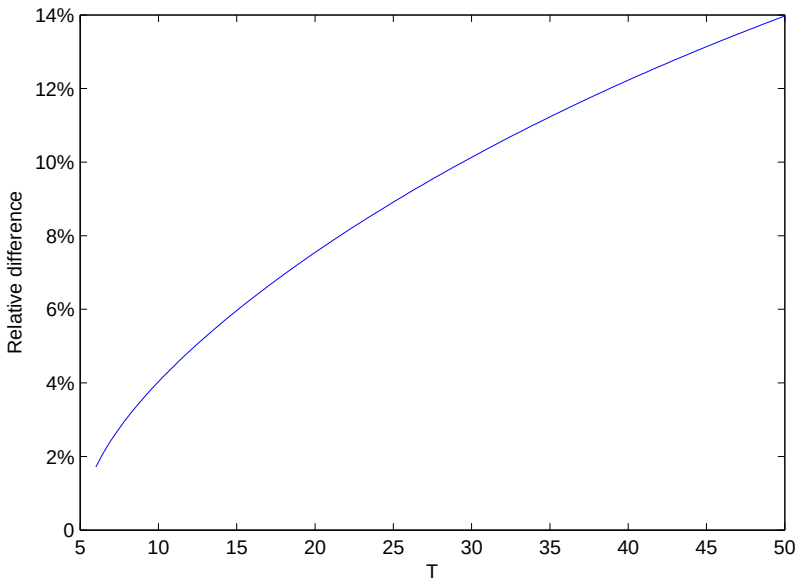

Figure 2.1: Differences among the two sides of the equation (2.9)

Plotted in Figure 2.1 are percentage differences between the two sides of Equation (2.9) with $\delta = 0.5$, $\sigma = \sqrt{0.4}$ and $t = 5$, when $T - t$ is varied with in a range of $T - t \in [1, 45]$. Indeed, the maximum difference for this set of parameters reaches 14%, which implies that (2.9) does not hold and thus completes our proof through contradiction. The incorrectness of (2.5) naturally leads us to draw a conclusion that the pricing formula (14) in [51] is incorrect.

We could not exactly identify the reason where the mistake was made until we had realized that Corns & Satchell [51] had taken the extension of $f(\ln S_t|S_0)$ to $f(\ln S_T|S_t)$ for

granted, which is not true since the reflected Brownian motion does not have a stationary increment. Then the question raised was that why they needed to make such an extension if they already knew the relationship between S_T and S_t. As we dug further, we eventually found another error that they had regarded $E^Q[e^{-rT}S_T \mid F_0] = S_0$ as the condition for the discounted asset price to be a martingale. However, this condition is actually only a necessary but not sufficient condition for $e^{-rt}S_t$ to be a martingale, which again shows that the obtained option price, based on a wrongly chosen condition, should not be a fair price.

This point deserves to be elaborated a bit further as there are authors who deliberately use the condition $E^Q[e^{-rT}S_T \mid F_0] = S_0$ in their papers to derive option pricing formulae [52, 156, 174]. Are they all wrong?

In the literature, there are two main kinds of option pricing models, the so-called structural models [19, 117, 173] and non-structural models [148]. While the former tries to capture the dynamics of the underlying stock price at every moment for a given period of time horizon, the latter only specifies the probability density function of the underlying at maturity conditional upon the filtration at the current time without completely describing the fine details of the stochastic process themselves at each moment. More specifically, the necessary and sufficient condition $E^Q[e^{-rT}S_T \mid F_t] = e^{-rt}S_t$ for any $t \in [0, T]$ is used in structural models to price an option [162], whereas only the necessary condition $E^Q[e^{-rT}S_T \mid F_0] = S_0$ is adopted in non-structural models as a so-called "martingale restriction" [170] rather than a full martingale, which financially implies that arbitrage opportunities may exist.

Now, in terms of option pricing, if one wants to develop a pricing formula under the risk-neutral measure, structural models must be adopted since in this case the goal of perfect hedging at any time $t \in [0, T]$ can be achieved under the martingale framework. With structural approaches, we focus on the dynamics of the underlying following a specific stochastic process. Once a process is chosen, one then has no control on the probability density function that describes the distribution of the underlying at the expiry, which may result in a mis-price of the option, a well known "volatility smile" phenomenon [195]. On the other hand, one may wish to have a better control on the statistic properties, such as skewness and kurtosis in addition to mean and variance, of the underlying distribution at the expiry, in order to alleviate the "volatility smile". But, then it is very difficult to

find a process that yields the desired distribution. So, the essence of the non-structural approaches is to obtain option pricing formulae that yield results closer to market data at the expenses of giving up the "risk neutral" assumption, or we could say that deliberately using a weaker condition, $E^Q[e^{-rT}S_T \mid F_0] = S_0$, to derive a pricing formula is the rational behind the development of non-structural models. Therefore in this sense, what Corns & Satchell [51] did is not completely wrong.

However, what Corns & Satchell [51] did get wrong is that they already assumed the underlying asset price follow a geometric skew Brownian motion in [51], which implies that a pricing formula should be derived within the framework of structural models. They only adopted the "martingale restriction" $E^Q[e^{-rT}S_T \mid F_0] = S_0$ (a weaker condition), instead of the full martingale condition, i.e. $E^Q[e^{-rT}S_T \mid F_t] = e^{-rt}S_t$, in their derivation process. An extremely simplified binomial tree with two steps is established to show the potential quantitative difference by imposing these two conditions.

Let's take Y_t as the underlying asset price and assume that it will move up to $\mu_i Y_t$ or fall to $d_i Y_t$ after each step, where $i = 1, 2$. We further assume that $Y_0 = K = 100, r = 0.05, dt = 1$, where K is the strike price, r represents the risk-free interest rate and dt denotes the time duration of one step. On one hand, if we only know the information at present and at expiry, we can give the states of the underlying prices after two steps, i.e. $Y_T = \{81, 99, 121\}$ and we do not know what values μ and d take in each step. As a result, we can only impose the necessary condition $E^Q[e^{-rT}Y_T \mid F_0] = Y_0$ and obtain the following equation

$$121e^{-0.1}p_1 + 99e^{-0.1}p_2 + 81e^{-0.1}(1 - p_1 - p_2) = 100,$$

which implies that p_1 should be in the range of $[0.5114, 0.7313]$. Therefore, the European call option price should be in the range of [9.7,13.9] instead of a unique price. On the other hand, if we know the exact μ_i and d_i in each period, for example, we just set $\mu_1 = \mu_2 = 1.1$ and $d_1 = d_2 = 0.9$, we can impose the necessary and sufficient condition $E^Q[e^{-rT}Y_T \mid F_t] = e^{-rt}Y_t$, which can certainly leads to a unique risk-neutral price 10.7. Hence, it is not difficult to find that the maximum mis-pricing could reach 30% in this case.

One of the possible reasons for them to do so could be that they could not find a true

martingale measure for the process constructed by the particular geometric skew Brownian motion, which was a major difficulty that we also faced and tried to overcome when we wanted to work out a correct option pricing formula with the full martingale condition imposed. At the end, we successfully found such a risk-neutral measure with respect to the geometric skew Brownian motion and derived a new pricing formula, as will be shown in the next Section.

2.3 New Formula

In this section we will first briefly introduce a particular kind of skew Brownian motions, which is applied to model underlying asset returns. And then a new martingale measure is introduced, based on which a martingale method is used to derive a pricing formula for European call options.

2.3.1 Introduction of skew Brownian motion

Let (Ω, F, P) define a probability space where F is a σ -algebra on Ω and P is a probability measure on (Ω, F).

Proposition 2.3.1. *The diffusion process* $\{X_t, t \geq 0\}$ *defined as follows*

$$X_t = \sqrt{1-\delta^2} W_{1,t} + \delta \mid W_{2,t} \mid, \quad \delta \in (-1, 1), \tag{2.10}$$

with $W_{1,t}$ *and* $W_{2,t}$ *being two independent standard Brownian motions, is a kind of skew Brownian motions, with known probability density function:*

$$f_{X_t}(x) = \frac{2}{\sqrt{t}} \phi(\frac{x}{\sqrt{t}}) \Phi(\lambda \frac{x}{\sqrt{t}}).$$

The proof of this proposition can be found in [51].

2.3.2 A new equivalent martingale measure

As we mentioned in the last Section that the martingale measure in [51] is not correct, we need to find a new martingale measure $\mathbb{Q}$, under which $e^{-rt} S_t$ is martingale. However, it has been pointed out by Nilsen & Sayit [186] and Rossello [193] that if the underlying price process follows a geometric skew Brownian motion under the physical measure, then

arbitrage opportunities can occur. As a result, in order to price options still under the framework of the skew Brownian motion, a new underlying price process under the physical measure should be proposed first.

If we let X_t be the skew Brownian motion defined in the last subsection, and let

$$W_t = \sqrt{1-\delta^2}W_{1,t}, \quad R_t = \delta \mid W_{2,t} \mid,$$

then the price process under the physical measure is assumed to follow

$$S_T = S_t e^{\mu(T-t)-l(R_t)+\sigma(X_T-X_t)}, \tag{2.11}$$

where $l(z) = \ln(\Phi[\frac{z+(T-t)\sigma^2\delta^2}{\sqrt{T-t}\sigma\delta}] + e^{-2z}\Phi[\frac{-z+(T-t)\sigma^2\delta^2}{\sqrt{T-t}\sigma\delta}])$. By adding this "adjusted" process $l(R_t)$ under the Physical measure, $e^{\sigma(R_T-R_t)-l(R_t)-0.5\sigma^2\delta^2(T-t)}$ itself becomes a martingale and the market driven by Process (2.11) can become arbitrage free since there exist equivalent martingale measures. To be more specific, if we make the measure transform of

$$\begin{aligned} \bar{W}_{1,t} &= W_{1,t} + \frac{(\mu - r + 0.5\sigma^2)t}{\sigma\sqrt{1-\delta^2}}, \\ \bar{W}_{2,t} &= W_{2,t}, \end{aligned} \tag{2.12}$$

where $\bar{W}_{1,t}$ and $\bar{W}_{2,t}$ are independent Brownian motions under the equivalent martingale measure $\mathbb{Q}$, then the underlying price process under this new risk-neutral measure should be

$$S_T = S_t e^{(r-0.5\sigma^2)(T-t)-l(\bar{R}_t)+\sigma(\bar{X}_T-\bar{X}_t)}, \tag{2.13}$$

where $\bar{X}_T$ and $\bar{R}_t$ represent the skew Brownian motion and reflected Brownian motion under $\mathbb{Q}$ respectively.

It should be noted that although a semimartingale representation for our model can hardly be derived due to the expression of $l(z)$, it is natural for us to view our model as an incomplete market model, since there exist two independent Brownian motions. As a result, there are different equivalent martingale measures one could choose to price an option [91, 201]. Our choice for this particular martingale measure is motivated by the so-called "minimal martingale measure" [201] in the sense that we assume only risks associated with

the Brownian motion $W_{1,t}$ need to be hedged. To be more specific, the stochastic process $e^{(\mu+0.5\sigma^2\delta^2)(T-t)+\sigma\sqrt{1-\delta^2}(W_{1,T}-W_{1,t})}$ constructed with $W_{1,t}$ represents the endogenous risk of the underlying itself while the stochastic process $e^{\sigma\delta(|W_{2,T}|-|W_{2,t}|)-l(\delta|W_{2,t}|)-0.5\sigma^2\delta^2(T-t)}$ constructed with $W_{2,t}$ is used to model all the exogenous risks. As shown before the process $e^{\sigma\delta(|W_{2,T}|-|W_{2,t}|)-l(\delta|W_{2,t}|)-0.5\sigma^2\delta^2(T-t)}$ is a martingale and thus there is no need for us to hedge the exogenous risk associated with $W_{2,t}$, over which we actually have no control. Therefore, we should only focus on hedging the endogenous risk associated with $W_{1,t}$. This implies that $W_{2,t}$ remains unchanged, whereas there is a shift for $W_{1,t}$ under the measure transform performed in Equation (2.12). For this reason, we have named this particular martingale measure "endogenous risk neutral measure" to suggest that only the risk associated with the endogenous process should be fully hedged and there is no need to hedge the exogenous part since it is already a martingale. It of course also reflects that there is no unique risk neutral martingale measure when the process (2.11) is adopted to simulate the dynamics of an underlying as a result that the risk associated with the exogenous process can not be fully hedged at all since it is beyond our control.

In fact, this concept of splitting the total risk into two parts, namely endogenous risk and exogenous risk, and then pricing a financial derivative with an "endogenous risk neutral measure" can be extended to other option pricing models with different stochastic processes being adopted for incomplete markets. Of course, the key to the success hinges on a successful split of an incomplete market under the physical measure into two processes that are independent with each other with one being a martingale, taking all exogenous risks into consideration while another representing endogenous risks. Then, the concept of enforcing an "endogenous risk neutral measure" through measure transformation can be adopted as a financial justification of pricing derivatives. Of course, like some other approaches proposed in the literature to price financial derivatives in incomplete markets, such as [91, 201], our proposed "endogenous risk neutral measure" approach adds a new "flavor" to the literature; whether or not it is superior to other approaches are yet to be tested by empirical studies.

After providing the financial interpretation for such a martingale measure, we are now ready to justify the mathematical correctness of this choice. Actually, it is not difficult to

obtain the following conditional expectation

$$E^Q[e^{-rT} \cdot e^{r(T-t)+\sigma \bar{X}_T} \mid F_t] = S_t e^{-rt} e^{-\sigma \bar{W}_t - \sigma \bar{R}_t} E[e^{\sigma \bar{W}_T + \sigma \bar{R}_T} \mid F_t].$$

In addition, it can be easily derived that

$$f_{\sigma \bar{W}_T | \sigma \bar{W}_t}(x_1 \mid y) = \frac{1}{\sigma \sqrt{2\pi (T-t)(1-\delta^2)}} e^{-\frac{(x_1 - y)^2}{2(T-t)(1-\delta^2)\sigma^2}}, \tag{2.14}$$

$$f_{\sigma \bar{R}_T | \sigma \bar{R}_t}(x_2 \mid z) = \frac{1}{\delta \sigma \sqrt{2\pi (T-t)}} (e^{-\frac{(x_2 - z)^2}{2(T-t)\delta^2\sigma^2}} + e^{-\frac{(x_2 + z)^2}{2(T-t)\delta^2\sigma^2}}). \tag{2.15}$$

Since $\{\bar{W}_t, t \geq 0\}$ and $\{\bar{R}_t, t \geq 0\}$ are independent, the vector $(\bar{W}_T, \bar{W}_t)$ and $(\bar{R}_T, \bar{R}_t)$ are independent of each other ($\forall t < T$). Then

$$\begin{aligned} f_{\sigma \bar{W}_T, \sigma \bar{R}_T | \sigma \bar{W}_t, \sigma \bar{R}_t} &= \frac{f_{\sigma \bar{W}_T, \sigma \bar{R}_T, \sigma \bar{W}_t, \sigma \bar{R}_t}}{f_{\sigma \bar{W}_t, \sigma \bar{R}_t}} \\ &= \frac{f_{\sigma \bar{W}_T, \sigma \bar{W}_t} \cdot f_{\sigma \bar{R}_T, \sigma \bar{R}_t}}{f_{\sigma \bar{W}_t} \cdot f_{\sigma \bar{R}_t}} \\ &= f_{\sigma \bar{W}_T | \sigma \bar{W}_t} \cdot f_{\sigma \bar{R}_T | \sigma \bar{R}_t}. \end{aligned} \tag{2.16}$$

As a result, we have

$$\begin{aligned} E^Q[e^{\sigma \bar{W}_T + \sigma \bar{R}_T} \mid F_t] &= \int_0^{+\infty} \int_{-\infty}^{+\infty} e^{x_1 + x_2} f_{\sigma \bar{W}_T, \sigma \bar{R}_T | \sigma \bar{W}_t, \sigma \bar{R}_t}(x_1, x_2 \mid y, z) dx_1 dx_2 \\ &= e^{y + z + 0.5\sigma^2 (T-t)} e^{l(z)}, \end{aligned}$$

and thus

$$E^Q[e^{-rT} \cdot e^{r(T-t)+\sigma \bar{X}_T} \mid F_t] = S_t e^{-rt} e^{0.5\sigma^2 (T-t)} e^{l(z)}. \tag{2.17}$$

This implies $E^Q[e^{-rT} S_T \mid F_t] = e^{-rt} S_t$, i.e. $e^{-rt} S_t$ is a martingale.

One of the important assumptions in option pricing theory for complete markets is that there are no arbitrage opportunities. According to the fundamental theorem of asset pricing [61], the market is arbitrage-free if and only if there exists an equivalent martingale measure. Thus, successfully obtaining such a measure as shown above has paved the way for the success of deriving a risk-neutral pricing formula for European call options.

2.3.3 A new closed-form option pricing formula

Now we are ready to derive the option pricing formula under $\mathbb{Q}$.

Proposition 2.3.2. *Let the underlying asset price S_t follow the particular process (2.13) under the martingale measure $\mathbb{Q}$ that we derive in the last subsection, the European call option pricing formula can be written as*

$$C(S,t) = S_t M_1(b_1) - Ke^{-r(T-t)} M_2(b_2), \tag{2.18}$$

where

$$\begin{aligned}
&M_1(b_1) = \int_{b_1}^{\infty} e^{-g(m)} L_1(x,m)dx, \quad M_2(b_2) = \int_{b_2}^{\infty} L_2(x,m)dx,\\
&L_1(x,m) = \phi(x)\Phi(F_1) + e^{-2m\delta}\phi(\frac{\sigma\sqrt{T-t}x + 2m\delta}{\sigma\sqrt{T-t}})\Phi(F_2),\\
&L_2(x,m) = \phi(x)\Phi(G_1) + \phi(\frac{\sigma\sqrt{T-t}x + 2m\delta}{\sigma\sqrt{T-t}})\Phi(G_2),\\
&F_1 = sgn(\delta)\frac{\delta[\sigma\sqrt{T-t}x + (T-t)\sigma^2] + m}{\sigma\sqrt{(T-t)(1-\delta^2)}},\\
&F_2 = sgn(\delta)\frac{\delta[\sigma\sqrt{T-t}x + (T-t)\sigma^2 + 2m\delta] - m}{\sigma\sqrt{(T-t)(1-\delta^2)}},\\
&G_1 = sgn(\delta)\frac{\delta\sigma\sqrt{T-t}x + m}{\sigma\sqrt{(T-t)(1-\delta^2)}}, \quad G_2 = sgn(\delta)\frac{\delta[\sigma\sqrt{T-t}x + 2m\delta] - m}{\sigma\sqrt{(T-t)(1-\delta^2)}},\\
&b_1 = \frac{\ln K - \ln S_t - (r + 0.5\sigma^2)(T-t) + g(m)}{\sigma\sqrt{T-t}},\\
&b_2 = \frac{\ln K - \ln S_t - (r - 0.5\sigma^2)(T-t) + g(m)}{\sigma\sqrt{T-t}},\\
&g(m) = \ln\Phi(C_1) + e^{-2m\delta}\Phi(C_2), \quad m = \mid W_{2,t} \mid,\\
&C_1 = sgn(\delta)\frac{m + (T-t)\sigma^2\delta}{\sqrt{T-t}\sigma}, \quad C_2 = sgn(\delta)\frac{-m + (T-t)\sigma^2\delta}{\sqrt{T-t}\sigma},\\
&sgn(x) = \begin{cases} 1, & x \geq 0,\\ -1, & x < 0. \end{cases}
\end{aligned}$$

Proof. A probability approach is applied to derive the closed-form formula for European call option price $C(S,t)$.

Let

$$a = \ln K - \ln S_t - (r - 0.5\sigma^2)(T-t) + l(z) + y + z,$$

we then have

$$\begin{aligned} C(S,t) &= e^{-r(T-t)}E^Q[(S_T-K)^+ \mid F_t], \\ &= e^{-r(T-t)}E^Q[S_T \cdot I_{(S_T>K)} \mid F_t] - e^{-r(T-t)}KE^Q[I_{(S_T>K)} \mid F_t], \\ &= S_t e^{-0.5\sigma^2(T-t)-l(z)-(y+z)}\int_a^\infty e^u f(u \mid y,z)du \\ &- Ke^{-r(T-t)}\int_a^\infty f(u \mid y,z)du. \end{aligned} \tag{2.19}$$

Here, $f(u \mid y,z)$ is regarded as the conditional probability density function $f_{\sigma W_T+\sigma R_T|\sigma W_t,\sigma R_t}$. What we need to know is the two integrals in Equation (2.19) since the other terms are known by now. Therefore, $f(u \mid y,z)$ should be firstly derived, which is needed in the calculation of the two integrals. Recall Equation (2.16) in the last subsection,

$$f_{\sigma W_T,\sigma R_T|\sigma W_t,\sigma R_t} = f_{\sigma W_T|\sigma W_t} f_{\sigma R_T|\sigma R_t}, \tag{2.20}$$

the conditional probability density function $f_{\sigma W_T+\sigma R_T|\sigma W_t,\sigma R_t}$ can be easily derived as

$$\begin{aligned} f(u \mid y,z) &= \int_0^\infty \frac{1}{2\pi(T-t)\sigma^2\delta\sqrt{1-\delta^2}} e^{-\frac{(u-v-y)^2}{2(1-\delta^2)\sigma^2(T-t)}}[e^{-\frac{(v-z)^2}{2(T-t)\sigma^2\delta^2}} + e^{-\frac{(v+z)^2}{2(T-t)\sigma^2\delta^2}}]dv, \\ &= \frac{1}{\sqrt{2\pi(T-t)}\sigma} e^{-\frac{(u-y-z)^2}{2\sigma^2(T-t)}}\Phi(a_1) + e^{-\frac{(u-y+z)^2}{2\sigma^2(T-t)}}\Phi(a_2), \end{aligned} \tag{2.21}$$

where

$$\begin{aligned} a_1 &= \frac{\delta^2(u-y-z)+z}{\delta\sigma\sqrt{(T-t)(1-\delta^2)}}, \\ a_2 &= \frac{\delta^2(u-y+z)-z}{\delta\sigma\sqrt{(T-t)(1-\delta^2)}}. \end{aligned}$$

As a result, we arrive at

$$\begin{aligned} \int_a^{+\infty} e^u f(u \mid y,z)du &= \frac{1}{\sigma\sqrt{2\pi(T-t)}} e^{y+z+0.5\sigma^2(T-t)} \int_a^{+\infty} [e^{-\frac{[u-y-z-\sigma^2(T-t)]^2}{2(T-t)\sigma^2}}\Phi(a_1) \\ &+ e^{-2z}e^{-\frac{[u-y+z-\sigma^2(T-t)]^2}{2(T-t)\sigma^2}}\Phi(a_2)]du. \end{aligned}$$

By means of transformation of the variable $x = \dfrac{u-y-z-(T-t)\sigma^2}{\sigma\sqrt{T-t}}$, the above equation

becomes

$$\begin{aligned}\int_a^\infty e^u f(u \mid y,z)du &= e^{y+z+0.5\sigma^2(T-t)}\int_{b_1}^\infty \phi(x)\Phi(\frac{\delta^2[\sigma\sqrt{T-t}x+(T-t)\sigma^2]+z}{\sigma\delta\sqrt{(T-t)(1-\delta^2)}})\\ &+ e^{-2z}\phi(x+\frac{2z}{\sigma\sqrt{T-t}})\Phi(\frac{\delta^2[\sigma\sqrt{T-t}x+(T-t)\sigma^2+2z]-z}{\sigma\delta\sqrt{(T-t)(1-\delta^2)}})dx,\\ &\triangleq e^{y+z+0.5\sigma^2(T-t)}\Psi_1(b_1), \end{aligned} \tag{2.22}$$

where $b_1 = \dfrac{\ln K - \ln S_t - (r+0.5\sigma^2)(T-t)+l(z)}{\sigma\sqrt{T-t}}$.
In a similar fashion, with $w = \dfrac{u-y-z}{\sigma\sqrt{T-t}}$, we can obtain

$$\begin{aligned}\int_a^\infty f(u \mid y,z)du &= \int_{b_2}^\infty \phi(x)\Phi[\frac{\delta^2\sigma\sqrt{T-t}w+z}{\sigma\delta\sqrt{(T-t)(1-\delta^2)}}]\\ &+ \phi(w+\frac{2z}{\sigma\sqrt{T-t}})\Phi[\frac{\delta^2(\sigma\sqrt{T-t}w+2z)-z}{\sigma\delta\sqrt{(T-t)(1-\delta^2)}}]dw,\\ &\triangleq \Psi_2(b_2), \end{aligned} \tag{2.23}$$

where $b_2 = \dfrac{\ln K - \ln S_t - (r-0.5\sigma^2)(T-t)+l(z)}{\sigma\sqrt{T-t}}$.
Consequently,

$$C(S,t) = S_t e^{-l(z)}\Psi_1(b_1) - Ke^{-r(T-t)}\Psi_2(b_2).$$

Now let $z = m\delta(z = \delta \mid W_{2,t} \mid)$, hence m have the density $h(m) = \frac{2}{\sqrt{2\pi t}}e^{-\frac{m^2}{2t}},\ m \geq 0$. Then

$$C(S,t) = S_t M_1(b_1) - Ke^{-r(T-t)}M_2(b_2). \tag{2.24}$$

This has completed the proof. □

The option pricing formula that we have just derived is of the same form as that of the B-S formula, except $N_1(d_1)$ and $N_2(d_2)$ have been replaced by $M_1(b_1)$ and $M_2(b_2)$, respectively. Thus, the financial interpretations of this new formula is exactly the same as that for the B-S formula, which can be obtained from the derivation of the new formula.

Specifically, $M_2(b_2)$ represents the probability of exercising the option when it expires under the risk-neutral probability measure $\mathbb{Q}$, which can be deduced from the following equation obtained from Equation (2.19):

$$M_2(b_2) = E^Q[I_{(S_T>K)}] = P^Q(S_T > K). \tag{2.25}$$

It may be a little more complicated to interpret $M_1(b_1)$. Actually, we have the following equation which can be easily derived again from Equation (2.19):

$$S_t M_1(b_1) = e^{-r(T-t)} E^Q[S_T \cdot I_{(S_T>K)}]. \tag{2.26}$$

In order to express it clearly, the risk-neutral measure $\mathbb{Q}$ is transformed to $\mathbb{Q}^s$ by

$$\frac{dQ}{dQ^s} = \frac{e^{-rt} S_t}{e^{-rT} S_T}.$$

As a result,

$$\begin{aligned} e^{-r(T-t)} E^Q[S_T \cdot I_{(S_T>K)}] &= S_t E^Q[\frac{e^{-rT} S_T}{e^{-rt} S_t} \cdot I_{(S_T>K)}], \\ &= S_t E^{Q^s}[\frac{e^{-rT} S_T}{e^{-rt} S_t} \cdot I_{(S_T>K)} \cdot \frac{dQ}{dQ^s}], \\ &= S_t E^{Q^s}[I_{(S_T>K)}], \\ &= S_t P^{Q^s}(S_T > K). \end{aligned} \tag{2.27}$$

Combining Equation (2.26) and (2.27) we can obtain

$$M_1(b_1) = P^{Q^s}(S_T > K), \tag{2.28}$$

which implies that $M_1(b_1)$ is the probability of exercising the option at the maturity under the measure $\mathbb{Q}^s$.

On the other hand, the newly derived formula is different from the B-S formula with a newly added parameter δ which represents skewness. When $\delta = 0$, one can easily verify that it does degenerate to the B-S formula as expected. In addition, our pricing formula depends on the initial value of $W_{2,t}$ and it is analogous to the stochastic volatility model where the option price will be dependent on the initial value of the volatility. However, unlike the stochastic volatility model, the newly proposed formula in this paper is really easy to compute since the integrals $M_1(b_1)$ and $M_2(b_2)$ can be numerically evaluated straightforwardly.

The corresponding Greeks Δ_c, Γ_c, R_c, and K_c, where the subscript c denotes the call option, can be easily worked out as those under the B-S model, and we omit the other two Θ_c and Λ_c due to the complicatedness of their expression. Here are the new Greeks

and the details of their derivation are left in the Appendix A:

$$\begin{aligned}
\Delta_c &= \frac{\partial C}{\partial S} = M_1(b_1) > 0, \\
\Gamma_c &= \frac{\partial^2 C}{\partial^2 S} = \frac{e^{-g(m)} L_1(b_1, m)}{S\sigma\sqrt{T-t}} > 0, \\
R_c &= \frac{\partial C}{\partial r} = Ke^{-r(T-t)} M_2(b_2) > 0, \\
K_c &= \frac{\partial C}{\partial K} = -e^{-r(T-t)} M_2(b_2) < 0, \\
\Omega_c &= \frac{\partial C}{\partial \delta} = SI_1 - Ke^{-r(T-t)} I_2 - SI_3,
\end{aligned}$$

where I_i, $i \in 1, 2, 3$ are defined as follows:

$$\begin{aligned}
I_1 = {} & e^{-g(m)} \int_{b_1}^{\infty} \phi(x)\phi(F_1) sgn(\delta) \frac{x + \sqrt{T-t}\sigma + \frac{m\delta}{\sigma\sqrt{T-t}}}{(1-\delta^2)^{1.5}} \\
& + \phi(\frac{\sigma\sqrt{T-t}x + 2m\delta}{\sigma\sqrt{T-t}}) \Phi(F_2) e^{-2m\delta} [-2m - \frac{-2m(\sigma\sqrt{T-t}x + 2m\delta)}{\sigma^2(T-t)}] \\
& + \phi(\frac{\sigma\sqrt{T-t}x + 2m\delta}{\sigma\sqrt{T-t}}) \phi(F_2) e^{-2m\delta} [sgn(\delta) \frac{x + \sigma\sqrt{T-t} + \frac{(3\delta - 2\delta^3)m}{\sigma\sqrt{T-t}}}{(1-\delta^2)^{1.5}}] dx, \\
I_2 = {} & \int_{b_1}^{\infty} \phi(x)\phi(G_1) sgn(\delta) \frac{x + \frac{m\delta}{\sigma\sqrt{T-t}}}{(1-\delta^2)^{1.5}} \\
& + \phi(\frac{\sigma\sqrt{T-t}x + 2m\delta}{\sigma\sqrt{T-t}}) \Phi(G_2) [-\frac{2m(\sigma\sqrt{T-t}x + 2m\delta)}{\sigma^2(T-t)}] \\
& + \phi(\frac{\sigma\sqrt{T-t}x + 2m\delta}{\sigma\sqrt{T-t}}) \phi(G_2) [sgn(\delta) \frac{x + \frac{(3\delta - 2\delta^3)m}{\sigma\sqrt{T-t}}}{(1-\delta^2)^{1.5}}] dx, \\
I_3 = {} & \int_{b_1}^{\infty} \frac{L_1(x, m)}{e^{2g(m)}} [\sigma\sqrt{T-t} sgn(\delta)(\phi(C_1) + e^{-2m\delta}\phi(C_2)) - 2me^{-2m\delta}\Phi(C_2)] dx.
\end{aligned}$$

Here, $F_1, F_2, G_1, G_2, C_1, C_2$ are defined as before.

The financial interpretations of Δ_c, Γ_c, R_c and K_c are similar to those in the B-S model. However, it is hard to decide how the changes of t and σ will affect the price of option due to the complicated formula of Θ_c and Λ_c. Another Greek Ω_c, which is introduced by the skewness parameter δ, will be studied further to see its impact on option pricing in the next Section.

2.4 Numerical examples and discussions

It is interesting to see if the corrected formula would result in some significant differences. In this section, we choose the same benchmark case as that presented in [51] in order to

demonstrate the differences between the two formulae. We also want to explore the rate of change of option price with respect to a change of the skewness parameter, δ, which is a new Greek as a result of introducing the skew feature of the underlying price observed in market data.

2.4.1 Comparison with Corns & Satchell's [51] results

With the same parameters as those used in [51], i.e., $S_t = 100, K = 100, r = 0.1, \sigma^2 = 0.4, t = 0.25, T = 0.5$ and the new time-dependent parameter m is set to be $m = E(\mid W_{2,t} \mid) = \sqrt{\frac{2t}{\pi}}$, the calculated call option prices for different values of δ and S_t are tabulated for comparison purpose in Table 2.1. For the easiness of comparison, the differences between the new results and those presented in [51] are shown by percentage in Table 2.2.

From Table 2.2 we can see that the difference in option prices between the two formulae becomes larger when the absolute value of the skewness parameter, $|\delta|$, is increased, which means the increase in the absolute value of δ enlarges the extent of the difference. This is somewhat expected as large $|\delta|$ implies that the probability density function of the underlying price is more skewed. What was not expected is that the values of the extent of the differences, for example when $|\delta| = 0.75$, could be even more than thirty percent! Such a significant difference suggests that using a wrongly derived pricing formula could lead to more than 30% errors than using the corrected formula. When $\delta = 0$, our results are the same as the original ones, which would happen only in this case, simply because the two pricing formulae will degenerate to B-S formula.

Table 2.1: $C(S_t, t)$ for different values of δ and S_t

S_t	$\delta = -0.75$	$\delta = -0.5$	$\delta = -0.25$	$\delta = 0$	$\delta = 0.25$	$\delta = 0.5$	$\delta = 0.75$
90	7.80	8.08	8.31	8.39	8.31	8.08	7.80
100	12.92	13.32	13.59	13.68	13.59	13.32	12.92
110	19.33	19.81	20.10	20.19	20.10	19.81	19.33

Table 2.2: Differences for different values of δ and S_t by percentage

S_t	$\delta = -0.75$	$\delta = -0.5$	$\delta = -0.25$	$\delta = 0$	$\delta = 0.25$	$\delta = 0.5$	$\delta = 0.75$
90	31.09%	9.04%	1.96%	0	1.71%	7.88%	23.42%
100	16.08%	5.46%	1.19%	0	1.12%	5.05%	14.34%
110	8.29%	3.18%	0.75%	0	0.75%	3.18%	8.66%

2.4.2 Discussion on Greeks

Among all Greeks, Ω_c, which describes the influence of the skewness parameter δ on European call option prices, is the most interesting one since there is no counterpart in the B-S model. In the following study, we only change one parameter at a time in the expression of Ω_c and while holding other parameters the same as those described in the previous sub-section.

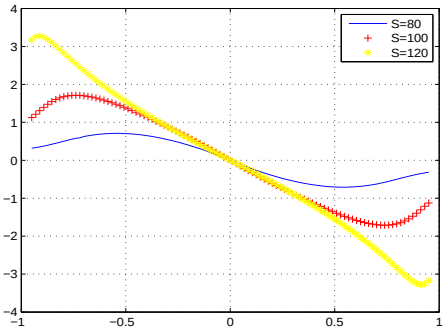

(a) Changes of Ω_c with three different values of S.

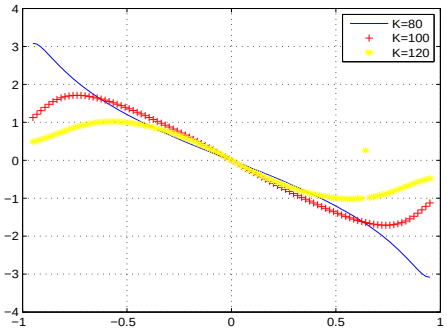

(b) Changes of Ω_c with three different values of K.

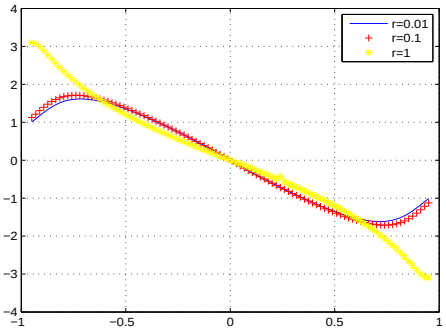

(c) Changes of Ω_c with three different values of r.

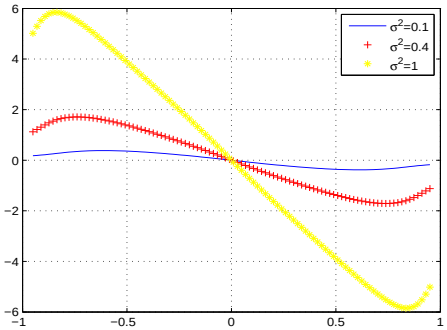

(d) Changes of Ω_c with three different values of σ.

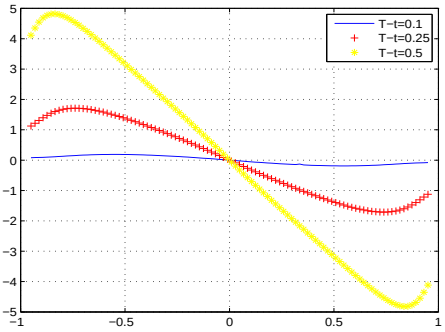

(e) Changes of Ω_c with three different values of $T-t$.

Figure 2.2: Changes of Ω_c according to δ

Depicted in Figure 2.2 are the variations of Ω_c vs. a set of δ values varying between

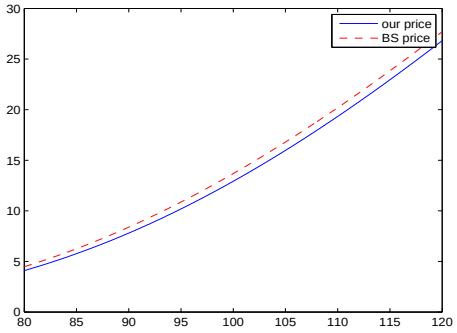

(a) Our price vs B-S price when $S \in (80, 120)$.

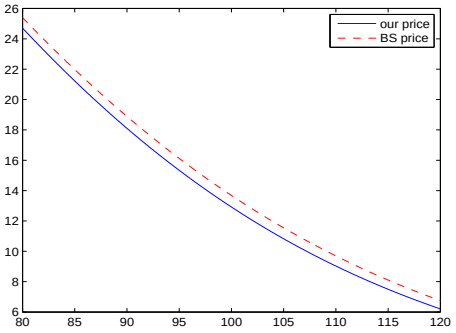

(b) Our price vs B-S price when $K \in (80, 120)$.

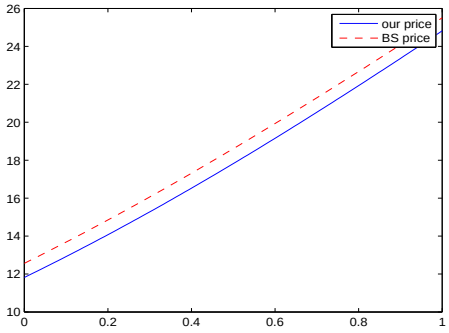

(c) Our price vs B-S price when $r \in (0, 1)$.

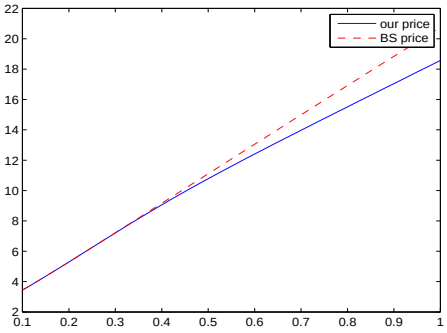

(d) Our price vs B-S price when $\sigma \in (0.1, 1)$.

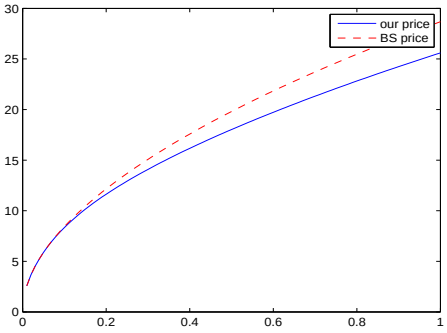

(e) Our price vs B-S price when $T - t \in (0.01, 1)$.

Figure 2.3: Our price vs B-S price for different ranges of different parameters

$-0.95 \leq \delta \leq 0.95$ with three discrete various chosen from each of the remaining 5 parameters to demonstrate the impact of these parameters on Ω_c. It is interesting to observe from Figure 2.2(a) and 2.2(b) that values of $|\Omega_c|$ for options that are clearly "in the money" are obviously larger than those for options that are "out of money" when $|\delta|$ approaches 1, whereas such a sharp contrast is not so clear when δ is close to zero. In other words, this suggests that option price is more sensitive to the skewness of the probability density function of the underlying asset when $|\delta|$ is close to 1 if options are "in the money". On the other hand, the variation of $|\Omega_c|$ taking the risk-free interest rate as a parameter seems to display something quite different. As is shown in Figure 2.2(c), changes of δ have almost the same effect on option prices when the risk-free interest rate r varies below 0.1. Furthermore, the variations of $|\Omega_c|$ taking the volatility and time to expiration as a parameter are shown in Figure 2.2(d) and 2.2(e), respectively. It should be noticed that the larger σ or $T-t$, the more impacts the changing δ will have on the option price in the whole region of $-0.95 \leq \delta \leq 0.95$.

One of the most important features, which is exhibited by all the five figures in Figure 2.2, is that Ω_c tends to be positive when δ is positive and vice versa, which means the option price will increase when the negative δ increases and it will drop when the positive δ increases. So we can conclude that the maximum option price is reached when $\delta = 0$, which is exactly the B-S price.

What is shown in Figure 2.3 is the comparison of the option price obtained from the newly derived formula with the B-S price. It should be noticed that the influence of S, K, r on the option price calculated with our formula is similar to that on the B-S price, which is clearly shown in Figure 2.3(a), 2.3(b) and 2.3(c) respectively while in Figure 2.3(d) and 2.3(e) the difference between our price and B-S price is enlarged when the value of volatility σ or time to expiration $T-t$ increases. Collectively, all the figures in Figure 2.3 confirm that the trend of the option price calculated with our formula is indeed the same as what we have discussed at the end of Section 3. In particular, our prices are lower than the B-S prices, which can be partly explained by the decrease in the variance of stock log-price when the absolute value of δ increases and thus leads to the decrease in option prices.

2.5 Conclusion

In this chapter, a new European call option pricing formula is derived when the dynamics of the underlying is modeled by a special kind of skew Brownian motions, which is introduced to capture the non-normal property of the distribution of log-returns. Upon identifying two errors in a key reference in this area, we introduced a new equivalent martingale measure named "endogenous risk neutral measure", based on which the analytical tractability of the problem is preserved and a new closed-form pricing formula is obtained. Using the newly derived formula, the quantitative impacts of different parameters, especially the skewness parameter δ, on the option price are discussed through numerical experiments. To be more specific, our price tends to decrease when the absolute value of δ increases, which implies that the maximum option price is reached when $\delta = 0$.

Chapter 3

An analytical approximation formula for European option pricing under a new stochastic volatility model with regime-switching

3.1 Introduction

Although the well-known Black-Scholes (B-S) model enjoys great popularity in the area of option pricing due to its simplicity and tractability, a lot of evidence has shown that it is inadequate to precisely model the dynamics of the underlying price. In real markets, the log-returns of the underlying price tend to be skew and fat-tailed [188], and the implied volatility extracted from market data often forms a "smile" curve [73], which is at odds with the constant volatility assumption. Hence, research interest has been led into finding more appropriate models for the underlying price.

In particular, one common modification to the B-S model is to relax the constant volatility assumption. Local volatility and stochastic volatility are two main approaches in the literature. Local volatility was proposed by Dupire [75], who assumed the volatility be a deterministic function of the underlying price and time. However, stochastic volatility

models are much more favored since the "smile dynamics" are poorly captured by local volatility models [102].

A number of authors has worked on stochastic volatility models. The addition of another stochastic source has made the option pricing problem much more complicated, and in most cases only numerical methods could be used to find the European option prices (e.g., [204],[224]). Moreover, although Hull & White [127] were able to derive a semi-closed form pricing formula under their model, their assumption that the volatility be independent of the underlying price is inappropriate since many empirical studies have shown that the volatility and the underlying price are negatively related [11]. A similar case is the Stein-Stein model [213], where a closed-form formula for European options exists. However, their volatility dynamic is again inconsistent with the fact that the volatility should always be positive. Fortunately, the famous Heston model [117] was proposed in 1993, the volatility dynamic of which satisfies a wide range of properties, such as the non-negative property and mean-reverting property, and most importantly, a closed-form pricing formula could be worked out for European options. However, it should also be pointed out that the Heston model is not perfect either since there already exists empirical evidence showing that the mean-reverting property for a volatility process is actually not linear [12].

In this chapter, we propose a new stochastic volatility model, where the volatility of volatility in the Heston model follows a Markov chain so that it could jump between two states. Our motivation stems from the fact that the Heston model with constant parameters may not provide good fit to market data, and the time-dependent Heston model has already been studied by Buhler [27], Mikhailov & Nogel [180] and so on. Moreover, the stochastic volatility of volatility has been considered in modeling the VIX dynamics [150], while variance and volatility swaps are priced under the regime-switching Heston model with the long-term mean following a Markov chain in [81]. In fact, quite a lot of empirical evidence already suggests that there are certain advantages to incorporate regime-switching into the volatility process. For example, Kalimipalli & Susmel [151] adopted a regime-switching stochastic volatility model to describe the short-term interest rate and they found that it can lead to a better in-sample performance than the classical stochastic volatility model, while results in [132] show that squared returns are better specified by regime-switching stochastic volatility models. Also, it has already been shown by So et

al. [212] that persistence in volatility can be explained by a regime-switching stochastic volatility model. In addition, Vo [219] found strong evidence of regime-switching in real markets, and he even pointed out that introducing regime-switching into the framework of stochastic volatility can bring two main advantages; one is that it can significantly enhance the forecasting power of the stochastic volatility model, and another is that the regime-switching stochastic volatility model does a better job in capturing major events affecting the market. Therefore, considering the fact that the Heston stochastic volatility model is a widely adopted model in real markets, it is natural for us to consider an introduction of regime-switching into this particular model, with the volatility of volatility in the Heston model being made regime-switching. Of course, since a great feature of the Heston model is the existence of a simple and analytical pricing formula for European options, the challenge we face is how to keep the tractability of the new model, which is more complicated than the Heston model. In this chapter, we present one way to preserve the tractability by deriving an approximation formula for European option prices at the expense of imposing a restriction that the formula is only suitable for short-tenor European options. In the following, this analytical approximation formula will be derived based on the perturbation method, which has been widely adopted in solving option pricing problems [123, 223, 234]. It should be noticed that our pricing formula is rather simple with only normal distribution function involved and is suitable for options with short tenors, which are dominated in real markets anyway. Finally, to show the performance of our model in real markets, empirical studies are carried out to compare our model and the Heston model with S&P 500 returns and short-tenor options. Results confirm that our model generally outperforms the Heston model, and thus it could be used as an alternative to the Heston model for some markets.

The rest of the chapter is organized as follows. In Section 3.2, we will first briefly introduce our new stochastic volatility model and present the coupled PDE (partial differential equation) system for European options, after which the perturbation method is applied to find pricing formula for options with short tenors. In Section 3.3, numerical experiments are carried out to show the accuracy of the approximation involved in our newly derived formula. In Section 3.4, empirical studies are carried out to show the performance of our newly proposed model, followed by some concluding remarks given in the last section.

3.2 European options with short tenors

In this section, the dynamics of the regime-switching Heston model are presented and the coupled PDE system governing the European put option prices is given, followed by the approximation formula obtained through the perturbation method.

Let S and v be the underlying price and the volatility respectively, the regime-switching Heston model under the risk-neutral measure is specified as

$$\begin{aligned} \frac{dS}{S} &= rdt + \sqrt{v_t}dW_t^1, \\ dv_t &= k(\theta - v_t)dt + \sigma_{X_t}\sqrt{v_t}dW_t^2, \end{aligned} \tag{3.1}$$

where W_t^1 and W_t^2 are two standard Brownian motions with correlation ρ. r is the risk-neutral interest rate. k and θ are the mean-reverting speed and level respectively. σ_{X_t} is the volatility of volatility controlled by the Markov chain X_t, which is independent of W_t^1 and W_t^2. In particular, X_t is defined as

$$X_t = \begin{cases} 1, & \text{when the economy is believed to be in State 1,} \\ 2, & \text{when the economy is believed to be in State 2,} \end{cases}$$

with the transition between the two states following a Poisson process as

$$P(t_{ij} > t) = e^{-\lambda_{ij}t}, i, j = 1, 2,\ i \neq j.$$

Here λ_{ij} is the transition rate from State i to j, and t_{ij} is the time spent in State i before transferring to State j. Apparently, when the two transition rates λ_{12} and λ_{21} take the value of zero, our model would surely degenerate to the Heston model.

Following [83], the state space of X_t could be taken to be the set of unit vectors $\{e_1, e_2\}$, with $e_1 = (1, 0)'$ and $e_2 = (0, 1)'$. Here, v' denotes the transpose of the vector v. Then, if we let the European put option price vector be denoted by

$$\widetilde{U}(S, v, t) = (U(S, v, t, e_1), U(S, v, t, e_2))',$$

it is not difficult to find that $U(S, v, t, X_t) =< \widetilde{U}(S, v, t), X_t >$, where $< \cdot, \cdot >$ denotes the

inner product of two vectors, which could certainly yield

$$dU =< d\widetilde{U}, X_t > + < \widetilde{U}, dX_t > .$$

By applying the Itô lemma to U, the following equation can be obtained

$$\begin{aligned} dU &= \frac{\partial U}{\partial t}dt + \frac{\partial U}{\partial v}dv + \frac{\partial U}{\partial S}dS + \frac{1}{2}\frac{\partial^2 U}{\partial S^2}(dS)^2 + \frac{1}{2}\frac{\partial^2 U}{\partial v^2}(dv)^2 \\ &+ \frac{\partial^2 U}{\partial S \partial v}dSdv + < \widetilde{U}, dX_t > . \end{aligned} \tag{3.2}$$

Considering the fact that the discounted option price $e^{-rt}U$ should be a martingale, the coupled PDE system can be derived as

$$\begin{aligned} \frac{\partial U_1}{\partial t} &+ \frac{1}{2}vS^2\frac{\partial^2 U_1}{\partial S^2} + rS\frac{\partial U_1}{\partial S} - rU_1 \\ &+ \frac{1}{2}\sigma_1^2 v\frac{\partial^2 U_1}{\partial v^2} + \sigma_1 v\rho S\frac{\partial^2 U_1}{\partial S \partial v} + k(\theta - v)\frac{\partial U_1}{\partial v} - \lambda_{12}(U_1 - U_2) = 0, \end{aligned} \tag{3.3}$$

and

$$\begin{aligned} \frac{\partial U_2}{\partial t} &+ \frac{1}{2}vS^2\frac{\partial^2 U_2}{\partial S^2} + rS\frac{\partial U_2}{\partial S} - rU_2 \\ &+ \frac{1}{2}\sigma_2^2 v\frac{\partial^2 U_2}{\partial v^2} + \sigma_2 v\rho S\frac{\partial^2 U_2}{\partial S \partial v} + k(\theta - v)\frac{\partial U_2}{\partial v} - \lambda_{21}(U_2 - U_1) = 0, \end{aligned} \tag{3.4}$$

where $U_1 = U(S, v, t, e_1), U_2 = U(S, v, t, e_2)$. The terminal condition for a put option[1] is

$$U_i(S, v, T) = \max(K - S, 0),$$

and the boundary conditions are

$$\begin{aligned} &\lim_{S\to 0} U_i(S, v, T) = Ke^{-r(T-t)}, \\ &\lim_{S\to +\infty} U_i(S, v, T) = 0, \\ &\lim_{v\to 0} U_i(S, v, T) = \max(Ke^{-r(T-t)} - S, 0), \\ &\lim_{v\to +\infty} \frac{\partial U_i(S, v, T)}{\partial v} = 0, \end{aligned}$$

for $i = 1, 2$. The boundary conditions along the v direction are discussed in [235].

[1] It suffices to derive a pricing formula for European put options. As for the call, we can just use the put-call parity to derive the formula.

To solve the above PDE system with the perturbation method, a small parameter should be introduced. As most of the options traded in real markets are short-tenor, it is reasonable to assume that the time to maturity is small. As a result, we let $\tau = T - t$, and assume $\tau = \epsilon T$, where ϵ is a small parameter. Moreover, following Zhu & Chen [234], we also introduce a scaled parameter $x = \dfrac{S-K}{\sqrt{\epsilon}K}$, so that the PDE system (3.3)-(3.4) could be converted into

$$\begin{aligned}\frac{\partial U_1}{\partial T} &= \frac{1}{2}v(\sqrt{\epsilon}x+1)^2\frac{\partial^2 U_1}{\partial x^2} + r(\sqrt{\epsilon}x+1)\sqrt{\epsilon}\frac{\partial U_1}{\partial x} + \sigma_1\rho v(\sqrt{\epsilon}x+1)\sqrt{\epsilon}\frac{\partial^2 U_1}{\partial x \partial v} \\ &+ \frac{1}{2}\sigma_1^2 v\epsilon\frac{\partial^2 U_1}{\partial v^2} + k(\theta - v)\epsilon\frac{\partial U_1}{\partial v} - r\epsilon U_1 - \lambda_{12}\epsilon(U_1 - U_2), \end{aligned} \tag{3.5}$$

and

$$\begin{aligned}\frac{\partial U_2}{\partial T} &= \frac{1}{2}v(\sqrt{\epsilon}x+1)^2\frac{\partial^2 U_2}{\partial x^2} + r(\sqrt{\epsilon}x+1)\sqrt{\epsilon}\frac{\partial U_2}{\partial x} + \sigma_2\rho v(\sqrt{\epsilon}x+1)\sqrt{\epsilon}\frac{\partial^2 U_2}{\partial x \partial v} \\ &+ \frac{1}{2}\sigma_2^2 v\epsilon\frac{\partial^2 U_2}{\partial v^2} + k(\theta - v)\epsilon\frac{\partial U_2}{\partial v} - r\epsilon U_2 - \lambda_{21}\epsilon(U_2 - U_1). \end{aligned} \tag{3.6}$$

In order to eliminate the factor $\sqrt{\epsilon}K$ in the initial condition, we set

$$P_i(x, v, T) = U_i(x, v, T)/(\sqrt{\epsilon}K),\ i = 1, 2,$$

and expand P_i in terms of $\sqrt{\epsilon}$ as

$$P_i = P_i^0 + \sqrt{\epsilon}P_i^1 + O(\epsilon),\ i = 1, 2. \tag{3.7}$$

By substituting Equation (3.7) into the system (3.5)-(3.6) and eliminate the $O(1)$ term, we can obtain

$$\begin{aligned}&\frac{\partial P_i^0}{\partial T} = \frac{1}{2}v\frac{\partial^2 P_i^0}{\partial x^2}, \\ &P_i^0(x, v, 0) = \max(-x, 0), \end{aligned} \tag{3.8}$$

for $i = 1, 2$. It should be noted that v can be regarded as a fixed constant when solving the newly obtained PDEs (3.8) since it does not involve the partial differential derivative with respect to v in the differential operator. As a result, it is clear that both of the newly obtained PDEs are homogeneous heat equation defined along the real axes, which can be

solved with the fundamental solution as

$$\begin{aligned} P_i^0 &= \frac{1}{\sqrt{2v\pi T}}\int_{-\infty}^{+\infty} e^{-\frac{(x-\xi)^2}{2vT}}d\xi, \\ &= \sqrt{\frac{vT}{2\pi}}e^{-\frac{x^2}{2vT}} - x[1-N(\frac{x}{\sqrt{vT}})]. \end{aligned}$$

In a similar fashion, we could obtain the PDE for $P_i^1, i = 1, 2$ by collecting the coefficients of $\sqrt{\epsilon}$ together, which is

$$\begin{aligned} &\frac{\partial P_i^1}{\partial T} = \frac{1}{2}v\frac{\partial^2 P_i^1}{\partial x^2} + xv\frac{\partial^2 P_i^0}{\partial x^2} + r\frac{\partial P_i^0}{\partial x} + \rho\sigma_i v\frac{\partial^2 P_i^0}{\partial x \partial v}, \\ &P_i^1(x, v, 0) = 0, \end{aligned} \tag{3.9}$$

for $i = 1, 2$. It should be noticed that PDE (3.9) is an inhomogeneous heat equation with homogeneous initial condition, which can be solved with green function. However, the calculation is rather complicated and thus alternative ways attempted. Luckily, one way would lead to much simpler formula, which is illustrated in the following. According to the results in [123], if $C_t - \frac{1}{2}C_{xx} = 0$, and $D_t - \frac{1}{2}D_{xx} = vC$, then a particular solution is $D = Cvt$. In addition, if $C_t - \frac{1}{2}C_{xx} = 0$ and $D_t - \frac{1}{2}D_{xx} = xvC$, then a particular solution is $D = xvtC + \frac{1}{2}(vt)^2 C_x$. As a result, considering the situation that $\frac{\partial P_i^0}{\partial x}$, $\frac{\partial^2 P_i^0}{\partial x^2}$ and $\frac{\partial^2 P_i^0}{\partial x \partial v}$ also satisfy the equation $C_t - \frac{1}{2}C_{xx} = 0$, a particular solution for P_i^1 could be obtained as

$$\begin{aligned} P_i^1 &= [\frac{r}{v}\frac{\partial P_i^0}{\partial x} + \rho\sigma_i\frac{\partial^2 P_i^0}{\partial x \partial v}]vT + \frac{\partial^2 P_i^0}{\partial x^2}xvT + \frac{1}{2}(vT)^2\frac{\partial^3 P_i^0}{\partial x^3}, \\ &= -rT[1-N(\frac{x}{\sqrt{vT}})] - \frac{\rho\sigma_1 vTx}{2\sqrt{2\pi vT}}e^{-\frac{x^2}{2vT}} + \frac{xvT}{2\sqrt{2\pi vT}}e^{-\frac{x^2}{2vT}}, \end{aligned} \tag{3.10}$$

for $i = 1, 2$. Therefore, after some algebraic manipulation, we can arrive at the final result written in the original parameters

$$\begin{aligned} U_i(S, v, \tau) &= \sqrt{\epsilon}KP_i = \sqrt{\epsilon}K[P_i^0 + \sqrt{\epsilon}P_i^1 + O(\epsilon)], \\ &= [\frac{\sqrt{v\tau}}{2\sqrt{2\pi}}(S+K) - \frac{\rho\sigma_i\sqrt{v\tau}}{2\sqrt{2\pi}}(S-K)]e^{-\frac{(S-K)^2}{2v\tau K^2}} \\ &- [S + (r\tau - 1)K][1 - N(\frac{S-K}{\sqrt{v\tau}K})] + O(\tau), \quad i = 1, 2. \end{aligned} \tag{3.11}$$

Obviously, the newly obtained formula is rather simple, which only involves the calculation of the normal distribution function, and thus the implementation of this formula

can be as easy as the B-S formula. This is a great advantage as the simplicity of a pricing formula presents enormous benefits in terms of model calibration as well as in line with the increasing demand of super fast computation of option price as a result of recent trend of algorithm trading. It should be pointed out that the mean-reversion speed k and the long-term mean θ of the volatility do not explicitly appear in the final approximation formula for short-tenor options, which implies that the two parameters have little influence on option prices with short time to expiry. This is also the main reason why we make k and θ the same for both regimes. It should also be noted that the small parameter ϵ does not explicitly appear in the final approximation formula, as it is a parameter determined by the tenor of a contract and used to judge the validity of the approximation. Therefore, all we need is to ensure that the time to expiry of a contact to be priced is small enough so that $\epsilon \ll 1$. Another point that should be emphasized is that although the techniques we employ in the regular perturbation are straightforward, proposing a new solution technique is not what we were trying to achieve in this chapter; proposing a new model by introducing regime-switching into the Heston model that can provide a better empirical performance than the classical Heston model is.

Once an approximation formula for short-tenor options is obtained, it is natural for us to numerically check its accuracy, which would be presented in the next section.

3.3 Numerical verification

In this section, numerical experiments are conducted to show the performance of Formula (3.11) when the time to expiry varies. The accuracy is demonstrated through a comparison of the option prices calculated with the newly derived formula and those obtained by Monte Carlo simulation of SDE (3.1). In the following, the current state is assumed to be 1, and the strike price of the option K is 10. The volatility of volatility for state 1 and 2, σ_1 and σ_2, takes the value of 0.3 and 0.6 respectively. The two transition rates λ_{12} and λ_{21} are 40 and 60, respectively. The mean reverting speed k is 2.5, the long-term mean θ is 0.16, and the initial value of the volatility v_0 is 0.2. The correlation between the underlying price and the volatility ρ is -0.5.

Depicted in Figure 3.1 are the option prices for different underlying prices when time to expiry is one month, and it is clear that the results obtained from our approximation

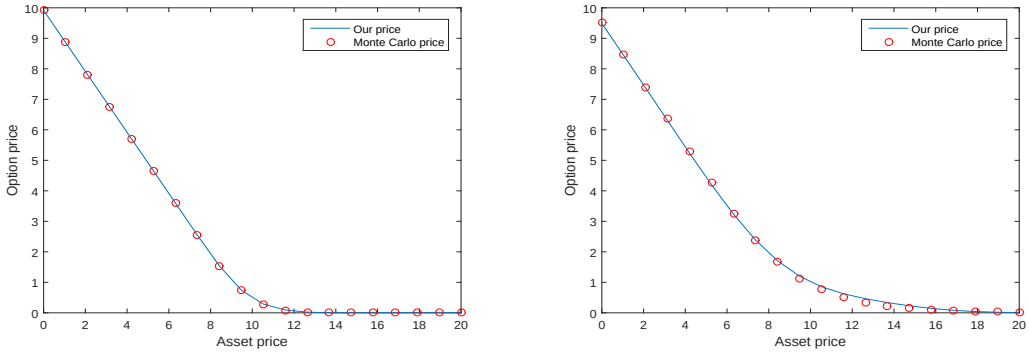

(a) $\tau = 1/12, r = 0.1$. (b) $\tau = 1/2, r = 0.1$.

Figure 3.1: Our price vs Monte Carlo price with different underlying prices.

agrees very well with the Monte Carlo prices. Specifically, the point-wise absolute error in Figure 3.1(a) less than 0.01, which demonstrates that our approximation is very accurate when the time to expiry is relatively short. On the other hand, When the time to expiry increases to six months, our approximation is still quite close to the Monte Carlo price as shown in Figure 3.1(b), though the performance of our approximation this time is clearly worse than the case when the time to expiry is short. This is expected since the approximation is made based on the assumption of small time to maturity. It is also interesting to notice that our approximation performs slightly better for in the money option than the out of money option.

With the confidence of our pricing formula for short-tenor options, empirical studies are carried out with the time to expiry of the chosen options being less than one month to make the comparison of our model and the well-known Heston model, which is a widely adopted stochastic volatility model in real markets, with the results presented in the next section.

3.4 Empirical studies

In this section, empirical results are presented and discussed with the Heston model being taken as a benchmark to assess the performance of our model in real markets. In the following, we will firstly describe the data we use and introduce the method adopted for parameter estimation. Then, the performance of these two models is quantitatively compared by the pricing errors measured with the "distance" between model-produced and market prices, and it is widely accepted that a model is regarded as the better one

if it exhibits less pricing errors. In fact, pricing errors usually consist of two parts: the so-called in-sample errors and out-of-sample errors. Conventionally, the period in which market data is available is divided into two; the first one refers to a period in which data is used for parameter determination (referred to as the "in-sample observations") and the second one then refers to the period in which data is used to verify the performance of a model through a comparison between the observed option prices and the calculated option prices based on the parameters determined from the "in-sample" period (in contrast to the first period, data in the second period is usually referred to as the "out-of-sample observations"). It should be remarked that it is usually difficult to achieve lower in- and out-of-sample errors simultaneously. When comparing two models through a comparison of the in- and out-of-sample errors, it is hard to draw a conclusion if only one part of errors is less than the other. However, there should be no doubt in one's mind which model is superior if both of its in- and out-of-sample fitness are better. This is the principle based on which we draw the conclusions of our empirical studies in the subsection 7.4.3.

3.4.1 Data description

Our empirical study is conducted on a data set of the S&P 500 Index and European call options written on the S&P 500 Index from Jan 2011 to Jun 2011[2]. However, raw data should not be adopted directly in the estimation since sample noise needs to be eliminated. Hence, two appropriate filters presented below were applied to the raw data, before they were used to estimate model parameters.

First of all, following a number of authors, such as Bakshi et. al [11] and Christoffersen et. al [41], only Wednesday and Thursday options data is adopted. In particular, Wednesday options data is used in estimation since Wednesday is least likely to be a holiday in a week and also less likely to be affected by the "day-of-the-week" effect than other days such as Monday and Friday, whereas the corresponding Thursday data serves as the market price to be compared with the predicted price calculated by the estimated parameters. Another motivation for only using Wednesday data in parameter estimation is that global optimization problems are usually quite time-consuming and choosing one day a week allows us to study a relatively longer time series yielding more reliable results. Secondly, very deep in-the-money and very deep out-of-money options are discarded due

[2]Since our formula could provide satisfactory accuracy for short-tenor options, all options used are to expire within one month.

to their inactivity in the market and may also have liquidity-related biases [209]. Specifically, options with the absolute moneyness, defined as the relative difference between the S&P 500 Index value and the corresponding strike price ($Moneyness = \frac{S-K}{K}$) over 10% are excluded.

It should be noted that after these filters are applied, more efficiency can be achieved in the process of parameter estimation with all the important information still preserved according to various previously conducted empirical studies in the literature [11, 41].

As for the risk-free interest rate, we choose the one-month U.S. Treasury Bill Rate, which is released daily, as a proxy of the risk-free rate [17, 209] since the time to expiry of the selected options is less than 30 days. Upon the preparation of all the data described above, parameter estimation was conducted, following a simple flow chart (cf. Figure 3.2) exhibiting the specific steps in our empirical studies. Clearly, adopting a genetic algorithm as the main tool of optimization forms the core of the determination of model parameters, the details of which are described in the next subsection.

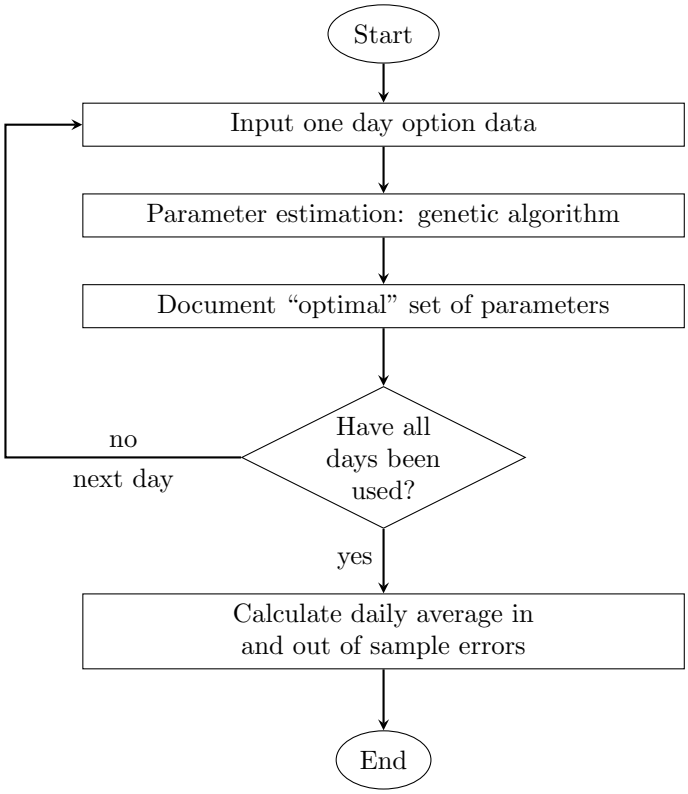

Figure 3.2: Flow chart on how our empirical studies are conducted.

3.4.2 Parameter estimation

In this section, we first provide a brief summary of the model parameters that need to be determined in both models and then introduce a genetic algorithm used to determine model parameters.

Recall that the Heston model is specified as

$$\begin{aligned} \frac{dS}{S} &= rdt + \sqrt{v}dW_t, \\ dv &= k(\theta - v)dt + \sigma\sqrt{v}dB_t, \end{aligned} \tag{3.12}$$

where the following five parameters, i.e. the mean-reversion speed k, the long-term mean θ, the volatility of volatility σ, correlation ρ between W_t and B_t and the initial value of volatility v_0, need to be determined from real market data, before the Heston pricing formula could be used to calculate the "fair" price of an option.

On the other hand, it should be pointed out that it is usually very difficult to determine which state the current underlying price belongs to in real markets. Thus, following [115], it is more reasonable to assume that the state is unobservable and regard the probability of each state at the point when the option contact needs to be priced as another parameter that needs to be estimated under a risk-neutral measure. To be more specific, if we let π denote the probability of the underlying price belonging to State 1, it is not difficult to find that the option price U^{model} under our newly proposed model should be calculated as

$$U^{model}(S, v, \tau) = \pi * U_1(S, v, \tau) + (1 - \pi) * U_2(S, v, \tau). \tag{3.13}$$

It should be pointed that there are actually five parameters which need to be estimated, i.e., the probability π and the four parameters, $\rho, \sigma_1, \sigma_2, v_0$, in the expression of U_1 and U_2. In other words, the size of parameter space remains the same as that of the Heston model. Specifically, the mean-reversion speed k and the long-term mean θ in the Heston model have disappeared in the new formula as a result of the restriction we imposed for pricing short-tenor contacts only, while the probability π and the two parameters representing the volatility of volatility in both regimes, σ_1 and σ_2, now appear in the new formula to capture the regime-switching dynamics. Coincidentally, the fact that the size of the parameter space of the new pricing formula is the same as that of the Heston model gives

an additional benefit that there is no extra burden when calibrating our model compared with the classical Heston model, as long as the new formula is only used for short-tenor contracts, which are the most popular cases in financial markets anyway. It should also be stressed that when using the pricing formula (3.13), the parameter estimation process for our model is similar to that for the classical Heston model, and there is no need to conduct separate estimation for the probability π and the two values for the volatility of volatility in the two regimes, σ_1 and σ_2. This is because the three parameters can be simultaneously obtained with other model parameters with optimization algorithms, which will be illustrated in the following.

Now we have figured out all the parameters that need to be determined, it is time to find an appropriate approach. A common one is to find the set of "optimal" parameters that minimizes the "distance" between market and model prices. Actually, there are different kinds of definition for the distance, a common one is to take the percentage mean squared error (PMSE)

$$PMSE = \frac{1}{N}\sum_{i=1}^{N}[\frac{U^{Market} - U^{Model}}{U^{Model}}]^2,$$

as the objective distance function to measure the relative difference between market and model prices. Here U^{Market} denotes the market price of an option contract from one sample, U^{Model} represents the corresponding calculated price with our pricing formula with a particular set of parameters and N is the total number of observations selected in a single estimation. However, the main disadvantage in choosing such an objective function is that a cheap option (i.e., low U^{Market}) could place an abnormally high amount of weight in PMSE. Therefore, following Christoffersen & Jacobs [39] and Lim & Zhi [169], we instead chose the dollar mean-squared errors

$$MSE = \frac{1}{N}\sum_{i=1}^{N}[U^{Market} - U^{Model}]^2, \tag{3.14}$$

as the objective function. In this case, with a given set of data, what we need to do is to use particular techniques to search the parameter space to find a set of parameters that can minimize the MSE between the model price and the market price.

Another issue is how to choose an appropriate optimization method. It should be noticed that although local minimization, which requires an initial guess that is very close

to the true optimal solution, can be much less time consuming, its results are usually not reliable since it depends too much on the selected initial guess. In fact, the objective function (3.14) is not necessarily convex and thus there could exist several local minima, which would probably result in a local minimum being taken as the global minimum. In contrast, a properly designed global optimization should be able to skip local minima and correctly identify the global minimum in an efficient way.

A genetic algorithm [46] is such a global optimization with some very nice properties. It is based on the idea of natural selection, introducing stochastic factors when searching for a satisfactory result in order to skip over local optima. One of the most important reasons for us to adopt this particular algorithm is that it randomly selects a number of different initial guesses to explore the entire solution space. Moreover, a so-called "mutation" step in the optimization process allows the algorithm to avoid local minima by preventing parameters from being restricted to a small region. In the literature, genetic algorithms have been applied in finance by quite a few researchers already. For instance, Gimeno & Nave [97] conducted estimation of the term structure of interest rates with a genetic algorithm while Grace [99], Cont & Ben Hamida [47] and He & Zhu [113] have adopted it in the area of option pricing. It is even pointed out by Bajpai & Kumar [10] that genetic algorithms are one of the best global optimization methods and can provide high quality solutions since they are intrinsically parallel and can explore the solution space in multiple directions at the same time.

It should be remarked that another advantage of adopting a genetic algorithm is its implementation in the Matlab is straightforward by using a built-in function *ga*. As a result of the numerical implementation, Table 3.1 exhibits the estimated daily averaged parameters extracted from the selected market data for the two models under consideration in this chapter, respectively.

Table 3.1: Estimated parameters

parameters	ρ	v_0	σ_1	σ_2	π	σ	k	θ
Our model	-0.2398	0.0218	2.0568	1.8818	0.5049			
Heston model	-0.7921	0.0666				1.7665	293.4422	0.0542

3.4.3 Empirical comparison

In this subsection, the performance of our model and the Heston model in real markets is compared using the extracted parameters. In terms of model performances, it is widely accepted that a model is regarded better if there exist less accumulated pricing errors calculated by the distance between model prices and market prices. Here, we adopt the root mean-squared error (RMSE), which is the square root of the objective function (MSE), as a measure of "goodness of fit". Table 3.2 exhibits the in- and out-of-sample errors for the two models.

Table 3.2: In- and out-of-sample errors for the two models

Error	In-sample	out-of-sample
Our model	0.5198	0.9221
Heston model	0.7753	1.3911
Relative difference	32.95%	33.71%

It is obvious from Table 3.2 that our model generally outperforms the Heston model in terms of both in- and out-of-sample errors. To be more specific, from the perspective of in-sample errors, the daily averaged RMSE for our model is only 0.5198, compared with 0.7753 for the Heston model. It is clear that our model is superior to the Heston model in this case since the relative difference[3] between the two models, as far as the daily averaged RMSE is concerned, is over 32%, which is surprisingly quite significant. On the other hand, when out-of-sample errors are taken into consideration, a similar pattern emerges; our model still shows a much better performance than that of the Heston model, and the relative difference between them is even a bit higher at 33.71%. Therefore, combining both in-sample and out-of-sample observations, we can conclude that our model serves as a better choice than the Heston model for the data set chosen in this comparison. One of the main reasons for such a significant improvement is that the chosen market does possess different regimes. Naturally it is expected that the market dynamics are better captured by a regime-switching stochastic volatility model.

It is also interesting to notice that the RMSE for out-of-sample errors is always much larger than that for in-sample errors. This is not difficult to understand since model prices are calculated with determined parameters. Those obtained with in-sample data

[3]The relative difference is defined as

$$\text{Relative difference} = \frac{|\text{Our model error} - \text{Heston model error}|}{\text{Heston model error}}.$$

are believed to be "closest" to market prices of the corresponding option contracts, which implies that in-sample errors should be relatively low, while out-of-sample data is only used as the verification of option prices and certainly there is no guarantee that out-of-sample errors be low.

On the other hand, options are traded with a wide range of strikes in real markets and thus it is important to check the out-of-sample valuation errors sorted by moneyness, which are shown in Table 3.3. While the range of moneyness is indicated on the top row of the table, the abbreviation in the parentheses indicate "out of money" "at the money" and "in the money", respectively, from the left to the right columns.

Table 3.3: Out-of-sample errors according to moneyness

Moneyness	$0.90 < S/K < 0.97(O)$	$0.97 \leq S/K \leq 1.03(A)$	$1.03 < S/K < 1.10(I)$
Our model	0.4266	1.1560	0.8171
Heston model	0.9546	1.5983	1.3162
Relative difference	55.31%	27.67%	37.93%

From this table, it is clear that the performance of our model is better than that of the Heston model in all of the three categories. Although the improvement for at-the-money options is lowest, the daily averaged pricing error for our model is around 27% less than that of the Heston model, which is quite significant. The maximal improvement occurs for the category of out-of-money options, where the relative difference even reaches over 50%. Thereby, we can confidently conclude that our model has given an overall better performance than that of the Heston model. Of course, this conclusion is based on the empirical test of one set of data. It is quite possible that the performance of these two models may reverse with some other data sets. However, our empirical study presented here can at least suggest it may offer as a good competitor of the Heston model for short-tenor options in some other markets, such as commodity and futures exchange markets.

3.5 Conclusion

In this chapter, an approximation pricing formula for European options under a newly-proposed stochastic volatility model is presented. The main contributions of our contribution can be summarized into three items: (i) A new stochastic volatility model is proposed with a key feature that the constant volatility of volatility in the original Heston model is now allowed to change randomly following a Markov chain. (ii) An analytical

pricing formula for short-tenor European options has been worked out with a key feature that the newly-obtained formula is fast and easy to implement with only normal distribution function involved. (iii) Not only have we tested the reliability and accuracy of the newly-obtained formula, we have also implemented it in an empirical experiment with real market data to demonstrate the superiority of the new model over the classical Heston model; empirical results based on S&P 500 returns and options demonstrate that our model significantly outperforms the Heston model for the case tested, and our empirical study suggests that the new model has a great potential to be used as an alternative to the Heston model for short-tenor options.

Chapter 4

A modified Black-Scholes pricing formula for European options with bounded underlying prices

4.1 Introduction

Financial derivatives have become increasingly popular among investors as well as academic researchers recently. Among these, options are one kind of the most basic and important instruments and thus option valuation receives high attention. An option is a right, not an obligation, to buy or sell the certain amount of a specified asset with the strike price according to the option contract. There are mainly four kinds of options traded in the open exchanges market, including European options, American options, Asian options and barrier options. In this chapter, we will focus on the pricing of European options, which are the most fundamental ones.

Although Black & Scholes [19] proposed the celebrated Black-Scholes (B-S) formula for pricing European options, which is still widely used in financial markets today, some fundamental assumptions made in the B-S model in order to achieve a simple and closed-form pricing formula have actually attracted critics; more and more revised B-S models and/or "modified" pricing formulae are proposed as a result. For example, the assumption of the constant volatility in the B-S model has been shown to be at odds with the so-called "volatility smile" [73] exhibited by the implied volatility of option prices. Moreover, observed returns of the underlying from financial markets are actually not normally

distributed and they are usually skewed [188] and fat-tailed [191]. As a result, quite a few approaches have been proposed to modify the B-S model in order to obtain more "accurate" option prices.

In the literature, there are mainly two kinds of modifications as far as option pricing is concerned, i.e. the so-called structural models and non-structural models. To be more specific, the former provide the dynamics of the underlying price at every moment for a given period of time horizon. Apparently, the B-S model belongs to this category. There are also other models of this type. For example, stochastic volatility is adopted by Scott [204], Wiggins [224], Heston [117] and many other authors in order to alleviate the well-known "volatility smile". Another common modification using structural models is to add components to the geometric Brownian motion or even replace the Brownian motion with other stochastic processes. For instance, jump-diffusion models [158, 178] add a jump term to the standard Brownian motion to reflect that the underlying price is discontinuous in real markets. Moreover, the Variance-Gamma and the CGMY model were proposed by Madan [173] and Carr et al. [29] respectively to capture various characteristics shown by real market data.

On the other hand, non-structural models only specify the probability density function of the underlying at maturity conditional upon the filtration at the current time without completely describing the fine details of the stochastic process themselves at each moment. With more flexible distributions, different characteristics of the asset returns and the volatility term structure that the B-S model failed to describe properly can be captured. In particular, generalized beta distribution of the second kind was used by Bookstaber & McDonald [174] while Burr-3 distribution was adopted by Sherrick et al. [207]. Other examples include Weibull distribution used by Savickas [197], g-and-h distribution studied by Dutta & Babbel [76] and generalized gamma distribution adopted by Fabozzi [87]. In addition, a density expansion approach was firstly developed by Jarrow and Rudd [143], who proposed an integrated Edgeworth series expansion of a log-normal density in pricing theory. After that, Madan & Milne [172] gave an expansion to approximate a risk-neutral density function while Corrado & Su [53] adopted the integrated Gram-Charlier series expansion of a normal density function.

Unfortunately, all the pricing models in the existing literature, including the structural and non-structural ones, assume that the underlying price is unbounded above, i.e., the

price range from zero to infinity. Although this assumption contains a clear "pitfall" as there is no way that any underlying price could reach infinity in reality, it is nevertheless a nice and elegant mathematical compromise to ensure the tractability. A "modification" to the B-S formula to take into account that option traders often have their own expected (finite) range of the underlying price in mind appears to be a very reasonable and attractive idea.

In this chapter, such a modification is presented, with a non-structural model being adopted under the assumption that the log-returns of the underlying asset follow a truncated normal distribution during a certain period with a finite upper and lower bound.

One question that could be raised is that unlike the use of the B-S formula, in which both the writer and buyer of an option know that the underlying has been assumed to vary, albeit unreasonable, from zero to infinity, traders using our newly derived formula would not know if the opposite side of the option has taken the same view in terms of these upper and lower bounds of the underlying. But, this is not a good reason to devalue our modified formula. Even if both sides agree to adopt the original B-S formula, their views on many market factors, such as the trend of the underlying would be different anyway; otherwise there would be no "deal". In fact, we believe that our formula could be at least used as a way to adjust the fair price of an option, after a trader adds a bit of his personal views on the range of the underlying, which he/she believes to be more reasonable to use than the $[0, \infty)$ range that was adopted in deriving the original B-S formula. For example, one could still use the original B-S formula to decide the volatility value from the historical market data. This has the effect of acknowledging that the opposite side has adopted the B-S formula. Then, he/she will stick the obtained volatility value into our new formula to obtain a "revised" option price based on his/her own view of what a reasonable price range of the underlying should be before the option expires.

In fact, there are many applications of the truncated normal distribution. For example, it has been applied to the theory of queues by Pender [189], while Dey & Chakraborty [70] introduced it into the inventory model as the distribution of a fuzzy random variable. Certainly, there also exist plenty of its financial applications. Specifically, truncated normal distribution was adopted in the analysis of investments and the measurement of stock market efficiency by Norgaard & Killeen [187] and Hasan et al. [109] respectively. Recently, portfolio insurance has been another application area of the truncated normal

distribution [119].

When the truncated normal distribution is chosen in option pricing, there would be a price range for the underlying. With martingale approach, a closed-form pricing formula is derived, which does not bring any significantly extra burden compared with the B-S formula as far as the computational efficiency is concerned. Moreover, the B-S model is a special case of our model since the truncated normal distribution could degenerate to the normal distribution when the lower and upper bound approach negative and positive infinity respectively. It should also be noticed that according to the numerical results, with the two bounds varying while other parameters being the same in both models, European call option prices calculated with our formula are no greater than those obtained from B-S formula, which is consistent with our expectation since the underlying price under our setting can not go beyond a certain level, while that in the B-S model can surely take any value. This is quite useful in real markets since sellers of a call option could give up some profits by choosing a lower price with our formula if they believe that the underlying price will not exceed a certain level. It should also be noted that although imposing upper (lower) bounds is similar to the up-and-out (down-and-out) barrier option in the sense that we all give up some space for increase (decrease), our prices are essentially different from barrier option prices under the B-S model in that the bounds for the underlying price in barrier options are specified in the option contract while our bounds are imposed on the pricing model, and this is also confirmed by our numerical results presented later. On the other hand, to demonstrate the pricing performance of the newly proposed model in real markets, empirical results for our model and the Black-Scholes model are presented based on S&P 500 Index and options.

The rest of the chapter is organized as follows. In Section 4.2, we will firstly introduce the truncated normal distribution and then a martingale restriction will be derived for our model. After that, a closed-form pricing formula for European call options will be presented. In particular, various basic properties of the option price formula will be examined. In Section 4.3, numerical examples and some useful discussions will be given. In Section 4.4, empirical studies are carried out to compare the performance of our model and that of the Black-Scholes model, followed by some concluding remarks presented in the last section.

4.2 Our model

In this section, the truncated normal distribution is briefly introduced first, followed by a necessary martingale restriction that needs to be imposed in order to avoid arbitrage opportunities. Finally, we derive a closed-form pricing formula for our model and a number of basic properties of our solution are investigated.

4.2.1 Truncated normal distribution

If a random variable X is assumed to follow a truncated normal distribution with $X \in [a, b]$, then its probability density function can be specified as

$$f(x;\mu,\sigma,a,b) = \begin{cases} \dfrac{\frac{1}{\sigma}\phi(\frac{x-\mu}{\sigma})}{\Phi(\frac{b-\mu}{\sigma}) - \Phi(\frac{a-\mu}{\sigma})}, & a \le x \le b, \\ 0, & otherwise. \end{cases}$$

Hence, its expectation and variance can be easily calculated as

$$E(X) = \mu + \frac{\phi(\frac{a-\mu}{\sigma}) - \phi(\frac{b-\mu}{\sigma})}{\Phi(\frac{b-\mu}{\sigma}) - \Phi(\frac{a-\mu}{\sigma})}\sigma, \tag{4.1}$$

$$V(X) = \sigma^2\left[1 + \frac{\frac{a-\mu}{\sigma}\phi(\frac{a-\mu}{\sigma}) - \frac{b-\mu}{\sigma}\phi(\frac{b-\mu}{\sigma})}{\Phi(\frac{b-\mu}{\sigma}) - \Phi(\frac{a-\mu}{\sigma})} - \Big(\frac{\phi(\frac{a-\mu}{\sigma}) - \phi(\frac{b-\mu}{\sigma})}{\Phi(\frac{b-\mu}{\sigma}) - \Phi(\frac{a-\mu}{\sigma})}\Big)^2\right], \tag{4.2}$$

which shows that the mean and variance of the truncated normal distribution are no longer μ and σ^2. In the following, Figure 4.1 exhibits the probability density function of truncated normal distribution and standard normal distribution, which further illustrates the differences between the two distributions. It can be seen clearly that with some parameters being kept the same, there would be higher probability for the truncated normal distribution in the truncated area than the standard normal distribution and the probability can become even higher if the particular area is further narrowed down.

4.2.2 Martingale restriction

The underlying log-price is now assumed to follow a truncated normal distribution under the martingale measure $\mathbb{Q}$, which can be described as

$$\ln(\frac{S_t}{S_0}) \sim f(x;\mu t, \sigma\sqrt{t}, a, b). \tag{4.3}$$

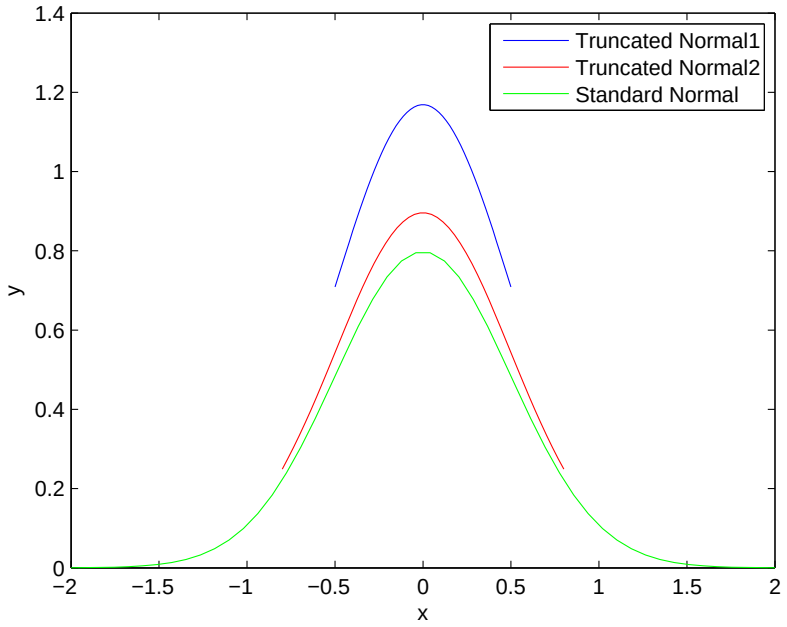

Figure 4.1: Differences between the two distributions. Model parameters are $\mu = 0, \sigma = 0.5, t = 1$; TN1: $a = -0.5, b = 0.5$, TN2: $a = -0.8, b = 0.8$.

Here, S_0 represents the current underlying price, and the underlying price will always be higher than $S_0 e^a$ but lower than $S_0 e^b$. Also, unlike the B-S model, the expected return and variance of the underlying log-returns no longer take the value of μ and σ^2 directly, but take the value of (4.1) and (4.2). After the model is established, one should notice that a certain condition needs to be imposed to guarantee the non-existence of arbitrage opportunities. In fact, as we mentioned before, the so-called structural models and non-structural models are mainly two kinds of option pricing models. On one hand, when we apply the former, we indeed specify the whole dynamics during the time period $[0, T]$ and in this case the goal of perfect hedging at any time $t \in [0, T]$ can be achieved under the martingale framework, which implies that the adopted model is arbitrage-free if we impose the condition $E^Q[e^{-rT} S_T \mid F_t] = e^{-rt} S_t$. However, once a process is chosen, one then has no control on the probability density function that describes the distribution of the underlying at the expiry, which may result in a mis-price of the option, the well known "volatility smile" phenomenon [195] is a typical example in this category. On the other hand, one could have a better control on the statistic properties, such as skewness and kurtosis in addition to mean and variance, of the underlying distribution at the expiry, in order to alleviate the "volatility smile", which prompted the development of the non-structural models since it is rather difficult to find a process with the desired distribution.

To be more specific, when non-structural models are adopted, we only know the information of the start date and expiry date denoted by 0 and T respectively, which stands for a two-date economy. As a result, a martingale restriction,

$$E^Q[e^{-rT}S_T \mid F_0] = S_0, \tag{4.4}$$

suggested by Longstaff [170], should be imposed in this kind of models. Although this is only a necessary condition, it is quite reasonable in the two-date economy since Harrison & Kreps [106] have shown that violation of the martingale restriction under the pricing measure can lead to arbitrage opportunities.

In this chapter, "non-structural" approach is adopted in order to capture the property that the underlying price could not be too high or low in a certain period. This means that the martingale restriction should be imposed to avoid arbitrage opportunities. If we apply the martingale restriction in the B-S model, the drift μ could be shifted to $r - \frac{1}{2}\sigma^2$, which means a reduction in the parameter space. As a result, when we apply the condition in our model, we can also expect such a phenomenon that the expected return μ will be represented by a function of the risk-free interest rate r and the volatility σ as well as the two bounds a and b, which will be presented in the following.

If we denote that $Y = \frac{S_t}{S_0}$, it is not difficult to find that the probability density for Y can be expressed as $\frac{1}{y}f(\ln y; \mu t, \sigma\sqrt{t}, a, b)$, which can be specified as

$$f_Y(y) = \begin{cases} \frac{1}{y} \cdot \frac{\frac{1}{\sigma\sqrt{t}}\phi(\frac{\ln y - \mu t}{\sigma\sqrt{t}})}{\Phi(\frac{b-\mu t}{\sigma\sqrt{t}}) - \Phi(\frac{a-\mu t}{\sigma\sqrt{t}})}, & e^a \le y \le e^b, \\ 0, & otherwise. \end{cases}$$

As a result, we can obtain

$$E[Y|F_0] = \int_{e^a}^{e^b} \frac{\frac{1}{\sigma\sqrt{t}}\phi(\frac{\ln y - \mu t}{\sigma\sqrt{t}})}{\Phi(\frac{b-\mu t}{\sigma\sqrt{t}}) - \Phi(\frac{a-\mu t}{\sigma\sqrt{t}})} dy. \tag{4.5}$$

With the transform of $z = \dfrac{\ln y - \mu}{\sigma}$, it can be further calculated as

$$\begin{aligned} E[Y|F_0] &= \frac{e^{(\mu+\sigma^2)t}}{\Phi(\frac{b-\mu t}{\sigma\sqrt{t}}) - \Phi(\frac{a-\mu t}{\sigma\sqrt{t}})} \int_{\frac{b-\mu t}{\sigma\sqrt{t}}}^{\frac{a-\mu t}{\sigma\sqrt{t}}} \frac{1}{\sqrt{2\pi}} e^{-\frac{(z-\sigma\sqrt{t})^2}{2}}, \\ &= e^{(\mu+\sigma^2)t} \frac{\Phi(\frac{b-\mu t}{\sigma\sqrt{t}} - \sigma\sqrt{t}) - \Phi(\frac{a-\mu t}{\sigma\sqrt{t}} - \sigma\sqrt{t})}{\Phi(\frac{b-\mu t}{\sigma\sqrt{t}}) - \Phi(\frac{a-\mu t}{\sigma\sqrt{t}})}. \end{aligned}$$

In order to avoid arbitrage opportunities, the martingale restriction (4.4) should be imposed, which implies that

$$E[Y|F_0] = e^{rt}. \tag{4.6}$$

Therefore, the following can be obtained

$$\frac{\Phi(\frac{b-\mu t}{\sigma\sqrt{t}} - \sigma\sqrt{t}) - \Phi(\frac{a-\mu t}{\sigma\sqrt{t}} - \sigma\sqrt{t})}{\Phi(\frac{b-\mu t}{\sigma\sqrt{t}}) - \Phi(\frac{a-\mu t}{\sigma\sqrt{t}})} = e^{(r-\frac{1}{2}\sigma^2-\mu)t}, \tag{4.7}$$

which yields μ being an implicit function of given parameters and time to maturity for the target options. In other words, once a, b, σ, r, t are given, μ needs to be computed from (4.7) as a "root finding" problem. Here, $\Phi(\cdot)$ represents the normal distribution function. It should be remarked that once an equation has been derived, the existence of the solution should be checked. In Equation (4.7), when μ approaches $+\infty$, the left hand side (LHS) and the right hand side (RHS) of the equation approaches 1 and 0 respectively, which implies that the LHS is greater than RHS. In contrast, when μ approaches $-\infty$, the LHS is still 1 while the RHS approaches $+\infty$, from which we can certainly know that the LHS is smaller than the RHS in this case. Therefore, the existence of the solution is verified.

After the martingale restriction is imposed, we are now ready to derive a closed-form pricing formula for European call options under our model with the martingale approach, which will be provided in the next subsection.

4.2.3 Closed-form pricing formula

In order to obtain the pricing formula for European call options, three cases with respect to the initial underlying price and the strike price should be taken into consideration. The first two cases are trivial and are illustrated in advance. When $\dfrac{K}{S_0} < e^a$, we should know that $S_t - K \geq 0$ always holds and thus the option price can be obtained easily as

$S_0 - Ke^{-rt}$. On the other hand, when $\frac{K}{S_0} > e^b$, the underlying price will always be lower than the strike price, which tells that the option is worthless.

Now let us turn to the final case, i.e. $e^a \leq \frac{K}{S_0} \leq e^b$, the option price can be obtained according to the definition

$$\begin{aligned} V_c &= e^{-rt}E[\max(S_t - K, 0)|F_0], \\ &= S_0 e^{-rt}\int_{-\infty}^{+\infty} \max\Big(y - \frac{K}{S_0}, 0\Big) f_Y(y)dy, \\ &= \frac{S_0 e^{-rt}}{\Phi(\frac{b-\mu t}{\sigma\sqrt{t}}) - \Phi(\frac{a-\mu t}{\sigma\sqrt{t}})}\left[\int_{\frac{K}{S_0}}^{e^b} \frac{1}{\sigma\sqrt{t}}\phi\Big(\frac{\ln y - \mu t}{\sigma\sqrt{t}}\Big)dy - \frac{K}{S_0\sigma\sqrt{t}y}\phi\Big(\frac{\ln y - \mu t}{\sigma\sqrt{t}}\Big)dy\right], \\ &\triangleq \frac{S_0 e^{-rt}}{\Phi(\frac{b-\mu t}{\sigma\sqrt{t}}) - \Phi(\frac{a-\mu t}{\sigma\sqrt{t}})}(A_1 + A_2). \end{aligned} \tag{4.8}$$

The first integral A_1 can be easily calculated according to the derivation process of the martingale restriction in the last subsection while the second one A_2 is the integral of the probability density of the standard normal distribution after applying the transform of $x = \ln y$. As a result, the following two should hold

$$\begin{aligned} A_1 &= e^{(\mu+\frac{1}{2}\sigma^2)t}\left[\Phi\Big(\frac{b-\mu t}{\sigma\sqrt{t}} - \sigma\sqrt{t}\Big) - \Phi\Big(\frac{\ln(\frac{K}{S_0}) - \mu t}{\sigma\sqrt{t}} - \sigma\sqrt{t}\Big)\right], \\ A_2 &= \frac{K}{S_0}\left[\Phi\Big(\frac{b-\mu t}{\sigma\sqrt{t}}\Big) - \Phi\Big(\frac{\ln(\frac{K}{S_0}) - \mu t}{\sigma\sqrt{t}}\Big)\right]. \end{aligned}$$

Combining the martingale restriction (4.7), we can finally arrive at

$$V_c = S_0\frac{\Phi(\frac{b-\mu t}{\sigma\sqrt{t}} - \sigma\sqrt{t}) - \Phi(\frac{\ln(\frac{K}{S_0})-\mu t}{\sigma\sqrt{t}} - \sigma\sqrt{t})}{\Phi(\frac{b-\mu t}{\sigma\sqrt{t}} - \sigma\sqrt{t}) - \Phi(\frac{a-\mu t}{\sigma\sqrt{t}} - \sigma\sqrt{t})} - Ke^{-rt}\frac{\Phi(\frac{b-\mu t}{\sigma\sqrt{t}}) - \Phi(\frac{\ln(\frac{K}{S_0})-\mu t}{\sigma\sqrt{t}})}{\Phi(\frac{b-\mu t}{\sigma\sqrt{t}}) - \Phi(\frac{a-\mu t}{\sigma\sqrt{t}})}. \tag{4.9}$$

With the newly derived option pricing formula, it is natural for us to consider some properties of the solution theoretically, which will be discussed in the next subsection.

4.2.4 Basic properties of the solution

In this subsection, various basic properties of the pricing formula would be investigated to show the rationale and validity of the solution.

Proposition 4.2.1. *(Monotonicity) The European call option price is a monotonic increasing function of the underlying price S.*

Proof. To show the Monotonicity of the option price with respect to S, we shall just derive $\frac{\partial V_c}{\partial S}$. A direct calculation can be made as

$$\begin{aligned}\frac{\partial V_c}{\partial S} &= \frac{\Phi(\frac{b-\mu t}{\sigma\sqrt{t}}-\sigma\sqrt{t})-\Phi(\frac{\ln(\frac{K}{S_0})-\mu t}{\sigma\sqrt{t}}-\sigma\sqrt{t})}{\Phi(\frac{b-\mu t}{\sigma\sqrt{t}}-\sigma\sqrt{t})-\Phi(\frac{a-\mu t}{\sigma\sqrt{t}}-\sigma\sqrt{t})}+\frac{1}{\sigma\sqrt{t}}\frac{\phi(\frac{\ln(\frac{K}{S_0})-\mu t}{\sigma\sqrt{t}}-\sigma\sqrt{t})}{\Phi(\frac{b-\mu t}{\sigma\sqrt{t}}-\sigma\sqrt{t})-\Phi(\frac{a-\mu t}{\sigma\sqrt{t}}-\sigma\sqrt{t})} \\ &- \frac{K}{S_0\sigma\sqrt{t}}\frac{\phi(\frac{\ln(\frac{K}{S_0})-\mu t}{\sigma\sqrt{t}})}{\Phi(\frac{b-\mu t}{\sigma\sqrt{t}})-\Phi(\frac{a-\mu t}{\sigma\sqrt{t}})}, \\ &\triangleq M_1+M_2-M_3. \end{aligned} \tag{4.10}$$

Actually, M_2 can be further simplified as

$$\begin{aligned}M_2 &= \frac{1}{\sigma\sqrt{t}[\Phi(\frac{b-\mu t}{\sigma\sqrt{t}}-\sigma\sqrt{t})-\Phi(\frac{a-\mu t}{\sigma\sqrt{t}}-\sigma\sqrt{t})]}\frac{1}{\sqrt{2\pi}}e^{-\frac{1}{2}(\frac{\ln(\frac{K}{S_0})-\mu t}{\sigma\sqrt{t}}-\sigma\sqrt{t})^2}, \\ &= \frac{1}{\sigma\sqrt{t}[\Phi(\frac{b-\mu t}{\sigma\sqrt{t}}-\sigma\sqrt{t})-\Phi(\frac{a-\mu t}{\sigma\sqrt{t}}-\sigma\sqrt{t})]}\frac{1}{\sqrt{2\pi}}e^{-\frac{1}{2}(\frac{\ln(\frac{K}{S_0})-\mu t}{\sigma\sqrt{t}})^2+\ln(\frac{K}{S_0})-\mu t-\frac{1}{2}\sigma^2 t}. \end{aligned} \tag{4.11}$$

Substituting Equation (4.7) into (4.11) yields

$$M_2 = \frac{K}{S_0}e^{-rt}\frac{1}{\sigma\sqrt{t}[\Phi(\frac{b-\mu t}{\sigma\sqrt{t}})-\Phi(\frac{a-\mu t}{\sigma\sqrt{t}})]} = M_3. \tag{4.12}$$

On the other hand, it is well-known that the normal distribution function $\Phi(x)$ is a monotonic increasing function of x. In addition, with $e^b > \frac{K}{S_0} > e^a$, we can also obtain that

$$\frac{b-\mu t}{\sigma\sqrt{t}}-\sigma\sqrt{t} \geq \frac{\ln(\frac{K}{S_0})-\mu t}{\sigma\sqrt{t}}-\sigma\sqrt{t} \geq \frac{a-\mu t}{\sigma\sqrt{t}}-\sigma\sqrt{t},$$

which implies that $M_1 > 0$. Therefore, we have shown that $\frac{\partial V_c}{\partial S} > 0$. This has completed the proof. □

The monotonicity of our pricing formula with respect to S is consistent with financial implications of the call options, showing the rationality of our formula. Furthermore, it is rather important to check the asymptotic behavior of the formula to further show its validity in the following.

Proposition 4.2.2. *(Asymptotics)*

$$\lim_{S\to+\infty} V_c = S, \quad \lim_{S\to 0} V_c = 0. \tag{4.13}$$

Proof. The proof of this proposition is trivial. In fact, it should be noticed that when the underlying price S approaches positive infinity, S must be larger than Ke^{-a}, which means that $V = S_0 - Ke^{-rt}$. As a result, the value of Ke^{-rt} can be ignored when S is large enough and thus the first limit should hold. Similarly, when S is close to zero, the inequality, $S < Ke^{-b}$, should be satisfied, which implies that $V = 0$. This has completed the proof. □

It should be noted that the asymptotic behavior of the current pricing formula is consistent with the financial settings of European call options, which verifies the correctness of our formula from one angle. On the other hand, the bounds a and b are newly introduced parameters. It should be pointed out that our price degenerates to the B-S price when the lower and upper bound approach negative and positive infinity respectively. This is clearly shown by the following proposition.

Proposition 4.2.3. *When a and b approach $-\infty$ and $+\infty$ respectively, our option price can degenerate to the B-S price.*

Proof. This proposition is also not difficult to verify. As we observe the newly derived pricing formula carefully, it is not hard to find that

$$\begin{aligned}
\lim_{b\to+\infty} \Phi(\frac{b-\mu t}{\sigma\sqrt{t}} - \sigma\sqrt{t}) &= 1, \\
\lim_{a\to-\infty} \Phi(\frac{a-\mu t}{\sigma\sqrt{t}} - \sigma\sqrt{t}) &= 0, \\
\lim_{b\to+\infty} \Phi(\frac{b-\mu t}{\sigma\sqrt{t}}) &= 1, \\
\lim_{a\to+\infty} \Phi(\frac{a-\mu t}{\sigma\sqrt{t}}) &= 0.
\end{aligned}$$

As a result, the martingale restriction under the limitation of a and b can be simplified as

$$\mu = r - \frac{1}{2}\sigma^2, \tag{4.14}$$

which is exactly the same as the one for the B-S model. Moreover, the following can also be obtained

$$\begin{aligned}
\lim_{a\to-\infty, b\to+\infty} V_c &= S_0[1 - \Phi(\frac{\ln(\frac{K}{S_0}) - \mu t}{\sigma\sqrt{t}} - \sigma\sqrt{t})] - Ke^{-rt}[1 - \Phi(\frac{\ln(\frac{K}{S_0}) - \mu t}{\sigma\sqrt{t}})], \\
&= S_0\Phi(\frac{\ln(\frac{S_0}{K}) + \mu t}{\sigma\sqrt{t}} + \sigma\sqrt{t}) - Ke^{-rt}\Phi(\frac{\ln(\frac{S_0}{K}) + \mu t}{\sigma\sqrt{t}}).
\end{aligned}$$

With Equation (4.14), it is straightforward that

$$\lim_{a\to-\infty,b\to+\infty} V_c = S_0\Phi(\frac{\ln(\frac{S_0}{K})+(r+\frac{1}{2}\sigma^2)t}{\sigma\sqrt{t}}) - Ke^{-rt}\Phi(\frac{\ln(\frac{S_0}{K})+(r-\frac{1}{2}\sigma^2)t}{\sigma\sqrt{t}}), \quad (4.15)$$

which is exactly the B-S price. This has completed the proof. □

Since the B-S formula is just a special case of our formula, it is natural for us to check whether the put-call parity under the B-S model still holds in our model. In addition, the put-call parity is a relationship between European call and put option prices and its validity is an indication that no arbitrage opportunity exists, which can reinforce that the derived martingale restriction is reasonable. Hence, its mathematical proof would be provided in the next proposition.

Proposition 4.2.4. *The put-call parity holds for our model with the truncated normal distribution and its form is the same as that in B-S model, i.e.*

$$V_c - V_p = S_0 - Ke^{-rt}. \quad (4.16)$$

Proof. According to the derivation process of the call option price, we can certainly obtain

$$\begin{aligned} V_c &= S_0e^{-rt}\int_{\frac{K}{S_0}}^{e^b} \frac{1}{y}\cdot\frac{\frac{1}{\sigma\sqrt{t}}\phi(\frac{\ln y-\mu t}{\sigma\sqrt{t}})}{\Phi(\frac{b-\mu t}{\sigma\sqrt{t}})-\Phi(\frac{a-\mu t}{\sigma\sqrt{t}})}(y-\frac{K}{S_0})dy, \\ V_p &= S_0e^{-rt}\int_{e^a}^{\frac{K}{S_0}} \frac{1}{y}\cdot\frac{\frac{1}{\sigma\sqrt{t}}\phi(\frac{\ln y-\mu t}{\sigma\sqrt{t}})}{\Phi(\frac{b-\mu t}{\sigma\sqrt{t}})-\Phi(\frac{a-\mu t}{\sigma\sqrt{t}})}(\frac{K}{S_0}-y). \end{aligned}$$

As a result, it is straightforward that

$$V_c - V_p = S_0e^{-rt}C_1 - Ke^{-rt}C_2, \quad (4.17)$$

where

$$\begin{aligned} C_1 &= \int_{e^a}^{e^b} \frac{\frac{1}{\sigma\sqrt{t}}\phi(\frac{\ln y-\mu t}{\sigma\sqrt{t}})}{\Phi(\frac{b-\mu t}{\sigma\sqrt{t}})-\Phi(\frac{a-\mu t}{\sigma\sqrt{t}})}dy, \\ C_2 &= \int_{e^a}^{e^b} \frac{\frac{1}{\sigma\sqrt{t}y}\phi(\frac{\ln y-\mu t}{\sigma\sqrt{t}})}{\Phi(\frac{b-\mu t}{\sigma\sqrt{t}})-\Phi(\frac{a-\mu t}{\sigma\sqrt{t}})}dy. \end{aligned}$$

Recall the martingale restriction, it is not difficult to find that C_1 is actually equal to e^{rt}.

On the other hand, if we apply the transform of $z = \dfrac{\ln y - \mu t}{\sigma\sqrt{t}}$, the value of C_2 can surely be worked out, which is exactly 1. Therefore, we finally arrive at the desired result

$$V_c - V_p = S_0 - Ke^{-rt}, \tag{4.18}$$

which indicates that the proof has been completed. □

With the same put-call parity being verified, it is clear that our model can be viewed as a more general model than the B-S model. It should also be noted that the put-call parity derived here has also brought the convenience in trading practice since to obtain both of the European call and put option prices, only one price needs to be figured out; its counterpart can be easily deduced with the parity.

After these basic properties of the newly derived option pricing formula have been studied, we then focus on some numerical examples, which will be given in the next section.

4.3 New Formula

In this section, the influence of parameters a and b on European call option prices will be first studied and then a comparison of option prices obtained from the newly derived formula is made with those calculated from the B-S formula. Finally, the difference between imposing bounds on the underlying price model and the barrier option will be discussed. In terms of numerical calculation of the option prices, although we have to work out the parameter μ with the martingale restriction (4.7), its calculation is rather rapid by making use of the Matlab built-in function $fzero$ with a recommended initial guess of $r - \dfrac{1}{2}\sigma^2$. Our motivation for choosing such an initial guess is that when the upper and lower bound take large and small values respectively, our model will be similar to the B-S model, in which μ would take the value of $r - \dfrac{1}{2}\sigma^2$. Hereafter, the risk-free interest rate r is set to be 0.01 and the volatility σ takes the value of 0.2.

Depicted in Figure 4.2 are our option prices with different bound values. To be more specific, it is interesting to notice that with lower bound set to be $\ln 0.85$, a higher price under our model can be expected when we increase the value of the upper bound b in Figure 4.2(a). It can be easily explained since the underlying price can take larger value

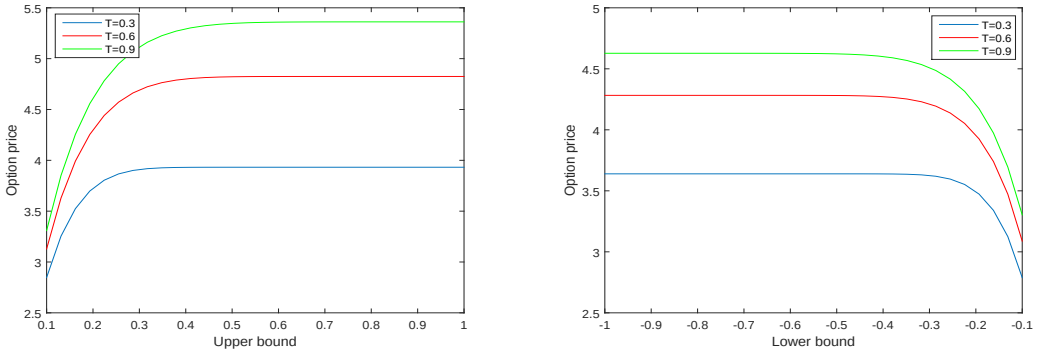

(a) Option prices with variable upper bound.

(b) Option prices with variable lower bound.

Figure 4.2: Option pricing with changing bounds. Model parameters are $S = 100, K = 100$.

with a higher upper bound, which can certainly give rise to a call option price. This also means that the price of a call option with a finite range of the underlying price is always lower than that obtained from the B-S formula. This does make sense financially too, because the underlying price in our model is assumed to be impossible to go beyond $S_0 e^b$, while that in the B-S model can take any value. Another important feature is that when the value of b becomes large enough, a further increase in the upper bound will make little difference to option prices, which is not difficult to understand since the right tail of the truncated normal distribution would become more similar to that of the standard normal distribution when we increase the value of b. Furthermore, higher upper bound is needed to observe this phenomenon with larger time to expiry mainly because a higher European call option price would be obtained in this case. On the other hand, Figure 4.2(b) exhibits that the smaller the lower bound a, the higher the call option price will be (here upper bound is $\ln 1.15$). It seemed rather confusing at first. However, we eventually understand it when we realized that the European put option price should decrease when the lower bound a takes a smaller value since the underlying price can decrease to a much lower value when a drops. As a result, with the help of the put-call parity derived in the previous section, the call option price should also be a decreasing function of a with other parameters unchanged. In addition, a similar observation can be obtained that if the lower bound keeps decreasing, the call option price would converge to a certain price. The interpretation for it is the same as that for the case of the upper bound.

As for Figure 4.3, it is clearly that our price for call options is an increasing function of the underlying price, which confirms the theoretical results obtained in the previous

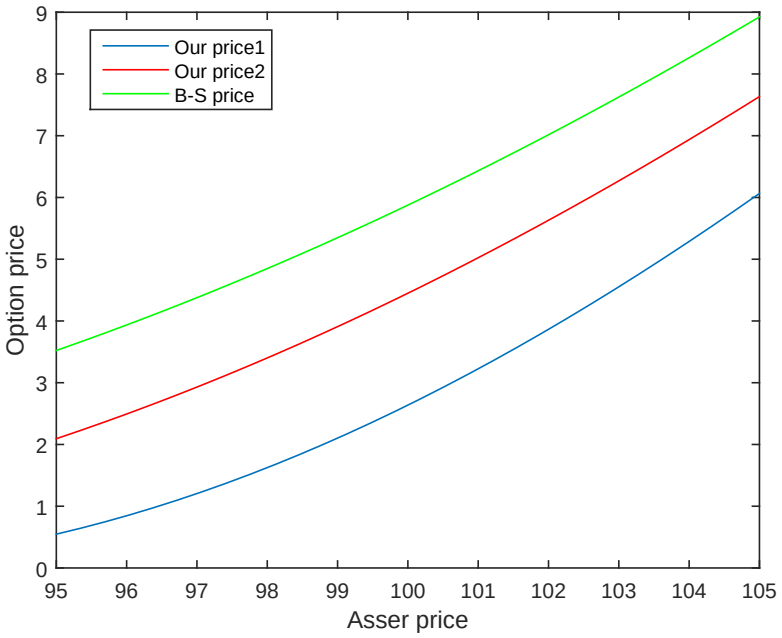

Figure 4.3: Our price vs B-S price with different underlying price. Our price1: $a = \ln 0.9, b = \ln 1.0$; Our price2: $a = \ln 0.8, b = \ln 1.2$.

section. Furthermore, it is always lower than the B-S price, no matter the option is "in the money", "at the money" or "out of money". This is quite reasonable because the call option price would increase when we enlarge the upper bound in the sense that it would be possible for the underlying price to become larger. On the other hand, the put option price would go down if we set the lower bound to be smaller since it would be more likely for the underlying price to decrease and thus there will also be a down trend for the call option price according to the put-call parity.

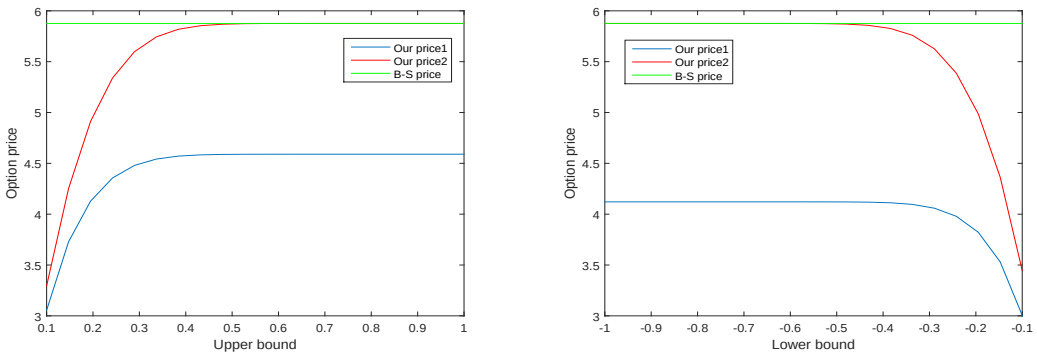

(a) Our price vs B-S price with different lower bound. Our price1: $a = \ln 0.85$; Our price2: $a = -2$.

(b) Our price vs B-S price with with variable upper bound. Our price1: $b = \ln 1.15$; Our price2: $b = 2$.

Figure 4.4: Our price vs B-S price with different bounds. Model parameters are $S = K = 100$.

What can be seen in Figure 4.4(a) is that when the upper bound is large enough, the option price surges from approximately 4.6 to 5.8, which is rather close to the B-S price, if the lower bound a decreases from $\ln 0.85$ to -2. This is because when the upper and lower bound are large and small enough respectively, our model will certainly become similar to the B-S model. A similar pattern appears in Figure 4.4(b) where our price tends to approach the B-S price when the bound range becomes larger, which is consistent with the fact that the truncated normal distribution would degenerate to the standard normal distribution if a and b are close to the negative and positive infinity respectively.

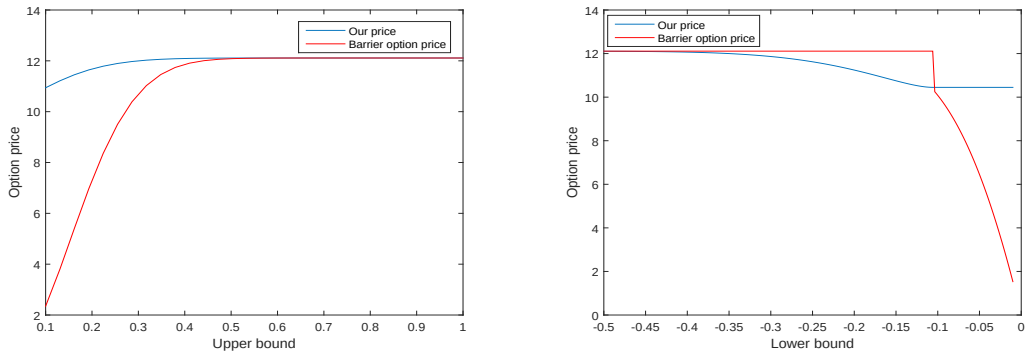

(a) Our price vs up-and-out call option price with changing upper bound.

(b) Our price vs down-and-out call option price with changing lower bound.

Figure 4.5: Option price vs B-S barrier option price with changing bounds. Model parameters are $S = 100, K = 90$.

Another interesting question is whether our prices would be similar to barrier option prices under the B-S framework. In fact, Figure 4.5 exhibits a comparison of our price with the barrier option price under the B-S model and it is very clear that the difference between the two kinds of option prices is distinct. As shown in Figure 4.5(a), with the lower bound a removed and the barrier level for the up-and-out call option being Se^b, the same as the upper bound for the underlying price, our price is always higher than the up-and-out option price, especially when the upper bound is small. This is caused by the intrinsic difference between the two prices. Although the two prices both give up some space for increase, the way to reach this goal is quite different in that it is a basic assumption in our model that the underlying price will not exceed a certain level, while the barrier level is actually introduced in the option contrast for the up-and-out options. In this case, there would be higher probability for the increase of the underlying price in our model, which leads to a higher price. In addition, when the upper bound becomes

larger, the up-and-out option price and our price become almost the same, which does make sense since the two prices eventually approach the B-S price in this case. When we turn to Figure 4.5(b), in which the upper bound b is removed and the barrier level is Se^a, it shows a similar pattern that our price is almost the same as the down-and-out call price and the two prices are close to the B-S price when the lower bound is small. This is reasonable since our price approaches the B-S price when the lower bound is small enough, while the barrier is meaningless when the barrier level for the down-and-out call option is smaller than the strike price. However, it appears to be quite different from the first case that when the lower bound increases to some extent, there is a sudden drop in the down-and-out option price, when our price begins to become constant. This is also not difficult to understand since the barrier level for the down-and-out option starts to take effect when it is higher than the strike price, in which case the underlying price will always be higher than the strike price in our model and thus our price can be expressed as $S - Ke^{-rT}$, which is stated in Section 2 already.

4.4 Empirical studies

In this section, the results of a preliminary study, comparing the market performance of our model and the Black-Scholes model, are presented, in order to show whether the underlying price is better described by our model when option pricing.

4.4.1 Data description

This empirical study is based on the data of S&P 500 European call options from Jan 2011 to Dec 2011. As usual, the average value of bid and ask prices is regarded as the option price, and several filters need to be applied to eliminate sample noise in the estimation of parameters [11].

First of all, only Wednesday options data (denoted by in-sample data) is used in the stage of parameter estimation mainly due to two reasons; the first is that Wednesday is least likely to be a holiday in a week and also less likely to be affected by day-of-the-week effect, while another is that parameter determination is time-consuming, and choosing one day a week allows us to study a relatively long period. It should be mentioned here that Thursday options data (denoted by out-of-sample data, in contrast to the concept

of in-sample) will be used to assess the model performance in the prediction of option prices calculated with parameters determined by the day before. Secondly, options closed to the expiry time (less than 7 days) are discarded since these options have less time value. Also, Options with more than 120 days to expiry were also excluded because of their unpopularity caused by high trading premiums. Thirdly, if we define the moneyness as $\frac{S-K}{K}$, then options with the absolute value of moneyness over 10% are deleted since very deep in-the-money and out-of-money options usually have liquidity-related problems. Finally, options with prices less than \$1/8 are removed as these prices are rather volatile in real markets. It should also be pointed out that the three-month U.S. Treasury Bill Rate released daily is chosen as a proxy of risk-free interest rate [209] since the time to expiry of options used is less than 120 days.

With all the option data needed at hand, we are now ready to determine model parameters with these data, the process of which will be illustrated in the following subsection.

4.4.2 Parameter estimation

The first step in assessing model performance is to estimate model parameters with real market data, which is a very difficult problem and time-consuming. To find out the "optimal" parameter set that best fits the chosen market data, one common approach is minimizing the "distance" between the model and market option price, which means we need to choose an appropriate function (known as objective function) for such a distance. Following Christoffersen & Jacobs [40] and many other authors, we adopt the dollar mean-squared errors, which is defined as

$$MSE = \frac{1}{N}\sum_{i=1}^{N}[C_{Market} - C_{Model}]^2, \tag{4.19}$$

with C_{Market} and C_{model} denoting the market and model price of an option respectively. N is the total number of observations used in one parameter estimation.

With the objective function chosen, we should choose a satisfactory approach to conduct parameter estimation. It should be pointed out that the objective function (4.19) is not necessarily convex, and thus local minimization algorithms will probably end up with a local minima. In this case, a global optimization is preferred, in which some stochastic factors are generally introduced in their search process so that it will not be stuck when

it reaches a local minima.

The method we adopt here is the Adaptive Simulated Annealing (ASA) [137], which is one of the most popular global optimization algorithms. In fact, Simulated Annealing was firstly developed in 1983 for highly nonlinear problems [155], and it was improved in [215] with the development of the so-called Fast Simulated Annealing, which allows the global minimum can be obtained within finite time. Later on, Very Fast Simulated Reannealing [135], which is now renamed as ASA, was established to further accelerate the speed with random step selection automatically adjusted according to algorithm progress. This particular optimization method has been widely applied in many areas [31, 32], and it has already been applied in the calibration of option pricing models [136, 180].

In our study, the adopted ASA is can be realized through the open-source code provided in [134], and the feedback from many users regularly assesses the source code to ensure its soundness so that it can become even more flexible and powerful. The estimated parameters (daily averaged) are reported in the following Table 4.1.

Table 4.1: Estimated parameters

parameters	σ	a	b
Our model	0.2401	-1.4879	0.5932
Black-Scholes	0.2213		

4.4.3 Empirical comparison

Once model parameters have been obtained with real market data, it is natural for us to assess the model performance. It is widely acknowledged that the performance of a model can be regarded better if there are lower pricing differences between the calculated option prices with model and the corresponding market prices.

Table 4.2: In- and out-of-sample errors for the two models

Error	In-sample	Out-of-sample
Our model	2.3905	12.7735
Black-Scholes	4.5396	14.5772
Relative difference	47.37%	12.37%

What are shown in Table 4.2 are the in-sample and out-of-sample errors under our model and the Black-Scholes model. It is not difficult to find that our model can certainly be regarded as superior over the Black-Scholes model in the tested case as our model can provide better fitness to both of the in-sample and out-of-sample market data. In specific,

if the Black-Scholes model is replaced by our model, there is a great improvement with the relative difference being approximately 50% as far as the in-sample errors are concerned, while a 12% less errors of our model can be witnessed when out-of-sample comparison is taken into consideration.

Table 4.3: Out-of-sample errors for the two models with different moneyness

Error	$0.90 < S/K < 0.97(O)$	$0.97 \leq S/K \leq 1.03(A)$	$1.03 < S/K < 1.10(I)$
Our model	2.6983	16.6294	11.3016
Black-Scholes	5.0314	20.8835	12.6835
Relative difference	46.37%	20.37%	10.90%

On the other hand, options are traded with a wide range of strikes in real markets and thus it is important to check the out-of-sample performance of the two models according to different moneyness, which is presented in Table 4.3 with the abbreviation in the parentheses representing out of money, at the money and in the money, respectively, from the left to the right columns. It is clear that our model can provide a better data fitness, no matter options belong to which sub-category, with out-of-money options experiencing the highest relative difference of approximately 50%. The improvement in the category of at-the-money and in-the-money is relatively smaller, being around 20% and 10% respectively.

4.5 Conclusion

In this chapter, the underlying log-price is assumed to follow a truncated normal distribution, which is able to describe the phenomenon that there should be reasonable bounds for the underlying price in a certain period. By adopting the non-structural model, the martingale restriction for our model is obtained and a closed-form pricing formula for European call options is derived, after which various basic properties of the newly derived formula are investigated, showing the validity of the solution. Furthermore, through numerical experiments, the influence brought by the introduction of upper and lower bounds on option prices is studied and results show that our price is an increasing function of the upper bound while it is a decreasing function with respect to the lower bound. Our price is also compared with the B-S price, and it is reasonable to find that our price will approach the B-S price if the lower bound and upper bound become small and large enough respectively since this case can be viewed as bounds removed. Finally, empirical studies show

that our model greatly outperforms the Black-Scholes model in the tested data set, which can certainly lead us to the conclusion that our model can at least act as an alternative to the Black-Scholes model in real markets.

Part II

Solution techniques

Chapter 5

An accurate approximation formula for pricing European options with discrete dividend payments

5.1 Introduction

One of the incentives for people to invest in stock market is the attraction of receiving dividend payments, in addition to the potential gain of appreciation of the stock value itself. For options written on stocks with dividend payments, an interesting problem is always to find out the correct way to count in the dividend payment in pricing option values. There are generally two kinds of models for pricing these options, i.e. continuous dividend and discrete dividend models. The former is firstly used by Merton [177] who incorporated the continuous dividend under the framework of the B-S (Black-Scholes) model [19] and provided a similar price formula. It is also adopted by a number of other authors, such as Krausz [160], Chung & Shackleton [44] and so on.

On the other hand, pricing options written on the underlying with discretely paid dividend is usually harder than the case with continuous dividend payment, simply because the latter does not involve any jump conditions in a PDE (partial differential equation) pricing system. However, the former is much closer to reality as hardly any underlying

asset involved in exchange-traded options bears with a continuous dividend yield. The only exception would be FX (foreign exchange) options, in which the involved underlying is usually another currency, the interest of which could be viewed as a continuous dividend yield if the compounding period is sufficiently small, say daily compounding, which is a usual case in today's markets.

In this chapter, we therefore focus on discrete dividends, which can themselves be divided in two types. One is paid proportional to the underlying price at the payment day (denoted by the proportional dividend), while another is paid independent of the underlying price level (denoted by the fixed-amount dividend). Firstly, we discuss an interesting phenomenon observed under the classic B-S framework; the option price is independent of the dividend payment date in the case of the proportional dividend. This appears to be at odds with one's intuition that dividend amount, as well as the dividend date, should both affect the price of a European call or put option. Through a proper discussion, we shall show, both mathematically and financially, that while a European option price indeed depends up on not only the amount of the dividend, but also the ex-dividend date when the declared dividend is a fixed amount, it depends on the dividend yield rate only in the case of the discrete dividend payment being proportional to the underlying asset value. Merton [177] seemed to be the first one to derive an analytical solution for European options with the proportional dividend under the B-S model.

However, when the discrete dividend is a fixed amount instead of being proportional to the underlying price, the simplicity and tractability can not be preserved and no exact solution has been discovered, and thus the European option pricing problem with fixed-amount dividend, which is the second issue discussed in this chapter, has drawn plenty of attention among academic researchers. This has prompted the development of a number of such models, including the three popular ones, i.e., Escrowed model, Forward model and Piecewise log-normal model [90], among which the Piecewise log-normal model, assuming that the stock price jumps down at the date of dividend payment and follows a geometric Brownian motion during each non-dividend payment period, can yield most close-to-reality results, as pointed out by Frishling [90] by comparing these three models. Unfortunately, there is no closed-form solution for this model, which makes it hard to be implemented in real markets since the calibration process is time consuming and the calculation of option prices with numerical methods can cost much more time. Therefore, we then derive a

general closed-form approximation formula similar to the B-S formula with the Taylor series approximation technique, specified as the sum of one-dimensional integrals, for all the cases of the single and multiple dividends. Subsequently, numerical experiments are established to show the accuracy of this approximation.

The rest of the Chapter is organized as follows. In Section 5.2, a detailed discussion on the reason why the dividend payment date has no effect on the option price in the case of the dividend yield is carried out. In Section 5.3, a good closed-form approximation for the European call option price with fixed-amount dividend is presented, followed by some numerical results demonstrating its accuracy. Concluding remarks are given in the last section.

5.2 European options with dividend yield

Unlike the materials presented in the next section, the key point of this section is to provide a convincing financial explanation, to a seemingly confusing conclusion that the option price of a European call or put with a discrete dividend payment is independent of the dividend payment date for the case of the proportional dividend to the underlying price at the ex-dividend day. Since such an explanation in this way is not well documented in the literature, we shall also provide a bit more detailed mathematical explanation for the completeness of the chapter as well as easiness for the readers.

In the classic B-S framework, the price of an option, $V(S,t)$, can be found by solving the celebrated B-S [19]

$$\frac{\partial V}{\partial t} + \frac{1}{2}\sigma^2 S^2 \frac{\partial^2 V}{\partial S^2} + rS\frac{\partial V}{\partial S} - rV = 0, \tag{5.1}$$

subject to a set of appropriately boundary and initial conditions. In (5.1), S is the price of the underlying asset, t is time, r is the risk-free interest rate, σ is the volatility of the underlying asset price and E is the strike price.

For a European call option, the boundary and initial conditions are

$$\begin{cases} V(0,t) = 0, \\ \lim\limits_{S\to\infty} V(S,t) = S, \\ V(S,T) = \max\{S-E, 0\}, \end{cases} \tag{5.2}$$

whereas for a European put, the corresponding ones are

$$\begin{cases} V(0,t) = Ee^{-r(T-t)}, \\ \lim\limits_{S\to\infty} V(S,t) = 0, \\ V(S,T) = \max\{E-S, 0\}. \end{cases} \tag{5.3}$$

There are several different ways to solve (5.1) subject to (5.2) or (5.3), for the price of call or put, respectively, which leads to the famous B-S formulae for the option price [226]. For the easiness of references, the option price for a call is denoted by $C(S,t)$ and that of a put is $P(S,t)$, respectively, as

$$C(S,t) = SN(d_1) - Ee^{-r(T-t)}N(d_2), \tag{5.4}$$

$$P(S,t) = Ee^{-r(T-t)}N(-d_2) - SN(-d_1). \tag{5.5}$$

where N is the cumulative distribution function and

$$\begin{aligned} d_1 &= \frac{\ln(S/E) + (r + \frac{1}{2}\sigma^2)(T-t)}{\sigma\sqrt{T-t}}, \\ d_2 &= \frac{\ln(S/E) + (r - \frac{1}{2}\sigma^2)(T-t)}{\sigma\sqrt{T-t}}. \end{aligned}$$

Formulae (5.4) and (5.5) are for the simplest case when there is no dividend payment between the current time t and the expiry date T. For the case with a continuous dividend yield paid to the underlying asset S, these formulae can be easily modified to account for the influence of the continuous dividend yield to the option price evaluated at time t [226].

On the other hand, if the dividend payments are discrete, a jump condition must be imposed at each dividend payment date and the evaluation needs to be carried out from

one dividend date to another, starting from the expiry time and moving backward until one reaches the current time t. Without loss of generality, all one needs to consider is a special case with one known discrete dividend payment between t and T.

If the ex-dividend date is denoted as t_d, the jump condition of the option price across the dividend payment date is

$$V(S(t_d^-), t_d^-) = V(S(t_d^+), t_d^+) \tag{5.6}$$

where t_d^- and t_d^+ denote the time immediately before and after the dividend date, respectively. From (5.6), one may be puzzled where the "jump" is, as the equation seems to suggest that the value of V does not change across the ex-dividend date. The right way to understand this jump condition is that it is a "horizontal jump" in the sense that there is a jump in the independent variable S

$$S(t_d^+) = S(t_d^-) - D_{t_d^-} \tag{5.7}$$

rather a "vertical jump" taking place in the dependent variable V. In (5.7), $D_{t_d^-}$ is the value of the dividend immediately before the dividend payment date.

For the case of the discrete dividend payment being declared as a given percentage of the underlying asset value right before the ex-dividend date, t_d, (i.e., $D_{t_d^-} = d_y S(t_d^-)$) with d_y being the given percentage, there is a closed-form pricing formula given in [226].

The derivation of this formula from the PDE point of view is quite simple. However, for the easiness of reference later and completeness of this chapter, the derivation is repeated here. Let $C_d(S, t; E, r, \sigma, T, t_d, d_y)$ denote the price of a European call option at time t, knowing that there is a discrete dividend payment proportional to the underlying asset value at t_d ($t \leq t_d \leq T$). Let's also re-denote the classic B-S formula for the corresponding call option without a dividend payment as $C_E(S, t; E, r, \sigma, T)$. Note that semicolons are introduced to separate variables from parameters of the problem.

The pricing task can be divided into three stages. In Stage 1, the option price $C_d(S, t_d^+; E, r, \sigma, T, t_d, d_y)$ is calculated. Since there is no more dividend to be paid in the time period, $t_d^+ \leq t \leq T$, i.e, between the time immediately after the dividend payment and the expiry

date, C_d is identical to the price of a vanilla call and thus

$$\begin{aligned} C_d(S, t_d^+;\, E, r, \sigma, T, t_d, d_y) &= C_d(S(t_d^+), t_d^+; E, r, \sigma, T, t_d, d_y) \\ &= C_E(S(t_d^+), t_d^+; E, r, \sigma, T). \end{aligned} \tag{5.8}$$

In Stage 2, we impose the jump condition (5.7) and obtain $C_d(S, t_d^-; E, r, \sigma, T, t_d, d_y)$ as

$$\begin{aligned} C_d(S, t_d^-; E, r, \sigma, T, t_d, d_y) &= C_d(S(t_d^-), t_d^-; E, r, \sigma, T, t_d, d_y) \\ &= C_d(S(t_d^+), t_d^+; E, r, \sigma, T, t_d, d_y) \\ &= C_E(S(t_d^+), t_d^+; E, r, \sigma, T) \\ &= C_E(S(t_d^-) - D_{t_d^-}, t_d^-; E, r, \sigma, T) \\ &= C_E(S(t_d^-) - d_y S(t_d^-), t_d^-; E, r, \sigma, T) \\ &= C_E(S(1 - d_y), t_d^-; E, r, \sigma, T). \end{aligned} \tag{5.9}$$

The remaining job, in Stage 3, is to price an option in the period $t < t_d^-$ with the terminal value $C_E(S(1 - d_y), t_d^-; E, r, \sigma, T)$. Since one can easily prove that a uniform scaling on S leaves the B-S equation invariant, $C_E(S(1-d_y), t; E, r, \sigma, T)$ is thus a solution of the B-S equation for any time t before t_d. In other words, at any time t prior to t_d, all one needs to do is to use the B-S formula for the corresponding vanilla call, except with the underlying pricing being replaced by the scaled $S(1-d_y)$. It should be remarked here that an equivalent approach to adjust the underlying price for the case of a fixed finite dividend amount as discussed in [110] leads only to an approximation, whereas for the discrete dividend being a percentage of the underlying asset price immediately before the dividend payment date, the adjustment of the underlying with a scale $(1-d_y)$ leads to an exact pricing formula!

Now, a better formula can be deduced with a scaled strike price, instead of a scaled underlying price, being used in the B-S formula for the corresponding vanilla option. The option contract $C_E(S(1 - d_y), t; E, r, \sigma, T)$ has the terminal value

$$C_d(S(1 - d_y), t_d; E, r, \sigma, T, t_d, d_y) = \max[S(1 - d_y) - E, 0], \tag{5.10}$$

at expiry. Re-scaling the above payoff function, we can easily show that this option has the same value as $(1-d_y)$ of an option with the exercise price $E(1-d_y)^{-1}$, simply because $\max[S(1 - d_y) - E, 0] = (1 - d_y)\max[S - E(1 - d_y)^{-1}, 0]$. Therefore, the final formula

to calculate a call option with a discrete dividend proportional to the underlying price immediately prior to the ex-dividend date is

$$C_d(S,t;E,r,\sigma,T,t_d,d_y) = (1-d_y)C_E(S,t;E(1-d_y)^{-1},r,\sigma,T). \tag{5.11}$$

Similarly, a corresponding formula for puts can be easily derived as

$$P_d(S,t;E,r,\sigma,T,t_d,d_y) = (1-d_y)P_E(S,t;E(1-d_y)^{-1},r,\sigma,T). \tag{5.12}$$

The disappearance of t_d in (5.11) and (5.12) implies that the option price at time t, prior to the dividend payment, has nothing to do with how long one has to wait until the dividend becomes ex-dividend. This may seem to be against one's financial instinct and needs a financial explanation. The key to reveal the financial interpretation of the option price being independent of the time to ex-dividend date for the case of a discrete dividend being proportional to the underlying asset price right before the ex-dividend date is the main reason for this article.

The fundamental reason is that in the classic B-S framework, the underlying asset is assumed to follow a geometric Brownian motion with a constant volatility rate $\sigma > 0$

$$dS_t = \mu S_t dt + \sigma S_t dW, \tag{5.13}$$

where μ is the drift rate and dW denotes increments of a standard Wiener process defined on a complete probability space $(\Omega, \mathcal{F}, Q)$. With this assumption, the discounted expectation of the underlying asset price $e^{-r(t_d-t)}E(S_{t_d})$ is nothing but S_t, which is independent from t_d and it is a known quantity at the time when an option contact needs to be priced. So, when an option needs to be priced at time t, knowing that there is a dividend payment at t_d but the dividend amount is not known at that moment (it is a random number $d_y S_{t_d^-}$), the only "fair" way, for both the buyer and the writer of the option, to account for the contribution of the dividend to the price of the option at time t is to count in its discounted expectation, just like we take the discounted expectation of the payoff function of an option as the "fair" price of the option under the no arbitrage argument. When the discounted expectation of the discrete dividend payment is independent of the time to dividend date (S_t in this case), it is the fundamental reason why the option price

evaluated at t is independent of t_d for the case when the dividend payment is assumed to be proportional to the underlying asset price right before the ex-dividend date as shown in (5.11) and (5.12).

Some people may try to understand the reason that a call option price does not change across the dividend payment with the argument that the option holder does not benefit from a dividend payment, such an argument certainly does not explain why a put option value does not change across a discrete dividend payment day, as the holder of a put option does pocket the dividend payment. The fundamental reason is that the effect of the dividend payment has already been factorized in formula (5.11) for a call or formula (5.12) for a put and the option holder cannot exercise their option until the expiry day, when he/she holds a European style option. For calls, it is straightforward to show that $C_d(S,t)$ is always less than its vanilla counterpart without dividend payment to count for the fact that the writer of the option will pocket the dividend. For puts, it can also be shown that $P_d(S,t)$ is always more than its vanilla counterpart without dividend payment to compensate the writer of the option as holder will receive the dividend. However, such a financial intuition is not so obvious mathematically. A put with a higher strike price is worth more. But, the less-than-one factor $(1-d_y)$ in front of $P_E(S,t;E(1-d_y)^{-1},r,\sigma,T)$ in (5.12) could make the product smaller and thus the price of a put with a discrete dividend could be cheaper than its counterpart without any dividend payment at all. Fortunately, to mathematically prove that $aP_E(S,t;\frac{E}{a},r,\sigma,T)$, with $0 < a \leq 1$, is a monotonically decreasing function for any $S > 0$ is not too difficult. The actual proof is thus omitted here.

It should be mentioned in passing that a very similar formula is given in [208]. However, no financial explanation was provided there, in terms of why the option price has no dependence on the dividend payment time. Also, the formula stated in [208] (pages 238-240) is in a format that the "initial stock price" has been replaced in the BS formula, in order to count in the effect of the discrete dividend payment. Mathematically, of course, there is nothing wrong there. But, financially, it is far better to adjust the strike price, as shown in [226], because the underlying price (or the "initial stock price") is usually a given value and the advantage of using (5.11) (or (5.12) for puts) is the interpretation that the reduced (or increased) option price is achieved through an equivalent option with a higher strike price.

Before leaving this section, it should be remarked that with discrete dividend payments, the put-call parity between European options is not of the same form as the case without the dividend payments. With no arbitrage argument, one can easily establish that the revised put-call parity for a single discrete dividend paid at t_d is

$$S_t - PV(D_{t_d^-}) + P_d(S,t) - C_d(S,t) = Ee^{-r(T-t)}, \tag{5.14}$$

as shown in [100]. In (5.14), $PV(D_{t_d^-})$ is the present value of the dividend value right before the ex-dividend date, $D_{t_d^-}$. For a discrete dividend proportional to the underlying price at t_d^-, $PV(D_{t_d^-}) = d_y S_t$, as discussed earlier. With the put-call parity (5.14), it is then consistent that both puts and calls do not change values, while there is a downward jump of the underlying price across the dividend payment date.

In contrast, as stated before that the European option price depends on not only the amount of the dividend, but also the dividend payment date when the amount of dividend is fixed, the price formula can be quite difficult to be derived and there exists no closed-form formula for it, which makes our accurate approximation formula presented in the next section rather valuable.

5.3 European options with fixed-amount dividend

In this section, we will present an excellent closed-form approximation for the European call option price with fixed-amount dividend under the B-S framework. In particular, we will firstly derive a closed-form pricing formula for options with single dividend and then extend it to a general case with multiple discrete dividends. Before we go any further, some notations used in this section should be introduced first. We let $f^{(n)}(S,t;t_{d_k},1\le k\le n)$ be the European call option price paying n-period dividend, T stand for the expiry time, S and K represent the underlying price and the strike price respectively. We also denote $C(S_t,t)$ to be the B-S European call option price at time t with no dividend paid in the life of the option contract.

5.3.1 Single fixed-amount dividend

In this subsection, a simple case is considered that a stock only pays one discrete dividend D at the time t_d before the expiry time T. Then it is not difficult to know that when

$t > t_d$, the option price is exactly the same as the B-S price $C(S_t, t)$ since there is no dividend to be paid after time t_d. As for the case of $t < t_d$, we can also easily find the pricing PDE, which is exactly the B-S equation specified as

$$\frac{\partial f^{(1)}}{\partial t} + \frac{1}{2}\sigma^2 S^2 \frac{\partial^2 f^{(1)}}{\partial S^2} + rS\frac{\partial f^{(1)}}{\partial S} - rf^{(1)} = 0, \quad t < t_d, \tag{5.15}$$

where r is the risk-free interest rate, σ is the volatility. According to the continuity of option prices, the boundary condition for PDE (5.15) can be derived as

$$f^{(1)}(S_{t_d}, t_d^-; t_d) = \begin{cases} C(S_{t_d} - D, t_d^+), & S_{t_d} \geq D, \\ 0, & S_{t_d} < D. \end{cases}$$

After making the transformation of

$$S = Ke^x, \tau = \frac{1}{2}\sigma^2(t_d - t), f^{(1)} = Ke^{-\frac{1}{2}(m-1)x - \frac{1}{4}(m+1)^2\tau}u(x,\tau), m = \frac{2r}{\sigma^2}, \tag{5.16}$$

PDE (5.15) can be simplified to

$$\frac{\partial u}{\partial \tau} = \frac{\partial^2 u}{\partial x^2}, \quad \tau > 0, \tag{5.17}$$

with the boundary condition

$$u(x,0) = \begin{cases} e^{\frac{1}{2}(m-1)x}[(e^x - \frac{D}{K})N(z_1) - e^{-r(T-t_d)}N(z_2)], & x \geq \ln(\frac{D}{K}), \\ 0, & x < \ln(\frac{D}{K}), \end{cases}$$

where $z_1 = \dfrac{\ln(e^x - \frac{D}{K}) + (r + \frac{1}{2}\sigma^2)(T - t_d)}{\sigma\sqrt{T - t_d}}, z_2 = z_1 - \sigma\sqrt{T - t_d}$, and $N(\cdot)$ denotes the normal cumulative distribution function. The newly obtained PDE system is a heat equation with an initial condition, which can be solved through a convolution of the initial condition with a fundamental solution [89] as follows

$$\begin{aligned} u(x,\tau) &= \frac{1}{2\sqrt{\pi\tau}}\int_{-\infty}^{+\infty} u(s,0)e^{\frac{(x-s)^2}{4\tau}}ds, \\ &= \frac{1}{2\sqrt{\pi\tau}}\int_{\ln(\frac{D}{K})}^{+\infty} e^{\frac{1}{2}(m-1)s - \frac{(x-s)^2}{4\tau}}[(e^s - \frac{D}{K})N(z_1) - e^{-r(T-t_d)}N(z_2)]ds. \end{aligned} \tag{5.18}$$

Ideally, we want to derive a formula in a nice form as the case when the dividend is paid proportional to the underlying price discussed in the previous section. Unfortunately, the analytic simplicity could not be preserved when dividends are paid with fixed amount and no exact solution exists [59]. This could make the model hard to be implemented in real markets since the calculation of European option prices with n-period dividends would involve the numerical computation of a $(n+1)$-dimensional integral, which is rather slow. As a result, some approximation methods have already been established to try to seek more efficient ways to price European options with discrete dividends. For example, Amaro [5] provided accurate bounds for the option price with a single dividend, while Dai & Lyuu [60] approximated fixed-amount dividends with continuous dividend yields and provided their solution with the aid of recursive formulae. However, none of these are satisfactory since they are not general or efficient. Therefore, we aimed to find an approximation method that can not only be applied when there is only a single dividend, but also be extended to the case of multiple dividends, with a closed-form pricing formula constructed by only one-dimensional integrals so that the calculation of this formula can be quite rapid, which is presented in the following.

Actually, it is not difficult to find that the existence of the term $\ln(e^s - \frac{D}{K})$ is the main reason that leads to the difficulty in carrying out the integral (5.18) with respect to s. Thereby, what we will do is to provide an appropriate approximation for this term through a truncated Taylor series expansion. Given that $N(\cdot)$ is a bounded function, it is natural to notice that the integrand in Equation (5.18) will approach zero if the absolute value of s is large enough since e^{-s^2} decreases rapidly as s becomes larger, which implies that we should focus on the case that the absolute value of s is not very large when we make approximation. As a result, if we take into account the fact that $\frac{D}{K}$ should be quite small in real markets, we can obtain

$$\begin{aligned}
\ln(e^s - \frac{D}{K}) &= \ln(e^s) - \frac{D}{K}e^{-s} + \mathbb{O}(\frac{D^2}{K^2}), \\
&= \ln(e^s) - \frac{D}{K}(1-s) + \mathbb{O}(\frac{D^2}{K^2}) + \frac{D}{K}\mathbb{O}(s^2), \\
&= s(1+\frac{D}{K}) - \frac{D}{K} + \mathbb{O}(\frac{D}{K}).
\end{aligned}$$

Hence, in the following, $\ln(e^s - \frac{D}{K})$ will be replaced by $s(1+\frac{D}{K}) - \frac{D}{K}$ in deriving the

closed-form approximation. Actually, if we rewrite Equation (5.18) as

$$(5.18) = A_1^{(1)} - A_2^{(1)} - A_3^{(1)}, \tag{5.19}$$

where

$$\begin{aligned} A_1^{(1)} &= \frac{1}{2\sqrt{\pi\tau}} \int_{\ln(\frac{D}{K})}^{+\infty} e^{\frac{1}{2}(m+1)s - \frac{(x-s)^2}{4\tau}} N(z_1) ds, \\ A_2^{(1)} &= \frac{D}{K} \frac{1}{2\sqrt{\pi\tau}} \int_{\ln(\frac{D}{K})}^{+\infty} e^{\frac{1}{2}(m-1)s - \frac{(x-s)^2}{4\tau}} N(z_1) ds, \\ A_3^{(1)} &= \frac{1}{2\sqrt{\pi\tau}} e^{-r(T-t_d)} \int_{\ln(\frac{D}{K})}^{+\infty} e^{\frac{1}{2}(m-1)s - \frac{(x-s)^2}{4\tau}} N(z_2) ds, \end{aligned}$$

we need to work out the above three integrals respectively. Then, applying the approximation $\ln(e^s - \frac{D}{K}) \doteq s(1 + \frac{D}{K}) - \frac{D}{K}$ yields

$$A_1^{(1)} \doteq \frac{1}{2\sqrt{\pi\tau}} e^{\frac{m+1}{2}x + \frac{(m+1)^2}{4}\tau} \int_{\ln(\frac{D}{K})}^{+\infty} e^{-\frac{[s-(m+1)\tau - x]^2}{4\tau}} N(\frac{s(1+\frac{D}{K}) - \frac{D}{K} + (r + \frac{1}{2}\sigma^2)(T - t_d)}{\sigma\sqrt{T - t_d}}) ds, \tag{5.20}$$

which can be further approximated to

$$(5.20) \doteq \frac{1}{2\sqrt{\pi\tau}} e^{\frac{m+1}{2}x + \frac{(m+1)^2}{4}\tau} \int_{-\infty}^{+\infty} e^{-\frac{[s-(m+1)\tau - x]^2}{4\tau}} N(\frac{s(1+\frac{D}{K}) - \frac{D}{K} + (r + \frac{1}{2}\sigma^2)(T - t_d)}{\sigma\sqrt{T - t_d}}) ds, \tag{5.21}$$

with the fact that $\ln(\frac{D}{K})$ will approach $-\infty$ when $\frac{D}{K}$ is close to zero. Then, applying the following transformation $y = \frac{s - (m+1)\tau - x}{\sqrt{2\tau}}$ yields

$$\begin{aligned} (5.21) &= e^{\frac{m+1}{2}x + \frac{(m+1)^2}{4}\tau} \int_{-\infty}^{+\infty} \frac{1}{\sqrt{2\pi}} e^{-\frac{y^2}{2}} \times \\ & N \left(\frac{(1+\frac{D}{K})[\sqrt{2\tau}y + x + (m+1)\tau] + (r + \frac{1}{2}\sigma^2)(T - t_d) - \frac{D}{K}}{\sigma\sqrt{T - t_d}}\right) dy, \\ &= e^{\frac{m+1}{2}x + \frac{(m+1)^2}{4}\tau} N\left(\frac{(1+\frac{D}{K})[x + (m+1)\tau] + (r + \frac{1}{2}\sigma^2)(T - t_d) - \frac{D}{K}}{\sigma\sqrt{T - t_d + (1+\frac{D}{K})^2(t_d - t)}}\right), \end{aligned} \tag{5.22}$$

the last step of which is obtained according to Lemma 2 in [8]. In a similar fashion, the

approximation of $A_2^{(1)}$ and $A_3^{(1)}$ can then be derived as

$$\begin{aligned} A_2^{(1)} &\doteq \frac{D}{K} e^{\frac{m-1}{2}x+\frac{(m-1)^2}{4}\tau} N\left(\frac{(1+\frac{D}{K})[x+(m-1)\tau]+(r+\frac{1}{2}\sigma^2)(T-td)-\frac{D}{K}}{\sigma\sqrt{T-t_d+(1+\frac{D}{K})^2(t_d-t)}}\right), \\ A_3^{(1)} &\doteq e^{-r(T-t_d)} e^{\frac{m-1}{2}x+\frac{(m-1)^2}{4}\tau} N\left(\frac{(1+\frac{D}{K})[x+(m-1)\tau]+(r-\frac{1}{2}\sigma^2)(T-td)-\frac{D}{K}}{\sigma\sqrt{T-t_d+(1+\frac{D}{K})^2(t_d-t)}}\right). \end{aligned}$$

Finally, to show the solution under the original parameters, we arrive at

$$f^{(1)}(S,t;t_d) = SN(d_0^{(1)}) - De^{-r(t_d-t)}N(d_1^{(1)}) - Ke^{-r(T-t)}N(d_2^{(1)}), \tag{5.23}$$

where

$$\begin{aligned} d_0^{(1)} &= \frac{(1+\frac{D}{K})\ln(\frac{S}{K})+(r+\frac{1}{2}\sigma^2)[T-td+(1+\frac{D}{K})(t_d-t)]-\frac{D}{K}}{\sigma\sqrt{T-t_d+(1+\frac{D}{K})^2(t_d-t)}}, \\ d_1^{(1)} &= \frac{(1+\frac{D}{K})\ln(\frac{S}{K})+(r+\frac{1}{2}\sigma^2)(T-td)+(r-\frac{1}{2}\sigma^2)(1+\frac{D}{K})(t_d-t)-\frac{D}{K}}{\sigma\sqrt{T-t_d+(1+\frac{D}{K})^2(t_d-t)}}, \\ d_2^{(1)} &= \frac{(1+\frac{D}{K})\ln(\frac{S}{K})+(r-\frac{1}{2}\sigma^2)[T-td+(1+\frac{D}{K})(t_d-t)]-\frac{D}{K}}{\sigma\sqrt{T-t_d+(1+\frac{D}{K})^2(t_d-t)}}. \end{aligned}$$

By now, we have established the closed-form formula for the case of the single fix-amount dividend and we name it "one-period formula". However, as known to us all that the stock could pay the dividend more than one time during the lifetime of an option in real markets, the one-period formula would become inadequate, and thus whether a simple formula could also be obtained for the case of multiple fixed-amount dividends with our approximation method is vital and will be presented in the next subsection.

5.3.2 Multiple fixed-amount dividends

In this subsection, we will show that our approximation approach in the last subsection can be extended to the multiple-period case, where the stock pays dividend D_n at time t_{d_n} with $t_{d_n} > t_{d_{n-1}}$. We will firstly consider a two-period case and then give a general formula for n-period case with the help of mathematical induction.

When the stock only pays D_1 and D_2 at time t_{d_1} and t_{d_2} respectively, it is easy to deduce that the option price will equal to the B-S price $C(S,t)$ if $t > t_{d_2}$, while it can be calculated from our one-period formula if $t_{d_1} < t < t_{d_2}$. So the only period that we

need to price is $[0,\ t_{d_1}]$, where the pricing PDE is still the B-S equation with the terminal condition

$$f^{(2)}(S_{t_{d_1}}, t_{d_1^-}; t_{d_1}, t_{d_2}) = \begin{cases} f^{(1)}(S_{t_{d_1}} - D_1, t_{d_1^+}; t_{d_2}), & S_{t_{d_1}} \geq D_1, \\ 0, & S_{t_{d_1}} < D_1, \end{cases}$$

With the same transformation (5.16) except that $f^{(1)}$ and t_d are replaced by $f^{(2)}$ and t_{d_1} respectively, we can certainly obtain the following PDE

$$\frac{\partial u}{\partial \tau} = \frac{\partial^2 u}{\partial x^2},$$

with the initial condition

$$u(x,0) = \begin{cases} e^{\frac{1}{2}(m-1)x}[(e^x - \frac{D}{K})N(d_{00}^{(1)}) - \frac{D}{K}e^{-r(t_{d_2}-t_{d_1})}N(d_{11}^{(1)}) + e^{-r(T-t_{d_1})}N(d_{22}^{(1)})], & x \geq \ln(\frac{D_1}{K}), \\ 0, & x < \ln(\frac{D_1}{K}), \end{cases}$$

where $\{d_{kk}^{(1)}, k = 0,1,2\}$ are the same as $\{d_k^{(1)}, k = 0,1,2\}$ but t and t_d are replaced by t_{d_1} and t_{d_2} respectively. To solve this heat equation, we can again apply the convolution and obtain

$$u(x,\tau) = A_1^{(2)} - A_2^{(2)} - A_3^{(2)} - A_4^{(2)}, \tag{5.24}$$

where

$$\begin{aligned} A_1^{(2)} &= \frac{1}{2\sqrt{\pi\tau}} \int_{\ln(\frac{D}{K})}^{+\infty} e^{\frac{1}{2}(m+1)s - \frac{(x-s)^2}{4\tau}} N(d_{00}^{(1)}) ds, \\ A_2^{(2)} &= \frac{D}{K}\frac{1}{2\sqrt{\pi\tau}} \int_{\ln(\frac{D}{K})}^{+\infty} e^{\frac{1}{2}(m-1)s - \frac{(x-s)^2}{4\tau}} N(d_{00}^{(1)}) ds, \\ A_3^{(2)} &= \frac{D}{K}e^{-r(t_{d_2}-t_{d_1})}\frac{1}{2\sqrt{\pi\tau}} \int_{\ln(\frac{D}{K})}^{+\infty} e^{\frac{1}{2}(m-1)s - \frac{(x-s)^2}{4\tau}} N(d_{11}^{(1)}) ds, \\ A_4^{(2)} &= e^{-r(T-t_{d_1})}\frac{1}{2\sqrt{\pi\tau}} \int_{\ln(\frac{D}{K})}^{+\infty} e^{\frac{1}{2}(m-1)s - \frac{(x-s)^2}{4\tau}} N(d_{22}^{(1)}) ds. \end{aligned}$$

It is obvious that all the above four integrals are to be worked out to find the final solution. When we apply the same approximation method as the last subsection, we would surely obtain

$$A_1^{(2)} \doteq \frac{1}{2\sqrt{\pi\tau}} e^{\frac{m+1}{2}x + \frac{(m+1)^2}{4}\tau} \int_{-\infty}^{+\infty} e^{-\frac{[s-(m+1)\tau - x]^2}{4\tau}} N(d_{00}^{(1)}) ds, \tag{5.25}$$

which can be further calculated as

$$\begin{aligned}(5.25) &= e^{\frac{m+1}{2}x+\frac{(m+1)^2}{4}\tau}\int_{-\infty}^{+\infty}\frac{1}{\sqrt{2\pi}}e^{-\frac{y^2}{2}}N(\frac{(1+\frac{D_2}{K})(1+\frac{D_1}{K})[\sqrt{2\tau}y+x+(m+1)\tau]+M}{\sigma\sqrt{T-t_{d_2}+(1+\frac{D_2}{K})^2(t_{d_2}-t_{d_1})}}),\\ &= e^{\frac{m+1}{2}x+\frac{(m+1)^2}{4}\tau}N(\frac{(1+\frac{D_2}{K})(1+\frac{D_1}{K})[x+(m+1)\tau]+M}{\sigma\sqrt{T-t_{d_2}+(1+\frac{D_2}{K})^2(t_{d_2}-t_{d_1})+(1+\frac{D_2}{K})^2(1+\frac{D_1}{K})^2(t_{d_1}-t)}}),\end{aligned}$$

with the transformation of $y=\dfrac{s-(m+1)\tau-x}{\sqrt{2\tau}}$. Here,

$$M=(r+\frac{1}{2}\sigma^2)[T-t_{d_2}+(1+\frac{D_2}{K})(t_{d_2}-t_{d_1})]-\frac{D_1}{K}(1+\frac{D_2}{K})-\frac{D_2}{K}.$$

With a similar manner, A_2^2, A_3^2 and A_4^2 could be figured out straightforwardly. Therefore, the final solution for this two-period case is derived in the form of original variables as

$$f^{(2)}(S,t;t_{d_1},t_{d_2})=SN(d_0^{(2)})-D_1e^{-r(t_{d_1}-t)}N(d_1^{(2)})-D_2e^{-r(t_{d_2}-t)}N(d_2^{(2)})-Ke^{-r(T-t)}N(d_3^{(2)}),$$

with $\{d_k^{(2)},k=1,2,3,4\}$ being

$$\begin{aligned}d_0^{(2)} &= \frac{L+(r+\frac{1}{2}\sigma^2)[T-t_{d_2}+(1+\frac{D_2}{K})(t_{d_2}-t_{d_1})+(1+\frac{D_2}{K})(1+\frac{D_1}{K})(t_{d_1}-t)]}{\sigma\sqrt{T-t_{d_2}+(1+\frac{D_2}{K})^2(t_{d_2}-t_{d_1})+(1+\frac{D_2}{K})^2(1+\frac{D_1}{K})^2(t_{d_1}-t)}},\\ d_1^{(2)} &= \frac{L+(r+\frac{1}{2}\sigma^2)[T-t_{d_2}+(1+\frac{D_2}{K})(t_{d_2}-t_{d_1})]+(r-\frac{1}{2}\sigma^2)(1+\frac{D_2}{K})(1+\frac{D_1}{K})(t_{d_1}-t)}{\sigma\sqrt{T-t_{d_2}+(1+\frac{D_2}{K})^2(t_{d_2}-t_{d_1})+(1+\frac{D_2}{K})^2(1+\frac{D_1}{K})^2(t_{d_1}-t)}},\\ d_2^{(2)} &= \frac{L+(r+\frac{1}{2}\sigma^2)(T-t_{d_2})+(r-\frac{1}{2}\sigma^2)[(1+\frac{D_2}{K})(t_{d_2}-t_{d_1})+(1+\frac{D_2}{K})(1+\frac{D_1}{K})(t_{d_1}-t)]}{\sigma\sqrt{T-t_{d_2}+(1+\frac{D_2}{K})^2(t_{d_2}-t_{d_1})+(1+\frac{D_2}{K})^2(1+\frac{D_1}{K})^2(t_{d_1}-t)}},\\ d_3^{(2)} &= \frac{L+(r-\frac{1}{2}\sigma^2)[T-t_{d_2}+(1+\frac{D_2}{K})(t_{d_2}-t_{d_1})+(1+\frac{D_2}{K})(1+\frac{D_1}{K})(t_{d_1}-t)]}{\sigma\sqrt{T-t_{d_2}+(1+\frac{D_2}{K})^2(t_{d_2}-t_{d_1})+(1+\frac{D_2}{K})^2(1+\frac{D_1}{K})^2(t_{d_1}-t)}},\\ L &= (1+\frac{D_2}{K})(1+\frac{D_1}{K})\ln(\frac{S}{K})-\frac{D_1}{K}(1+\frac{D_2}{K})-\frac{D_2}{K}.\end{aligned}$$

Although it seems that there is a long way to go before we can find a general solution for the n-period case, the derivation of this general case is actually similar to the two-period case if the time period [0,T] is separated into two parts, i.e., [0,t_{d_1}] and [t_{d_1},T]. In this sense, what we only need is the solution of the $(n-1)$-period case, which apparently depends on the $(n-2)$-period case. As a result, with the essence of the mathematical induction method, we could eventually show that the general solution for the n-period

case can be specified as

$$f^{(n)}(S,t;t_{d_k},1\le k\le n)=SN(d_0^{(n)})-\sum_{k=1}^{n}D_ke^{-r(t_{d_k}-t)}N(d_k^{(n)})-Ke^{-r(T-t)}N(d_{n+1}^{(n)}), \tag{5.26}$$

where

$$\begin{aligned}
&d_k^{(n)}=\frac{B+C}{\sigma\sqrt{\sum_{j=1}^{n+1}\{[\Pi_{i=j}^{n+1}(1+\frac{D_i}{K})]^2(t_{d_j}-t_{d_{j-1}})\}}},0\le k\le n+1,n\ge 0,\\
&B=[\Pi_{j=1}^{n+1}(1+\frac{D_j}{K})]\ln(\frac{S}{K})-\sum_{j=1}^{n+1}\{[\Pi_{i=j+1}^{n+1}(1+\frac{D_i}{K})]\frac{D_j}{K}\},\\
&C=(r-\frac{1}{2}\sigma^2)\sum_{j=1}^{k}\{[\Pi_{i=j}^{n+1}(1+\frac{D_i}{K})](t_{d_j}-t_{d_{j-1}})\}+(r+\frac{1}{2}\sigma^2)\sum_{j=k+1}^{n+1}\{[\Pi_{i=j}^{n+1}(1+\frac{D_i}{K})](t_{d_j}-t_{d_{j-1}})\},\\
&T=t_{d_{n+1}},\quad t=t_{d_0},\quad D_{n+1}=0.
\end{aligned}$$

It should be particularly stressed that we have now approximated European option prices with n-period dividends, which is originally in the form of $(n+1)$-dimensional integrals, by the sum of $(n+2)$ one-dimensional integrals. This could certainly save us much effort in the numerical calculation of option prices. It should also be noticed that this general formula also suits the non-dividend case ($n=0$), where our formula becomes the B-S price formula, and this is consistent with our expectation. On the other hand, after an approximation formula is derived, it is natural for us to consider its accuracy, which will be presented in the next subsection.

5.3.3 Numerical verification

In this subsection, we will show the behavior of our approximation by comparing our prices with those true values obtained through direct numerical integration of the exact solution. For simplicity, the case of the single fixed-amount dividend will be used as a representative to show the comparison results. In our numerical experiment, the expiry time of the European call option T is set to be 1 and the present time is 0. The risk-free interest rate and the initial stock price take the value of 0.03 and 100 respectively.

Depicted in Figure 5.1 is the comparison of our price with the true price calculated from Equation (5.18) and results show that our approximation is quite accurate. To be more specific, what can be easily found in Figure 5.1(a) is that no matter the European

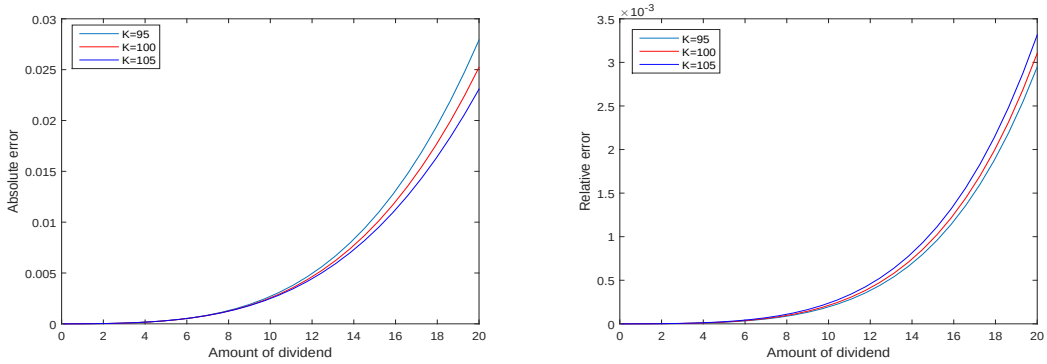

(a) Absolute error between our approximation and true price.

(b) Relative error between our approximation and true price.

Figure 5.1: Our approximation vs true price with different amount of dividend. Model parameters are: $\sigma = 0.4, t_d = 0.3$.

call option is "in the money", "at the money" or "out of money", the absolute error is a monotonic increasing function with respect to the amount of dividend, which is consistent with our expectation since our approximation is based on the fact that the dividend is relatively small according to the stock price level. Furthermore, the "in the money" option price suffers from the largest absolute error, which is also reasonable if we take into consideration that its price is also the largest among the three kinds of options. When we turn to Figure 5.1(b), a similar pattern could be witnessed that the relative error between the two prices is still an increasing function of the dividend level. However, if we take a close look, there exists some difference that the "out of money" options, instead of the "in the money" ones, experience the most relative error. The main explanation for it can be that the price for this kind of option is quite low. To view these two sub-figures together, it is not difficult to find that when the dividend rate reaches approximately 20%, the maximum absolute and relative error are only 0.028 and 0.33% respectively, which are rather small, in contrast to the huge dividend rate.

A completely different picture is exhibited in Figure 5.2, where the error is shown according to the dividend payment time. As shown in Figure 5.2(a), with dividend payment time becoming closer to expiry, the absolute error will increase to some extent and then fall below the initial level for all the options included in different "moneyness". Although it seems to be strange at first glance of this peculiar shape, it is not difficult to explain the behavior of the errors as a function of the time to dividend payment, if we go back to the place where the approximation was made, i.e., Equation (5.20). If the dividend payment

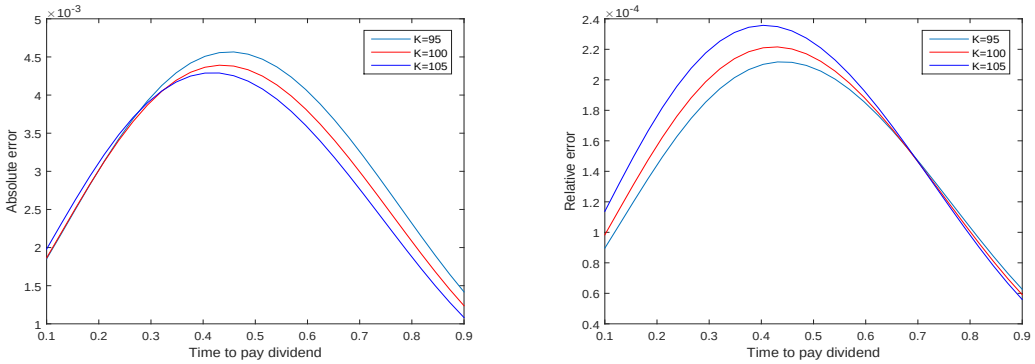

(a) Absolute error between our approximation and true price.

(b) Relative error between our approximation and true price.

Figure 5.2: Our approximation vs true price with different dividend payment time. Model parameters are: $\sigma = 0.6, D = 10$.

time is increased, the remaining time between this dividend payment time and expiry time is decreased, which would lead to more time range being exposed to approximation and thus has increased the total error. However, once the dividend payment time is increased beyond a critical point, a further increase does not contribute to more errors, as a result of the change of the slopes in the normal distribution function involved in approximation formula beyond this critical point. Furthermore, the absolute errors for the three kinds of options are quite close when the dividend payment day is near the present time with "out of money" options possessing the largest error. When the payment day becomes closer to expiry, the distance between the three errors enlarges and the "in the money" option price takes the place of possessing the largest error. In contrast, a different phenomenon could be observed in Figure 5.2(b). Although the relative error experiences a similar increase and a subsequent decrease when the dividend payment time increase from 0.1 to 0.9, and it for the "out of money" option price also changes from the highest to the lowest, an opposite phenomenon appears, showing that the gap among the relative errors for three kinds of options is relatively large if the dividend is paid early and it will be narrowed down when the dividend payment time is close to expiry. This is mainly because the price of options will increase if the stock pay the dividend later. Again, the whole Figure 5.2 demonstrates the fact that although the dividend rate is as high as around 10%, the absolute and relative error are less than 0.005 and 0.024% respectively, which reflects that our approximation is satisfactory.

It should be stressed that one great advantage of our approximation is the speed with

Table 5.1: The comparison of CPU time (seconds) with both approaches.

Number of dividends	Exact solution	Our approximation
One	$2.94 * 10^{-3}$	$2.09 * 10^{-4}$
Two	$9.10 * 10^{-1}$	$2.48 * 10^{-4}$
Three	$3.21 * 10^{+2}$	$3.17 * 10^{-4}$

which option price can be fast calculated. Such an advantage of an enormously faster calculation speed at the expenses of a minor sacrificed accuracy, compared with the case if the price has to be calculated with the exact solution procedure stage by stage (denoted by exact solution in the following), justifies the potential application of the newly proposed approximation formula in finance industry, particularly in current algorithmic trading rage, since the Black-Scholes formulae are still heavily used in Finance industry today. To substantiate our claim, the CPU times needed to evaluate option prices with exact solution and our approximation, respectively, for the cases of one, two, and three dividends are presented in Table 5.1. Clearly, it only takes very little time, which is around the order of $10^{-4}s$ when pricing options with our formula, and this order remains the same as the number of dividends is increased. This is expected since the increased number of discrete dividend payments only leads to more one-dimensional integrals to be calculated, which is not time-consuming at all. In contrast, it costs a lot more when we evaluate options with the exact solution procedure stage by stage. Even for the case of one dividend, the consumed CPU with exact solution is already about 10 times more than that with our approximation. The consumed CPU time with exact solution has increased exponentially and by the time when we need to calculate the option price with only three dividend payments, the order of the consumed CPU has already reached $10^{+2}s$ or it is 10^6 times more than that of our formula!

Table 5.2: The relative errors between our approximation and exact solution.

Number of dividends	Case A	Case B
One	$4.35 * 10^{-7}$	$2.10 * 10^{-4}$
Two	$1.14 * 10^{-6}$	$9.47 * 10^{-4}$
Three	$2.18 * 10^{-6}$	$2.6 * 10^{-3}$

Having already known the advantage of our approximation in terms of the CPU time, the accuracy of our formula should also be checked against the increase of the number of dividends, making sure that one does not lose too much in terms of accuracy while gaining speed. Table 5.2 displays the relative errors between our approximation and exact

solution. To ensure that a meaningful discussion is carried out, with regard to accuracy as well as its sensitivity against dividend amount, we have presented here with two cases representing low and high dividends respectively. In Case A, a relatively small dividend of \$1 is set for each dividend payment, while in Case B we have increased the dividend amount 10-folds higher. From Table 5.2, we can observe that the relative error between our formula and exact solution will increase when the number of dividends is increased, which is also shown in previous figures. It should also be pointed out that the order of the relative error remains almost the same with the increased number of dividends, which implies that the relative error would still stay in a satisfactory range when the number of dividends is relatively large, considering the fact that the relative error is less than 10^{-5} when the dividend is around 1% of the underlying price. Even in the extreme cases with dividend level being around 10%, our formula can still be regarded as a good approximation of the true formula as the relative error is only $2.6 * 10^{-3}$ for the case of three-dividend payments.

5.4 Conclusion

In this chapter, two relevant issues regarding discrete dividends are considered. First of all, a paradox that the dividend payment date of a discrete dividend that is proportional to the value of the underlying asset value right before the dividend payment time appears to have no influence on the option price is explained mathematically and financially. The fundamental reason that the time of dividend payment is not involved in the pricing formula under the B-S framework is because this is the only "fair" way to count in the effect of a discrete dividend payment under the risk-neutral assumption when an option is priced. Then, a closed-form approximation formula for the price of European options with fixed-amount dividends is presented and its accuracy is also numerically checked. Obviously, our formula could certainly facilitate the application in real markets since no matter how many times the underlying pay its dividends before the expiry of the option, the formula is always the sum of one-dimensional integrals, the calculation of which can be rather rapid.

Chapter 6

Pricing European options with stochastic volatility under the minimal entropy martingale measure

6.1 Introduction

Although Black & Scholes [19] made a great contribution to the area of option pricing by proposing a simple and closed-form pricing formula for European options in 1973, their assumption for the log-returns of the underlying asset to follow a normal distribution proves to be an over simplification in some cases (it can not capture the features like skewness [188] and fat-tails [191] exhibited by the real market data), which may lead to the problem of mispricing. As a result, many modifications to the Black-Scholes model have been proposed, including one of the most well-known ways by relaxing the assumption of the constant volatility due to the observed "volatility smile" from market data [73].

In the literature, there are mainly two kinds of non-constant volatility models, i.e. local volatility and stochastic volatility model. Local volatility models were adopted by Dupire [74], Derman & Kani [67] and Rubinstein [195] and the volatility in their models was defined as a deterministic function of asset price and time. Although this kind of model appears to have certain advantages since it may relieve some computational burden

and fit well with a given market, it was shown that local volatility model is not as flexible as the stochastic volatility models [73] and it is even suggested in Hagan et. al [102] that the "smile dynamics" are poorly predicted by the local volatility model. Such kind of observations have made stochastic volatility models much more popular over local volatility models.

Stochastic volatility was first systematically studied by Scott [204] who numerically solved the option pricing problem with Monte Carlo simulations. It was further investigated by Hull & White [127] and Stein & Stein [213]; the former proposed a series approximation solution and the latter presented a closed-form formula for European option price. Unfortunately, their models are not satisfying since some drawbacks do exist. For example, the stochastic volatility process of Hull & White model does not possess the mean-reverting property, which is at odds with observations from many empirical studies [14], while the volatility can not always remain positive under some parameter settings of Stein & Stein model.

A breakthrough took place in 1993 when Heston [117] incorporated a specific model with the stochastic volatility possessing the mean-reverting and non-negative properties and derived a closed-form pricing formula based on the Fourier transform technique. However, despite its great success, one should notice that the pricing formula obtained by Heston is not the only price formula under the proposed model. This is because the market described by the Heston model is actually incomplete as a result of introducing stochastic volatility and thus derivative pricing is no longer independent of investors' risk preference. Thus, different choice of equivalent martingale measures will lead to different risk-neutral prices. There are then two issues one may face; a) we need a reasonable principle to select an appropriate martingale measure, and b) we need to overcome the difficulty of deriving a closed-form pricing formula associated with the chosen martingale measure.

In fact, there are several different martingale measures, such as minimal martingale measure [201], variance-optimal measure [164, 202], minimal reverse entropy martingale measure [203] and so on. The minimal entropy martingale measure considered here is one of them and is chosen by minimizing the relative entropy between the pricing measures and the physical measure. A financial interpretation for choosing the minimal entropy martingale measure was originally given in [91], which is related to the concept of expected utility maximization, and will be further illustrated later in this chapter showing that

choosing the minimal entropy martingale measure is equivalent to attaining the maximum expected utility, an action axiom in finance. Unfortunately, to the best of our knowledge, only numerical methods are applied to option pricing under this particular measure, and a closed-form pricing formula has hitherto not been found. A great advantage of having analytical closed-form formula in terms of option pricing is that considerable amount of time and effort can be spared when these formula are involved in the determination of model parameters; a feature that none of numerical pricing approaches could match. This is the main thrust behind our effort of searching for a closed-form solution of the Heston stochastic volatility model under the minimal entropy martingale measure.

Entropy is a concept originated from thermodynamics [64] and it has been applied to portfolio selection and asset pricing by a number of different authors, such as Philippatos & Wilson [190], who were believed to be the first to apply this concept to portfolio selection and adopted it as a measure of risk, and Buchen & Kelly [25], who estimated the distribution of the underlying from a set of option prices with the principle of maximum entropy. In contrast, we adopt the concept but use it in the context of pricing options in an incomplete market. Let us consider a stochastic process $S = (S_t)_{t\geq 0}$ defined on a probability space $(\Omega,\ \mathcal{F},\ \mathrm{P})$ and adapted to the filtration $\boldsymbol{F} = (\mathcal{F}_t)_{t\geq 0}$. The relative entropy $H(Q, P)$ of an equivalent martingale measure Q for S is then defined as

$$H(Q,P) = \begin{cases} E\left[\dfrac{dQ}{dP}\ln\left(\dfrac{dQ}{dP}\right)\right], & Q \ll P, \\ +\infty, & \text{otherwise}, \end{cases}$$

where E represents the expectation operator under measure P. We denote M as the set of martingale measures and Q_e as the minimal entropy martingale measure satisfying

$$H(Q_e, P) = \min_{Q\in M} H(Q, P).$$

It is proved by Frittelli [91] that a unique minimal entropy martingale measure equivalent to P exists under the assumption that there is an equivalent martingale measure Q_0 such that $H(Q_0, P) < +\infty$. Under this assumption, Hobson [118] managed to obtain an explicit expression of the dynamics for the underlying price and the volatility under the minimal entropy martingale measure with some particular settings. Following him, we take zero interest rate as a leading order approximation. This is a reasonable approximation because

the tenor of most exchange-traded options is often less than three months, which means the risk-free interest rate (often approximated by Treasury Bill Rates) should be quite low [1], and the changes in the value of the interest rate has little influence on option prices [211]. In this case, although the new PDE (partial differential equation) system governing the option price contains variable coefficients as a result of the introduction of time-dependent drift term in the volatility process, which has made the task of finding closed-form solutions much more difficult, we still managed to find a closed-form pricing formula in series form together with a lower bound for the radius of convergence. In addition, two numerical examples are provided to further demonstrate the speed of convergence of the series solution. To further validate the newly derived pricing formula, we have also carried out additional comparison of the results produced with the new formula and those directly obtained from solving the PDE with the finite difference method and from solving the SDE (stochastic differential equation) with Monte Carlo simulation.

The rest of the chapter is organized as follows. In Section 6.2, we will provide the financial meaning of the minimal entropy martingale measure. In Section 6.3, we will first briefly introduce the model we adopt and then derive a series solution to our PDE governing the European option price. Also, the convergence of our solution will be proved theoretically by giving a lower bound for the radius of convergence. In Section 6.4, the speed of convergence will be tested numerically, after which our formula is further verified by making comparison with the results obtained by the finite difference method and Monte Carlo simulation. In Section 6.5, the case when the time to expiry exceeds the derived lower bound is discussed, and a set of converged pricing formulae that suit different time ranges are presented, followed by some concluding remarks given in the last section.

6.2 Financial explanation for minimal entropy martingale measure

In this section, we will briefly review the relationship between minimizing the relative entropy and maximizing the expected exponential utility, which is actually one of the most important areas of research on the minimal entropy martingale measure.

According to the existing literature, Frittelli [91] and Bellini & Frittelli [15] provided an elaborate illustration about the link between the minimal entropy martingale measure

and maximum expected utility. By setting w_T be the attainable terminal wealth and the utility function be exponential, i.e.

$$u(x) = -e^{-x}, \tag{6.1}$$

the results were presented as

$$H(Q,P) = \sup_{w_T \in L^\infty : e^{-rT} E_Q(w_T) \leq 0} u^{-1}(E_P[u(w_T)]), \tag{6.2}$$

which implies that the relative entropy is indeed the maximum certainty equivalent [161], $u^{-1}(E_P[u(w_T)])$, of attainable wealth w_T with prices less than or equal to zero. Then the characteristics of the density of the minimal entropy martingale measure were given, showing the equivalence between maximization of the expected utility and adopting the minimal entropy martingale measure. In addition, Delbaen et. al [66] obtained a more generalized result, which considers a self-financing strategy and an extra contingent claim, further demonstrating that maximizing the expected utility is equivalent to minimizing the relative entropy with an exponential utility function specified as

$$u(x) = 1 - e^{-\alpha x}, \qquad \alpha > 0. \tag{6.3}$$

Moreover, how to construct an optimal strategy for a utility optimization problem through the dual problem of martingale measures was also documented in [228]. It should also be noticed that the minimal entropy martingale measure is quite useful when pricing contingent claims with utility indifference approaches [133, 214].

After the financial justification for choosing the minimal entropy martingale measure is illustrated, we are now ready to price European call options under this particular martingale measure, which will be presented in the next Section.

6.3 Closed-form formula

In this section we will firstly specify our model under the physical measure and then pricing dynamics will be proposed by means of measure transformation. After the model is established, the derivation of a closed-form pricing formula for European call options is provided based on the series expansion.

Let S_t be the underlying asset price and v_t be the volatility, the dynamics under the physical measure are specified as follows

$$\begin{aligned} \frac{dS_t}{S_t} &= \mu v_t dt + \sqrt{v_t} dB_t, \\ dv_t &= k(\theta - v_t)dt + \beta\sqrt{v_t} dW_t, \end{aligned}$$

where B_t and W_t are two standard Brownian motions with correlation ρ. It is obvious that this market is incomplete, where a claim can not be perfectly replicated, and there exists a set of equivalent martingale measures and correspondingly arbitrage-free prices. As a result, we need to choose an appropriate equivalent martingale measure for pricing contingent claims. Over the years, many principles have been developed, such as the minimal martingale measure [201], under which the price of "risk premium" is zero, and variance-optimal measure [164, 202], which is connected with quadratic utility function. The minimal entropy martingale measure adopted in this chapter is reasonable to choose according to the utility maximization argument in Section 6.2. Furthermore, no one has derived a closed-form solution under this measure. As a result, following [118], if we set

$$W_t = \rho B_t + \sqrt{1-\rho^2} C_t, \tag{6.4}$$

where B_t and C_t are two independent Brownian motions, the dynamics under the minimal entropy martingale measure Q can be obtained by the following transformation

$$\begin{aligned} dB_t^Q &= dB_t + \mu v \sqrt{v_t} dt, \\ dC_t^Q &= dC_t + \frac{1}{\beta\sqrt{1-\rho^2}} \lambda(\tau)\sqrt{v_t} dt, \end{aligned}$$

where $\tau = T - t$ and $\lambda(\tau) = 2\Delta \tanh(\Delta\tau + b) - k - \rho\beta\mu$. Here $\Delta = \sqrt{\frac{1}{4}k^2 + \frac{1}{2}k\rho\beta\mu + \frac{1}{4}\beta^2\mu^2}$ and $b = \tanh^{-1}(\frac{1}{2}\frac{k+\beta\rho\mu}{\Delta})$. Therefore, the corresponding expression for the dynamics can be derived as

$$\begin{aligned} \frac{dS_t}{S_t} &= \sqrt{v_t} dB_t^Q, \\ dv_t &= [k(\theta - v_t) - \beta\rho\mu v_t - \lambda(\tau)v_t]dt + \beta\sqrt{v_t} dW_t^Q. \end{aligned} \tag{6.5}$$

Let $U(S, v, t)$ be the European call option price written on the underlying asset S_t, then

according to the Feynman-Kac theorem [208], we can easily show that $U(S,v,t)$ satisfies the PDE

$$\begin{aligned}\frac{1}{2}vS^2\frac{\partial^2 U}{\partial S^2} &+ \rho\sigma vS\frac{\partial^2 U}{\partial S\partial v}+\frac{1}{2}\sigma^2 v\frac{\partial^2 U}{\partial v^2}\\ &+ [k(\theta-v)-\beta\rho\mu v-\lambda(\tau)v]\frac{\partial U}{\partial v}+\frac{\partial U}{\partial t}=0,\end{aligned} \tag{6.6}$$

with terminal condition:

$$U(S,v,T)=\max(S-K,0), \tag{6.7}$$

and boundary conditions:

$$\begin{aligned}&U(0,v,t)=0, \quad \lim_{S\to+\infty}U(S,v,t)=S,\\ &U(S,\infty,t)=S, \quad \lim_{v\to 0}U(S,v,t)=\max(S-K,0).\end{aligned}$$

Here, the reason for the option price to be equal to the payoff function at $v=0$ is illustrated in [235]. On the other hand, $U(S,v,t)$ can also be equivalently calculated as

$$\begin{aligned}U(S,v,t) &= e^{-r(T-t)}E^Q[(S_T-K)^+|S_t=S]\\ &= SE^Q[e^{-r(T-t)}\frac{S_T}{S}I_{\{S_T>K\}}|S_t=S]-Ke^{-r(T-t)}E^Q[I_{\{S_T>K\}}|S_t=S].\end{aligned}$$

To seek a solution in an affine form later, we can let $U(S,v,t)$ take the form of

$$U(S,v,t)=SP_1(x,v,t)-Ke^{-r(T-t)}P_2(x,v,t). \tag{6.8}$$

Substituting Equation (6.8) into (6.6) and applying transformation of $x=\ln(S)$ yield the following PDE

$$\begin{aligned}\frac{1}{2}v\frac{\partial^2 P_j}{\partial x^2} &+ \rho\sigma v\frac{\partial^2 P_j}{\partial x\partial v}+\frac{1}{2}\sigma^2 v\frac{\partial^2 P_j}{\partial v^2}+l_j v\frac{\partial P_j}{\partial x}\\ &+ [k(\theta-v)-\beta\rho\mu v-\lambda(\tau)v+m_j v]\frac{\partial P_j}{\partial v}+\frac{\partial P_j}{\partial t}=0,\end{aligned} \tag{6.9}$$

for $j=1,2$, where $l_1=\frac{1}{2}, l_2=-\frac{1}{2}, m_1=\rho\sigma, m_2=0$. Now the terminal conditions for P_j become

$$P_j(x,v,T;\ln[K])=I_{\{x\geq\ln[K]\}}.$$

Let us denote $y = \ln[K]$ and assume that $f_j(x, v, t; \phi)$ be the conditional characteristic function of x_T, i.e.

$$f_j(x, v, t; \phi) = E^Q[e^{i\phi x_T} | x_t = x, v_t = v]. \tag{6.10}$$

It is not difficult to deduce that $f_j(x, v, t; \phi)$ satisfies the same PDE as $P_j(x, v, t; y)$ and thus we obtain

$$\begin{aligned} \frac{1}{2}v\frac{\partial^2 f_j}{\partial x^2} &+ \rho\sigma v\frac{\partial^2 f_j}{\partial x \partial v} + \frac{1}{2}\sigma^2 v\frac{\partial^2 f_j}{\partial v^2} + l_j v\frac{\partial f_j}{\partial x} \\ &+ [k(\theta - v) - \beta\rho\mu v - \lambda(\tau)v + m_j v]\frac{\partial f_j}{\partial v} + \frac{\partial f_j}{\partial t} = 0, \end{aligned} \tag{6.11}$$

with known terminal condition $f_j(x, v, T; \phi) = e^{i\phi x}$. Considering the results in [117], it is natural for us to assume that there exists an affine structure solution to PDE (6.11) as

$$f_j = e^{C(\tau;\phi) + D(\tau;\phi)v + i\phi x}. \tag{6.12}$$

Hereafter, i denotes the imaginary unit. Therefore, by substituting (6.12) into (6.11), we can obtain the following equation after some calculation

$$\{\frac{1}{2}\sigma^2 D^2 + [i\rho\sigma\phi - k + m_j - \beta\rho\mu - \lambda(\tau)]D + (l_j i\phi - \frac{1}{2}\phi^2) - D^{'}(\tau)\}v + [k\theta D - C^{'}(\tau)] = 0, \tag{6.13}$$

which implies that the coefficients of v^n should be set to be zero for every n respectively since v is arbitrary. As a result, we have the following two ODEs (ordinary differential equations)

$$D^{'}(\tau) = \frac{1}{2}\sigma^2 D^2 + [i\rho\sigma\phi - k + m_j - \beta\rho\mu - \lambda(\tau)]D + (l_j i\phi - \frac{1}{2}\phi^2), \tag{6.14}$$

$$C^{'}(\tau) = k\theta D, \tag{6.15}$$

with initial condition $C(0) = D(0) = 0$. It is obvious that if we can derive the solution of $D(\tau; \phi)$, then $C(\tau; \phi)$ will be obtained straightforwardly by direct integration. As a result, what we need to do is to focus on $D(\tau; \phi)$. Actually, it should be noticed that ODE (6.14) is actually a Riccati Equation with variable coefficients, which brings extra burden in finding a closed-form solution for it.

We set $q_0 = l_j i\phi - \frac{1}{2}\phi^2$, $q_1 = i\rho\sigma\phi - k + m_j - \beta\rho\mu - \lambda(\tau)$ and $q_2 = \frac{1}{2}\sigma^2$. After this

crucial change of the variables, it is easy to find that q_1 can be further simplified as

$$q_1 = i\rho\sigma\phi + m_j - 2\Delta \tanh(\Delta\tau + b).$$

By applying the transformation of $D = -\dfrac{u^{'}}{q_2 u}$, the Riccati equation becomes a second-order linear ODE with variable coefficients as

$$u^{''} - q_1 u^{'} + q_0 q_2 u = 0, \tag{6.16}$$

with $u^{'}(0) = 0$. Although this kind of ODE can be easily solved when its coefficients are all constant, it still poses an obstacle when its coefficients are a function of the variable τ as the case we end up with in (6.16). By setting

$$u = \sum_{n=0}^{\infty} a_n \tau^n, \tag{6.17}$$

we obtain

$$\begin{aligned} u^{'} &= \sum_{n=0}^{\infty} (n+1) a_{n+1} \tau^n, \\ u^{''} &= \sum_{n=0}^{\infty} (n+1)(n+2) a_{n+2} \tau^n. \end{aligned} \tag{6.18}$$

What we need to do now is to expand $\tanh(\Delta\tau + b)$ as a series with respect to τ. However, the coefficients of the series would be very complicated and the property of convergence can hardly be studied as far as the Taylor series for $\tanh(x)$ is concerned, which is a major reason for us to seek alternative ways.

Since e^x can be expanded as

$$e^x = \sum_{n=0}^{\infty} \frac{x^n}{n!}, \tag{6.19}$$

and the RHS (right hand side) of Equation (6.19) is a power series, whose radius of convergence for any given x can be calculated as

$$\lim_{n\to\infty} \left| \frac{\frac{1}{n!} x^n}{\frac{1}{(n+1)!} x^{n+1}} \right| = \lim_{n\to\infty} \left| \frac{n+1}{x} \right| = +\infty, \tag{6.20}$$

we rewrite $\tanh(x)$ as

$$\tanh(x) = \frac{e^{2x}-1}{e^{2x}+1}, \tag{6.21}$$

since Equation (6.20) means that Equation (6.19) holds for any x. As a result, ODE (6.16) can be rearranged as

$$(e^{2b}\cdot e^{2\Delta\tau}+1)u^{''} - [(i\rho\sigma\phi+m_j-2\Delta)e^{2b}e^{2\Delta\tau}+(i\rho\sigma\phi+m_j+2\Delta)]u^{'} + (e^{2b}\cdot e^{2\Delta\tau}+1)q_0q_2u = 0. \tag{6.22}$$

According to Equation (6.19) we know that

$$e^{2\Delta\tau} = \sum_{n=0}^{\infty} c_n\tau^n, \tag{6.23}$$

where $c_n = \frac{1}{n!}(2\Delta)^n$. Therefore, applying Equation (6.18) and (6.23) into (6.22) yields

$$\begin{aligned}(e^{2b}\sum_{n=0}^{\infty} c_n\tau^n + 1)\sum_{n=0}^{\infty}(n+1)(n+2)a_{n+2}\tau^n + (e^{2b}\sum_{n=0}^{\infty} c_n\tau^n + 1)q_0q_2\sum_{n=0}^{\infty} a_n\tau^n \\ -[(i\rho\sigma\phi + m_j - 2\Delta)e^{2b}\sum_{n=0}^{\infty} c_n\tau^n + (i\rho\sigma\phi + m_j + 2\Delta)]\sum_{n=0}^{\infty}(n+1)a_{n+1}\tau^n = 0.\end{aligned} \tag{6.24}$$

As Equation (6.24) should hold for any τ, the coefficients of $\{\tau^k, \forall k \geq 0\}$ should be equal to zero and thus we have

$$(k+1)(k+2)a_{k+2} + e^{2b}\sum_{i=0}^{k}[(k-i+2)(k-i+1)a_{k-i+2}c_i] + I_2 - I_1 = 0, \tag{6.25}$$

for $k \geq 0$, where

$$\begin{aligned} I_1 &= \{(i\rho\sigma\phi + m_j - 2\Delta)e^{2b}\sum_{i=0}^{k}[(k-i+1)a_{k-i+1}c_i] + (i\rho\sigma\phi + m_j + 2\Delta)(k+1)a_{k+1}\} = 0, \\ I_2 &= e^{2b}q_0q_2\sum_{i=0}^{k}(a_{k-i}c_i) + q_0q_2a_k. \end{aligned}$$

As a result, $\{a_{k+2}, k \geq 0\}$ can be easily obtained once $\{a_n, n = 0, 1, 2, .., k+1\}$ according to the following equation derived from Equation (6.25)

$$a_{k+2} = \frac{I_1 - I_2 - e^{2b}\sum_{i=1}^{k}[(k-i+1)(k-i+2)a_{k-i+2}c_i]}{(e^{2b}+1)(k+2)(k+1)}, \quad k \geq 0. \tag{6.26}$$

One may think that $D(\tau;\phi)$ has been solved by now. However, we only have $a_1 = 0$ from $u^{'}(0) = D(0) = 0$, which keeps $\{a_{k+2}, k \geq 0\}$ still unknown without the value of a_0. Fortunately, $D(\tau;\phi)$ takes the form as

$$D(\tau) = -\frac{1}{q_2} \cdot \frac{\sum_{n=0}^{\infty}(n+1)a_{n+1}\tau^n}{\sum_{n=0}^{\infty} a_n\tau^n}, \tag{6.27}$$

which means that we do not have to derive a_n since $D(\tau)$ can be further represented by

$$D(\tau) = -\frac{1}{q_2} \cdot \frac{\sum_{n=0}^{\infty}(n+1)\frac{a_{n+1}}{a_0}\tau^n}{\sum_{n=0}^{\infty} \frac{a_n}{a_0}\tau^n}. \tag{6.28}$$

It should be noticed that if we define

$$\hat{a}_k = \frac{a_k}{a_0}, \quad k \geq 0, \tag{6.29}$$

all $\{\hat{a}_k, k \geq 0\}$ can be immediately derived due to the expression

$$\hat{a}_{k+2} = \frac{\hat{I}_1 - \hat{I}_2 - e^{2b}\sum_{i=1}^{k}[(k-i+1)(k-i+2)\hat{a}_{k-i+2}c_i]}{(e^{2b}+1)(k+2)(k+1)}, \quad k \geq 0, \tag{6.30}$$

with $\hat{a}_0 = 1, \hat{a}_1 = 0$. Here, $\hat{I}_1$ and $\hat{I}_2$ can be respectively expressed as

$$\begin{aligned}
\hat{I}_1 &= \{(i\rho\sigma\phi + m_j - 2\Delta)e^{2b}\sum_{i=0}^{k}[(k-i+1)\hat{a}_{k-i+1}c_i] + (i\rho\sigma\phi + m_j + 2\Delta)(k+1)\hat{a}_{k+1}\}, \\
\hat{I}_2 &= e^{2b}q_0q_2\sum_{i=0}^{k}(\hat{a}_{k-i}c_i) + q_0q_2\hat{a}_k.
\end{aligned}$$

Therefore, we have finally arrived at the desired result with

$$D(\tau) = -\frac{1}{q_2} \cdot \frac{\sum_{n=0}^{\infty}(n+1)\hat{a}_{n+1}\tau^n}{\sum_{n=0}^{\infty} \hat{a}_n\tau^n}, \tag{6.31}$$

according to Equation (6.28). As for $C(\tau;\phi)$, it is calculated from

$$C(\tau) = \int_0^{\tau} k\theta D(t)dt. \tag{6.32}$$

since $D(\tau;\phi)$ has been worked out. As stated previously, f_j is the conditional characteristic function of x_T, thus P_j can be derived according to the Gil-Pelaez Theorem [96] once f_j

is obtained as follows

$$P_j = \frac{1}{2} + \frac{1}{\pi}\int_0^{+\infty} Re\left[\frac{e^{-i\phi \ln[K]} f_j}{i\phi}\right] d\phi. \tag{6.33}$$

By now a formula in series expansion for the price of European call options is derived and can be calculated by Equation (6.8).

Once a series solution is obtained, it is natural for us to consider its convergence. Although the convoluted and recursive structure of Equation (6.30) posed an obstacle when we tried to prove its convergence theoretically, we finally figured out an alternative way. In fact, the series solution is introduced when we seek solutions to ODE (6.16) and thus our final formula will converge if this series solution converges. Therefore, we provide the radius of convergence for the series solution in the following proposition.

Proposition 6.3.1. *The series solution* $u = \sum_{n=0}^{\infty} a_n \tau^n$ *will always converge if*

$$\tau \leq \frac{1}{\Delta}\sqrt{b^2 + \frac{\pi^2}{4}}. \tag{6.34}$$

Proof. According to one existing theory that the radius of convergence of the series solution to a second order linear ODE near an ordinary point is at least as large as the distance from the ordinary point to the nearest singularity of the ODE [16], all we need to do for our model is to find the nearest singularity to zero of (6.16). Now if we let

$$\begin{aligned} F_1(\tau) &= (i\rho\sigma\phi + m_j)(e^{2(\Delta\tau+b)} + 1) - 2\Delta(e^{2(\Delta\tau+b)} - 1), \\ F_2(\tau) &= e^{2(\Delta\tau+b)} + 1, \end{aligned}$$

it is not difficult to verify that $F_1(\tau)$ and $F_2(\tau)$ are both analytic in the entire complex domain. Furthermore, as we notice that q_1 equals $F_1(\tau)/F_2(\tau)$ and $q_0 q_2$ is a constant, all singularities can be obtained when we set $F_2(\tau) = 0$ and are specified as follows

$$\tau_k = -\frac{b}{\Delta} + i\frac{(2k+1)\pi}{2\Delta}, \qquad k = 0, 1, 2... \tag{6.35}$$

Therefore, the nearest singularity to zero is $-\frac{b}{\Delta} + i\frac{\pi}{2\Delta}$ and it is actually a simple pole. This implies that the radius of convergence is at least $\frac{1}{\Delta}\sqrt{b^2 + \frac{\pi^2}{4}}$, which has completed

the proof. □

Except the radius of convergence, the speed of convergence is also an important factor for the series solution and should be examined. Moreover, we will further check the validity of our pricing formula by comparing European option prices calculated by pricing formula (6.8) with those obtained directly from the SDE (6.5) controlling the dynamics with Monte Carlo simulation and from the PDE (6.6) governing the option price with finite difference methods to further demonstrate the speed of convergence and accuracy. These two issues will be shown in the next Section.

6.4 Numerical examples and discussions

In this section, two different examples will be given respectively to show the convergence and the validity of our pricing formula. Of course, the parameters used are chosen under the restriction (6.34).

As shown from the derivation process in Section 3 that the obtained pricing formula (6.8) can be expressed as

$$U(S,t,v) = \lim_{n\to\infty} G(S,t,v;n), \tag{6.36}$$

where n represents the number of terms we use in calculating the option price, the convergence of our formula can be shown if there exists N and $K \in (0,1)$ such that when $n > N$, the following is valid

$$|G(S,t,v;n+2) - G(S,t,v;n+1)| \leq K|G(S,t,v;n+1) - G(S,t,v;n)|, \tag{6.37}$$

according to the compression conditions for sequences. As a result, when $G(S,t,v;n+1) - G(S,t,v;n) \neq 0$, the following is the only one that need to be considered to check the convergence of the solution

$$\lim_{n\to\infty} \left| \frac{G(S,t,v;n+2) - G(S,t,v;n+1)}{G(S,t,v;n+1) - G(S,t,v;n)} \right| = 0. \tag{6.38}$$

In contrast, when $G(S,t,v;n+1) - G(S,t,v;n) = 0$ holds for all $n > N$, the solution should be regarded as converged. In the following, the values of $G(S,t,v;n)$ are all calculated in

the order of 10^{-16}.

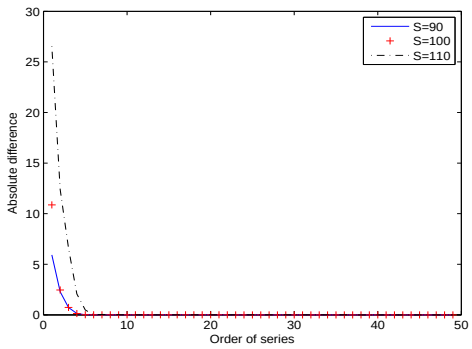

(a) Value of $G(S,t,v;n+1)-G(S,t,v;n), 3 \leq n \leq 49$.

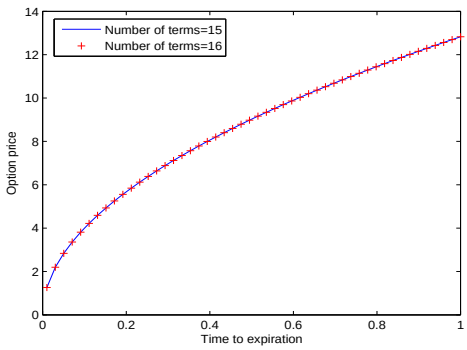

(b) Option price when number of terms chosen to be 15 and 16.

Figure 6.1: Convergence of our price in the first example. Parameters are $\rho = -0.5, k = 2, \theta = 0.1, \beta = 0.1, u = 4, \tau = 0.5, v = 0.1, K = 100$.

As is shown in Figure 6.1(a), the value of $G(S,t,v;n+1) - G(S,t,v;n)$ decreases rapidly when n increases and it becomes zero when n reaches 8, independent of whether the option is "in the money", "at the money" or "out of money". Moreover, it should be noted that the speed of convergence for "in the money" option is slower than that for "out of money" option. To exhibit the convergence of the series solution more clearly, Figure 6.1(b) displays two option prices corresponding to the cases with 15 terms and 16 terms of the series solution picked respectively when S is set to be 100. What we can observe first is that the calculated option price is a monotonic increasing function of time to expiration. Furthermore, two different curves are pictured with a difference of 10^{-5} order, which can be tolerated when operating in financial markets and thus the 15-term price can be regarded as the converged option price.

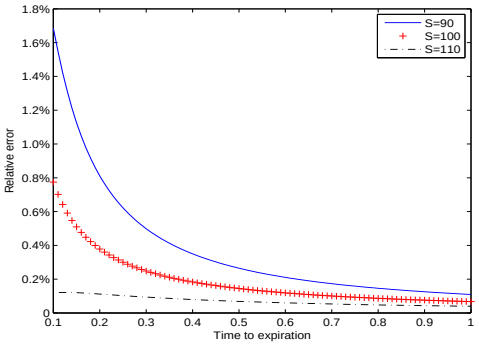

(a) Our price vs finite difference method price.

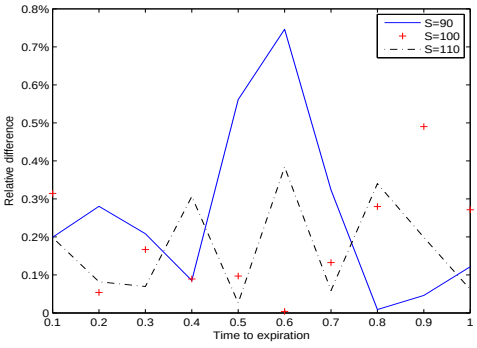

(b) Our price vs Monte Carlo price.

Figure 6.2: Comparison of our price with those obtained by other numerical methods in the first example. Parameters are $\rho = -0.5, k = 2, \theta = 0.1, \beta = 0.1, u = 4, v = 0.1, K = 100$.

What we can see in Figure 6.2(a) is the relative difference between our price calculated by 20 terms in the series solution and FDM (finite difference method) price, which is calculated by the explicit scheme. We try to make the results of comparison more convincing by setting $S = 90, 100, 110$ respectively. The maximum difference shown in this sub-figure is less than 1.8%, which could certainly be accepted in real markets. Figure 6.2(b) further show that our price is quite accurate since there are only no more than 0.8% difference when our price is compared with Monte Carlo price, which is calculated with 500,000 simulations. When these two sub-figures are viewed together, it should be noticed that prices for "out of money" option exhibit higher relative difference than those for options in other positions as expected since prices are smaller for "out of money" call options. On the other hand, as for the speed of calculation, it only takes 2.77 seconds to work out a converged 15-term price with the closed-form solution, while it costs 639.66 seconds for Monte Carlo simulation and 909.21 seconds for finite different method with the same set of parameters. This implies that working with our closed-form formula can be really time-saving compared with those numerical methods.

Since only one example given by the same set of parameters may not be sufficient to lead to reliable conclusions, another example is chosen. The values of parameters are selected to be quite different from those in the first example to show that it converges for a wide range of parameters as long as the parameters are chosen within the radius of convergence (6.34). As a result, we again calculate the value of $|G(S, t, v; n + 1) - G(S, t, v; n)|$ when n increases from 13 to 49, which is shown in Figure 6.3(a). It is obvious that our price still converges in either moneyness of options, although the converging rate is slower than that in the first example. It should also be noticed that the converging speed for "in the money" options is slowest. Figure 6.3(b) is the one showing how close it is for the price of 25-team and 26-term picked in the series of our solution. Apparently, the order of difference is again only 10^{-5}, which means that prices of more than 25 terms can be seen as converged.

Comparison with prices obtained through other numerical methods for this case is also given in Figure 6.4. This time the relative difference between our price and FDM price is narrowed down to maximum 1.2% while the distance between our price and Monte Carlo price is still less than 0.8%. Besides, one can still observe that option prices calculated by the closed-form pricing formula have lower relative difference with those obtained through

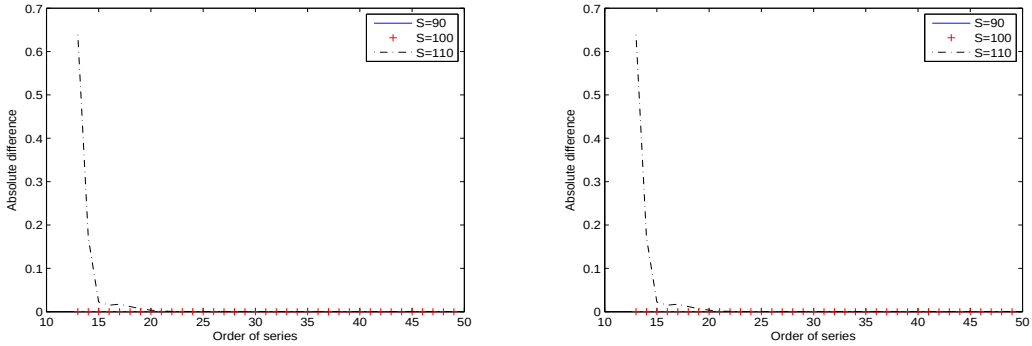

(a) Value of $G(S,t,v;n+1)-G(S,t,v;n), 13 \leq n \leq 49$.

(b) Option price when number of terms chosen to be 25 and 26.

Figure 6.3: Convergence of pur price in the second example. Parameters are $\rho = 0.5, k = 5, \theta = 0.01, \beta = 0.05, u = 0.8, v = 0.2, \tau = 0.5, K = 100$.

both of the numerical methods when the initial underlying price is no less than the strike price. It should be pointed out that although 25 terms are needed for a converged price, the time it consumes to figure out one price in this case is still very low, at about 4.72 seconds, which is less than $\frac{1}{120}$ of the time that the two numerical methods require. This can significantly raise the efficiency of option pricing in real markets.

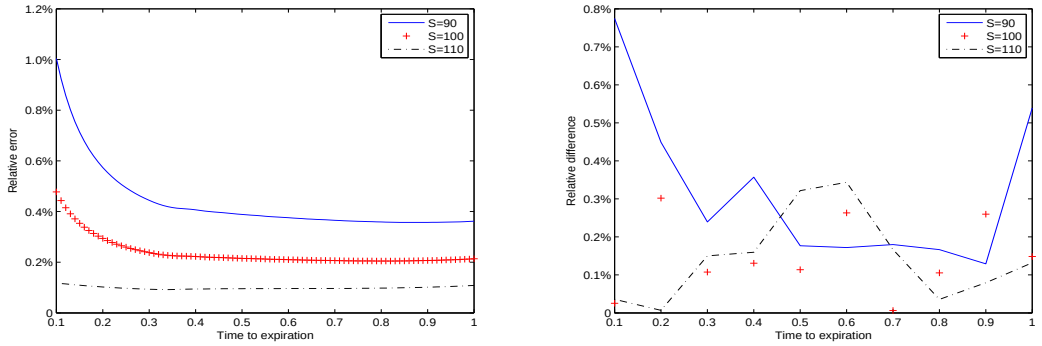

(a) Our price vs finite difference method price.

(b) Our price vs Monte Carlo price.

Figure 6.4: Comparison of our price with those obtained by other numerical methods in the second example. Parameters are $\rho = 0.5, k = 5, \theta = 0.01, \beta = 0.05, u = 0.8, v = 0.2, K = 100$.

6.5 What if $\tau > \frac{1}{\Delta}\sqrt{b^2 + \frac{\pi^2}{4}}$

It should be noticed that to seek a series solution to Equation (6.16) in Section 6.3, we expanded the solution at $\tau = 0$, which converges in the region of $\tau \leq \frac{1}{\Delta}\sqrt{b^2 + \frac{\pi^2}{4}}$. Obviously, when τ is larger than this radius, the convergence of the solution could not be

guaranteed. As a result, other solutions should be found in this case. In this section, a set of option pricing formulae for different time range under the Heston stochastic volatility model with the minimal entropy martingale measure that converges outside the converged area is derived.

In particular, if we assume that

$$t_m = \sum_{k=1}^{m} \frac{1}{\Delta}\sqrt{b^2 + \frac{\pi^2}{4} * k} - \frac{b}{\Delta},$$

then we would expand the solution u at the point $\tau = t_m$ when $t_m \leq \tau \leq t_{m+1}$, i.e.

$$u = \sum_{n=0}^{\infty} a_n(\tau - t_m)^n. \tag{6.39}$$

As $\tanh(x)$ could be expressed as $\tanh(x) = \frac{e^{2x}-1}{e^{2x}+1}$, and $e^{2\Delta\tau}$ could be expanded as $e^{2\Delta\tau} = e^{2\Delta t_m}\sum_{n=0}^{+\infty} c_n(\tau - t_m)^n$ with $c_n = \frac{1}{n}(2\Delta)^n$, ODE (6.16) could be converted into the following equation

$$\begin{aligned}
&[e^{2b+2\Delta t_m}\sum_{n=0}^{\infty} c_n(\tau - t_m)^n + 1]\sum_{n=0}^{\infty}(n+1)(n+2)a_{n+2}(\tau - t_m)^n \\
&-[(i\rho\sigma\phi + m_j - 2\Delta)e^{2b+2\Delta t_m}\sum_{n=0}^{\infty} c_n(\tau - t_m)^n + (i\rho\sigma\phi + m_j + 2\Delta)]\sum_{n=0}^{\infty}(n+1)a_{n+1}(\tau - t_m)^n \\
&+[e^{2b+2\Delta t_m}\sum_{n=0}^{\infty} c_n(\tau - t_m)^n + 1]q_0q_2\sum_{n=0}^{\infty} a_n(\tau - t_m)^n = 0.
\end{aligned} \tag{6.40}$$

It should be remarked that Equation (6.40) should hold for any τ, which implies that the coefficients of $\{(\tau - t_m)^k, \forall k \geq 0\}$ should be equal to zero. Hence, we could obtain the following equation

$$(k+1)(k+2)a_{k+2} + e^{2b+2\Delta t_m}\sum_{i=0}^{k}[(k-i+2)(k-i+1)a_{k-i+2}c_i] + I_2 - I_1 = 0, \tag{6.41}$$

for any $k \geq 0$. Here, I_1 and I_2 are defined as

$$\begin{aligned}
I_1 &= \{(i\rho\sigma\phi + m_j - 2\Delta)e^{2b+2\Delta t_m}\sum_{i=0}^{k}[(k-i+1)a_{k-i+1}c_i] + (i\rho\sigma\phi + m_j + 2\Delta)(k+1)a_{k+1}\} = 0, \\
I_2 &= e^{2b+2\Delta t_m}q_0q_2\sum_{i=0}^{k}(a_{k-i}c_i) + q_0q_2a_k.
\end{aligned}$$

In order to reach the final solution, a_0 and a_1 should be calculated. However, from the boundary condition $u^{'}(0) = 0$, one can only obtain $a_1 = 0$, while the value of a_0 keeps unknown. To solve this problem, both sides of Equation (6.41) are divided by a_0, and we define

$$\hat{a}_k = \frac{a_k}{a_0}, \quad k \geq 0. \tag{6.42}$$

In this case, $\{\hat{a}_k, k \geq 0\}$ could all be evaluated with $\hat{a}_0 = 1, \hat{a}_1 = 0$ through

$$\hat{a}_{k+2} = \frac{\hat{I}_1 - \hat{I}_2 - e^{2b+2\Delta t_m} \sum_{i=1}^{k} [(k-i+1)(k-i+2)\hat{a}_{k-i+2} c_i]}{(e^{2b+2\Delta t_m} + 1)(k+2)(k+1)}, \quad k \geq 0, \tag{6.43}$$

where

$$\begin{aligned}
\hat{I}_1 &= \{(i\rho\sigma\phi + m_j - 2\Delta)e^{2b+2\Delta t_m} \sum_{i=0}^{k} [(k-i+1)\hat{a}_{k-i+1} c_i] + (i\rho\sigma\phi + m_j + 2\Delta)(k+1)\hat{a}_{k+1}\}, \\
\hat{I}_2 &= e^{2b+2\Delta t_m} q_0 q_2 \sum_{i=0}^{k} (\hat{a}_{k-i} c_i) + q_0 q_2 \hat{a}_k.
\end{aligned}$$

Once $\{\hat{a}_k, k \geq 0\}$ have been derived, D could be easily worked out by

$$D(\tau) = -\frac{1}{q_2} \frac{\sum_{n=0}^{\infty} (n+1)\hat{a}_{n+1}(\tau - t_m)^n}{\sum_{n=0}^{\infty} \hat{a}_n (\tau - t_m)^n}, \tag{6.44}$$

and thus C could be calculated as

$$C(\tau) = \int_0^{\tau} k\theta D(t) dt. \tag{6.45}$$

By now, we have derived a set of pricing formulae based on different points at which the series is expanded. In the following, the convergence of these solutions in the considered region is verified. It is well-known that the radius of convergence of the series solution to a second order linear ODE near an ordinary point is at least as large as the distance from the ordinary point to the nearest singularity of the ODE [16]. Moreover, from the discussion above, all the singularities in ODE (6.16) could be specified as

$$\tau_k = -\frac{b}{\Delta} + i\frac{(2k+1)\pi}{2\Delta}, \quad k = 0, 1, 2... \tag{6.46}$$

Combining both of the two facts, it is not difficult to find that the nearest singularity to

any expansion point is always $-\frac{b}{\Delta}+i\frac{\pi}{2\Delta}$. As a result, the radius of convergence for the series solution expanded at t_m is at least

$$R_m=\sqrt{(\sum_{k=1}^{m}\frac{1}{\Delta}\sqrt{b^2+\frac{\pi^2}{4}*k})^2+\frac{1}{\Delta^2}\frac{\pi^2}{4}}>\frac{1}{\Delta}\sqrt{b^2+\frac{\pi^2}{4}*(m+1)}, \tag{6.47}$$

which shows that the solution expanded at $\tau=t_m$ converges in the region $t_m\leq\tau\leq t_{m+1}$. It should also be noticed that

$$\lim_{m\to+\infty}t_m=+\infty, \tag{6.48}$$

which implies that when $\tau>t_1$, there always exists $m>1$ such that $\tau<t_m$.

Another issue that should also be mentioned is whether all these solutions, including the formula obtained in the previous section as well as those derived here, have already covered the whole region $[0,+\infty]$. Given that the converged region for the solution presented in [114] is $[0,\frac{1}{\Delta}\sqrt{b^2+\frac{\pi^2}{4}}]$, it is not difficult to find that when $b>0$, $\frac{1}{\Delta}\sqrt{b^2+\frac{\pi^2}{4}}>t_1$ holds. In this case, we have already finished our task. On the other hand, when $b\leq 0$, our solution expanded at t_1 could be used if τ falls in the gap $[\frac{1}{\Delta}\sqrt{b^2+\frac{\pi^2}{4}},t_1]$ since the radius of convergence for this solution is at least $\frac{1}{\Delta}\sqrt{b^2+\frac{\pi^2}{4}*2}$, which is obviously larger than the length of the interval $-\frac{b}{\Delta}$. Therefore, we could certainly reach the conclusion that for any $\tau\in[0,+\infty]$, we could always find a converged solution.

6.6 Conclusion

In this chapter, a closed-form pricing formula for European options is obtained under the minimal entropy martingale measure in the Heston stochastic volatility model with several particular settings. This is a reasonable choice since the specific equivalent martingale measure can be connected with the principle of maximum expected utility. A great advantage of our newly-derived pricing formula is that the convergence of the solution in series form can be proved theoretically; such a proof of the convergence has also been complemented by some numerical examples to demonstrate the speed of convergence. Our numerical evidence has further substantiated that the series solution indeed converges very rapidly; when the relative differences with respect to FDM prices and MC prices are maintained to be no more than 1.8% and 0.8% respectively, the computational cost associated with

adopting the closed-form solution is less than 1% of those associated with purely numerical methods such as the FDM and MC methods. Finally, we present a set of slightly modified formulae for European options accompanied by a set of complete convergence proofs for the solution that would cover the entire time horizon of a European option contact.

Chapter 7

A new integral equation for American put options

7.1 Introduction

Financial derivatives are becoming increasingly popular means of investment, speculation and risk management; market demands on faster and more accurate valuation for these contracts have prompted researchers to continue seeking alternative solution approaches for pricing various derivative contracts. Options, as one kind of the most well-known and useful derivatives, have received a lot of attention ever since Black-Scholes [19] derived a simple and elegant pricing formula for European options with the underlying price following a geometric Brownian motion. However, it is widely acknowledged that pricing American options is a much more intriguing problem [125, 171]; the main reason is the inherent characteristic that an American option can be exercised at any time before the expiry time. This additional right for the holder of an American option over that of its European counterpart has cast the American option pricing problem into a free boundary problem, and the so-called "optimal exercise price" (hereafter referred to as "optimal exercise boundary") at which the option contract should be early exercised needs to be determined together with the option price itself. Mathematically, the existence of the optimal exercise boundary has made the problem of pricing American options highly nonlinear since the domain of such a problem is not only unknown in advance but also "moving" with time, and a closed-form analytic solution is not attainable unless in some special cases, such as perpetual American options and the series solutions for American

puts in Zhu [232]. Thus, much of the research in pricing American options involves the development of accurate and efficient valuation methods.

Among various numerical approaches proposed in the literature, one of the most common methods is to numerically solve the partial differential equation (PDE) governing the price of an American option (referred to as the PDE approach hereafter), and this particular approach can be further divided into several sub-categories. On one hand, with the optimal exercise boundary being implicitly located, the pricing problem can be transformed into a linear complementarity problem [124], which can be solved with various numerical algorithms [159, 221]. On the other hand, the optimal exercise boundary can be explicitly tracked and simultaneously found together with the price function. A well-known approach in the latter sub-category is the finite difference method (FDM), based on which many different algorithms have been developed [179, 227]. Other kinds of numerical approaches often used in solving the option pricing problem are the Monte Carlo simulation technique and the tree approach. Typical examples are a least square Monte Carlo method proposed by Longstaff & Schwartz [171] and a modified binomial tree method for pricing American options mentioned in [237].

A main disadvantage of purely numerical approaches is that errors are introduced at very early stage of computation. One way to overcome such a disadvantage is to develop semi-analytical approaches, in which analytical analysis is performed until a point beyond which numerical calculations must be resorted to. There are several well-known papers in this category. For example, Geske & Johnson [95] proposed the compound-option approximation method such that an American option is decomposed into a finite number of European options, while Carr [28] presented a semi-explicit approximation with a randomization technique. Zhu [233] developed an analytic approximation method for American options with a pseudo-steady-state approximation of the moving boundary. In order to seek a good balance between maximizing analytical tractability and minimizing the computational time, integral equation approaches are a good compromise between the two[1]. The essence of this particular method is to cast the differential equation into an integral equation, so that the analytical tractability is preserved in the form of an integral equation and yet the eventual numerical calculations, should numerical values need to be

[1]Ideally, a closed-form solution in terms of elementary functions like the Black-Scholes pricing formula for European options is ultimately preferred, in terms of rendering both analytical tractability as well as computational efficiency. Unfortunately, such kind of solution has not been found yet.

computed, can be completed with a relatively efficient algorithm. Of course, a crucial measure of the performance of this approach is the specific form of the integral equation analytically derived as various forms have been proposed in the past.

McKean [175] seems to be the first to derive an integral equation for American option prices using the technique of incomplete Fourier transform. The advantage of this particular integral equation is that it only involves two one-dimensional integrals. However, there are two main drawbacks for this representation, which may cause problems when conducting numerical experiments; one is that the presence of the derivative of the optimal exercise boundary can create numerical difficulties because of the infinite slope of the optimal exercise boundary at maturity [37], and another is that the value of the integral equation at the optimal exercise boundary only equals to half of its original value due to the fact that the inverted Fourier transform of a discontinuous function will converge to the midpoint of the discontinuity [69]. Jamshidian [141] derived a different integral equation for American option prices by transforming the homogeneous Black-Scholes equation into an inhomogeneous one. Although this formulation does not involve the derivative of the optimal exercise boundary, the integral equation contains a two-dimensional integral, which is much more computational intensive than those involving one-dimensional integrals only. One of the most famous integral equations for American option prices was derived by Kim [154] through taking the limit of compound option prices. A very useful feature of Kim's formulation is its quantification of the value of an American option in two parts; a base value that corresponds to its European option and an early exercise premium that is associated exclusively with the early exercise right of an American option. On the other hand, one of its main drawbacks is still the relatively excessive computational time needed for the computation of the two-dimensional integrals involved in finding the unknown optimal exercise boundary.

In this chapter, we present a new integral equation (IE) formulation for American put option prices under the Black-Scholes model. Our derivation procedure involves several steps. Firstly, we cast the original problem into a new free boundary problem for the option Theta (the first-order derivative with respect to the time to maturity as one of the important Greeks in option pricing). Taking the advantage of the free boundary being a monotonic decreasing function of the time to expiry, we adopt a novel approach in which the optimal exercise price itself is taken as an independent variable first, replacing an

original independent variable, the time to expiry. Mathematically, we transform a problem governed by a linear PDE defined on a domain bounded by an unknown free boundary into one governed by a nonlinear PDE with a fixed boundary. After applying a Fourier transform to this particular nonlinear PDE, an analytical solution in the Fourier space is successfully derived. However, our approach should not be regarded as successful if we could not obtain the analytical inversion of the solution since the numerical inversion of a function in the Fourier space is not desirable and should be avoided whenever possible. Fortunately, we have finally managed to derive a simple and elegant integral equation after analytically performing the inverse Fourier transform. Once this integral equation is solved, the optimal exercise price as a function of the time to expiry can be retrieved.

It should be pointed out here that this newly derived integral equation possesses two distinguishable advantages over all the existing IE formulations. The first one is that the integral equation only involves a one-dimensional integral. The advantage associated with this is clearly its numerical realization being far less computational intensive than that involving two-dimensional integrals. The second unique feature of the newly derived integral equation is that it does not suffer from any discontinuity problem, and singularities associated with the optimal exercise boundary at the expiry time are totally avoided as a result of taking the moving boundary itself as an independent variable in the newly formulated nonlinear PDE system; the computational accuracy and efficiency can thus be further enhanced.

It should also be remarked here that our method can be extended to the valuation problem of American option prices under other models, such as stochastic volatility models and jump-diffusion models. For any stochastic volatility model such as the well-known Heston model [117], although volatility becomes another state variable (see [235]), the free boundary is essentially only "moving" in the direction of the underlying price. Thus, the same technique presented here would still apply, transforming a two-dimensional free boundary surface, instead of a one-dimensional free boundary curve like in the Black-Scholes' case, into a two-dimensional fixed boundary first and then a "retrieving" process similar to what has been presented here is used to restore the needed two-dimensional free boundary surface. On the other hand, when jump-diffusion models are to be dealt with, there is an added integral component in the PDE, so that a partial integro-differential equation needs to be solved. Our proposed technique can still be adopted, with a difference

that the ordinary differential equation (ODE) in the Fourier space presented in Theorem 1 of this chapter becomes an ODE with a modified coefficient. A challenge then is to find the analytical solution for this modified ODE and to perform the Fourier inversion analytically as we did in this chapter. Therefore, specifically dealing with these issues will be left in future research with results shown in a forthcoming paper.

The rest of the chapter is organized as follows. In Section 7.2, a new PDE system governing the Theta of American puts is presented. This new free boundary problem is further transformed into a fixed boundary problem through a novel approach, and a new integral equation containing only a one-dimensional integral is derived. In Section 7.3, numerical experiments and related discussions are presented, followed by some concluding remarks given in the last section.

7.2 A new integral equation

In this section, we use the Black-Scholes PDE system for American put option prices to illustrate our approach. The Black-Scholes PDE system is first transformed into another system with two different free boundary conditions by simply differentiating the PDE with respect to the time to expiry. This new free boundary problem is then formulated into a fixed boundary problem by using the free boundary as the new variable to replace the time to expiry. The PDE of this fixed boundary problem is actually nonlinear, from which we obtain a new integral equation with the aid of the Fourier transform.

7.2.1 A new PDE system

If the underlying price S_t follows a geometric Brownian motion under the risk-neutral measure as

$$\frac{dS}{S} = rdt + \sigma dW_t, \tag{7.1}$$

with r and σ representing the risk-free interest rate and the volatility respectively, and W_t being the standard Brownian motion, the PDE system[2] governing the American put price

[2]The problem of pricing American options is a non-linear problem, if one looks from the whole PDE system point of view, even though the involved PDE itself is a linear one. The main reason is due to the existence of the unknown free boundary, which needs to be determined as part of the solution.

$P(S,t)$ can be derived according to the Feynman-Kac formula

$$\begin{cases} \dfrac{\partial P}{\partial t}+\dfrac{1}{2}\sigma^2S^2\dfrac{\partial^2P}{\partial S^2}+rS\dfrac{\partial P}{\partial S}-rP=0,\ S>S_f(t), \\ P(S,t)|_{S=S_f(t)}=K-S_f(t), \\ \dfrac{\partial P}{\partial S}|_{S=S_f(t)}=-1, \\ \lim\limits_{S\to+\infty}P(S,t)=0, \\ P(S,t)|_{t=T}=\max(K-S,0), \end{cases} \tag{7.2}$$

in which T is the expiry time, K denotes the strike price, and $S_f(t)$ is the optimal exercise boundary with K being its terminal value, i.e., $S_f(t)|_{t=T}=K$. It should be noted that there are altogether three boundary conditions for the reason that the existence of the unknown free boundary has added one degree of freedom and thus a second-order PDE system needs to be supplied with an additional boundary condition to properly close the system. Details on the existence and uniqueness of the solution to System (7.2) can be found in [33].

To efficiently solve System (7.2), all variables are firstly non-dimensionalized with the following transform

$$x=\ln\frac{S}{K}, p=\frac{P}{K}, \tau=\frac{\sigma^2}{2}(T-t), \tag{7.3}$$

from which we can obtain a dimensionless PDE

$$\begin{cases} \dfrac{\partial p}{\partial \tau}=\dfrac{\partial^2p}{\partial x^2}+(k-1)\dfrac{\partial p}{\partial x}-kp,\ x>b(\tau) \\ p(x,\tau)|_{x=b(\tau)}=1-e^{b(\tau)}, \\ \dfrac{\partial p}{\partial x}|_{x=b(\tau)}=-e^{b(\tau)}, \\ \lim\limits_{x\to+\infty}p(x,\tau)=0, \\ p(x,\tau)|_{\tau=0}=\max(1-e^x,0), \end{cases} \tag{7.4}$$

where $k=\dfrac{2r}{\sigma^2}$ and $b(\tau)=\ln\dfrac{S_f(\tau)}{K}$ with the initial condition

$$b(\tau)|_{\tau=0}=0. \tag{7.5}$$

From System (7.4), it is not very difficult to obtain the following two identities[3]

$$\frac{\partial p}{\partial \tau}|_{x=b(\tau)} = 0, \tag{7.6}$$

$$\frac{\partial^2 p}{\partial x \partial \tau}|_{x=b(\tau)} = -k\frac{db}{d\tau}. \tag{7.7}$$

Clearly, these two identities are the conditions defined on the free boundary for the Theta of American puts, that is, $\theta(x,\tau) \triangleq \frac{\partial p}{\partial \tau}$.

To form a complete PDE system for θ, we still need an initial condition and a boundary condition. In particular, if $\tau = 0$ is substituted into the PDE in System (7.4), the following equation can be derived

$$\begin{aligned} \frac{\partial p}{\partial \tau}|_{\tau=0} &= \frac{\partial^2 p}{\partial x^2}|_{\tau=0} + (k-1)\frac{\partial p}{\partial x}|_{\tau=0} - kp|_{\tau=0} \\ &= \frac{\partial^2 p_0(x)}{\partial x^2} + (k-1)\frac{\partial p_0(x)}{\partial x} - kp_0(x), x \geq 0 \end{aligned} \tag{7.8}$$

where $p_0(x) = \max(1 - e^x, 0)$. This further leads to

$$\theta(x,0) = \frac{\partial p}{\partial \tau}|_{\tau=0} = \delta(x) - kH(-x), x \geq 0 \tag{7.9}$$

where $\delta(x)$ is the Dirac delta function.

On the other hand, the boundary condition of American puts $p(x,\tau)$ is given by

$$\lim_{x \to +\infty} p(x,\tau) = 0,$$

and this can further yield the boundary condition for θ

$$\lim_{x \to +\infty} \theta(x,\tau) = \lim_{x \to +\infty} \frac{\partial p}{\partial \tau} = 0, \tag{7.10}$$

the proof of which is not difficult and has thus been left in Appendix B. Differentiating the PDE in System (7.4) with respect to the time to expiry τ, and collecting boundary conditions (7.6), (7.7), (7.10) and the initial condition (7.9), we arrive at a new PDE

[3] Although these two properties have already been presented in [34], their derivation is still included the in Appendix B.1, for the easiness of reference and completeness of this chapter.

system for $\theta(x,\tau)$ as

$$\begin{cases} \dfrac{\partial\theta}{\partial\tau} = \dfrac{\partial^2\theta}{\partial x^2} + (k-1)\dfrac{\partial\theta}{\partial x} - k\theta, \ x > b(\tau), \\ \theta(x,\tau)|_{x=b(\tau)} = 0, \\ \dfrac{\partial\theta}{\partial x}|_{x=b(\tau)} = -k\dfrac{db}{d\tau}, \\ \lim\limits_{x\to+\infty}\theta(x,\tau) = 0, \\ \theta(x,\tau)|_{\tau=0} = \delta(x) - kH(-x), x \geq 0. \end{cases} \tag{7.11}$$

It should be remarked that the PDE system governing $\theta(x,\tau)$ does not possess any essential change on the fundamental characteristics as it is still a free boundary problem with a linear PDE. However, it has facilitated the conversion of a moving boundary problem to a fixed boundary problem as a result of the second boundary on $x = b(\tau)$ being inserted into the PDE as demonstrated in the next subsection.

7.2.2 Analytical pricing formula for American put

In this subsection, the free boundary problem contained in System (7.11) is transformed into a fixed boundary problem with a non-linear PDE defined on a fixed domain. The solution of the new PDE system in the Fourier space is then obtained by applying the Fourier transform, the analytical inversion of which yields an integral equation.

In the literature, there are many ways in which a free boundary problem can be converted into a fixed boundary problem. Specifically, in the context of transforming the American option pricing problem into a fixed boundary problem, Zhu [232] adopted the well-known Landau transform [227], and obtained an exact and explicit pricing formula for American puts in an infinite series form. However, this technique is not suitable for the integral equation approach, as the adoption of Landau transform would introduce the derivative of the optimal exercise boundary into the non-linear PDE and consequently in the final expression of the integral equation as well. To overcome this problem, we take the advantage of a well-known property of the optimal exercise boundary, namely, the monotonicity of the optimal exercise boundary, and introduce an alternative method with one of the independent variables in the original PDE system being replaced by a new independent variable, the free boundary itself being treated as "parameter".

More specifically, from the monotonicity of $b(\tau)$, we can take b as a new independent variable and view $\theta(x,\tau)$ as $\theta(x,b(\tau))$. Then, using the chain rule on the l.f.s. (left hand

side) of the first equation in (7.11), we obtain

$$\frac{\partial\theta}{\partial b}\frac{db}{d\tau} = \frac{\partial^2\theta}{\partial x^2} + (k-1)\frac{\partial\theta}{\partial x} - k\theta. \tag{7.12}$$

On the other hand, the second boundary condition in (7.11) can be rewritten as

$$\frac{\partial\theta}{\partial x}|_{x=b} = -k\frac{db}{d\tau}, \tag{7.13}$$

which is now used to facilitate the elimination of $\dfrac{db}{d\tau}$ in (7.12) and complete the change of one of the independent variables as far as the new PDE is concerned[4]. As for the remaining two boundary conditions in (7.11), they now simply become the boundary conditions of the new system in the x-direction with b being no longer viewed as a function of τ. Also, taking (7.5) into account, the PDE system for $\theta(x,b)$ can be summarized as

$$\begin{cases} -\dfrac{1}{k}\dfrac{\partial\theta}{\partial x}|_{x=b}\dfrac{\partial\theta}{\partial b} = \dfrac{\partial^2\theta}{\partial x^2} + (k-1)\dfrac{\partial\theta}{\partial x} - k\theta, \ x > b, \\ \theta(x,b)|_{x=b} = 0, \\ \lim\limits_{x\to+\infty}\theta(x,b) = 0, \\ \theta(x,b)|_{b=0} = \delta(x) - kH(-x), x \geq 0. \end{cases} \tag{7.14}$$

It should be pointed out that the PDE system (7.14) is obtained after introducing a new independent variable to the original PDE system (7.11). Thus, the existence and uniqueness of the solution to the new system are preserved as a result of the one-to-one explicit relationship between the new independent variable b and the old independent variable τ. To obtain the solution, a Fourier transform is performed as presented in the following theorem. It should be remarked here that although the PDE in (7.14) is a nonlinear one due to the presence of a product of the unknown function and its first order derivative, one can still establish an integral equation by performing a Fourier transform, which would normally be a powerful tool only for solving linear PDEs. The key of the success hinges on a careful observation that the PDE in System (7.14) can be treated as a linear PDE with constant coefficients as far as a Fourier transform with respect to x is concerned, because the source of the nonlinearity, $\dfrac{\partial\theta}{\partial x}|_{x=b}$, is a function b only, albeit unknown. Once the solution for $\theta(x,b)$ is obtained for every given x and b, $b(\tau)$ can be

[4]the subtle difference on the left hand side of (7.13) from that of the second equation in (7.11) should be noted too as a result of change of independent variables.

then easily retrieved from using essentially the third equation in (7.11) and $p(x,\tau)$ can be recovered from integrating $\theta(x,b)$ with respect to τ.

Theorem 5. *If $\theta(x,b)$ is the solution to the PDE system (7.14), then an integral equation for $\theta(x,b)$ can be derived as*

$$\begin{aligned}\theta(x,b) &= \frac{e^{-k^2 m(b)-\frac{1}{2}m(b)[k-1+\frac{x}{km(b)}]^2}}{2\sqrt{\pi k m(b)}} \\ &+ \int_0^b \frac{e^{-k^2[m(b)-m(y)]-\frac{1}{2}[m(b)-m(y)]\{k-1+\frac{x-y}{k[m(b)-m(y)]}\}^2}}{2\sqrt{\pi k[m(b)-m(y)]}}dy, \end{aligned} \tag{7.15}$$

where $m(b)$ is defined as

$$m(b) = \int_0^b -\frac{1}{\frac{\partial\theta(x,s)}{\partial x}|_{x=s}}ds. \tag{7.16}$$

Proof. We begin with treating the nonlinear PDE in System (7.14) as a linear one with constant coefficients in the process of performing an incomplete Fourier transform, after denoting $\frac{\partial\theta}{\partial x}|_{x=b}$ as $f(b)$[5]. With such a notation deliberately emphasizing that all the coefficients of the PDE in System (7.14) are a function of b only, we can perform an incomplete Fourier transform on the PDE in System (7.14) with respect to x, the operator of which, $F(\cdot)$, is defined as

$$F[g(x)] = \int_b^{+\infty} e^{-i\phi x} g(x)dx, \tag{7.17}$$

where i denotes the imaginary unit. It should be pointed out here that the incomplete Fourier transform can be viewed as an ordinary one if we assume that the function $g(x)$ is also defined on $(-\infty, b)$ where $g(x) = 0$.

After applying the incomplete Fourier transform to the unknown function $\theta(x,b)$ and its derivatives with respect to x, we have

$$\begin{aligned} F(\frac{\partial\theta}{\partial x}) &= i\phi\bar{\theta}, \\ F(\frac{\partial^2\theta}{\partial x^2}) &= -e^{-i\phi b}f(b) - \phi^2\bar{\theta}, \\ F(\frac{\partial\theta}{\partial b}) &= \frac{d\bar{\theta}}{db}, \end{aligned}$$

[5]It should be remarked that this elegant treatment does not mean that the Fourier transform technique can be extended to solve nonlinear equations in general; we have merely utilized the fact that when the source of the nonlinearity becomes a known function of one variable only, as in this case, the power of the Fourier transform can still be "displayed" as the PDE would appear to be a pseudo "linear" as long as the Fourier transform is performed against another variable (or variables in a more general case).

where $\bar{\theta}(\phi, b) = F[\theta(x, b)]$. Consequently, after the incomplete Fourier transform is performed, the PDE in System (7.14) becomes an ODE (ordinary differential equation)

$$\frac{d\bar{\theta}}{db} - \frac{k[\phi^2 - (k-1)i\phi + k]}{f(b)}\bar{\theta} = ke^{-i\phi b}, \tag{7.18}$$

with the initial condition

$$\bar{\theta}(\phi, b)|_{b=0} = F[\delta(x)H(x)]. \tag{7.19}$$

where $H(x)$ is a Heaviside function. Such a first-order ODE with variable coefficients can be solved analytically with the solution

$$\bar{\theta} = e^{-\int_0^b \frac{k[\phi^2-(k-1)i\phi+k]}{-f(s)}ds}\{\int_0^b ke^{-i\phi y}e^{\int_0^y \frac{k[\phi^2-(k-1)i\phi+k]}{-f(s)}ds}dy + F[\delta(x) - kH(-x)]\}. \tag{7.20}$$

If we further let

$$m(b) = \int_0^b \frac{1}{-f(s)}ds, \tag{7.21}$$

Equation (7.20) can then be simplified as

$$\bar{\theta} = \int_0^b ke^{-i\phi y}e^{-k[\phi^2-(k-1)i\phi+k][m(b)-m(y)]}dy + e^{-k[\phi^2-(k-1)i\phi+k]m(b)}F[\delta(x)H(x)]. \tag{7.22}$$

This means that we have successfully obtained the analytical solution in the Fourier space and the remaining work is to apply the inverse Fourier transform.

Let us denote $F^{-1}[\cdot]$ as the inverse Fourier transform operator. Our target solution can be expressed as

$$\begin{aligned}\theta &= F^{-1}[\int_0^b ke^{-i\phi y}e^{-k[\phi^2-(k-1)i\phi+k][m(b)-m(y)]}dy] + F^{-1}\{e^{-k[\phi^2-(k-1)i\phi+k]m(b)}F[\delta(x)H(x)]\} \\ &\triangleq U_1 + U_2,\end{aligned} \tag{7.23}$$

which means that the calculation of $\theta(x, b)$ can be divided into two parts. In particular,

the first part U_1 can be evaluated as

$$\begin{aligned} U_1 &= \frac{1}{2\pi}\int_0^b \int_{-\infty}^{+\infty} k e^{i\phi(x-y)} e^{-k[\phi^2-(k-1)i\phi+k][m(b)-m(y)]} d\phi dy \\ &= \frac{k}{2\pi}\int_0^b e^{-k^2[m(b)-m(y)]} \int_{-\infty}^{+\infty} e^{-k[m(b)-m(y)]\{\phi^2-(k-1)i\phi-\frac{x-y}{k[m(b)-m(y)]}\}} d\phi dy \\ &= \frac{k}{2\pi}\int_0^b e^{-k^2[m(b)-m(y)]-\frac{1}{4}k[m(b)-m(y)]\{k-1+\frac{x-y}{k[m(b)-m(y)]}\}^2} \\ &\times \int_{-\infty}^{+\infty} e^{-k[m(b)-m(y)]\{\phi-\frac{1}{2}i[k-1+\frac{x-y}{k[m(b)-m(y)]}]\}^2} d\phi dy. \end{aligned} \tag{7.24}$$

In order to work out the integration with respect to ϕ in Equation (7.24), we need to firstly study the property of the function $m(b)$. The definition of $f(b)$, $f(b) = -k\dfrac{db}{d\tau}$, certainly implies that $f(b)$ is always positive since b is a monotonically decreasing function of the time to expiry. Moreover, considering the fact that $m(b)$ defined in Equation (7.16) is non-negative as b is non-positive, we can reach a conclusion that the decrease in b will result in the increase in $m(b)$. Therefore, we have $m(b) > m(y)$ when $y > b$, and thus U_1 in Equation (7.24) can be further simplified as

$$U_1 = \int_0^b \frac{e^{-k^2[m(b)-m(y)]-\frac{1}{4}k[m(b)-m(y)]\{k-1+\frac{x-y}{k[m(b)-m(y)]}\}^2}}{2\sqrt{k\pi[m(b)-m(y)]}} dy. \tag{7.25}$$

By now, the first part of $\theta(x,b)$ has been analytically inverted and what we need to do is its second part U_2. Similar to the above derivation process, it is quite straightforward to obtain

$$F^{-1}[e^{-k[\phi^2-(k-1)i\phi+k]m(b)}] = \frac{e^{-k^2m(b)-\frac{1}{4}km(b)[k-1+\frac{x}{km(b)}]^2}}{2\sqrt{k\pi m(b)}}. \tag{7.26}$$

Thus, according to the convolution theorem for inverse Fourier transform, we can obtain

$$U_2 = F^{-1}[e^{-k[\phi^2-(k-1)i\phi+k]m(b)}] * F^{-1}\{F[\delta(x)H(x)]\}, \tag{7.27}$$

with $*$ as the convolution notation. This further gives

$$\begin{aligned} U_2 &= \int_{-\infty}^{+\infty} \frac{e^{-k^2m(b)-\frac{1}{4}km(b)[k-1+\frac{x-u}{km(b)}]^2}}{2\sqrt{k\pi m(b)}} \delta(u)H(u)du \\ &= \frac{e^{-k^2m(b)-\frac{1}{4}km(b)[k-1+\frac{x}{km(b)}]^2}}{2\sqrt{k\pi m(b)}}. \end{aligned} \tag{7.28}$$

Therefore, Equations (7.25) and (7.28) can lead to the final solution of $\theta(x,b)$. This has

completed the proof. □

Obviously, $\theta(x,b)$ can finally be worked out through Equation (7.15) once the function $m(b)$ is solved. Therefore, in order to obtain $m(b)$, we make use of $\theta(x,b)|_{x=b}=0$, which can yield

$$\frac{e^{-k^2m(b)-\frac{1}{2}m(b)[k-1+\frac{b}{km(b)}]^2}}{2\sqrt{\pi km(b)}}+\int_0^b\frac{e^{-k^2[m(b)-m(y)]-\frac{1}{2}[m(b)-m(y)]\{k-1+\frac{b-y}{k[m(b)-m(y)]}\}^2}}{2\sqrt{\pi k[m(b)-m(y)]}}dy=0. \tag{7.29}$$

It should be noted that there is no discontinuity in this equation because the value of $\theta(x,b)$ at the boundary condition $x=b$ is zero, which is the same as that outside the continuously holding region. It should also be remarked here that while there always exists a singularity at $\tau=0$ in all the existing integral equations for optimal exercise boundary of the American option in the literature due to the presence of the negative infinite slope of the optimal exercise boundary, i.e.,

$$\frac{db}{d\tau}|_{\tau=0}=-\infty, \tag{7.30}$$

we have successfully avoided directly dealing with this singularity when eventually solving the integral equation numerically. This is achieved as a direct result of taking the free boundary b itself as an independent variable, rather than an unknown function in the original system. In other words, one can easily verify that there are no singularities in (7.29) when b approaches zero, i.e., the slope of $m(b)$ is actually

$$\frac{dm(b)}{db}|_{b=0}=-\frac{1}{\frac{\partial\theta(x,b)}{\partial x}|_{x=b}}\bigg|_{b=0}=\frac{1}{k\frac{db}{d\tau}}\bigg|_{\tau=0}=0. \tag{7.31}$$

Thus, a notoriously difficult problem of numerically dealing with the resolution near $\tau=0$ in almost all numerical solution approaches proposed to price American options is avoided here as a result of $b=0(\tau=0)$ being dealt with "exactly" in our newly derived integral equation. Furthermore, the singular behavior of $b(\tau)$ at $\tau=0$ is recovered analytically through Equation (7.32), so we can claim that there is no loss of accuracy in our newly derived integral equation as far as dealing with the well-known singularity at $\tau=0$ is concerned. In addition, Equation (7.29) only involves a one-dimensional integral and thus its computation should be very efficient.

Once $m(b)$ is found Equation (7.29), the time to expiry that corresponds to each b can be calculated straightforwardly via

$$\tau = km(b), \tag{7.32}$$

which is the result of a direct integration of the ODE

$$\frac{db}{d\tau} = -\frac{1}{k} f(b), \tag{7.33}$$

with the utilization of Equation (7.21) and the initial condition (7.5).

Consequently $\theta(x, \tau)$ can be computed through (7.15) making use of equation (7.32). Finally, the dimensionless option price, $p(x, \tau)$, can be obtained from

$$p(x, \tau) = p(x, 0) + \int_0^\tau \theta(x, s) ds = \max(1 - e^x, 0) + \int_0^\tau \theta(x, s) ds, \tag{7.34}$$

and the corresponding dimensional option price posted in the original problem can be calculated from

$$P(x, \tau) = K[\max(1 - e^x, 0) + \int_0^\tau \theta(x, s) ds], \tag{7.35}$$

where $x = \ln(\frac{S}{K})$ and $\tau = \frac{1}{2}\sigma^2(T - t)$.

In summary, to work out the American option price and the optimal exercise boundary with respect to the time to expiry, the integral equation (7.29) should be numerically solved to obtain $m(b)$ values for each discrete b value step by step[6]. Then, by utilizing the obtained $m(b)$, corresponding τ and $\theta(x, b)$ values can be successfully obtained with Equation (7.32) and (7.15) respectively. Finally, the American put prices can be figured out from Equation (7.35). In the next section, this solution procedure is numerically realized, and the accuracy and efficiency of the newly derived integral equation are demonstrated.

[6]To a certain extent, this first part of the solution procedure in the proposed new approach is similar to the concept of inverse finite element method proposed by Zhu & Chen [236] for solving the American option pricing problem, in which a set of unknown function values are "prescribed" first and then the corresponding values of the original independent variable are found through an efficient nonlinear iteration scheme.

7.3 Numerical examples and discussions

In this section, the accuracy and efficiency of our integral equation approach will be numerically verified. In the following calculations, the risk-free interest rate r is set to be 0.1, the strike price K is 100, and other model parameters are $\sigma = 0.3$ and $T = 1$.

Unlike the solution procedure for American option prices with other integral equation approaches, where the time to expiry is discretized first and the optimal exercise boundary is obtained by solving the corresponding integral equation step by step, the free boundary b is discretized in our approach before the integral equation (7.29) is solved numerically to obtain $m(b)$. Once $m(b)$ is found, τ, the time to expiry that corresponds to each b is computed by using Equation (7.32) to obtain discrete values of the optimal exercise boundary $b(\tau)$.

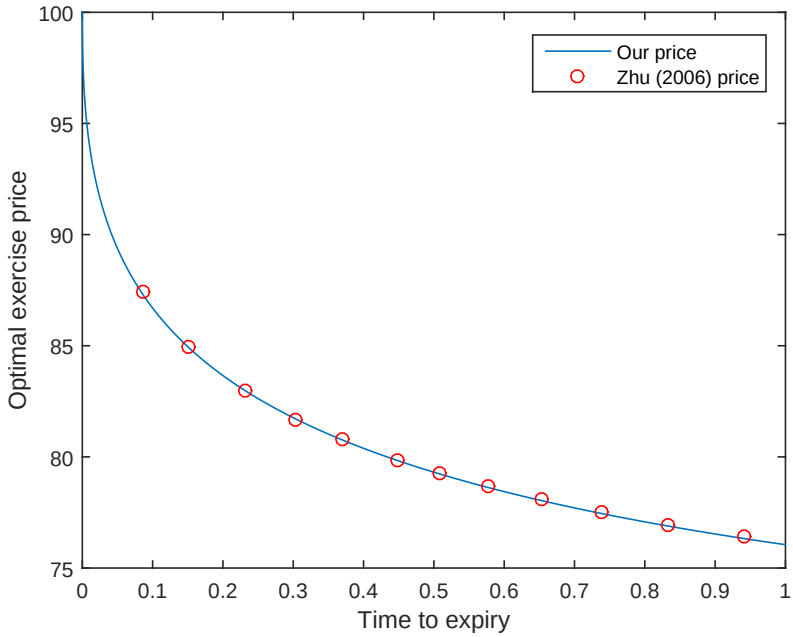

Figure 7.1: Comparison of optimal exercise prices with two different approaches. Model parameters are $\sigma = 0.3, \tau = 1$.

Depicted in Figure 7.1 is the comparison of optimal exercise prices calculated with our integral equation with those obtained from Zhu's formula. What should be noticed first is that the optimal exercise price of an American put option is a monotonic decreasing function of the time to expiry, which can partially verify our formula. Moreover, it is obvious that our results agree very well with those obtained from Zhu's formula. To further demonstrate this issue, the two sets of optimal exercise prices are listed in Table

7.1, and clearly the maximum relative error between the two results is less than 0.2%, which can certainly show the accuracy of our integral equation. On the other hand, the speed with which the optimal exercise boundary is calculated by solving our newly formulated integral equation is much, much faster than that through Zhu's formula by summing up an infinite series. As Medvedev and Scaillet [176] pointed out in their paper, Zhu [232] did not focus on computational efficiency at all; in fact, the two approaches are not even comparable in terms of computational efficiency, as it would take hours to compute the optimal exercise boundary on a same resolution if we were trying to compute the optimal exercise boundary with Zhu's approach, whereas it only takes few seconds to do the same job with the current approach.

Table 7.1: Comparison of optimal exercise prices with our and Zhu's approach.

Time to expiry	Our results	Zhu's results	Relative error
0.0868	87.4347	87.2748	0.18%
0.1515	84.9193	84.9158	0.004%
0.2321	82.9560	82.9710	0.02%
0.3039	81.6967	81.7036	0.008%
0.3697	80.7728	80.7625	0.01%
0.4480	79.8654	79.8408	0.03 %
0.5083	79.2696	79.2349	0.04%
0.5761	78.6813	78.6336	0.06%
0.6521	78.1008	78.0411	0.08%
0.7376	77.5284	77.4571	0.09%
0.8335	76.9635	76.8856	0.10%
0.9413	76.4007	76.3263	0.09%

Table 7.2: Comparison of the CPU time

	CPU Time
Our equation	6.0s
Kim's equation	11.5s

As far as the computational efficiency is concerned, we make comparison of the CPU times consumed by computing our new integral equation and Kim's integral equation to obtain a single set of the optimal exercise boundary. As can be seen in Table 7.2, it is clear that to obtain a similar accuracy with a relative difference being in the order of 1%, it only takes 6.0 seconds to compute for one particular set of the optimal exercise prices with the time to expiry $T = 1$. This means that our time savings is about 50% over Kim's approach, which is as expected since solving integral equations requires iteration, and Kim's integral equation actually involves a two-dimensional integral while our integral

equation only contains a one-dimensional integral. On the other hand, this significant enhancement of numerical efficiency further justifies the usefulness of the new approach as an alternative to the traditional integral equations derived in the past.

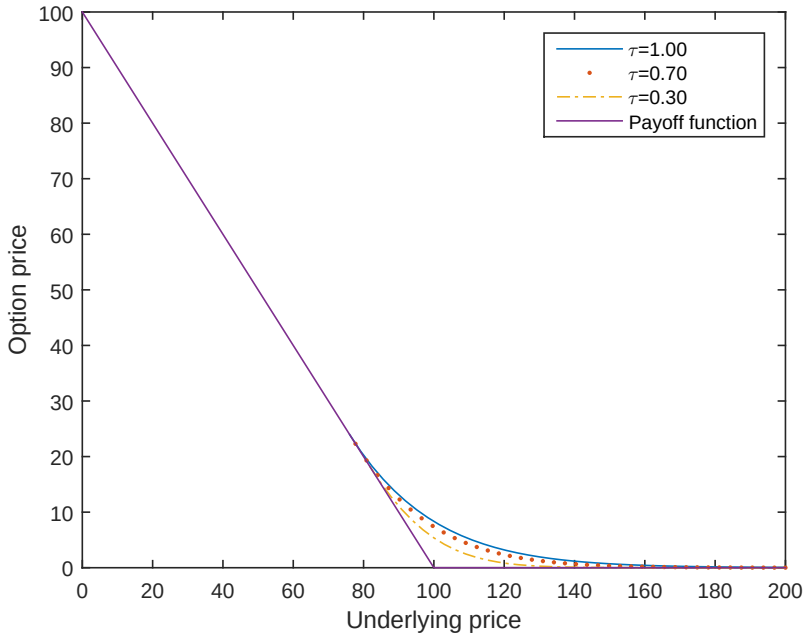

Figure 7.2: Option prices with different time to expiry. Model parameters are $\sigma = 0.3$.

With the confidence of our integral equation, we present American put option prices against the underlying price with different values of time to expiry in Figure 7.2. Obviously, the option price will take a downward trend when we increase the value of the underlying price. This is as expected since the payoff function is also a decreasing function of the underlying price. Furthermore, when the time to expiry is less than one year, the option becomes almost worthless when the underlying price approaches approximately 2 times of the strike price, which is consistent with the fact that the value of the option will become zero when the underlying price is large enough.

The volatility σ of the underlying price is a very important parameter in the determination of American option prices, and thus its influence on the optimal exercise price and the option price is shown in Figure 7.3. Specifically, Figure 7.3(a) shows the difference of optimal exercise prices caused by the different value of the volatility. It is clear that the higher the volatility level, the smaller the optimal exercise price. This is mainly because when the underlying price becomes more volatile, the optimal exercise price should be lowered down to prevent potential losses. On the other hand, the phenomenon shown in

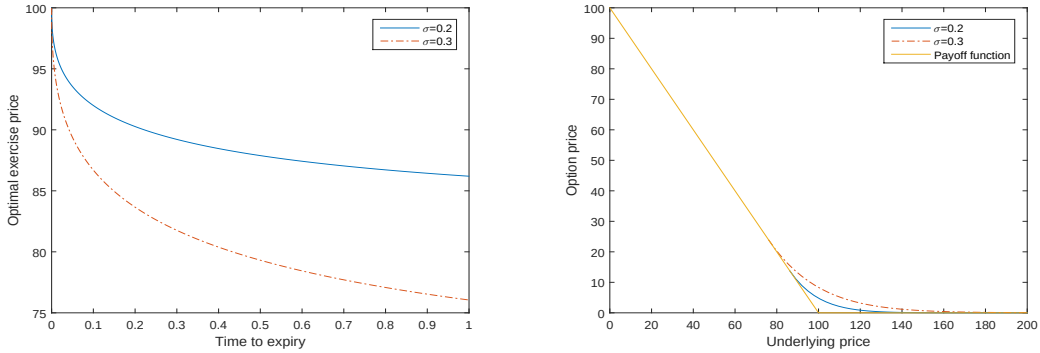

(a) Optimal exercise prices with different value of the volatility σ.

(b) Option prices with different value of the volatility σ.

Figure 7.3: The influence of the volatility σ.

Figure 7.3(b) is that a larger volatility will result in the increase of American put option prices, which is financially meaningful since a larger volatility implies higher uncertainty of the underlying price, and the seller of the option will suffer from a higher probability to lose. In this case, they should be compensated with higher option prices.

7.4 Conclusion

In this chapter, we first present a PDE system for the first-order derivative of American put prices with respect to the time to expiry, and then this new free boundary problem is further transformed into a fixed boundary problem with a novel approach by making the unknown free boundary as a new variable replacing the time to expiry. This new fixed boundary problem actually contains a nonlinear PDE with one initial condition and two fixed boundary conditions, which leads to a new integral equation involving only a one-dimensional integral as one of its main advantages. Another great advantage is that the discontinuity of the integral equation and singularities associated with the optimal exercise boundary at expiry are avoided so that the accuracy and efficiency can be further enhanced. It should be noted that the option Theta, which is one of the important Greeks in option pricing, is computed directly in our formulation.

Chapter 8

A hybrid computational approach for option pricing

8.1 Introduction

In 1973, Black & Scholes [19] made a landmark contribution to the literature in the area of option pricing by deriving a closed-form pricing formula for European options with the underlying price following a geometric Brownian motion. Despite their great success, the Black-Scholes model suffered from the mis-pricing problem as some over simplified assumptions made to achieve analytical tractability are inappropriate. A typical example is the constant volatility assumption being at odds with the phenomenon of the so-called "volatility smile" [73], which has led a large amount of research interest in modifying the Black-Scholes model.

Among all these attempts, stochastic volatility models, which make the volatility as another random variable in addition to the underlying price, have received a lot of attention since stochastic volatility is believed to better capture different properties of underlying returns [102]. However, it needs to be pointed out that the introduction of another stochastic source has made the option pricing problem even more difficult, and it is usually very hard to find closed-form pricing formula even for European options, although there are several models, such as the Stein-Stein model [213] and the Heston model [117], for which analytical solutions can be found. Besides, American options and exotic options are also widely traded in real markets, and it is almost impossible to analytically evaluate these options, even under the Black-Scholes model. As a result, numerical methods must be

resorted to in most cases when pricing options.

In the literature, a number of different numerical approaches have been proposed and adopted to efficiently price options. One of the most basic ones is the so-called binomial tree approach [54], in which a tree of the underlying price is generated and option prices are evaluated backwards from the expiry time to the current time. A distinguished feature of this particular method is that it is very easy and straightforward to implement. Although this method can clearly reflect the construction of the replicating portfolio, it can cause some biases since the underlying price actually does not discretely change within a two-valued framework. As another basic approach, the Monte-Carlo simulation technique, which directly simulates the dynamics of the underlying price to find option prices without using any boundary conditions, is also quite popular in option pricing [23, 171, 200] as it has two main advantages; the first is that it can easily deal with path dependent options, and it can handle high-dimensional pricing problems in which options are written on underlying assets. However, this approach suffers from the inefficiency problem due to the requirement of large number of paths being generated to achieve enough accuracy especially for low dimensional problems [129]. Being different from the above two methods, both of which directly simulate the underlying price process, the finite difference method, which is based on the discretization of the differential operators, can be certainly employed if a PDE (partial different equation) system governing option prices is derived first. Then, depending on how the differential operator is discretized, different schemes, such as the explicit method, implicit scheme, the ADI (alternating direction implicit) method [138], the predictor-corrector scheme [235] and many others, form all the specific approaches under the umbrella of the PDE approach. This method is firstly applied to option pricing by Schwartz [199] and Brennan & Schwartz [24], and it has been widely used by many others [50, 128]. One of the main advantages for the finite difference method is that a set of option prices can be obtained simultaneously in one computation with a relatively small amount of computational time, while an obvious disadvantage is that boundary conditions are imposed at infinity for any PDE system when pricing options, and its truncation will certainly affect the accuracy of the calculation. Of course, there are some other well-known numerical approaches that have already been used in dealing with option pricing problems, such as the finite element method [121].

It should be remarked that when using PDE approaches, the operating domain needs

to be truncated as the underlying price and the volatility range from zero to infinity under stochastic volatility option pricing models, and a large enough boundary for the underlying price and the volatility should be chosen respectively so that the boundary values at the truncated domain can be a good approximation of those at infinity. However, short-term options are dominated in most of derivative markets, which means that the probability for a dramatic change in the underlying price or the volatility taking place is quite low. Thus, option traders will probably focus on a relatively small region around the current value of the underlying price [241] and the volatility (denoted by interested region in the following), and want to accurately figure out the influence of a small change in this region on option prices, while they do not care too much about the information outside this particular region. In this case, it will be a waste of time to determine option prices outside the interested region since we will have to discretize the entire pricing domain if we employ PDE approaches. Naturally, one wonder if one could only truncate the interested domain, and thus alternative ways should be found.

In this chapter, we propose a new numerical method that is able to cope with the situation illustrated above. This particular method is actually a combination of the Monte-Carlo simulation technique and the PDE approach (we name it as "the MCPDE method") that we artificially generate boundary values for the interested region so that we can avoid being restricted to work on a very large domain, and option prices inside this region can be efficiently obtained through the PDE approach (we use the ADI method as an example) with the generated boundary condition. To clearly illustrate this particular method, a sample figure is presented in Figure 8.1. Assume that we are currently at the point $M(S_0, v_0)$, and we are only interested in Domain ABCD around M. What we need to do first is to find the boundary values of this particular domain, and thus Monte-Carlo simulation should be used to generate option prices on every point we need like P. Then, option prices inside Domain ABCD can be worked out through PDE approaches. Furthermore, in order to show the accuracy of this newly proposed approach, we use the pricing of European options under the Heston model as an example since it possesses a closed-form pricing formula for European options. Moreover, its efficiency is also numerically demonstrated by comparing the computational time it takes to obtain option prices in a same discretized interested region with purely ADI method, purely Monte-Carlo simulation and this new approach.

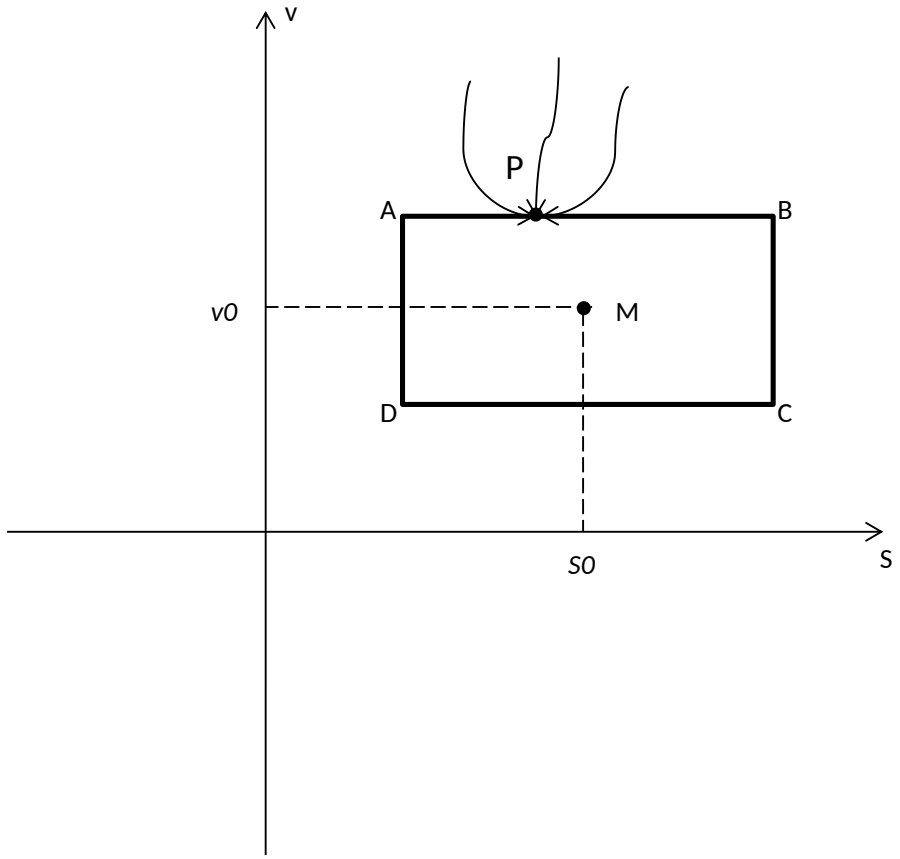

Figure 8.1: Sample figure on how the MCPDE method can be implemented.

The rest of the chapter is organized as follows. In Section 8.2, a new numerical approach combining Monte-Carlo simulation and the ADI method is introduced. In Section 8.3, numerical experiments are carried out to show the accuracy as well as efficiency of the new approach, followed by some concluding remarks given in the last section.

8.2 A new numerical approach

In this section, we formally introduce the MCPDE method to evaluate options. We choose the Heston model as an example to illustrate the newly proposed approach since it possesses a closed-form pricing formula for European options, with which its accuracy can be easily assessed.

To start, let us denote S_t and v_t as the underlying price and the volatility respectively. Then, the dynamics of the Heston model under the risk-neutral measure can be specified

as

$$\begin{aligned} \frac{dS}{S} &= rdt + \sqrt{v}dW_1, \\ dv &= k(\theta - v) + \sigma\sqrt{v}dW_2, \end{aligned} \tag{8.1}$$

where r is the risk-free interest rate, k is the mean-reverting speed, θ is the mean-reverting level, and σ is the volatility of volatility. W_1 and W_2 are two standard Brownian motions with correlation ρ. If we further let $U(S, v, t)$ denote the price of a European call option, then the governing PDE for U has been shown in many previous papers (e.g., see [113, 117])

$$\frac{\partial U}{\partial t} + \frac{1}{2}vS^2\frac{\partial^2 U}{\partial S^2} + \rho\sigma vS\frac{\partial^2 U}{\partial S \partial v} + \frac{1}{2}\sigma^2 v\frac{\partial^2 U}{\partial v^2} + rS\frac{\partial U}{\partial S} + k(\theta - v)\frac{\partial U}{\partial v} - rU = 0, \tag{8.2}$$

Introducing a new variable, the time to expiry $\tau = T - t$, the terminal value problem can be transformed into an initial value problem. On the other hand, to eliminate the variable coefficients in PDE (8.2), we adopt the log-transform as $x = \log(S)$. Therefore, PDE (8.2) can be transformed into

$$\frac{\partial U}{\partial \tau} = AU, \tag{8.3}$$

where the operator is defined as

$$A = a(v)\frac{\partial^2}{\partial x^2} + b(v)\frac{\partial^2}{\partial v^2} + c(v)\frac{\partial^2}{\partial x \partial v} + d(v)\frac{\partial}{\partial x} + e(v)\frac{\partial}{\partial v} - r, \tag{8.4}$$

with

$$a(v) = \frac{1}{2}v,\ b(v) = \frac{1}{2}\sigma^2 v,\ c(v) = \rho\sigma v,\ d(v) = r - \frac{1}{2}v,\ e(v) = k(\theta - v).$$

Here, the initial condition is $U(x, v, \tau)|_{\tau=0} = \max(e^x - K, 0)$. Usually, the domain $[-\infty, +\infty] \times [0, +\infty]$ should be truncated as $[-X_{max}, X_{max}] \times [0, V_{max}]$ with X_{max} and V_{max} chosen to be large enough so that the boundary conditions at infinity can be regarded as a good approximation for those at the truncated points. However, as stated above, this can previous computational time on computing values of the unknown function in the area that we have no interest in.

In contrast, our MCPDE approach combines the Monte-Carlo method and the PDE method to avoid such kind of waste. In particular, it directly generates the boundary value

for our interested region by simulation with the Monte-Carlo method so that we will be able to save certain amount of time. If we denote the interested region as $[X_1, X_2]\times[V_1, V_2]$, then the boundary values we need to generate are actually $U(x, V_1, \tau)$, $U(x, V_2, \tau)$, $U(X_1, v, \tau)$ and $U(X_2, v, \tau)$. Then, with the initial condition and all the boundary values in hands, we are able to price options in the interested region with PDE approaches. In the following, we choose one kind of the most popular PDE approaches, the ADI method, since it is a very useful tool for solving parabolic equations on rectangular domains. Generally speaking, it is of great efficiency since it can reduce a two-dimensional problem to a succession of many one-dimensional problems, whose final matrix is tridiagonal and can thus be easily solved. Before the ADI method is formally applied, the time derivative of U should be discretized in advance. We first split the operator A as

$$A = A_0 + A_1 + A_2, \tag{8.5}$$

such that A_0, A_1 and A_2 represent the mixed derivative, the spatial derivative in the x direction and the spatial derivative in the v direction respectively, i.e.,

$$\begin{aligned} A_0 &= c(v)\frac{\partial^2}{\partial x \partial v}, \\ A_1 &= a(v)\frac{\partial^2}{\partial x^2} + d(v)\frac{\partial}{\partial x} - \frac{1}{2}r, \\ A_2 &= b(v)\frac{\partial^2}{\partial v^2} + e(v)\frac{\partial}{\partial v} - \frac{1}{2}r. \end{aligned}$$

Then, if a uniform discretization in the τ direction is performed with the number of steps and the step size being $\Delta\tau = \frac{T}{N_\tau}$, applying the first-order implicit Euler scheme to PDE (8.3) yields

$$\frac{U^{n+1} - U^n}{\Delta\tau} = (A_0 + A_1 + A_2)U^{n+1} + \mathbb{O}(\Delta\tau),$$

with $U^n = U(x, v, n\Delta\tau)$, which can be rearranged as

$$[I - \Delta\tau(A_0 + A_1 + A_2)]U^{n+1} = U^n + \mathbb{O}(\Delta\tau^2).$$

Similarly, the first-order explicit Euler scheme of (8.2) can be derived as

$$U^{n+1} = [I + \Delta\tau(A_0 + A_1 + A_2)]U^n + \mathbb{O}(\Delta\tau^2).$$

As a result, the weighted average of implicit and explicit scheme can be obtained

$$[I - \theta\Delta\tau(A_0 + A_1 + A_2)]U^{n+1} = [I + \theta\Delta\tau(A_0 + A_1 + A_2)]U^n + \mathbb{O}(\Delta\tau^2). \tag{8.6}$$

It should be remarked that if $\theta = 0$ or $\theta = 1$, (8.6) degenerates to the explicit scheme or implicit scheme respectively. When θ takes the value of $\frac{1}{2}$, (8.6) becomes the Crank-Nicolson scheme. In order to solve this problem separately in two directions with the ADI method, (8.6) is further expressed as

$$\begin{aligned}(I - \theta\Delta\tau A_1)(1 - \theta\Delta\tau A_2)U^{n+1} &= [I + \Delta\tau A_0 + (1-\theta)\Delta\tau A_1 + (1-\theta)\Delta\tau A_2 + \theta^2(\Delta\tau)^2 A_1 A_2]U^n \\ &+ [\theta\Delta\tau A_0 + \theta^2(\Delta\tau)^2 A_1 A_2](U^{n+1} - U^n) + \mathbb{O}(\Delta\tau^2). \end{aligned} \tag{8.7}$$

Since the order of $U^{n+1} - U^n$ is $\mathbb{O}(\Delta\tau)$, $[\theta\Delta\tau A_0 + \theta^2(\Delta\tau)^2 A_1 A_2](U^{n+1} - U^n)$ can certainly be merged into the error term and thus we can obtain

$$(I-\theta\Delta\tau A_1)(1-\theta\Delta\tau A_2)U^{n+1} = [I+\Delta\tau A_0+(1-\theta)\Delta\tau A_1+(1-\theta)\Delta\tau A_2+\theta^2(\Delta\tau)^2 A_1 A_2]U^n+\mathbb{O}(\Delta\tau^2).$$

Therefore, we finally arrive at the finite difference equation we need as

$$(I-\theta\Delta\tau A_1)(1-\theta\Delta\tau A_2)U^{n+1} = [I+\Delta\tau A_0+(1-\theta)\Delta\tau A_1+\Delta\tau A_2]U^n-(I-\theta\Delta\tau A_1)\theta\Delta\tau A_2 U^n, \tag{8.8}$$

if we omit the error term.

With Equation (8.8) in hands, we are now ready to proceed to the ADI method. In fact, there are different schemes, such as the Craig-Sneyd scheme [55] and the Hundsdorfer-Verwer scheme [130]. What we adopt here is the Douglas-Rachford scheme [71] since it is a two-step scheme, which is more convenient to be implemented. In particular, the first step of the Douglas-Rachford scheme for our case is to compute an intermediate variable (we denote it as Y) from

$$(I - \theta\Delta\tau A_1)Y = [I + \Delta\tau A_0 + (1-\theta)\Delta\tau A_1 + \Delta\tau A_2]U^n, \tag{8.9}$$

by fixing the variable in the v direction. If the interested region $[X_1, X_2] \times [V_1, V_2]$ is discretized with the number of steps in the x and v direction being set to be N_x and N_v

respectively, the value of a European option at a grid point can be expressed as

$$U(x,v,\tau) = U(i\Delta x, j\Delta v, n\Delta\tau) = U^n_{i,j}. \tag{8.10}$$

Moreover, the first-order and the second-order non-cross spacial derivatives are approximated by the standard central difference scheme, while the crossed spatial derivative is calculated as

$$\frac{\partial^2 U^n_{i,j}}{\partial x \partial v} = \frac{\frac{U^n_{i+1,j+1} - U^n_{i-1,j+1}}{2\Delta x} - \frac{U^n_{i+1,j-1} - U^n_{i-1,j-1}}{2\Delta x}}{2\Delta v}.$$

Therefore, Equation (8.9) can be split into $(N_v - 1)$ algebraic equations, the matrix form of which can be derived as

$$B^1 Y_j = P^1_j + R^1_j, \ j = 1, 2, ..., N_v - 1, \tag{8.11}$$

where R^1_j is a $(N_x - 1)$-dimensional row vector, whose first element and last element are $\theta\Delta\tau(\frac{a_j}{\Delta x^2} - \frac{d_j}{2\Delta x})Y_{0,j}$ and $\theta\Delta\tau(\frac{a_j}{\Delta x^2} + \frac{d_j}{2\Delta x})Y_{N_x,j}$ respectively while other elements take the value of zero, $Y_j = (Y_{1,j}, Y_{2,j}, ..., Y_{N_x-1,j})'$, $P^1_j = (p^1_{1,j}, p^1_{2,j}, ..., p^1_{N_x-1,j})'$ with $p^1_{i,j}$ expressed as

$$\begin{aligned} p^1_{i,j} &= U^n_{i,j} + c_j\Delta\tau\frac{U^n_{i+1,j+1} - U^n_{i+1,j-1} - U^n_{i-1,j+1} + U^n_{i-1,j-1}}{4\Delta x\Delta v} \\ &+ (1-\theta)\Delta\tau(a_j\frac{U^n_{i+1,j} - 2U^n_{i,j} + U^n_{i-1,j}}{\Delta x^2} + d_j\frac{U^n_{i+1,j} - U^n_{i-1,j}}{2\Delta x} - \frac{1}{2}rU^n_{i,j}) \\ &+ \Delta\tau(b_j\frac{U^n_{i,j+1} - 2U^n_{i,j} + U^n_{i,j-1}}{\Delta v^2} + e_j\frac{U^n_{i,j+1} - U^n_{i,j-1}}{2\Delta x} - \frac{1}{2}rU^n_{i,j}), \end{aligned} \tag{8.12}$$

and B^1 is a tridiagonal matrix defined as

$$B^1 = \begin{bmatrix} 1 + \theta\Delta\tau(\frac{2a_j}{\Delta x^2} + \frac{1}{2}r) & -\theta\Delta\tau(\frac{a_j}{\Delta x^2} + \frac{d_j}{2\Delta x}) & & 0 \\ -\theta\Delta\tau(\frac{a_j}{\Delta x^2} - \frac{d_j}{2\Delta x}) & \ddots & \ddots & \\ & \ddots & \ddots & -\theta\Delta\tau(\frac{a_j}{\Delta x^2} + \frac{d_j}{2\Delta x}) \\ 0 & & -\theta\Delta\tau(\frac{a_j}{\Delta x^2} - \frac{d_j}{2\Delta x}) & 1 + \theta\Delta\tau(\frac{2a_j}{\Delta x^2} + \frac{1}{2}r) \end{bmatrix}.$$

Once we have obtained the solution of the intermediate variable Y, we can move on to the second step to find the solution to U^{n+1} through

$$(I - \theta\Delta\tau A_2)U^{n+1} = Y - \theta\Delta\tau A_2 U^n, \tag{8.13}$$

by fixing the variable in the x direction since the operator in the left hand side of Equation (8.13) is with respect to v only. Similarly, we only need to solve (N_x-1) algebraic equations

$$B^2 U_i^{n+1} = P_i^2 + R_i^2,\ i = 1, 2, ..., N_x - 1, \tag{8.14}$$

where all the elements of the row vector R_i^2 are zero except that the first and the last element take the value of $\theta\Delta\tau(\frac{b_j}{\Delta v^2} - \frac{e_j}{2\Delta v})U_{i,0}$ and $\theta\Delta\tau(\frac{b_j}{\Delta v^2} + \frac{e_j}{2\Delta v})U_{i,N_v}$ respectively. U_i^{n+1} and P_i^2 are defined as $(U_{i,1}, U_{i,2}, ..., U_{i,N_v-1})'$, $P_j^2 = (p_{i,1}^2, p_{i,2}^2, ..., p_{i,N_v-1}^2)'$ respectively, with $p_{i,j}^2$ expressed as

$$p_{i,j}^2 = Y_{i,j} - \theta\Delta\tau(b_j\frac{U_{i,j+1}^n - 2U_{i,j}^n + U_{i,j-1}^n}{\Delta v^2} + e_j\frac{U_{i,j+1}^n - U_{i,j-1}^n}{2\Delta v} - \frac{1}{2}rU_{i,j}^n). \tag{8.15}$$

The Matrix B^2 is also a tridiagonal matrix and it can be specified as

$$B^2 = \begin{bmatrix} 1+\theta\Delta\tau(\frac{2b_j}{\Delta v^2} + \frac{1}{2}r) & -\theta\Delta\tau(\frac{b_j}{\Delta v^2} + \frac{e_j}{2\Delta v}) & & 0 \\ -\theta\Delta\tau(\frac{b_j}{\Delta v^2} - \frac{e_j}{2\Delta v}) & \ddots & \ddots & \\ & \ddots & \ddots & -\theta\Delta\tau(\frac{b_j}{\Delta v^2} + \frac{e_j}{2\Delta v}) \\ 0 & & -\theta\Delta\tau(\frac{b_j}{\Delta v^2} - \frac{e_j}{2\Delta v}) & 1+\theta\Delta\tau(\frac{2b_j}{\Delta v^2} + \frac{1}{2}r) \end{bmatrix}.$$

By now, we have presented our MCPDE method for option pricing. In summary, once a discretization of $[X_1, X_2] \times [V_1, V_2] \times [0, T]$ is chosen, the first step of our newly proposed approach is to generate boundary values, $U_{0,j}^n$, $U_{N_x,j}^n$, $U_{i,0}^n$ and U_{i,N_v}^n for each $n = 0, 1, ..., N_\tau$, $i = 0, 1, ..., N_x$, and $j = 0, 1, ..., N_v$ by directly simulating Dynamic (8.1) with the Monte Carlo technique. Then the second step is to work out an intermediate variable Y with Equation (8.11) with the obtained U^n. It should be remarked here that we need to find the boundary values for Y, i.e., $Y_{0,j}$ and $Y_{N_x,j}$ before we are able to solve Equation (8.11). In fact, the calculation of Y on the two boundaries can be dealt with similarly by utilizing Equation (8.13), which can yield

$$\begin{aligned} Y_0 &= (I - \theta\Delta\tau A_2)U_0^{n+1} + \theta\Delta\tau A_2 U_0^n, \\ Y_{N_x} &= (I - \theta\Delta\tau A_2)U_{N_x}^{n+1} + \theta\Delta\tau A_2 U_{N_x}^n, \end{aligned} \tag{8.16}$$

since we have generated all the boundary conditions for $U^n, n = 0, 1, ..., N_\tau$. Once we have successfully obtained Y, the last step is to derive U^{n+1} with Equation (8.14).

Once a new numerical approach is proposed, its accuracy needs to be verified first. Moreover, it is also of interest to show whether the new method is advantageous than those existing methods, as far as the computational speed is concerned since our initial aim is to find an alternative method, which can save us some time when pricing options if we only focus on an interested region with a high resolution. These two issues will be illustrated in the next section.

8.3 Numerical examples and discussions

In this section, the accuracy of the newly proposed numerical approach is demonstrated by making comparison of our results and those obtained through the closed-form pricing formula for European options in the Heston model. Then, the computational time of our approach, purely Monte Carlo approach and purely ADI approach to work out the same set of option prices is presented for the purpose of assessing efficiency. Unless otherwise stated, the values of parameters we use are listed as follows. The risk-free interest rate r is 0.03 and the correlation between the underlying price and the volatility ρ is 0.8. The mean-reverting speed k and level θ are set to 2 and 0.5, respectively. The volatility of volatility σ is chosen to be 0.3, while the initial value of the volatility v_0 is 0.3. The time to expiry T is set to 1, and the number of discretization in the time direction N_τ is 100, while the number of paths in the Monte-Carlo simulation is set to be 200,000. The lower bound and the upper bound for the underlying price, X_1 and X_2, are chosen to be $\log(90)$ and $\log(110)$ respectively.

Depicted in Figure 8.2 are European put option prices calculated from the MCPDE method and the analytical formula. What can be observed first is that option prices are a monotonic decreasing function of the underlying price, which is consistent with the property of European puts. Moreover, we can witness an excellent agreement between option prices calculated with the MCPDE method and the analytical formula that the relative error between the two prices at the generated boundaries and internal points being approximately 0.3% and less than 0.1% respectively.

One may also be interested in how the accuracy is affected by the number of grids in the x and v direction, and thus we also present numerical results under different sizes of discretization in Table 1 with the relative difference between option prices calculated from

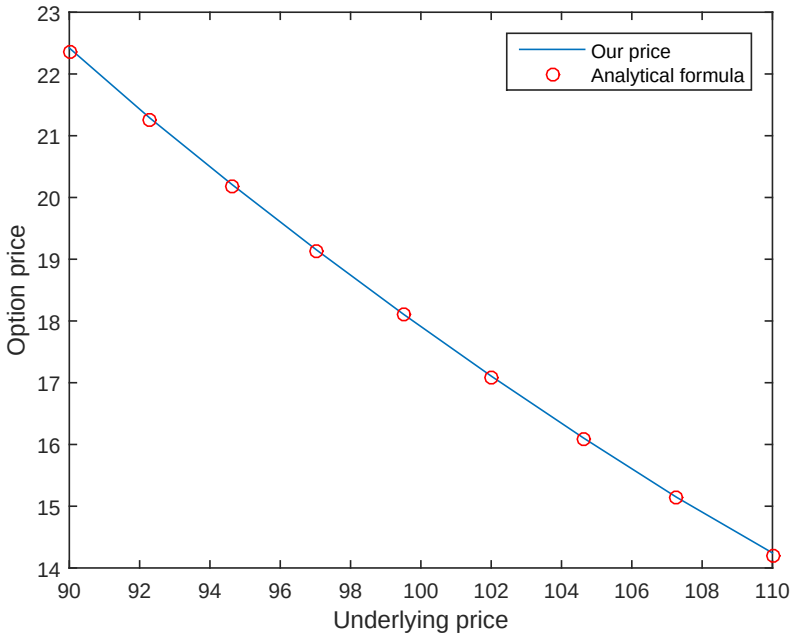

Figure 8.2: Comparison of European put option prices with our approach and analytical formula.

Table 8.1: Accuracy with different discretization ($S = 99.5$)

	$v_0 = 0.1$	$v_0 = 0.2$	$v_0 = 0.3$	$v_0 = 0.4$	$v_0 = 0.5$
$nv = nx = 4$	14.281(0.03%)	16.337 (0.24%)	18.076 (0.12%)	19.710(0.14%)	21.249 (0.01%)
$nv = nx = 8$	14.296(0.12%)	16.298 (0.01%)	18.125 (0.14%)	19.742(0.03%)	21.258 (0.05%)
$nv = nx = 12$	14.294(0.12%)	16.290 (0.04%)	18.134 (0.19%)	19.734(0.02%)	21.315 (0.32%)
$nv = nx = 16$	14.282(0.03%)	16.289 (0.05%)	18.105 (0.04%)	19.729(0.04%)	21.320 (0.35%)

our approach and those from analytical formula. In this example, we choose V_1 and V_2 to be 0.1 and 0.5 respectively, which means that the prices in the first and last column of Table 1 are generated with Monte Carlo simulation. From Table 8.1, it is not difficult to find that with the maximum relative difference between option prices calculated with the MCPDE method and the analytical pricing formula being less than 0.4%, the MCPDE method can provide satisfactory results, even when the number of grids in the x and v directions is only 4. Moreover, when the number of grids is 4, the relative difference inside the interested region is relatively large, though the generated boundary values is rather accurate with less than 0.3% relative difference. In contrast, when the number of discretization becomes 16, the relative difference inside the interested region experiences a significant decrease, although the generated boundary condition now is not as close to the true value as that for the case where the number of discretization is 4. This clearly demonstrates that if we increase the number of discretization, we can certainly decrease

the influence of the generated boundary values and obtain more accurate results.

Table 8.2: CPU time (seconds) with different numerical approaches

	Our method	Purely Monte-Carlo	Purely ADI
$nv = nx = 50$	204	2127	208
$nv = nx = 100$	407	8471	804
$nv = nx = 200$	805	34721	3337

With the gained confidence of our newly proposed approach, we can now proceed to comparing the computational time cost to evaluate option prices at same sets of points with a similar order of accuracy that the average relative error is less than 1%, and the results are presented in Table 8.2 with V_1 and V_2 chosen to be 0.1 and 0.2 respectively. Specifically, although it is clear that purely using Monte Carlo simulation is advantageous over the other two methods when we are only interested in a small number of points as it only takes 0.8 seconds to obtain one accurate option price compared with 19 seconds of our method and 2 seconds of purely ADI method, its computational time increases sharply with the interested number of points. More computational time than the other two methods is needed when the grids in the x and v directions of the interested region exceeds 4, and more than 10 times of the computational time is needed to obtain the same set of option prices if the number of discretization is over 50. On the other hand, when the grids in the interested region is slowly enlarged to some extent from zero, purely ADI method is clearly the most efficient method (take 10 for the grids as an example), and when the number of discretization is around 50, it will cost almost the same time with the MCPDE method and purely ADI. Moreover, if we increase the grids, the time consumed by the MCPDE method becomes less than that cost by purely ADI method, and the gap is even bigger if the number of discretization is further enlarged. By the time when the number of discretization is 200, the computational time the MCPDE method needs is only one fourth of that with purely ADI method. This can certainly demonstrate that our newly proposed approach is competitive when option traders focus on a particular region of high resolution.

8.4 Conclusion

In this chapter, the MCPDE method is proposed that is advantageous than classical numerical approaches in dealing with the situation where option traders are particularly

interested in the influence of a small change of variables in a certain region on option prices, while they do not care much about option prices outside this region. Under this method, boundary values of the interested region are generated with Monte Carlo simulation, while option prices inside this region are calculated with the PDE approach. In this way, we can surely save a large amount of time, especially when we need a large discretization in the interested region, in the sense that we are not forced to derive option price outside the interested region to ensure accuracy. The superiority of this newly proposed numerical approach is also shown by comparing the computational time of our approach, purely Monte Carlo method and purely ADI method cost to evaluate a same set of option prices on the interested domain.

Part III

Model calibration

Chapter 9

An alternative form used to calibrate the Heston option pricing model

9.1 Introduction

There is a long history in the development of the option valuing problem, which is basic and essential in risk management today. Bachelier [9] seems to be the first person to use Brownian motion to model stock price and value stock options, which was provided in his PhD thesis in 1900. However, he assumed that the stock price follow a Brownian motion with normal distribution, which would lead to negative stock and option prices, as pointed out by Merton [177]. After more than 70 years' research and development, Black & Scholes [19] finally made a landmark contribution by presenting a simple and closed-form pricing formula after some simple assumptions were made to capture the essence of the problem while preserving analytical tractability. However, the implied volatility from the real market data tends to exhibit a curve of the shape of a "smile" or "smirk", referred to as the volatility smile in the literature (e.g., [73]), which is at odds with one of those basic assumptions, i.e. the constant volatility, in Black-Scholes model. As a result, this has stimulated widely-spread research interest in proposing various forms of non-constant volatility processes in option pricing models to avoid the apparent "paradox".

Among many attempts to modify the "constant volatility" assumption in the Black-Scholes model, the two most natural ones are either to choose a deterministic function

of underlying and time as the volatility, called "local volatility model" or make volatility another random variable described by a stochastic process, called "stochastic volatility model"[1]. While the former was proposed by Dupire [74] and Derman & Kani [67], with the deterministic volatility function being determined from the well known Dupire formula, the latter is much more popular now among market traders and academic researchers since many empirical studies suggest the "smile dynamics" are poorly captured by the local volatility model (e.g., Hagan et. al [102]).

Models in the category of "stochastic volatility" were first systematically studied by Johnson & Shanno[147], Scott [204], and Wiggins [224] with numerical methods. Specifically, Monte Carlo simulation was adopted by Johnson & Shanno and Scott, while Wiggins proposed that the finite difference method be adopted in solving the corresponding PDEs for pricing financial derivatives, such as options. Unfortunately, neither of them is satisfactory due to the lack of closed-form solution, which could make it quite time-consuming when operating in real markets. Furthermore, although Hull & White [127] proposed a simple form of stochastic volatility process and adopted a power series approximation method, one of its main drawbacks is the zero correlation assumption. This is not reasonable since it violates the so-called "leverage effects" that the underlying price and the volatility should be negatively correlated [11]. Another well-known model is presented by Stein & Stein [213] several years later, who assumed that the volatility follow an Ornstein-Uhlenbeck process [93] and derived a closed-form pricing formula. However, except the assumption of no correlation between the underlying price and volatility, this model could not prevent the volatility from going negative, which was certainly not appropriate. Finally, a great progress was made by Heston [117] in 1993, who proposed the correlated stochastic volatility model and derived an analytic solution based on the inverse Fourier transform. Two aspects can account for the success of the Heston model; one is that the volatility process itself satisfies a wide range of basic properties, such as the obvious non-negative property and the mean-reverting property being consistent with the results of empirical studies [14], and another is that there exists a closed-form formula when pricing options, which can bring a number of advantages. In particular, with closed-form solutions, computational accuracy could certainly be guaranteed while there would exist systematical errors when numerical solutions must be resorted to for models that no

[1]Recently, there are hybrid models that combine both [217].

closed-form solutions are associated with. Most importantly, having closed-form solution can spare us considerable amount of time and effort in parameter estimation, a vitally important process for any mathematical model to function properly as model parameters always need to be extracted from real market data during model calibration.

In this chapter, we propose an alternative form of the Heston model based on a proof for the necessary and sufficient conditions to obtain an affine solution, and thus the new form also captures the essential ingredients of the original Heston version. In particular, our formula preserves the analytical tractability and has substantially reduced the computational effort in terms of parameter determination. To make this new form more attractive, the Feller condition and the non-explosion condition are also imposed on the parameter space to guarantee that the volatility will not drop below and reach infinity respectively. The mean-reverting property is also preserved since it is consistent with real market data.

Analytically, this form is actually equivalent to the original Heston version and there would be no difference of using this form or the original Heston model, if one could determine all model parameters analytically. However, the calibration of a model in reality is so complicated that model parameters always need to be determined numerically with an optimization algorithm. In the latter case, one would never be able to obtain the "optimized" set of parameters, but probably would have to settle near it. It is for this reason that we shall show, through some empirical evidence, that the newly proposed form may yield better results than the original one in some cases. Let's use a simple example to illustrate this point. Imagine that we want to minimize an objective function $g(y) = (\frac{y}{3})^2 - 2(\frac{y}{3}) + 1$ numerically with an optimization algorithm being adopted to find the optimal solution y^*. In doing so, any numerical algorithm needs to impose a stopping criterion so that the search of the optimal solution would cease, once an approximation of the optimal solution is close to the true one within a pre-given tolerance level ϵ. One of the common choices is that when the changing amount, i.e. $|\frac{g(y_{n+1}) - g(y_n)}{g(y_n)}|$, is lower than a chosen ϵ in the searching process, the algorithm will stop and return the optimal y_n. If this is the case for this example, the optimization would stop when $|g'(y)| = |\frac{2}{9}y - \frac{2}{3}| = \epsilon$, and thus $y^* = 3 + \frac{9}{2}\epsilon$ can be easily obtained as the optimal solution. On the other hand, if we make a transformation of $x = \frac{y}{3}$ first to the undetermined parameter, it is not difficult to work out that the returned point then becomes $x = 1 + \frac{1}{2}\epsilon$, which implies that

the optimal solution will be $y^* = 3 + \frac{3}{2}\epsilon$. Clearly, the obtained optimal solution with a simple transformation has made a difference; the latter is closer to the true optimal solution. Based on this simple concept, we propose a different form of the Heston model and demonstrate the possible advantages of adopting this form in some cases through an empirical study.

The rest of the chapter is organized as follows. In Section 9.2, following a brief introduction of general underlying dynamics and the proved conditions for the existence of an affine solution, a closed-form pricing formula for European call options is presented. In Section 9.3, some necessary parameter restrictions such as Feller condition, non-explosion condition and the mean-reverting property are imposed. In Section 9.4, the results of some preliminary empirical studies for a comparison of the performances between our form and the original Heston version are discussed, followed by some concluding remarks given in the last section.

9.2 A new form of the Heston model

In this section we firstly introduce a general stochastic volatility model and then provide the necessary and sufficient conditions for the existence of an affine solution to the governing PDE (partial differential equation) of the option price.

Let $\{S_t, t \geq 0\}$ denote the underlying price and $\{v_t, t \geq 0\}$ represent the dynamic of the volatility. Then the general stochastic volatility model under the risk-neutral measure is characterized as

$$\begin{aligned} \frac{dS}{S} &= rdt + v^{\alpha} dW_t, \\ dv &= \lambda(v)dt + \sigma v^{\beta} dB_t, \end{aligned} \tag{9.1}$$

where W_t and B_t are two standard Brownian motions with correlation ρ. It is obvious that $\alpha \neq 0$, otherwise the underlying asset is not related to the stochastic volatility.

Here, this particular model can be regarded as a general one since it includes a number of different stochastic volatility models and three examples are listed below to further illustrate this point. First of all, if $\alpha = \beta = \frac{1}{2}$ and $\lambda(v) = k(\theta - v)$, our model will surely degenerate to the Heston model. Secondly, if β is set to be zero and the values of other two terms, i.e. α and $\lambda(v)$, remain unchanged as the first case, the model is then the

Stein-Stein model. In addition, when α and β take the value of $\frac{1}{2}$ and $\frac{3}{2}$ respectively, and $\lambda(v) = kv(\theta - v)$, this model degenerates to another well-known model, the so-called "$\frac{3}{2}$ model" [168].

Now let $U(S, v, t)$ denote the European call option price written on the underlying asset S_t, then according to the martingale pricing theory, which requires that $e^{-rt}U_t$ be a martingale, we can obtain the following PDE

$$\begin{aligned} \frac{1}{2}v^{2\alpha}S^2\frac{\partial^2 U}{\partial S^2} &+ \rho\sigma v^{\alpha+\beta}S\frac{\partial^2 U}{\partial v \partial S} + \frac{1}{2}\sigma^2 v^{2\beta}\frac{\partial^2 U}{\partial v^2} \\ &+ rS\frac{\partial U}{\partial S} + \lambda\frac{\partial U}{\partial v} - rU + \frac{\partial U}{\partial t} = 0, \end{aligned} \tag{9.2}$$

with boundary conditions

$$\begin{aligned} U(S, v, T) &= \max(S - K, 0), \\ U(0, v, t) &= 0, \\ \lim_{S\to\infty}\frac{U(S, v, t)}{S} &= 1, \end{aligned}$$

for the price of a European call option. Then, based on the form of Black-Scholes formula, we assume that the solution to PDE (9.2) takes the form of

$$U = SP_1(S, v, t) - Ke^{-r(T-t)}P_2(S, v, t), \tag{9.3}$$

with K as the strike price. As a result, by substituting Equation (9.3) into (9.2) and applying the transform $x = \ln S$ we can finally arrive at

$$\begin{aligned} \frac{1}{2}v^{2\alpha}\frac{\partial^2 P_j}{\partial x^2} &+ \rho\sigma v^{\alpha+\beta}\frac{\partial^2 P_j}{\partial x \partial v} + \frac{1}{2}\sigma^2 v^{2\beta}\frac{\partial^2 P_j}{\partial v^2} \\ &+ (r + a_j v)\frac{\partial P_j}{\partial x} + [\lambda(v) + b_j v^{\alpha+\beta}]\frac{\partial P_j}{\partial v} + \frac{\partial P_j}{\partial t} = 0, \end{aligned} \tag{9.4}$$

where $u_j = \frac{(-1)^j}{2}$ and $b_j = \rho\sigma(2 - j)$ for $j = 1, 2$. As a result, the terminal condition for P_j becomes

$$P_j(x, v, T) = I_{\{x>\ln K\}}.$$

To solve PDE (9.4), we only need to find the characteristic function of x_T conditional on x_t and v_t denoted by $f_j(x, v, t; \phi)$ satisfying the same PDE as $P_j(x, v, t; \ln[K])$ for $j = 1, 2$

respectively. Actually, according to the results in [117] with an affine structure solution in the closed-form pricing formula, we also try to seek a solution of $f_j(x, v, t; \phi)$ in a particular affine form [117] with respect the v^θ, which is stated in the following theorem.

Theorem 6. *Let $f_j(x, v, t; \phi)$ be the solution to (9.4) with terminal condition $f_j(x, v, T; \phi) = e^{i\phi x}$, then $f_j(x, v, t; \phi)$ takes the affine form*

$$f(x, v, \tau; \phi) = e^{C(\tau;\phi)+D(\tau;\phi)v^\theta+i\phi x}, \tag{9.5}$$

with arbitrary θ and if and only if $\alpha + \beta = 1$, $\lambda(v) = \lambda_1 v + \lambda_2 v^{1-2\alpha}$, $\theta = 2\alpha$. Here, $\tau = T - t$, and the two functions $C(\tau; \phi)$ and $D(\tau; \phi)$ are set to be independent of x and v.

Proof. By substituting (9.5) into (9.4) and after some simplifications, we can reach

$$\begin{aligned}(\frac{\partial C}{\partial t} + ir\phi) \quad &+ \quad [-\frac{1}{2}\phi^2 + iu_j\phi]v^{2\alpha} + \frac{\partial D}{\partial t}v^\theta + (i\phi\rho\sigma + b_j)\theta D v^{\alpha+\theta+\theta-1} \\ &+ \quad \frac{1}{2}\sigma^2\theta(\theta-1)Dv^{2\beta+\theta-2} + \frac{1}{2}\sigma^2\theta^2 v^{2\beta+2\theta-2} + \theta D\lambda(v)v^{\theta-1} = 0. \end{aligned} \tag{9.6}$$

As mentioned before that $\alpha \neq 0$, we can obviously obtain $2\alpha \neq 0$. If we assume that $2\alpha \neq \theta$, then by setting $\tau = 0$ we can obtain

$$\frac{1}{2}\phi^2 v_0^{2\alpha} + (r + u_j v_0^{2\alpha})i\phi + \frac{\partial C}{\partial t}\Big|_{\tau=0} + \frac{\partial D}{\partial t}\Big|_{\tau=0} v_0^\theta = 0,$$

which holds for any v_0. Therefore the coefficients of $v^{2\alpha}$ should be zero, i.e.

$$\frac{1}{2}\phi^2 + ia_j\phi = 0,$$

which is not always true. As a result, our assumption was incorrect and we should conclude with

$$2\alpha = \theta. \tag{9.7}$$

Now we assume that $2\beta + 2\theta - 2 \neq \{0, \theta\}$, and then we can deduce that the coefficients of $v^{2\beta+2\theta-2}$ should satisfy

$$\frac{1}{2}\sigma^2\theta^2 D^2 + kD = 0,$$

where k is an arbitrary complex constant. To seek non-trivial solution, we must obtain

$$D = -\frac{k}{\frac{1}{2}\sigma^2\theta^2},$$

which means that D is not related to τ. Thus it contradicts to the fact that $D(0) = 0$. As a result, our assumption is again incorrect and we have

$$2\beta + 2\theta - 2 = \{0, \theta\}. \tag{9.8}$$

To complete the proof, two cases need to be considered here.

(1) $2\beta + 2\theta - 2 = 0$.

Combining Equation (9.7) and the condition $2\beta + 2\theta - 2 = 0$, Equation (9.6) can be further simplified as

$$\begin{aligned}(-\frac{1}{2}\phi^2 + ia_j\phi + \frac{\partial D}{\partial t})v^{2\alpha} \quad &+ \quad 2\alpha D(i\phi\rho\sigma + b_j)v^{\alpha} + \alpha(2\alpha - 1)\sigma^2 D v^{-2\alpha} \\ &+ \quad (2\alpha^2\sigma^2 D^2 + ir\phi + \frac{\partial C}{\partial t}) + 2\alpha\lambda(v)Dv^{2\alpha-1} = 0,\end{aligned}$$

which should hold for any v. As a result, the coefficient of the v^{α} should be equal to zero, i.e.

$$2\alpha D(i\phi\rho\sigma + b_j + \lambda^0) = 0. \tag{9.9}$$

Here λ^0 should be the coefficient of the element $v^{1-\alpha}$ in $\lambda(v)$, which is an arbitrary real number, and should take the value to make the above Equation (9.9) hold. Thereby,

$$\lambda^0 = -b_j - i\phi\rho\sigma.$$

This means that λ^0 is not a real number, which is at odds with the fact that λ^0 is supposed to be a real number stated above. Hence, we have no such solution in this situation.

(2) $2\beta + 2\theta - 2 = \theta$.

Now we have

$$\alpha + \beta = 1, \tag{9.10}$$

and thus Equation (9.6) becomes

$$\begin{aligned}[\frac{\partial D}{\partial t} &+ 2\alpha^2\sigma^2 D^2 + 2\alpha(i\phi\rho\sigma + b_j)D + (ia_j\phi - \frac{1}{2}\phi^2)]v^{2\alpha} \\ &+ [\frac{\partial C}{\partial t} + \alpha(2\alpha-1)\sigma^2 D + ir\phi]v^0 + 2\alpha D\lambda(v)v^{2\alpha-1} = 0, \end{aligned} \tag{9.11}$$

which should hold for any v. Therefore, $\lambda(v)$ must satisfy

$$\lambda(v) = \lambda_1 v + \lambda_2 v^{1-2\alpha}. \tag{9.12}$$

Otherwise, with another term $f(v)$ being added in $\lambda(v)$ in (9.12), it would certainly lead to a conclusion that $f(v) \equiv 0$ due to the arbitrariness of v.

According to condition (9.7), (9.10) and (9.12), we finally obtain the desired result. This has completed the proof. □

With Theorem 1 being verified, it is clear that to make the general model (9.1) to possess such an affine structure solution, the pricing dynamics are specified as

$$\begin{aligned} \frac{dS}{S} &= rdt + v^\alpha dW_t, \\ dv &= (\lambda_1 v + \lambda_2 v^{1-2\alpha})dt + \sigma v^{1-\alpha} dB_t. \end{aligned} \tag{9.13}$$

In this case, our closed-form pricing formula is presented as follows, which is the same as Equation (9.3), and we have left the proof in the Appendix C since the derivation process is similar to that of the Heston model.

$$U = SP_1(S, v, t) - Ke^{-r(T-t)}P_2(S, v, t), \tag{9.14}$$

where

$$
\begin{aligned}
&P_j = \frac{1}{2} + \frac{1}{\pi}\int_0^{+\infty} RE[\frac{e^{-i\phi lnK}\cdot f_j}{i\phi}]d\phi,\\
&f_j(x,v,\tau;\phi) = e^{C(\tau;\phi)+D(\tau;\phi)v^{2\alpha}+i\phi x},\\
&C(\tau;\phi) = ri\phi\tau + \frac{\alpha(2\alpha-1)\sigma^2}{4\alpha^2\sigma^2}p(\tau;\phi),\\
&D(\tau;\phi) = \frac{d-2\alpha(b_j+\lambda_1+i\phi\rho\sigma)}{4\alpha^2\sigma^2}\cdot\frac{1-e^{d\tau}}{1-ge^{d\tau}},\\
&p(\tau;\phi) = [d-2\alpha(b_j+\lambda_1+i\phi\rho\sigma)]\tau - 2ln[\frac{1-ge^{d\tau}}{1-g}],\\
&d = 2\alpha\sqrt{(b_j+\lambda_1+i\phi\rho\sigma)^2-\sigma^2(2u_ji\phi-\phi^2)},\\
&g = \frac{2\alpha(b_j+\lambda_1+i\phi\rho\sigma)-d}{2\alpha(b_j+\lambda_1+i\phi\rho\sigma)+d},\\
&u_j = \frac{(-1)^j}{2}, \quad b_j = \rho\sigma(2-j),
\end{aligned}
$$

for $j = 1, 2$.

Although the closed-form solution is obtained under certain settings, we still need to check whether our model is suitable to be applied in real markets. In fact, the volatility process is expected to be mean-reverting, and it should also be bounded and never fall below zero. All of these features will be discussed in the next section.

9.3 Parameter restrictions

Like some other closed-form solutions, there are usually some restrictions that need to be imposed in the parameter space [72, 117]. To ensure that the volatility will never become negative nor reach infinity, the Feller condition [7, 79] and the non-explosion condition [72, 157] are imposed respectively. Moreover, according to some empirical studies [14], volatility displays the mean-reverting trend and thus this would further give some limitations on the parameter space of our model in order to show this property. As a result, we will put forward and verify several propositions below to set limitations for parameters in our model to meet these requirements.

Proposition 9.3.1. *If we impose* $\alpha \in (-\infty, \frac{1}{2})$ *or* $\lambda_2 \geq \sigma^2(1-\alpha)$ *and* $\alpha \in [\frac{1}{2}, 1)$, *volatility will always stay non-negative.*

Proof. Let us first denote $\beta(v,t) = \lambda_1 v + \lambda_2 v^{1-2\alpha}$ and $c(v,t) = \sigma v^{1-\alpha}$ in our model. According to the Feller condition, we have the assumption that $\beta(0,t) \geq 0$ and $c(0,t) = 0$,

which imply

$$\alpha < 1, \tag{9.15}$$

and λ_2 should be non-negative when $\alpha \in [\frac{1}{2}, 1)$. To ensure that volatility remains non-negative, the Feller condition specified in the following should be satisfied

$$\lim_{v\to 0} \beta(v,t) - \frac{1}{2}\frac{\partial c^2}{\partial v} \geq 0, \tag{9.16}$$

the LHS (left hand side) of which can be calculated as

$$\begin{aligned} \lim_{v\to 0}[\beta(v,t) - \frac{1}{2}\frac{\partial c^2}{\partial v}] &= \lim_{v\to 0}\{\lambda_1 v + \lambda_2 v^{1-2\alpha} - (1-\alpha)\sigma^2 v^{1-2\alpha}\}, \\ &= \lim_{v\to 0}[\lambda_2 - \sigma^2(1-\alpha)]v^{1-2\alpha}. \end{aligned} \tag{9.17}$$

Thus we can immediately get the condition we need according to (9.16) and (9.17). This has completed the proof. □

Proposition 9.3.2. *If we impose $\alpha > -\frac{1}{2}$, or $\alpha \in (-1, -\frac{1}{2}]$ and $\lambda_2 \leq \sigma^2$, volatility will obey the non-explosion condition, which means that the volatility will be bounded.*

Proof. It is obvious that v never reaches infinity is equivalent to $\frac{1}{v}$ will never take negative values. By applying the Itô lemma and setting $u = \frac{1}{v}$ we have

$$\begin{aligned} du &= d\frac{1}{v}, \\ &= -v^{-2}dv + v^{-3}(dv)^2, \\ &= (-\lambda_1 v^{-1} - \lambda_2 v^{-1-2\alpha} + \sigma^2 v^{-1-2\alpha})dt - \sigma v^{-1-\alpha}dB_t, \\ &= [-\lambda_1 u + (\sigma^2 - \lambda_2)u^{1+2\alpha}]dt - \sigma u^{1+\alpha}dB_t. \end{aligned}$$

Now we set $\beta(u,t) = -\lambda_1 u + (\sigma^2 - \lambda_2)u^{1+2\alpha}$ and $c(u,t) = -\sigma u^{1+\alpha}$. According to the assumption in the Feller condition, we should have $\beta(0,t) \geq 0$ and $c(0,t) = 0$, which imply

$$\alpha > -1, \tag{9.18}$$

and

$$\begin{cases} \lambda_2 \in (-\infty, +\infty), & \alpha > -\frac{1}{2}, \\ \lambda_2 \in (-\infty, \sigma^2), & \alpha \leq -\frac{1}{2}, \end{cases}$$

respectively. Now again imposing the Feller condition, the following should be satisfied

$$\lim_{u \to 0} \beta(u,t) - \frac{1}{2}\frac{\partial c^2}{\partial u} = \lim_{u \to 0}(-\alpha\sigma^2 - \lambda_2)u^{1+2\alpha} \geq 0. \tag{9.19}$$

As a result, condition (9.19) yields

$$\begin{cases} \lambda_2 \in (-\infty, +\infty), & \alpha > -\frac{1}{2}, \\ \lambda_2 \in (-\infty, -\alpha\sigma^2), & \alpha \leq -\frac{1}{2}. \end{cases}$$

Combining all the conditions above, we will finally arrive at what we try to prove. □

Proposition 9.3.3. *If we impose $\lambda_1 > 0, \lambda_2 < 0$ and $\alpha < 0$, or $\lambda_1 < 0, \lambda_2 > 0$ and $\alpha > 0$, the volatility process is mean-reverting.*

Proof. Recall that the stochastic volatility follows

$$dv = (\lambda_1 v + \lambda_2 v^{1-2\alpha})dt + \sigma v^{1-\alpha} dB_t. \tag{9.20}$$

To set it mean-reverting, we should consider the ODE below

$$dv = (\lambda_1 v + \lambda_2 v^{1-2\alpha})dt, \tag{9.21}$$

which can be simplified as

$$\frac{\frac{1}{2\alpha} dv^{2\alpha}}{\lambda_1 v^{2\alpha} + \lambda_2} = dt. \tag{9.22}$$

Therefore, ODE (9.22) can be easily solved as

$$v^{2\alpha} = Ce^{2\alpha\lambda_1 t} - \frac{\lambda_2}{\lambda_1}. \tag{9.23}$$

The following two cases are considered to find the needed restriction on parameters for the volatility process to become mean-reverting.

(1) $\alpha < 0$.

In this scenario, when we set $\lambda_1 < 0$,

$$\lim_{t\to+\infty} v^{2\alpha} = \lim_{t\to+\infty} Ce^{2\alpha\lambda_1 t} - \frac{\lambda_2}{\lambda_1} = \infty,$$

which is not suitable. When we set $\lambda_1 > 0$,

$$\lim_{t\to+\infty} v^{2\alpha} = \lim_{t\to+\infty} Ce^{2\alpha\lambda_1 t} - \frac{\lambda_2}{\lambda_1} = -\frac{\lambda_2}{\lambda_1}.$$

To keep v non-negative, obviously $\lambda_2 < 0$.

(2) $\alpha > 0$.

Following the similar law of the first situation, to keep the mean-reverting property in this case, we can easily obtain

$$\lambda_1 < 0, \qquad \lambda_2 > 0. \tag{9.24}$$

This has completed the proof. □

In conclusion, to meet the requirement of the Feller condition, non-explosion condition and the mean-reverting property for the volatility, α should be limited in $(-1, 1)$ and other parameters should be restricted as

$$\begin{cases} \lambda_1 > 0, \lambda_2 < 0, & \alpha \in (-1, 0), \\ \lambda_1 < 0, \lambda_2 > 0, & \alpha \in (0, \frac{1}{2}), \\ \lambda_1 < 0, \lambda_2 \geq \sigma^2(1-\alpha), & \alpha \in [\frac{1}{2}, 1). \end{cases}$$

Although some people may argue that if we make the the transformation of $\bar{v}_t = v_t^{2\alpha}$, $\bar{\sigma} = 2\alpha\sigma$ and $k = -2\alpha\lambda_1$ together with $\theta = \frac{\frac{1}{2}(\alpha(1-2\alpha)\sigma^2 - 2\alpha\lambda_2}{2\alpha\lambda_1}$, our form will degenerate to the following original Heston version

$$\begin{aligned} \frac{dS}{S} &= r dt + \sqrt{\bar{v}} dW_t, \\ d\bar{v} &= k(\theta - \bar{v})dt + \bar{\sigma}\sqrt{\bar{v}} dB_t, \end{aligned} \tag{9.25}$$

our work is still meaningful since as stated before, our form could yield better results than the original Heston version under certain conditions. To further demonstrate this point,

the behavior of our form in real markets will be compared with the original Heston version through a carefully designed empirical study in the next section.

9.4 Empirical studies

In this section, we shall present and discuss the results of an empirical study, aimed to benchmark the performance between our form and that of the Heston version in terms of the closeness between the calculated option prices with model parameters extracted from the "historical data" and market prices, in order to show whether it is meaningful to propose another form of the Heston model.

9.4.1 Data description

Our empirical study was conducted on the data of S&P 500 European call options for two separate periods with each period containing two-year data. Actually, one period was deliberately chosen during the financial crisis (between Jan 2007 and Dec 2008), while another was selected for a post-crisis period from Sept 2011 to Aug 2013, the market during which can be viewed as under a normal condition. To simplify the calculations without losing key information for the purpose of this study, we took the average value of bid and ask prices as the option price.

In order to eliminate sample noise in the estimation of parameters, appropriate filters were applied to the raw data. First, following Bakshi et. al [11] and Christoffersen et. al [41], only Wednesday options data is used in the stage of parameter estimation since Wednesday is least likely to be a holiday in a week and also less likely to be affected by day-of-the-week effect. Moreover, since global optimization problems are quite time consuming, choosing one day a week helped us to effectively reduce the size of the data set so that a longer time series can be included in the process of parameter determination. Second, options with time to maturity less than 30 days were discarded since they usually possess less time value and less information about the future dynamics of the firm [165]. Options with more than 120 days to expiry were also excluded because there would be a high premium if they are traded, which makes them unpopular. Third, very deep in-the-money and very deep out-of-money options were discarded since they are not active in the market and may have liquidity-related biases [209]. More specifically, if moneyness is defined as

the percentage difference between the S&P 500 Index value and the corresponding strike price, i.e. $Moneyness = \frac{S-K}{K}$, then options with the absolute value of moneyness over 10% were excluded. Finally, options with prices less than \$1/8 were all removed since these prices are rather volatile [62] and such abnormal volatility may result in unusual option prices. As a summary, the numbers of observations for original data and filtered data are reported in Table 9.1. It needs to be emphasized that by applying these filters, all the important information is still preserved, while higher efficiency and accuracy can be obtained in the process of parameter estimation, according to various empirical studies conducted before.

Table 9.1: Yearly number of observations

Time	2007.1-2007.12	2008.1-2008.12	2011.9-2012.8	2012.9-2013.8
Original	112144	158732	294825	382637
Filtered(Whole week)	22095	23935	35452	48713
Filtered(Only Wednesday)	4684	5202	7235	9403

An important parameter that needs to be determined first is the risk-free interest rate. As time to maturity of options used is less than 120 days, it is reasonable to choose the three-month U.S. Treasury Bill Rate (T-Bill rate) released daily as a proxy of the risk-free rate [17, 209].

The total set of data is divided into two consecutive subsets, with the 1st one being used for parameter determination, while the 2nd one is used for comparison. Data in the first period of each example is referred to as in-sample observations which are used for parameter determination, whereas data in the latter period serves for the purpose of out-of-sample comparison. In the current study, both periods are of the duration of one year. To illustrate it more clearly, three steps are listed as follows with the first period (2007.1-2008.12) as an example.

- First of all, filtered Wednesday data during the period of Jan 2007 to Dec 2007 was used as the input to estimate model parameters.
- Second, with a genetic algorithm, parameters in our form and the original Heston version were determined respectively and in-sample errors were calculated based on the obtained "optional" parameters for this period.
- Finally, by applying the filtered Wednesday and whole week data from Jan 2008 to Dec 2008, out-of-sample errors were calculated so that the performance of the two

forms could be compared.

9.4.2 Parameter estimation

Model comparison empirically involving market data always begins with parameter estimation, which itself is a difficult problem. One of the most commonly adopted approaches is to find the parameter set that minimizes the distance between model and market prices. In our empirical study, a genetic algorithm was adopted to search for a solution of global minimization from the S&P 500 Index and options, in order to compare the pricing performance of the two forms.

To find the "optimal" parameter set that best fits the chosen market data, what we need to do is to minimize the distance between market and model prices. Therefore, one of the most important steps is to choose an appropriate objective function (loss function) [40]. Following Christoffersen & Jacobs [39] and Lim & Zhi [169], we adopt the dollar mean-squared errors defined as

$$MSE = \frac{1}{N}\sum_{i=1}^{N}[C^{Market} - C^{Model}]^2, \tag{9.26}$$

where C^{Market} denotes the market price of an option contract, C^{Model} represents the corresponding calculated price with the pricing formula by using a particular set of parameters, and N is the total number of observations selected for parameter estimation. It should be noted that the objective function (9.26) is not necessarily convex and there may exist several local minima. In this case, if a local optimization approach, such as the non-linear least squared method, is employed, we would not be sure whether the solution is a local minimum or a global one. Furthermore, if a local one is reached, it is still hard for us to attain the global solution and thus there is no point of using any local minimization technique. As a result, a global optimization is preferred, in which some stochastic factors are generally introduced in their search process. This means that it will not stop searching when it finds a potential solution.

In fact, the method for optimization we adopted is a genetic algorithm [46], which is one of the most popular types of evolutionary algorithm [149] and based on the idea of natural selection. One of the most important qualities in the algorithm is that random changes are made to the potential solution to check whether there would be an improvement,

instead of following the known information to determine the next step. This very special feature has made genetic algorithms very reliable. In fact, there are a number of financial applications of genetic algorithms. For example, Sefiane & Benbouziane [206] adopted a genetic algorithm in optimal portfolio selection while Gimeno & Nave conducted estimation of the term structure of interest rates with genetic algorithms. Furthermore, it has also been applied in the area of option pricing [47, 99]. It is even pointed out by Bajpai & Kumar [10] that genetic algorithms are one of the best global optimization methods and can provide high quality solutions since they are intrinsically parallel and can explore the solution space in multiple directions each time.

In our study, the adopted genetic algorithm is Matlab built-in function *ga*, which has made it easy for us to implement. In Tables 9.2 and 9.3, estimation results obtained with data in a financial crisis and a normal market are exhibited, respectively.

Table 9.2: Estimation results with option data ranging from 2007.1 to 2007.12

parameters	σ	ρ	v_0	α	λ_1	λ_2	k	θ
Our form	0.6861	-0.7082	0.0981	0.9008	-16.4877	0.1882		
Heston	0.6684	-0.6223	0.0188				7.3249	0.0305

Table 9.3: Estimation results with option data ranging from 2011.9 to 2012.8

parameters	σ	ρ	v_0	α	λ_1	λ_2	k	θ
Our form	0.7224	-0.7093	0.0781	0.6911	-7.6438	0.2637		
Heston	0.8775	-0.6916	0.0298				7.5539	0.0510

The estimated parameters in Table 9.2 and Table 9.3 all appear to be in very reasonable range. For example, θ in the Heston model denotes the long-term mean of the volatility process and the extracted values are 0.0305 for the period with a financial crisis and 0.0510 for the normal period, respectively. On the other hand, the long-term mean for our form can be calculated from $-\frac{\lambda_2}{\lambda_1}$ and thus the results are 0.0114 and 0.0345 for the first and second example, respectively. These results are rather close to the one reported in [11] at 0.04. It is also interesting to notice that the long-term mean of the volatility in financial crisis is lower than that in the normal market for both forms.

Moreover, our estimated values of the so-called volatility of volatility range from 0.6684 to 0.8775, which are a little larger than those in Bakshi [11] and Eraker [86] using joint data of underlying returns and option prices. However, our results are quite similar to the results obtained in more recent studies [182]. Also, it should be noticed that 15 different

sets of parameters were obtained by Christoffersen et al. [43], who repeatedly used yearly option data as the input of the estimation between 1990 and 2004. According to their results, the value for the volatility of volatility can be as low as 0.3796 and as high as 0.8516. So, values we obtained for volatility of volatility are quite reasonable.

In addition, our estimation of the "leverage effect" ρ for the two models in two different cases is quite similar, ranging from -0.7093 to -0.6223. This result is rather satisfactory since most of the empirical studies show that the value for ρ was negative [11, 43, 231, 243]. In particular, if we again compare with the results in [43], it provided a quite wide range from -0.8519 to -0.5061, in which range our result is included.

With the reasonable parameters extracted from the filtered data, we are now ready to compare the performance of our form and the original Heston model with these reported parameters, which is presented in the next subsection.

9.4.3 Empirical comparison

Once model parameters have been estimated, it is natural for us to empirically compare performance of these two forms. It is obvious that we regard the performance of a model better if it results in lower pricing differences between the calculated option prices with model and the corresponding market prices. Specifically, root mean-squared error (RMSE) is adopted as a measure, which is the square root of the objective function (MSE), to reflect the pricing difference for both in-sample and out-of-sample comparison.

As for the in-sample comparison, it is clear that for both examples, the performance of the two forms is really similar. In fact, the Heston version performs slightly better than our form from the perspective of in-sample comparison. Specifically, the RMSE of the Heston version is 8.2767, while that for our form is 8.2954 in the the period of financial crisis (2007.1-2007.12) with the average call option price being $ 51.6222. As for the normal market (2011.9-2012.8), the average call option price is lower at $ 46.5101. In this case, although the absolute value of the RMSE for the two models increases, the gap between them is narrowed down, with 9.2802 and 9.2819 for the Heston version and our form respectively.

However, when we turn to the out-of-sample errors, it is quite a different story. In fact, Table 9.4 and 9.5 display the out-of-sample errors for the two periods (2008.1-2008.12, 2012.9-2013.8) respectively. It is clear that both forms generally perform better in the

normal market than in the financial crisis since the RMSE between Jan 2008 and Dec 2008 is approximately twice of that from Sept 2012 to Aug 2013. Specifically, our form is only slightly better than the Heston version in the financial crisis since by replacing the Heston version with our form, the maximum improvement in the RMSE is merely 1.33% with only Wednesday data and whole week data. In contrast, when we turn to the results in the normal market, what we can see first is that using only Wednesday data and employing all the filtered data for the whole year exhibit almost same results, which show that our form is much more attractive than the Heston version in this case. In particular, the RMSE of our form is smaller than that of the Heston version in both of the two cases, with the former being 83% of the latter.

Table 9.4: Out-of-sample errors for the first example

Data type	Model	Average price	RMSE
Wednesday	Ours	53.0310	20.7824
	Heston	53.0310	21.0616
	Rate		98.67%
All	Ours	53.7271	21.3709
	Heston	53.7271	21.6545
	Rate		98.69%

Table 9.5: Out-of-sample errors for the second example

Data type	Model	Average price	RMSE
Wednesday	Ours	44.4747	10.8238
	Heston	44.4747	12.8878
	Rate		83.98%
All	Ours	44.3649	10.5969
	Heston	44.3649	12.8659
	Rate		82.36%

On the other hand, the valuation errors for the option data of the whole year considered by moneyness are shown in Table 9.6 and 9.7. It should be noticed that the column of "No." refers to the observation numbers and "Difference" in these tables stands for the relative difference defined as

$$\text{difference} = \frac{|\text{Our form error} - \text{Heston version error}|}{\text{Heston version error}}. \tag{9.27}$$

In addition, an option is regarded as "at the money" (A) if $0.97 \leq S/K \leq 1.03$. The position of "in the money" (I) and "out of money" (O) refer to the case of $S/K > 1.03$ and $S/K < 0.97$, respectively.

Table 9.6 exhibits the performance of the two forms in financial crisis. Although our form generally performs better than the Heston model in this case, which is mentioned above, it turns out that the Heston version is a better choice when predicting out-of-money option prices since there would be 8.1% less errors. In contrast, when at-the-money and in-the-money options are taken into consideration, it is not difficult to find that there can be a more precise prediction with our form and its improvement can be 7.8% and 4.7% respectively.

Table 9.6: Out-of-sample errors of the first example according to moneyness

Moneyness	Model	Average price	No.	RMSE
$0.90 < S/K < 0.97(O)$	Ours	19.4995	9688	21.5817
	Heston	19.4995	9688	19.9681
	Difference			8.1%
$0.97 \leq S/K \leq 1.03(A)$	Ours	54.0624	7572	22.5165
	Heston	54.0624	7572	24.4305
	Difference			7.8%
$1.03 < S/K < 1.10(I)$	Ours	103.0018	6675	19.6566
	Heston	103.0018	6675	20.6272
	Difference			4.7%

A different phenomenon is shown by Table 9.7 that our forms greatly outperforms the Heston version for options either "in the money", "at the money" or "out of money". To be more specific, although "at-the-money" options exhibit the largest value of RMSE for both models, the maximum absolute difference of RMSE between our form and the Heston version is shown by "in-the-money" options to be 3.86. On the other hand, the relative difference of errors between our form and the Heston version for "out-of-money" options is the lowest at 6.7%, which is only approximately one half of that for "at-the-money" options. The largest improvement appears in the category of "in-the-money" options, almost reaching 30% when we replace the Heston version with our form, which is rather significant.

Therefore, based on these observations, we can certainly conclude that our form has certain advantages over the original Heston version in the normal market for S&P 500 with a genetic algorithm, which implies that it may provide more accurate results than the original Heston version for some cases.

Table 9.7: Out-of-sample errors of the second example according to moneyness

Moneyness	Model	Average price	No.	RMSE
$0.90 < S/K < 0.97(O)$	Ours	4.0590	17472	8.5902
	Heston	4.0590	17472	9.2077
	Difference			6.7%
$0.97 \leq S/K \leq 1.03(A)$	Ours	33.0472	15783	13.6092
	Heston	33.0472	15783	15.9021
	Difference			14.4%
$1.03 < S/K < 1.10(I)$	Ours	100.8722	15618	9.0335
	Heston	100.8722	15618	12.8935
	Difference			29.9%

9.5 Conclusion

In this chapter, the necessary and sufficient conditions to ensure the existence of a solution in an affine form are proved and imposed to establish an alternative form of the Heston model. This alternative form could offer certain advantages in parameter determination. After deriving the semi-closed pricing formula, our form is empirically compared with the Heston version by incorporating data of S&P 500 returns and options, with the Feller condition and another non-explosion condition correctly imposed in the parameter space to prevent the volatility from taking negative values or reaching infinity. Results show that our form generally outperforms the original Heston version for the case tested so far and it could be used as an alternative to the Heston version for some markets.

Chapter 10

An alternative form to calibrate the correlated Stein-Stein option pricing model

10.1 Introduction

With the rapid development of financial markets, investments on financial assets are really popular today. Financial derivatives, as one of the main kinds of financial assets, have received enormous attention, as a result of high demand for accurate pricing of them. Among these, European options considered here are one of the most significant and basic financial instruments, which can be used for hedging or speculations.

Despite the great success of B-S (Black-Scholes) model [19] for option pricing, in which asset returns are assumed to follow a log-normal distribution, and a simple and closed-form formula for European options can be obtained, it fails to reflect the phenomenon observed in the real market, such as skew [188] and leptokurtic [191] property of financial data. The constant volatility assumption, as another main disadvantage of this model, contradicts the results of empirical studies [73, 194], which show that the volatility varies randomly. Both of the two major unrealistic assumptions together with some other minor ones, have certainly led to mis-pricing of options with the classical B-S formula, which has thus encouraged the development of various modifications to the B-S model.

In an attempt to deal with the mis-pricing problem of the B-S model, jumps were included to model the underlying asset. Merton [178] proposed a modification by adding

a Poisson jump component to the original dynamics of the B-S model. Another well-known jump-diffusion model was proposed by Kou [158] with jump sizes modeled by a double exponential distribution. The B-S model could also be further modified with Brownian motion being replaced by a pure jump process, such as the VG model suggested by Madan et al. [173] and the CGMY model proposed by Carr et al. [29].

Another popular approach to improve the behavior of B-S model is to incorporate non-constant volatility. Among all these attempts, the two most natural ones are to either let the volatility be a deterministic function of underlying and time, the so-called "local volatility model" or make volatility another random variable described by another stochastic process, the so-called "stochastic volatility model". While the former was proposed by Dupire [74] and Derman & Kani [67], with the deterministic volatility function being determined from the well-known Dupire formula, the latter is much more popular now since many empirical studies suggest the "smile dynamics" are poorly captured by local volatility models (e.g., Hagan et. al [102]). Therefore, stochastic volatility models receive much more attention among researchers and market practitioners. In fact, the continuous-time stochastic volatility model was first studied by Johnson [146]. Later on Johnson & Shanno [147], Scott [204], and Wiggins [224] worked on option pricing problems under different stochastic volatility models with numerical methods. In particular, Johnson & Shanno adopted the Monte Carlo techniques to simulate SDE (stochastic differential equation) directly while Wiggins proposed a finite difference method to solve the involved PDE (partial differential equation). Unfortunately, neither of them is satisfactory due to the lack of closed-form solution, which could make it quite time-consuming when the model is applied in real markets. Furthermore, although Hull & White [127] made a progress and managed to obtain a power series approximation for option prices in their model, which seemed to be more attractive than those derived simply through numerical methods, there were two major disadvantages in their model. One is that they assumed zero correlation between the underlying price and the volatility, which is at odds with the reality since it violates the so-called "leverage effects" that the underlying price and the volatility should be negatively correlated [11]. Another is that the volatility process also did not possess the mean-reverting property, which contradicted the fact that the stochastic process for volatility is actually mean-reverting [14].

Two of the most famous models are the Stein-Stein model [213] and the Heston model

[117]. The former incorporated an Ornstein-Uhlenbeck process [93], while the latter used the CIR model to describe the volatility process. Their popularity can be mainly attributed to the existence of a closed-form solution for European option prices, which can have some obvious advantages over other models with which option prices need to be obtained numerically. In particular, with closed-form solutions, computational accuracy could certainly be guaranteed while there would exist systematical errors when numerical solutions must be resorted to for models that no closed-form solutions are associated with. Most importantly, having closed-form solution can spare us considerable amount of time and effort in parameter estimation, a vitally important process for any mathematical model to function properly as model parameters always need to be extracted from real market data during model calibration.

In this chapter, we present an alternative form of the correlated Stein-Stein model [198], which preserves its analytical tractability. Although the newly proposed form is equivalent to the original version and there would be no difference if one could work out all the model parameters analytically, the model calibration process in practice is so complicated that model parameters always need to be determined through an optimization algorithm. Moreover, as shown in [113], different forms of a certain model could yield quite different results when empirical studies are conducted. In this sense, we propose a different form of the correlated Stein-Stein model, and empirical comparison of our form and the original form is conducted based on the S&P 500 Index and options. Our results demonstrate that under certain market conditions, our new form could provide generally better results than the original Stein-Stein form.

The rest of the chapter is organized as follows. In Section 10.2, we will introduce the new form of the correlated Stein-Stein model with the closed-form solution for European call option. In Section 10.3, some preliminary empirical studies are conducted based on the S&P 500 Index returns and options to make comparison of our new form with the original Stein-Stein form, followed by some concluding remarks given in the last section.

10.2 The new form of the correlated Stein-Stein model

In this section, the new form is proposed under the risk-neutral measure first and then some conditions are imposed to keep the mean-reverting property of the volatility process.

10.2.1 Introduction of the new form

We begin by specifying the new model of the underlying asset S_t and the volatility v_t below.

$$\frac{dS}{S} = rdt + v^{\alpha}dW_t, \tag{10.1}$$

and

$$dv = [\frac{1}{2}(1-\alpha)\sigma^2 v^{1-2\alpha} + \lambda_1 v^{1-\alpha} + \lambda_2 v]dt + \sigma v^{1-\alpha}dB_t, \tag{10.2}$$

where W_t and B_t are Brownian motions with correlation ρ. We set $\sigma > 0$, $\alpha \in (-1,1)\backslash\{0\}$, while other requirements for parameters α, λ_1 and λ_2 will be given later.

10.2.2 Mean-reversion

A mean-reverting volatility model tells us that the high and low value of the volatility is temporary and it will tend to be the average over time. Thus when the mean-reverting feature is taken into account, we ignore the stochastic term in the process of volatility and only focus on the following ordinary differential equation.

$$dv = [\frac{1}{2}(1-\alpha)\sigma^2 v^{1-2\alpha} + \lambda_1 v^{1-\alpha} + \lambda_2 v]dt. \tag{10.3}$$

To find the long-term trend for v_t according to (10.3), three scenarios are discussed respectively as follows.

(1) $\lambda_2 = 0$.

In this case we only need to consider $dv = [\frac{1}{2}(1-\alpha)\sigma^2 v^{1-2\alpha} + \lambda_1 v^{1-\alpha}]dt$. As a result,

$$\frac{v^{2\alpha-1}dv}{\lambda_1 v^{\alpha} + \frac{1}{2}(1-\alpha)\sigma^2} = dt. \tag{10.4}$$

Setting $u = v^{\alpha}$ in Equation (10.4) yields

$$\frac{udu}{\lambda_1 u + \frac{1}{2}(1-\alpha)\sigma^2} = \alpha dt,$$

which implies

$$[\frac{1}{\lambda_1} - \frac{(1-\alpha)\sigma^2}{\lambda_1}\frac{1}{\lambda_1 u + \frac{1}{2}(1-\alpha)\sigma^2}]du = \alpha dt. \tag{10.5}$$

Integrating on the both sides of Equation (10.5) yields

$$[\lambda_1 u + \frac{1}{2}(1-\alpha)]e^{-\frac{2\lambda_1 u}{(1-\alpha)\sigma^2}} = C \cdot e^{-\frac{2\alpha\lambda_1^2}{(1-\alpha)\sigma^2}t}, \tag{10.6}$$

where C is a constant. As shown in the last two subsections, α should satisfy $\alpha \in (-\frac{1}{2}, 0) \cup (0, \frac{1}{2})$. In addition, the RHS (right hand side) of (10.6) is controlled by the value of α when $t \to +\infty$. Therefore, discussions with two separated parts are presented with α being positive and negative, respectively.

- If $\alpha \in (-1, 0)$, then

$$\lim_{t\to\infty}[\lambda_1 u + \frac{1}{2}(1-\alpha)]e^{-\frac{2\lambda_1 u}{(1-\alpha)\sigma^2}} = \infty,$$

from which we can obtain $\lim_{t\to\infty} u = \infty$. As a result,

$$\lim_{t\to\infty} v = \lim_{t\to\infty} u^{\frac{1}{\alpha}} = 0,$$

which contradicts the fact that $v > 0$.

- If $\alpha \in (0, 1)$, we have

$$\lim_{t\to\infty}[\lambda_1 u + \frac{1}{2}(1-\alpha)]e^{-\frac{2\lambda_1 u}{(1-\alpha)\sigma^2}} = 0,$$

from which we have

$$\lim_{t\to\infty} v = [-\frac{\frac{1}{2}(1-\alpha)\sigma^2}{\lambda_1}]^{\frac{1}{\alpha}}. \tag{10.7}$$

It is obvious that λ_1 should be negative since $v_t > 0$.

(2) $\lambda_2 < 0$.

We set $k = \dfrac{\lambda_2}{\frac{1}{2}(1-\alpha)\sigma^2 - \frac{\lambda_1^2}{4\lambda_2}}$. Obviously $k < 0$. So Equation (10.3) becomes

$$\frac{dv^{2\alpha}}{1 + k(v^\alpha + \frac{\lambda_1}{2\lambda_2})^2} = \frac{2\alpha\lambda_2}{k}dt. \tag{10.8}$$

By applying the transform $u = v^\alpha$ into Equation (10.8), the following is obtained.

$$\frac{udu}{1 + k(u + \frac{\lambda_1}{2\lambda_2})^2} = \frac{\alpha\lambda_2}{k}dt,$$

which can be further calculated as

$$[\frac{A}{1+\sqrt{-k}(u+\frac{\lambda_1}{2\lambda_2})}+\frac{B}{1-\sqrt{-k}(u+\frac{\lambda_1}{2\lambda_2})}]du=-\frac{\alpha\lambda_2}{k}dt, \tag{10.9}$$

where

$$A=\frac{\lambda_1}{4\lambda_2}+\frac{1}{2\sqrt{-k}},\quad B=\frac{\lambda_1}{4\lambda_2}-\frac{1}{2\sqrt{-k}}. \tag{10.10}$$

No matter what the value of λ_1 is, we can always show that $A>0, B<0$ (the proof is left in Appendix D.1). As a result, Equation (10.9) can be solved as

$$[1+\sqrt{-k}(u+\frac{\lambda_1}{2\lambda_2})]^A\cdot[1-\sqrt{-k}(u+\frac{\lambda_1}{2\lambda_2})]^{-B}=C\cdot e^{\frac{\alpha\lambda_2}{\sqrt{-k}}t}. \tag{10.11}$$

Since α can take either positive or negative values, we have the following two scenarios.

- If $\alpha\in(-1,0)$, then

$$\lim_{t\to\infty}[1+\sqrt{-k}(u+\frac{\lambda_1}{2\lambda_2})]^A\cdot[1-\sqrt{-k}(u+\frac{\lambda_1}{2\lambda_2})]^{-B}=\infty, \tag{10.12}$$

  which implies $\lim_{t\to\infty}u=\infty$. As a result,

$$\lim_{t\to\infty}v=\lim_{t\to\infty}u^{\frac{1}{\alpha}}=0,$$

  which contradicts the fact that $v>0$.

- If $\alpha\in(0,1)$, we have

$$\lim_{t\to\infty}[1+\sqrt{-k}(u+\frac{\lambda_1}{2\lambda_2})]^A\cdot[1-\sqrt{-k}(u+\frac{\lambda_1}{2\lambda_2})]^{-B}=0. \tag{10.13}$$

  What can be inferred from Equation (10.13) is that

$$\lim_{t\to\infty}1-\sqrt{-k}(u+\frac{\lambda_1}{2\lambda_2})=0, \tag{10.14}$$

  since $1+\sqrt{-k}(u+\frac{\lambda_1}{2\lambda_2})>1+\sqrt{-k}\frac{\lambda_1}{2\lambda_2}=2A\sqrt{-k}>0$. As a result, Equation (10.14) implies that

$$\lim_{t\to\infty}v=(-2B)^{\frac{1}{\alpha}}. \tag{10.15}$$

(3) $\lambda_2>0$.

In this case, it is impossible for the process v_t to be mean-reverting; the proof is given below according to different values of α.

- If $\alpha \in (0, 1)$, then

$$dv = v^{1-2\alpha}(\lambda_2 v^{2\alpha} + \lambda_1 v^{\alpha} + \frac{1}{2}(1-\alpha)\sigma^2)dt.$$

  Hence there exists a positive number p_1 that $dv > 0$ when $v^{\alpha} > p_1$, which means that v will keep increasing in this case and this is no mean-reverting.

- If $\alpha \in (-1, 0)$, then

$$dv = v(\lambda_2 + \lambda_1 v^{-\alpha} + \frac{1}{2}(1-\alpha)\sigma^2 v^{-2\alpha})dt,$$

  which implies that there exists a positive number p_2 that $dv > 0$ when $v^{-\alpha} > p_2$. In this case the process is again not a mean-reverting process.

All the discussion above leads to the following restrictions being imposed on the parameters in our model. In particular,

$$\alpha \in (0, 1), \tag{10.16}$$

$$\lambda_2 \in (-\infty, 0]. \tag{10.17}$$

As for λ_1, there exist two scenarios that $\lambda_1 < 0$ when $\lambda_2 = 0$, and $\lambda_1 \neq 0$ when $\lambda_2 < 0$.

After all the parameter restrictions are imposed, we are now ready to derive the pricing formula for European call options, which is presented in the next Section.

10.2.3 Analytic pricing formula

In this section the underlying asset price and the volatility are assumed to follow the dynamics introduced in Section 10.2.1, with which a closed-form pricing formula can be obtained.

Theorem 7. *Let $U(S, v, t)$ be the call option price with S_t and v_t following the new*

dynamics proposed in Section 10.2. Then

$$U(S,v,t) = SP_1 - Ke^{-r(T-t)}P_2, \tag{10.18}$$

where

$$\begin{aligned}
&P_j = \frac{1}{2} + \frac{1}{\pi}\int_0^\infty Re[\frac{e^{-i\phi ln(K)}f_j}{i\phi}]d\phi, \quad f_j = e^{C(\tau;\phi)+D(\tau;\phi)v^{2\alpha}+E(\tau;\phi)v^{\alpha}+i\phi x}, \quad j=1,2,\\
&D(\tau;\phi) = \frac{d-2\alpha(b_j+\lambda_2+i\phi\rho\sigma)}{4\alpha^2\sigma^2}(\frac{1-e^{d\tau}}{1-ge^{d\tau}}),\\
&E(\tau;\phi) = \frac{\lambda_1[d-2\alpha(b_j+\lambda_2+i\phi\rho\sigma)]}{2\alpha\sigma^2 d(1-ge^{d\tau})}(4e^{\frac{1}{2}d\tau}-2e^{d\tau}-2),\\
&C(\tau;\phi) = w(\tau;\phi) - w(0;\phi) + ri\phi\tau + \frac{1}{4}q(\tau),\\
&w(t;\phi) = \frac{\lambda_1^2[d-2\alpha(b_j+\lambda_2+i\phi\rho\sigma)]}{2\sigma^2 d^3}\{\frac{4arctan(i\sqrt{g}e^{\frac{dt}{2}})h}{ig\sqrt{g}} + [-2\alpha(b_j+\lambda_2+i\phi\rho\sigma)-d]td\\
&\qquad + \frac{[2\alpha(b_j+\lambda_2+i\phi\rho\sigma)-d](6g-4ge^{\frac{1}{2}dt}-4g^2e^{\frac{1}{2}dt}+g^2+1)}{g^2(ge^{dt}-1)} + \frac{(g+1)h\ln(ge^{dt}-1)}{g^2}\},\\
&d = 2\alpha\sqrt{(b_j+\lambda_2+i\phi\rho\sigma)^2-\sigma^2(2a_ji\phi-\phi^2)}, \quad g = \frac{2\alpha(b_j+\lambda_2+i\phi\rho\sigma)-d}{2\alpha(b_j+\lambda_2+i\phi\rho\sigma)+d},\\
&h = d(1+g) - 2\alpha(b_j+\lambda_2+i\phi\rho\sigma) + 2\alpha g(b_j+\lambda_2+i\phi\rho\sigma),\\
&q(t) = [d-2\alpha(b_j+\lambda_2+i\phi\rho\sigma)]t - 2ln(\frac{1-ge^{dt}}{1-g}), \quad p(t) = \alpha(b_j+\lambda_2+i\phi\rho\sigma)t + \frac{1}{2}q(t),\\
&a_1 = \frac{1}{2}, a_2 = -\frac{1}{2}, b_1 = \rho\sigma, b_2 = 0.
\end{aligned}$$

The proof of this proposition is left in Appendix D.2.

Although our form would degenerate to the original version

$$\begin{aligned}
\frac{dS}{S} &= rdt + \bar{v}dW_t,\\
d\bar{v} &= k(\theta-\bar{v})dt + \bar{\sigma}dB_t,
\end{aligned}$$

if we make the transformation of $\bar{v} = v^\alpha$, $k = -\alpha\lambda_2$, $\theta = -\frac{\lambda_1}{\lambda_2 k}$ and $\bar{\sigma} = \alpha\sigma$, our results are still meaningful since different forms of a certain model could yield different results in the model calibration process due to its complicatedness, as stated in [113]. In order to further demostrate this point, the behavior of our form in real markets will be compared with the original Stein-Stein form through a carefully designed empirical study in the next section.

10.3 Empirical studies

In this section, empirical results are presented and discussed with the Heston model being taken as a benchmark to assess the performance of our form in real markets. In the following, we will firstly describe the data we use and introduce the method adopted for parameter estimation. Then, the performance of these two models is quantitatively compared by the pricing errors measured with the "distance" between model-produced and market prices, and it is widely accepted that a model is regarded as the better one if it exhibits less pricing errors. In fact, pricing errors usually consist of two parts: the so-called in-sample errors and out-of-sample errors. Conventionally, the period in which market data is available is divided into two; the first one refers to a period in which data is used for parameter determination (referred to as the "in-sample observations") and the second one then refers to the period in which data is used to verify the performance of a model through a comparison between the observed option prices and the calculated option prices based on the parameters determined from the "in-sample" period (in contrast to the first period, data in the second period is usually referred to as the "out-of-sample observations"). It should be remarked that it is usually difficult to achieve lower in- and out-of-sample errors simultaneously. When comparing two models through a comparison of the in- and out-of-sample errors, it is hard to draw a conclusion if only one part of errors is less than the other. However, there should be no doubt in one's mind which model is superior if both of its in- and out-of-sample fitness are better. This is the principle based on which we draw the conclusions of our empirical studies in the subsection 10.3.3.

10.3.1 Data description

Our empirical study is conducted on a data set of the S&P 500 Index and European call options written on the S&P 500 Index from Sept 2010 to Aug 2012. However, raw data should not be adopted directly in the estimation since sample noise needs to be eliminated. Hence, several appropriate filters presented below were applied to the raw data, before they were used to estimate model parameters.

First of all, mid-prices, which equal to the average value of bid and ask prices, are used as option prices. It is well-known that wide bid-ask spread would discourage investors from trading. Thus, those samples with too much relative difference between offer and

bid prices, say $\frac{\text{offer} - \text{bid}}{\text{bid}} \geq 0.05$, are removed. Secondly, following a number of authors, such as Bakshi et. al [11] and Christoffersen et. al [41], only Wednesday and Thursday options data is adopted. In particular, Wednesday options data is used in estimation since Wednesday is least likely to be a holiday in a week and also less likely to be affected by the "day-of-the-week" effect than other days such as Monday and Friday, whereas the corresponding Thursday data serves as the market price to be compared with the predicted price calculated by the estimated parameters. Another motivation for only using Wednesday data in parameter estimation is that global optimization problems are usually quite time-consuming and choosing one day a week allows us to study a relatively longer time series yielding more reliable results. Thirdly, options with less than 30 days and more than 120 days to maturity are removed since there are less time values and less information about the future dynamics of the firm [165] for options with short time to expiry, and options with long time to expiry are traded at a high premium. Fourthly, very deep in-the-money and very deep out-of-money options are discarded due to their inactivity in the market and may also have liquidity-related biases [209]. Specifically, options with the absolute moneyness, defined as the relative difference between the S&P 500 Index value and the corresponding strike price ($Moneyness = \frac{S-K}{K}$) over 10% are excluded. Fifthly, options with prices less than 1/8 are all removed since these prices are rather volatile [62] and such abnormal volatility may result in unusual option prices. Finally, with dividend rate assumed to be zero, options not satisfying the general arbitrage restriction, i.e. $C \geq \max(0, S-K)$, are discarded.

It should be noted that after applying the above six filters, the daily average observations on Wednesday are over 30. Thus, we have also removed those days with only less than 5 sets of option data left to avoid biases when we analyze final results. This is because our estimation is conducted daily, and with a too-small number of samples (say, less than 5 sets of daily options data), we may end up obtaining better in-sample fitness at the expense of severely losing out-of-sample fitness. In Table 10.1, the numbers of observations for original data and filtered data are presented, respectively. It should be noted that after these filters are applied, more efficiency can be achieved in the process of parameter estimation with all the important information still preserved according to various previously conducted empirical studies in the literature [11, 41].

As for the risk-free interest rate, we chose the three-month U.S. Treasury Bill Rate,

Table 10.1: Number of observations

	Total	Daily average
Original data	543197	743
Filtered Wednesday data	3442	34
Filtered Thursday data	4070	41

which is released daily, as a proxy of the risk-free rate [17, 209] since the time to expiry of the selected options is less than 120 days. Upon the preparation of all the data described above, parameter estimation was conducted with a genetic algorithm as the main tool of optimization, the details of which are described in the next subsection.

10.3.2 Parameter estimation

In this section, we first provide a brief summary of the model parameters that need to be determined in the original Stein-Stein form and then introduce a genetic algorithm used to determine model parameters.

Recall that the correlated Stein-Stein model is specified as

$$\begin{aligned} \frac{dS}{S} &= rdt + vdW_t, \\ dv &= k(\theta - v)dt + \sigma dB_t, \end{aligned}$$

where the following five parameters, i.e. the mean-reversion speed k, the long-term mean θ, the volatility of volatility σ, correlation ρ between W_t and B_t and the initial value of volatility v_0, need to be determined from real market data.

A common approach to determine model parameters is to find the set of "optimal" parameters that minimizes the "distance" between market and model prices. Actually, there are different kinds of definition for the distance, a common one is to take the percentage mean squared error (PMSE)

$$PMSE = \frac{1}{N}\sum_{i=1}^{N}[\frac{C^{Market} - C^{Model}}{C^{Model}}]^2,$$

as the objective distance function to measure the relative difference between market and model prices. Here C^{Market} denotes the market price of an option contract from one sample, C^{Model} represents the corresponding calculated price with our pricing formula with a particular set of parameters and N is the total number of observations selected

in a single estimation. However, the main disadvantage in choosing such an objective function is that a cheap option (i.e., low C^{Market}) could place an abnormally high amount of weight in PMSE. Therefore, following Christoffersen & Jacobs [39] and Lim & Zhi [169], we instead chose the dollar mean-squared errors

$$MSE = \frac{1}{N}\sum_{i=1}^{N}[C^{Market} - C^{Model}]^2, \tag{10.19}$$

as the objective function.

Another issue is how to choose an appropriate optimization method. It should be noticed that although local minimization, which requires an initial guess that is very close to the true optimal solution, can be much less time consuming, its results are usually not reliable since it depends too much on the selected initial guess. In fact, the objective function (10.19) is not necessarily convex and thus there could exist several local minima, which would probably result in a local minimum being taken as the global minimum. In contrast, a properly designed global optimization should able to skip local minima and correctly identify the global minimum in an efficient way.

A genetic algorithm [46] is such a global optimization with some very nice properties. It is based on the idea of natural selection, introducing stochastic factors when searching for a satisfactory result in order to skip over local optima. One of the most important reasons for us to adopt this particular algorithm is that it randomly selects a number of different initial guesses to explore the entire solution space. Moreover, a so-called "mutation" step in the optimization process allows the algorithm to avoid local minima by preventing parameters from being restricted to a small region. In the literature, genetic algorithms have been applied in finance by quite a few researchers already. For instance, Gimeno & Nave [97] conducted estimation of the term structure of interest rates with a genetic algorithm while Grace [99] and Cont & Ben Hamida [47] have adopted it in the area of option pricing. It is even pointed out by Bajpai & Kumar [10] that genetic algorithms are one of the best global optimization methods and can provide high quality solutions since they are intrinsically parallel and can explore the solution space in multiple directions at the same time.

It should be remarked that another advantage of adopting a genetic algorithm is its implementation in the Matlab is straightforward by using a built-in function *ga*. As a

result of the numerical implementation, Table 10.2 exhibits the estimated daily parameters extracted from the selected market data for the two models under consideration in this chapter, respectively.

Table 10.2: Estimated parameters

parameters	σ	ρ	v_0	α	λ_1	λ_2	k	θ
Our form	1.4233	-0.5186	0.0363	0.4278	-2.1002	-12.3563		
Stein-Stein form	1.5710	-0.8170	0.0527				64.7818	0.0461

A careful analysis of the extracted parameters has led to some very interesting observations/remarks on the reasonableness of the obtained parameter values. First of all, the long-term mean in the original Stein-Stein form, denoted by the parameter θ, is 0.0461, while that for our form is 0.0510, which are quite similar to each other. In addition, our results are in the reasonable region since both of these values are also very close to many other results using different sets of data in the literature (e.g., see [11, 42]).

Secondly, the extracted volatility of volatility in our form is 1.4233, which is slightly smaller than that of the original Stein-Stein form. Although these results are larger than those reported in [43, 86], they are obviously smaller than those obtained in [167], which are over 2. Therefore, our results in this category are also in line with the existing literature and thus we believe that they are reasonable and acceptable.

Moreover, the values of correlation ρ (also known as "leverage effect") for our form and the original Stein-Stein form are -0.5186 and -0.8170 respectively. Although it seems that the results are quite distinct with each other, our results are still reasonable since the value for correlation could vary in a large range with different sets of data. For example, the value of ρ was documented to be in the range of -0.39 in [140] and -0.40 in [86]. In contrast, the results in [43] showed that it could be more negatively correlated as much as $\rho = -0.8519$.

An further check of the reasonableness of determined parameters is of course to conduct empirical comparison of the performance of our form with that of the original Stein-Stein form using these parameters, which is presented in the next subsection.

10.3.3 Empirical comparison

In this subsection, the performance of our form and the original Stein-Stein form in real markets is compared using the extracted parameters. Actually, it is widely accepted that

a model is regarded better if there exist less accumulated pricing errors calculated by the distance between model prices and market prices. Here, we adopt the root mean-squared error (RMSE), which is the square root of the objective function (MSE), as a measure of "goodness of fit". Table 4 exhibits the in- and out-of-sample errors for the two models.

Table 10.3: In- and out-of-sample errors for the two models

Error	In-sample	out-of-sample
Our form	0.2806	1.7558
Stein-Stein form	0.3715	1.8309
Relative difference	22.80%	4.10%

It is obvious from Table 10.3 that our form generally outperforms the original Stein-Stein form in terms of both in- and out-of-sample errors. To be more specific, from the perspective of in-sample errors, the daily averaged RMSE for our form is only 0.2806, compared with 0.3715 for the original Stein-Stein form. It is clear that our form is superior to the original Stein-Stein form in this case since the relative difference[1] between the two models, as far as the daily averaged RMSE is concerned, is almost 25%, which is quite significant. On the other hand, when out-of-sample errors are taken into consideration, a similar pattern emerges; our form still shows a better performance than the original Stein-Stein form, although the relative difference between them has narrowed down to 4.10%. Therefore, combining both in-sample and out-of-sample observations, we can conclude that our form serves as a better choice than the original Stein-Stein form for the data set chosen in this comparison.

It is also interesting to notice that the RMSE for out-of-sample errors is always much larger than that for in-sample errors. This is not difficult to understand since model prices are calculated with determined parameters; those obtained with in-sample data are believed to be "closest" to market prices of the corresponding option contracts, which implies that in-sample errors should be relatively low, while out-of-sample data are only used as the verification of option prices and certainly there is no guarantee that out-of-sample errors be low.

On the other hand, options are traded with a wide range of strikes in real markets and thus it is important to check the out-of-sample valuation errors sorted by moneyness,

[1] The relative difference is defined as

$$\text{Relative difference} = \frac{|\text{Our form error} - \text{Stein-Stein form error}|}{\text{Stein-Stein form error}}.$$

which are shown in Table 10.4. While the range of moneyness is indicated on the top row of the table, the abbreviation in the parentheses indicate "out of money" "at the money" and "in the money", respectively, from the left to the right columns.

Table 10.4: Out-of-sample errors according to moneyness

Moneyness	$0.90 < S/K < 0.97(O)$	$0.97 \leq S/K \leq 1.03(A)$	$1.03 < S/K < 1.10(I)$
Our form	0.9363	2.0645	1.6968
Stein-Stein form	0.9216	2.2155	1.7509
Relative difference	1.60%	6.82%	3.09%

From this table, we can see that although the original Stein-Stein form is a better choice as far as out-of-money option prices are concerned, the performance of our form is better than that of the original Stein-Stein form in the next two categories. However, the worse-off part is only 1.60% whereas the better-off parts are roughly at least doubled this percentage. Thereby, we can confidently conclude that our form has given an overall better performance than that of the original Stein-Stein form, particularly given that at or in the money performance of a model is far more important than its out of money performance. Of course, this conclusion is based on the empirical test of one set of data. It is quite possible that the performance of these two models may reverse with some other data sets. However, our empirical study presented here can at least suggest it may offer as a good competitor of the original Stein-Stein form for some other markets, such as commodity and futures exchange markets.

10.4 Conclusion

In this chapter, an alternative form of the correlated Stein-Stein model is proposed for option pricing and model calibration. Knowing that different forms of a certain model may yield different results in the model calibration process, our form is empirically compared with the well-known original Stein-Stein form with S&P 500 returns and options. Results show that our form generally outperforms the original Stein-Stein form, and thus it could be used as an alternative to the original Stein-Stein form for some markets.

Chapter 11

How should a local regime-switching model be calibrated?

11.1 Introduction

Despite the great success of the Black-Scholes model [19], in which the returns of the underlying were assumed to follow a log-normal distribution and a closed-form pricing formula for European options was derived, some of its simplified assumptions made to achieve analytical tractability are inappropriate and may lead to large pricing errors. In particular, one of its main drawbacks is the unrealistic assumption of constant volatility since the implied volatility extracted from market data tends to exhibit a "smile" curve with respect to the strike price [73], indicating that the assumption of constant volatility needs to be revised. As a result, a number of modifications have been proposed by introducing non-constant volatility in modeling underlying prices so that options can be priced with a model closer to reality.

In the literature, the non-constant volatility models can mainly be divided into two categories, i.e. stochastic volatility and local volatility. The former was investigated by a number of authors, such as Heston [117] with a CIR (Cox-Ingersoll-Ross) model to describe the volatility dynamic, and Hegan et al. [102] with a SABR model. Moreover, jump-diffusion dynamics are also combined with stochastic volatility by a number of authors, such as Bates [13], and Scott [205]. On the other hand, local volatility models were

considered by Dupire [75], Rubinstein [195], and Derman & Kani [67], who introduced the concept of taking volatility as a deterministic function of the underlying price and time, the specific form of which can be determined from market data through a model calibration process. There are a number of attractive features of local volatility models [68, 152, 183]. For example, local volatility models are easy and fast to calibrate since the only source of randomness is the underlying price. Also, the market becomes complete when adopting local volatility models and thus any contingent claim can be perfectly replicated with a portfolio consisting of the underlying and bond only. Most importantly, local volatility models can perfectly match any arbitrage-free set of European option prices. On the other hand, the generated local volatility surface in any local volatility model is actually static, which may yield poor hedging results [88, 102], and thus some hybrid models that combine local volatility and stochastic volatility have been proposed as a result [38, 217].

Recently, another kind of stochastic volatility models, the regime-switching model, is becoming quite popular since it proves to better capture the changing beliefs of investors towards the states of certain financial markets [104]. It was first introduced by Hamilton [103] and the volatility in this model can jump between different states controlled by a Markov chain. Its main attraction comes from a lot of empirical evidence, which suggests that the dynamics of the underlying price are better captured by allowing volatility to switch between different states [35, 86]. Therefore, it has been introduced to the area of financial derivative pricing and extensively studied by a number of researchers. For example, under regime-switching models, Naik [184] and Zhu et al. [244] worked on the valuation problem of European options, while Buffington & Elliott [26] and Bollen [20] priced American option contracts. Recently, the regime-switching mechanism has also been introduced into classical stochastic volatility models to form a regime-switching stochastic volatility models. In specific, Elliott et al. [82] introduced regime-switching into the Heston model with the long-term mean of the volatility process allowed to jump between different states and analytically evaluated volatility swaps, while the option pricing problem under general regime-switching stochastic volatility models was considered in [98]. Another example is [210], where the currency options are evaluated under a two-factor stochastic volatility model with regime-switching.

However, like in the Black-Scholes model, the assumptions of the classical regime-switching model with a constant volatility in each state may also need to be relaxed, in

order to better fit to market prices of options. This idea has prompted the development of the so-called local regime-switching model, where the volatility is a deterministic function of the underlying price and time rather than a constant that can switch among different states. Although Elliott et al. [85] have derived a Dupire equation (denoted by Elliott formula in the following) for the regime-switching model recently, they do not investigate the recovery of local volatility functions from market data, which is what we focus on throughout this chapter[1].

In fact, it should be emphasized that there are few empirical studies on regime-switching option pricing models, and it is even unclear on how to calibrate regime-switching models. Therefore, it is necessary to first develop an approach to implement Elliott's formula. In particular, the main two challenges in this model calibration process are a) the derived volatility function for each state involves all the state price variables whereas only one market price is available for model calibration; b) a direct implementation of Elliott et al.'s formula may not yield stable results. Hence, their formula alone does not allow the recovery of local volatility functions, and what will be presented first is a closed system on how to price options in real markets with classical regime-switching models, based on which one market price is split into two market-implied state prices through two financially meaningful equations. Once we have successfully obtained two market-implied state prices, another problem will certainly appear that Elliott formula can not be directly implemented since it may not yield accurate results due to the denominator being directly affected by the second-order derivative of option prices, the problem of which is similar to the case for the implementation of the Dupire formula in the Black-Scholes model [152, 230].

Specifically, under local volatility models, option prices as well as their derivatives can rarely be analytically derived, which implies that numerical approximations for the derivatives have to be made in the evaluation of the local volatility. However, the value of the second-order derivative of the option price with respect to the strike price is usually very small, and its approximation can result in large errors of the obtained local volatility as it appears in the denominator [152, 230]. The problem further deteriorates when the approximation of this particular second-order derivative becomes negative, in which case

[1]For illustration purpose, we shall focus on discussing the two-state regime-switching model in this chapter; the extension to arbitrary but finite number of states should be in principle very similar to what we present here.

the local volatility model fails as the calculated volatility is no longer a real number. For this reason, two main kinds of approaches have been proposed to solve this problem for the Black-Scholes model.

The first is to express local volatility in terms of a function of implied volatility [94] so that the second-order derivative does not soly appear in the denominator, which means that a small error induced on the second-order derivative does not necessarily lead to large errors of the entire volatility surface any more. However, this approach has a shortfall; the implied volatility remains a discontinuous function as a result of only scarce values of strike price and maturities being available in practice. This means that to obtain a local volatility function, one still needs to make necessary interpolation and extrapolation for a set of given data, which is a very difficult task itself with the constraint that no arbitrage opportunities should be introduced in the process of these numerical treatments. Another popular method is to use regularized approach to develop different algorithms so as to stably and accurately recover the local volatility function [78, 144]. Having been aware of the advantage of the regularized approach over the implied volatility approach, we will also adopt the regularized approach, and formulate the calibration problem associated with the local regime-switching model into an inverse problem of PDEs (partial differential equations) in this chapter. However, it should also be stressed that inverse problems are typically ill posed [220], and the situation is even worse in finance since not only option prices available in real markets are discontinuous, but also inadequate option data in terms of strikes and maturities is a serious issue that needs to be dealt with [45, 57, 63, 120]. In order to obtain stable results for this inverse problem, it is further transformed into an optimal control problem with the Tikhonov regularization [216]. Then, two necessary conditions that the optimal solution should satisfy are derived, based on which a numerical algorithm for iteration is proposed to obtain the optimal solution. Numerical experiments with synthetic are subsequently carried out to show the accuracy and stability of our algorithm, after which the performance of our algorithm is further tested with real market data.

The rest of the chapter is organized as follows. In Section 11.2, we will firstly propose a closed system to price options under the regime-switching model and then the specific steps to split one market price into two market-implied state prices for an option under this system will be introduced. In Section 11.3, the calibration problem will be formulated

into an inverse problem, which is further formed as an optimal control problem and is solved by a Tikhonov regularization approach. Two necessary conditions are also derived so that the numerical algorithm can be developed to find the optimal solution. In Section 11.4, numerical experiments and market tests for our algorithm are presented, followed by some concluding remarks given in the last section.

11.2 A closed system for calibration

In this section, a closed system should be established first for option pricing under regime-switching models with the constant volatility in each state, based on which how to split one market price of a European option into two market-implied state prices will be illustrated.

Let S_t be the price process of the underlying asset, then it follows a two-state regime-switching model under the risk-neutral measure as

$$\frac{dS_t}{S_t} = rdt + \sigma_{X_t}(S,t)dW_t, \tag{11.1}$$

where W_t is a Brownian motion independent of X_t and r represents the risk-free interest rate. In addition, X_t is a two-state Markov chain, which jumps between two states, i.e., $X_t \in \{(1,0)', (0,1)'\}$. Here, v' denotes the transpose of the vector v. If we define $\bar{\sigma}(S,t) = (\sigma_1(S,t), \sigma_2(S,t))'$ and let $< \cdot, \cdot >$ be the inner product of two vectors, $\sigma_{X_t}(S,t)$ can be expressed as

$$\sigma_{X_t}(S,t) =< \bar{\sigma}(S,t), X_t > . \tag{11.2}$$

Moreover, the transition between the two states follows a Poisson process as

$$P(t_{ij} > t) = e^{-\lambda_{ij}t}, i, j = 1, 2,\ i \neq j.$$

Here λ_{ij} is the transition rate from State i to j, and t_{ij} is the time spent in State i before transferring to State j.

It should be noted that there can be different ways to price options under this model. One approach is to assume that the market state is observable and the price of an option is the corresponding state price. However, it is usually difficult to determine which state the underlying asset price belongs to in practice, and thus it is more reasonable that the states of a financial market are treated as unobservable. The justification of the latter approach

lies in the stochastic nature of the volatility under a regime-switching model. In fact, for any stochastic volatility model, the current value of stochastic volatility is an unknown variable which needs to be estimated from real market data together with other model parameters. Such an "unobservable" nature has been discussed in the literature [3]. Due to the existence of Markov chain, regime-switching models are a special kind of stochastic volatility models and thus the volatility in any regime-switching model, together with the status of the regime the market is currently in, should all be assumed unobservable, as we do in this chapter.

Some people may argue that we are not able to obtain option prices without knowing the current state. However, this does not have to be true because when pricing an option, the probability of the underlying price being in each state at the current time should be known and be regarded as a model parameter. In this case the market price should be the expectation of the two state prices. Specifically, if we let C_1 and C_2 be the two state prices of a European option, and make π the probability of the underlying price that stays at the regime 1 at the current time (obviously the probability for the regime 2 is $1-\pi$), then it is reasonable to argue that the option price C should be

$$C = C_1\pi + C_2(1-\pi).$$

On the other hand, it is not clear how a regime switching model should be calibrated from a given set of data. Unlike the B-S model, where only the volatility needs to be estimated, the initial state probability, with which the state probability at any later time can be calculated, should be another parameter that needs to be determined through market data, apart from the two constant volatilities and two transition rates, when empirical studies are conducted for the classical regime-switching model. This can be analogous to the stochastic volatility model, in which the initial volatility level needs to be estimated too. In this case model prices can be calculated through $C_1\pi + C_2(1-\pi)$ and all model parameters can be estimated through some global optimization approaches by minimizing the "distance" between market prices and corresponding model prices, which can be done similarly as a lot of existing empirical studies [11, 30].

Considering all the discussion above, the closed system for option pricing under classical regime-switching models with the constant volatility in each state has already been set

up.

However, this is not enough when we take into account the local regime-switching model since to determine the two local volatility functions in this model, one market price of a European option should be split into two corresponding state prices since both of two state prices need to be used to recover the local volatility of any state. Therefore, if we still assume C_1 and C_2 be the two market-implied state prices corresponding to the market price C^{market}, we still need an extra equation to determine C_1 and C_2, apart from the following equation

$$C^{market} = C_1\pi + C_2(1-\pi). \tag{11.3}$$

In fact, the choice for such an equation is quite free as as long as this equation always holds when the regime-switching model degenerates to the Black-Scholes model.

One method that we believe is reasonable is that first of all, λ_{12} and λ_{21} and the two constant volatilities as well as the initial state probability are estimated with historical underlying and option data [142, 181], with which two state prices V_1 and V_2 can be worked out. It should be remarked that the two market-implied state prices C_1 and C_2 does not equal to the calculated V_1 and V_2 since V_1 and V_2 are obtained based on the assumption that the volatility in each state is constant. We then treat V_1 and V_2 as an approximation of C_1 and C_2 respectively and the relationship between them is imposed to serve as another equation

$$f(W_1, W_2, C_1, C_2) = 0. \tag{11.4}$$

The intuition behind such an approximation is that extracting parameters from real market data under classical regime-switching models has already made the model prices C^{model} calculated with these parameters very close to real market prices, and thus the corresponding state prices should also be a good approximation for the market-implied state prices. In this sense, one of the simplest examples is

$$(V_1 - V_2) - (C_1 - C_2) = 0, \tag{11.5}$$

the choice of which is based on two main reasons. One is that it obviously meets the requirement that it always holds when the regime-switching model degenerates to the

Black-Scholes model since in this case $V_1 = V_2$ and $C_1 = C_2$. Moreover, it is obvious that the biases between market prices and classical regime-switching model prices are caused by the difference between each state price of local regime-switching models and that of classical regime-switching models, and we make a reasonable assumption that the amount of these biases contributed by each state is the same.

With Equation (11.3) and Equation (11.4), it is not difficult to find that given one set of market prices, we could split them into two sets of market-implied state prices. Therefore, we are now ready to proceed to the calibration problem, which will be presented in the next section.

11.3 Calibration problem

In this section, a well-posed inverse problem for the calibration of local regime-witching models will be pointed out, and then a Tikhonov regularization approach will be introduced to recover smooth local volatility functions with the two sets of market-implied state prices obtained in the last section. Afterwards, two necessary conditions can be derived in order to reach the optimal solution, followed by the numerical algorithm showing the procedure of iteration to obtain the recovered local volatility functions.

11.3.1 An inverse problem

In this subsection, recovering the local volatility functions will firstly be formed into an ill-posed inverse problem, which will be further transformed into a well-posed inverse problem, before it could be properly solved.

If we let $V_1(S,t;K,T)$ and $V_2(S,t;K,T)$ be European call option prices for State 1 and State 2 respectively with K being the strike price and T being the expiry time, a system of coupled Black-Scholes equations for the option prices can be derived according to [26]

$$\begin{cases} \dfrac{\partial V_1}{\partial t} + \dfrac{1}{2}\sigma_1^2 S^2 \dfrac{\partial^2 V_1}{\partial S^2} + rS\dfrac{\partial V_1}{\partial S} - rV_1 - \lambda_{12}(V_1 - V_2) = 0,\ S > 0,\ t \in [0,T], \\ V_1(S,T) = \max(S-K,0), \\ V_1(0,t) = 0, \end{cases} \tag{11.6}$$

$$\begin{cases} \dfrac{\partial V_2}{\partial t} + \dfrac{1}{2}\sigma_2^2 S^2 \dfrac{\partial^2 V_2}{\partial S^2} + rS\dfrac{\partial V_2}{\partial S} - rV_2 - \lambda_{21}(V_2 - V_1) = 0, \ S > 0, \ t \in [0, T], \\ V_2(S, T) = \max(S - K, 0), \\ V_2(0, t) = 0. \end{cases} \tag{11.7}$$

Given the two sets of market-implied state prices $V_1^*(S_0, t_0; K, T)$ and $V_2^*(S_0, t_0; K, T)$ with different maturities and strike prices at time t_0, we want to recover the local volatility functions $\sigma_1(S, t)$ and $\sigma_2(S, t)$ for the two states from these market state prices, which formulate the following inverse problem.

Problem 1. *Find the two functions $\sigma_1(S, t)$ and $\sigma_2(S, t)$ such that the solution to the coupled PDE system (11.6) and (11.7), $V_1(S_0, t_0; K, T)$ and $V_2(S_0, t_0; K, T)$, satisfy the following two equations*

$$\begin{aligned} V_1(S_0, t_0; K, T) &= V_1^*(S_0, t_0; K, T), \\ V_2(S_0, t_0; K, T) &= V_2^*(S_0, t_0; K, T), \end{aligned}$$

respectively for all T and K.

Unfortunately, it should be noted that Problem 1 is not well-posed [192] since the variables of the coupled PDE system (11.6) and (11.7) are S and t, whereas $V_1^*(S_0, t_0; K, T)$ and $V_2^*(S_0, t_0; K, T)$ are observed with respect to K and T at a particular time t_0 and underlying price S_0. Thereby, alternative ways should be found to obtain the two local volatility functions. With the help of [85], in which a Dupire equation for the regime-switching model is derived, the coupled PDE system (11.6) and (11.7) is established with new variables K and T as

$$\begin{cases} \dfrac{\partial V_1}{\partial T} - \dfrac{1}{2}\sigma_1^2(K, T)K^2 \dfrac{\partial^2 V_1}{\partial K^2} + rK\dfrac{\partial V_1}{\partial K} - \lambda_{12}V_1 + \lambda_{21}V_2 = 0, \ K > 0, \ T \geq t_0, \\ V_1(K, t_0) = \max(S_0 - K, 0), \\ V_1(0, T) = S_0, \end{cases} \tag{11.8}$$

$$\begin{cases} \dfrac{\partial V_2}{\partial T} - \dfrac{1}{2}\sigma_2^2(K, T)K^2 \dfrac{\partial^2 V_2}{\partial K^2} + rK\dfrac{\partial V_2}{\partial K} - \lambda_{21}V_2 + \lambda_{12}V_1 = 0, \ K > 0, \ T \geq t_0, \\ V_2(K, t_0) = \max(S_0 - K, 0), \\ V_2(0, T) = S_0. \end{cases} \tag{11.9}$$

In theory, it is quite easy to work out the local volatility by simply differentiating the state prices once with respect to strike and expiry respectively, and twice with respect to the strike. However, the computation may not be stable since it involves the second-order derivative with respect to the strike and we can not guarantee that the variance be positive. Furthermore, the state prices are discontinuous and the numerical differentiation requires interpolation and extrapolation, which can affect the accuracy of the obtained local volatility. Therefore, another inverse problem should be formulated as summarized below. In this newly formulated problem, we have simplified the solution procedure for the inverse problem by assuming that the volatility be independent of time, in order to focus on the core issue for this chapter, i.e., to illustrate how a local regime-switching model can be calibrated. Of course, as a progressive approach to tackle the complexity arisen from the multi-dimensionality of an inverse problem, such kind of simplified assumptions has already been adopted in calibrating local Black-Scholes model with real market data (e.g., [21]).

Problem 2. *Given the fixed maturity T, find the two functions $\sigma_1(K)$ and $\sigma_2(K)$ such that the solution to the coupled PDE system (11.8)-(11.9), $V_1(K)$ and $V_2(K)$, satisfy the following two equations*

$$\begin{aligned} V_1(K,T) &= V_1^*(K), \\ V_2(K,T) &= V_2^*(K), \end{aligned}$$

respectively for all K.

Here, for simplicity, we denote

$$\begin{aligned} V_i(K,T) &= V_i(S_0,t_0;K,T), \\ V_i^*(K) &= V_i^*(S_0,t_0;K,T), \end{aligned}$$

for $i = 1, 2$.

By now, we have already formed a well-posed inverse problem for the recovery of local volatility functions in the sense that the market data is observed with respect to the strike price K and the maturity T, which are exactly the same as the variables in the PDE system (11.8)-(11.9). This has paved the way for us to solve this problem, which is illustrated in

the next subsection.

11.3.2 Tikhonov regularization

In this subsection, Tikhonov regularization will be used to solve Problem 2. The motivation for us to adopt this particular regularization technique is that it allows us to obtain stable solutions to optimal control problems. In particular, the two local volatility functions in regime-switching models should be determined simultaneously so that the following cost function is minimized

$$J(\sigma_1,\sigma_2)=\frac{\delta}{2}\int_0^{+\infty}(\frac{\partial\sigma_1}{\partial K})^2+(\frac{\partial\sigma_2}{\partial K})^2dK+\frac{1}{2}\int_0^{+\infty}[V_1(K,\tau_0)-V_1^*(K)]^2+[V_2(K,\tau_0)-V_2^*(K)]^2dK, \tag{11.10}$$

where $\tau = T - t$, and δ is called the Tikhonov regularization parameter. Therefore, Problem 2 derived in the last subsection is now turned to an optimal control problem that we should find $\bar{\sigma}_1(K)$ and $\bar{\sigma}_2(K)$ such that

$$J(\bar{\sigma}_1,\bar{\sigma}_2)=\inf_{\sigma_1,\sigma_2\in A}J(\sigma_1,\sigma_2), \tag{11.11}$$

where $A=\{\sigma\in C(R)|\dfrac{\partial\sigma}{\partial K}\in L^2(R)\}$.

Therefore, recovering the two local volatility functions reduces to solve this optimal control problem, for which we would derive two necessary conditions. If we assume $\bar{\sigma}_1(K)$ and $\bar{\sigma}_2(K)$ be the solution of the optimal control problem (11.11), it is clear that for any $h\in A$, both of the following two functions, i.e. $J(\bar{\sigma}_1+\lambda h,\bar{\sigma}_2)$ and $J(\bar{\sigma}_1,\bar{\sigma}_2+\lambda h)$, reach their minimum when $\lambda=0$, which implies

$$\frac{d}{d\lambda}J(\bar{\sigma}_1+\lambda h,\bar{\sigma}_2)|_{\lambda=0}=0,\quad \frac{d}{d\lambda}J(\bar{\sigma}_1,\bar{\sigma}_2+\lambda h)|_{\lambda=0}=0. \tag{11.12}$$

This could certainly yield

$$\delta\int_0^{+\infty}\frac{\partial\bar{\sigma}_1}{\partial K}\frac{\partial h}{\partial K}dK+\int_0^{+\infty}[V_1(K,\tau_0)-V_1^*(K)]\xi_1(K,\tau_0)+[V_2(K,\tau_0)-V_2^*(K)]\xi_2(K,\tau_0)dK=0, \tag{11.13}$$

$$\delta \int_0^{+\infty} \frac{\partial \bar{\sigma}_2}{\partial K} \frac{\partial h}{\partial K} dK + \int_0^{+\infty} [V_1(K,\tau_0) - V_1^*(K)]\eta_1(K,\tau_0) + [V_2(K,\tau_0) - V_2^*(K)]\eta_2(K,\tau_0) dK = 0, \tag{11.14}$$

where $\xi_i(K,\tau) = \frac{dV_i(K,\tau;\bar{\sigma}_1+\lambda h,\bar{\sigma}_2)}{d\lambda}|_{\lambda=0}$, $\eta_i(K,\tau) = \frac{dV_i(K,\tau;\bar{\sigma}_1,\bar{\sigma}_2+\lambda h)}{d\lambda}|_{\lambda=0}$ for $i = 1, 2$.

To work out the necessary condition (11.13), what we should do first is to calculate the two functions $\xi_1(K,\tau)$ and $\xi_2(K,\tau)$. In fact, $V_i(K,\tau;\bar{\sigma}_1+\lambda h,\bar{\sigma}_2), i = 1, 2$ should satisfy the PDE in (11.8) and (11.9), respectively, except that σ_1 is replaced by $\bar{\sigma}_1+\lambda h$. Therefore, by taking the derivative on both sides of the coupled PDEs governing $V_i(K,\tau;\bar{\sigma}_1+\lambda h,\bar{\sigma}_2), i = 1, 2$ with respect to λ and then setting $\lambda = 0$, we can find that $\xi_1(K,\tau)$ and $\xi_2(K,\tau)$ satisfy the following coupled PDE system

$$\begin{aligned} L_1\xi_1 &\triangleq \frac{\partial \xi_1}{\partial \tau} - \frac{1}{2}\sigma_1^2 K^2 \frac{\partial^2 \xi_1}{\partial K^2} + rK\frac{\partial \xi_1}{\partial K} - \lambda_{12}\xi_1 + \lambda_{21}\xi_2 = h\sigma_1 K^2 \frac{\partial^2 V_1}{\partial K^2}, \\ L_2\xi_2 &\triangleq \frac{\partial \xi_2}{\partial \tau} - \frac{1}{2}\sigma_2^2 K^2 \frac{\partial^2 \xi_2}{\partial K^2} + rK\frac{\partial \xi_2}{\partial K} - \lambda_{21}\xi_2 + \lambda_{12}\xi_1 = 0, \end{aligned}$$

with the initial conditions

$$\xi_1|_{\tau=0} = 0, \quad \xi_2|_{\tau=0} = 0.$$

It should be remarked here that it is very difficult to directly figure out $\xi_1(K,\tau)$ and $\xi_2(K,\tau)$ from the above coupled PDEs as the existence of the unknown function h, and thus we have to find an alternative way. Now, we let $L = (L_1, L_2)$, and denote $L^* = (L_1^*, L_2^*)$ as the adjoint operator of L [85]. We further assume ϕ_1 and ϕ_2 be the solution to the adjoint PDEs

$$L_1^*\phi_1 \triangleq -\frac{\partial \phi_1}{\partial \tau} - \frac{\partial^2(\frac{1}{2}\sigma_1^2 K^2 \phi_1)}{\partial K^2} - \frac{\partial (rK\phi_1)}{\partial K} - \lambda_{12}\phi_1 + \lambda_{12}\phi_2 = 0, \tag{11.15}$$

$$L_2^*\phi_2 \triangleq -\frac{\partial \phi_2}{\partial \tau} - \frac{\partial^2(\frac{1}{2}\sigma_2^2 K^2 \phi_2)}{\partial K^2} - \frac{\partial (rK\phi_2)}{\partial K} - \lambda_{21}\phi_2 + \lambda_{21}\phi_1 = 0, \tag{11.16}$$

with the terminal conditions given by

$$\phi_1|_{\tau=\tau_0} = V_1(K,\tau_0) - V_1^*(K), \quad \phi_2|_{\tau=\tau_0} = V_2(K,\tau_0) - V_2^*(K).$$

Then, it is not difficult to obtain

$$\begin{aligned} Z &\triangleq \int_0^{\tau_0}\int_0^{+\infty}(\phi_1 L_1\xi_1+\phi_2 L_2\xi_2)-(\xi_1 L_1^*\phi_1+\xi_2 L_2^*\phi_2)dKd\tau, \\ &= \int_0^{\tau_0}\int_0^{+\infty}(\phi_1\frac{\partial\xi_1}{\partial\tau}+\xi_1\frac{\partial\phi_1}{\partial\tau})+(\phi_2\frac{\partial\xi_2}{\partial\tau}+\xi_2\frac{\partial\phi_2}{\partial\tau})dKd\tau \\ &+ \int_0^{\tau_0}\int_0^{+\infty}(\phi_1\hat{L}_1\xi_1+\phi_2\hat{L}_2\xi_2)-(\xi_1\hat{L}_1^*\phi_1+\xi_2\hat{L}_2^*\phi_2)dKd\tau, \end{aligned} \tag{11.17}$$

where $\hat{L}(=(\hat{L}_1,\hat{L}_2))$ and $\hat{L}^*(=(\hat{L}_1^*,\hat{L}_2^*))$ are derived by removing the derivative with respect to τ in L and L^* respectively. As a result, $\hat{L}^*$ is also the adjoint operator of $\hat{L}$ with respect to K, which could lead to

$$<\hat{L}\xi,\phi>=<\xi,\hat{L}^*\phi>, \tag{11.18}$$

according to the property of adjoint operators with $\xi=(\xi_1,\xi_2)$ and $\phi=(\phi_1,\phi_2)$. This implies

$$\int_0^{+\infty}(\phi_1\hat{L}_1\xi_1+\phi_2\hat{L}_2\xi_2)-(\xi_1\hat{L}_1^*\phi_1+\xi_2\hat{L}_2^*\phi_2)dK=0. \tag{11.19}$$

Therefore, Equation (11.17) can be further simplified as

$$\begin{aligned} Z &= \int_0^{+\infty}\int_0^{\tau_0}(\phi_1\frac{\partial\xi_1}{\partial\tau}+\xi_1\frac{\partial\phi_1}{\partial\tau})+(\phi_2\frac{\partial\xi_2}{\partial\tau}+\xi_2\frac{\partial\phi_2}{\partial\tau})d\tau dK, \\ &= \int_0^{+\infty}\xi_1\phi_1|_0^{\tau_0}+\xi_2\phi_2|_0^{\tau_0}dK, \\ &= \int_0^{+\infty}[V_1(K,\tau_0)-V_1^*(K)]\xi_1(K,\tau_0)+[V_2(K,\tau_0)-V_2^*(K)]\xi_2(K,\tau_0)dK, \end{aligned} \tag{11.20}$$

the last step of which is obtained by the substitution of the initial condition for ξ and the terminal condition for ϕ. On the other hand, Z can be calculated directly through its definition as

$$Z=\int_0^{\tau_0}\int_0^{+\infty}\phi_1 h\bar{\sigma}_1K^2\frac{\partial^2V_1}{\partial K^2}dKd\tau, \tag{11.21}$$

since $L_1\xi_1=h\sigma_1K^2\frac{\partial^2V_1}{\partial K^2}$, $L_2\xi_2=0$, $L_1^*\phi_1=0$, and $L_2^*\phi_2=0$. Thereby, combining Equation (11.13), (11.20) and (11.21) yields

$$\delta\int_0^{+\infty}\frac{\partial\bar{\sigma}_1}{\partial K}\frac{\partial h}{\partial K}dK+\int_0^{\tau_0}\int_0^{+\infty}\phi_1 h\bar{\sigma}_1K^2\frac{\partial^2V_1}{\partial K^2}dKd\tau=0, \tag{11.22}$$

which should hold for any $h\in A$. This demonstrates that $\bar{\sigma}_1$ is the weak solution to the

following equation

$$-\delta\frac{\partial^2\bar{\sigma}_1}{\partial K^2}+\int_0^{\tau_0}\phi_1\bar{\sigma}_1K^2\frac{\partial^2V_1}{\partial K^2}d\tau=0. \tag{11.23}$$

In a similar fashion, another necessary (11.14) for $\bar{\sigma}_2$ can also be written in a simpler form

$$-\delta\frac{\partial^2\bar{\sigma}_2}{\partial K^2}+\int_0^{\tau_0}\phi_2\bar{\sigma}_2K^2\frac{\partial^2V_2}{\partial K^2}d\tau=0. \tag{11.24}$$

By now, we have obtained the optimality conditions for our optimal control problem (11.11), and thus the problem of recovering the two local volatility functions is now equivalent to finding the solutions of $\phi_i, i=1,2$ to the coupled PDEs (11.15) and (11.16) so that $\bar{\sigma}_1$ and $\bar{\sigma}_2$ are solutions to Condition (11.23) and (11.24) respectively. Hence, in the next subsection, a numerical algorithm will be designed to find the optimal solution.

11.3.3 Numerical algorithm

In this subsection, an algorithm is established to obtain the optimal solution to the optimal control problem (11.11). It should be noticed that the algorithm involves solving a system of equation (11.8)-(11.9), (11.15)-(11.16) and (11.23)-(11.24).

Specifically, the semi-infinite operating domain is truncated into a bounded one as

$$\tau\in[0,\tau_0],\quad K\in[0,2S_0], \tag{11.25}$$

where S_0 is the underlying price at τ_0. Let $d\tau$ and dK be the step size in the time direction and the space direction respectively with $N_1=\dfrac{2S_0}{dK}, N_2=\dfrac{\tau_0}{d\tau}$, and thus the truncated domain $[0,2S_0]\times[0,\tau_0]$ is discretized uniformly as

$$\begin{aligned} K_n &= (n-1)\frac{2S_0}{N_1},\quad n=1,2...N_1+1,\\ \tau_m &= (m-1)\frac{\tau_0}{N_2},\quad m=1,2...N_2+1. \end{aligned}$$

We also denote the functions at j-th step iteration as $\bar{\sigma}_{i,j}, V_{i,j}, \phi_{i,j}, i=1,2$. Then, given two sets of market-implied state prices, we are now ready to present the iteration procedure.

1. Let $j=0$. The value of a tolerance parameter ϵ used to control the convergence of the iteration is set. Also, initial guesses for the volatility functions $\sigma_{i,0}, i=1,2$, need to be chosen.

2. Two sets of option prices $V_{i,j}(K,\tau), i=1,2$, can be calculated through PDEs (11.8)-(11.9) corresponding to $\sigma_{i,j}, i=1,2$, with an implicit discretization as

$$\begin{aligned}\frac{V_{1,j}^{n,m+1}-V_{1,j}^{n,m}}{d\tau} &- \frac{(\sigma_{1,j}^n)^2(K_n)^2[V_{1,j}^{n+1,m+1}-2V_{1,j}^{n,m+1}+V_{1,j}^{n-1,m+1}]}{2(dK)^2} \\ &- rK_n\frac{V_{1,j}^{n+1,m+1}-V_{1,j}^{n-1,m+1}}{2dK}-\lambda_{12}V_{1,j}^{n,m+1}+\lambda_{21}V_{2,j}^{n,m+1}=0,\end{aligned}$$

and

$$\begin{aligned}\frac{V_{2,j}^{n,m+1}-V_{2,j}^{n,m}}{d\tau} &- \frac{(\sigma_{2,j}^n)^2(K_n)^2[V_{2,j}^{n+1,m+1}-2V_{2,j}^{n,m+1}+V_{2,j}^{n-1,m+1}]}{2(dK)^2} \\ &- rK_n\frac{V_{2,j}^{n+1,m+1}-V_{2,j}^{n-1,m+1}}{2dK}-\lambda_{21}V_{2,j}^{n,m+1}+\lambda_{12}V_{1,j}^{n,m+1}=0.\end{aligned}$$

3. With $\bar{\sigma}_{i,j}, i=1,2$, and the obtained $V_{i,j}(K,\tau_0), i=1,2$, in Step 2, $\phi_{i,j}, i=1,2$, can be calculated by solving PDEs (11.15)-(11.16) with an implicit discretization, which is similar to that in step 2 and thus the scheme is omitted.

4. By making use of $V_{i,j}(K,\tau_0), i=1,2$, and $\phi_{i,j}, i=1,2$, obtained in Step 2 and 3 respectively, the updated local volatility functions $\bar{\sigma}_{i,j+1}, i=1,2$, can be derived by solving the coupled ordinary differential equations (11.23)-(11.24). It should be noted that the integration in the two equations can be carried out with the trapezoidal rule, which is given as

$$\begin{aligned}W_{i,j}^n &\triangleq \int_0^{\tau_0}\phi_{i,j}\bar{\sigma}_{i,j}K^2\frac{\partial^2 V_1}{\partial K^2}\tau, \\ &= \frac{d\tau}{2}\sum_{m=1}^{N_2}[\phi_{i,j}^{n,m}\sigma_{i,j}^n(K_n)^2\frac{V_{i,j}^{n+1,m}-2V_{i,j}^{n,m}+V_{i,j}^{n-1,m}}{(dK)^2} \\ &+ \phi_{i,j}^{n,m+1}\sigma_{i,j}^n(K_n)^2\frac{V_{i,j}^{n+1,m+1}-2V_{i,j}^{n,m+1}+V_{i,j}^{n-1,m+1}}{(dK)^2}],\end{aligned}$$

for $i=1,2$. In addition, to make the iteration smoother, we introduce a "false" time θ in solving the two equations. The algorithm is provided in the following

$$\frac{\sigma_{i,j+1}^n-\sigma_{i,j}^n}{\theta}-\delta\frac{\sigma_{i,j}^{n+1}-2\sigma_{i,j}^n+\sigma_{i,j}^{n-1}}{(dK)^2}+W_{i,j}^n=0, \tag{11.26}$$

for $i=1,2$.

5. If

$$||\sigma_{1,j+1} - \sigma_{1,j}|| + ||\sigma_{2,j+1} - \sigma_{2,j}|| < \epsilon, \tag{11.27}$$

then we let $\bar{\sigma}_i = \sigma_{i,j+1}, i = 1, 2$, and stop the iteration. Otherwise, set $j = j + 1$ and go back to Step 2.

After the algorithm is designed, a natural question is how it performs and whether the recovered volatility functions would be accurate. Numerical experiments will be presented in the next section.

11.4 Numerical examples and market tests

In this section, numerical experiments are firstly conducted to show the accuracy and the stability of our numerical algorithm, and then the performance of our approach is further tested with real market data.

11.4.1 Accuracy tests

In this subsection, results of numerical experiments are presented to realize the designed algorithm in the last section. In order to demonstrate the accuracy of the algorithm, we carry out tests with exact solutions of the two volatility functions. To be more specific, the two "true" volatility functions denoted by $\sigma_i^*(S), i = 1, 2$, are pre-set, through which two sets of state prices $V_i(S_0, t_0; K_n, T), i = 1, 2$, can be generated with the coupled PDE system (11.6)-(11.7). Afterwards, we treat $V_i(S_0, t_0; K_n, T), i = 1, 2$ as market state prices, i.e.

$$V_i^*(K_n) = V_i(S_0, t_0; K_n, T), \quad i = 1, 2, \tag{11.28}$$

which will be used to recover the volatility functions through our algorithm.

In fact, these tests can be viewed as a pseudo-empirical study, because they were conducted in such a way that a time series of discrete data is generated from a stochastic process with two given volatility functions. Then we tried to see if we could recover the volatility function using the proposed algorithm as an inverse problem. When a hierarchy of given test functions is employed to go through these tests, starting from the simplest constant functions, they are the necessary conditions to ensure that the proposed algorithm is able to cope with much more complicated volatility functions to be recovered from real

market data, as any complicated function can be somewhat viewed as a decomposition of these simple functions.

Three test volatility functions were chosen in order to show that our algorithm is able to recover different shapes of volatility curve. In all these tests, model parameters were set to be

$$\begin{aligned} S_0 &= 10,\ t_0 = 0,\ r = 0.05,\ T = 1,\ \lambda_{12} = 0.1,\ \lambda_{21} = 0.2,\ N_1 = 30,\ N_2 = 50, \\ \delta &= 0.2,\ \theta = 10^{-3},\ \epsilon = 5 * 10^{-12}. \end{aligned}$$

In the first experiment, we start with the lowest order of test function in the hierarchy of the test functions, i.e., with the volatility being "flat" as

$$\sigma_1(S) = 0.4, \quad \sigma_2(S) = 0.2. \tag{11.29}$$

Of course, this does not mean that the volatility function to be recovered in practice will be of such a simple form. But, if the designed algorithm is even unable to recover such simplest form of local volatility functions, this algorithm can never be trusted and should certainly not be adopted for real markets. In other words, this is a necessary step, as the most fundamental function in the hierarchy of test functions to be tested, in order to know how accurately our algorithm can "recover" the true volatility functions in a local regime switching model. Since we don't know the specific forms of the volatility functions in reality, more complicated test functions will be used to gain confidence on the reliability and accuracy of the proposed algorithm to eventually employed to recover volatility functions when real market data are used.

The recovery results for this are shown in Figure 11.1. What we can see from Figure 11.1 is that with the initial guess of 0.35 for State 1 volatility and 0.15 for State 2 volatility respectively, the two recovered volatility functions are quite fit to the "true" pre-specified ones with errors only in the order of 10^{-8}, which is rather satisfactory.

When the shape of the true volatility functions is no longer flat, but exhibits a "smile" curve, which is a common phenomenon observed in real markets [73], we also try to recover them using our algorithm and these results are shown in Figure 11.2. In this case, the two

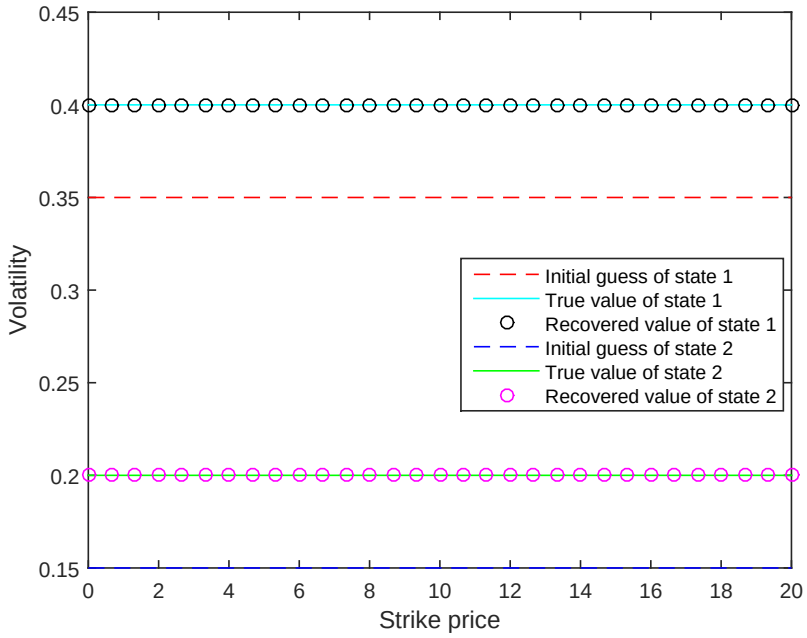

Figure 11.1: Recovery of the flat-shape volatility

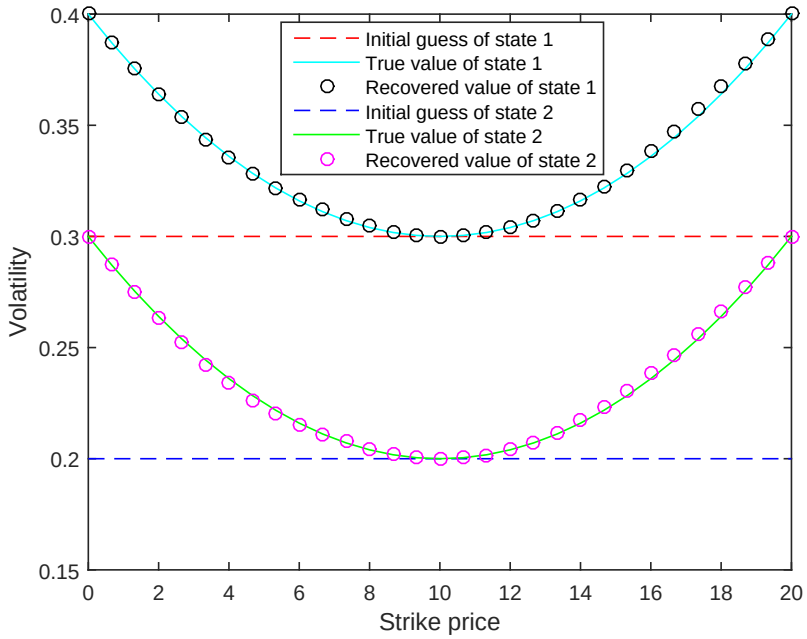

Figure 11.2: Recovery of the smile-shape volatility

"true" volatility functions are

$$\sigma_1(S) = 0.3 + \frac{(S-10)^2}{1000}, \quad \sigma_2(S) = 0.2 + \frac{(S-10)^2}{1000}. \tag{11.30}$$

It is clear that with initial guesses being two flat lines, our algorithm is still able to provide

quite accurate results of recovery with errors in the order of 10^{-4}.

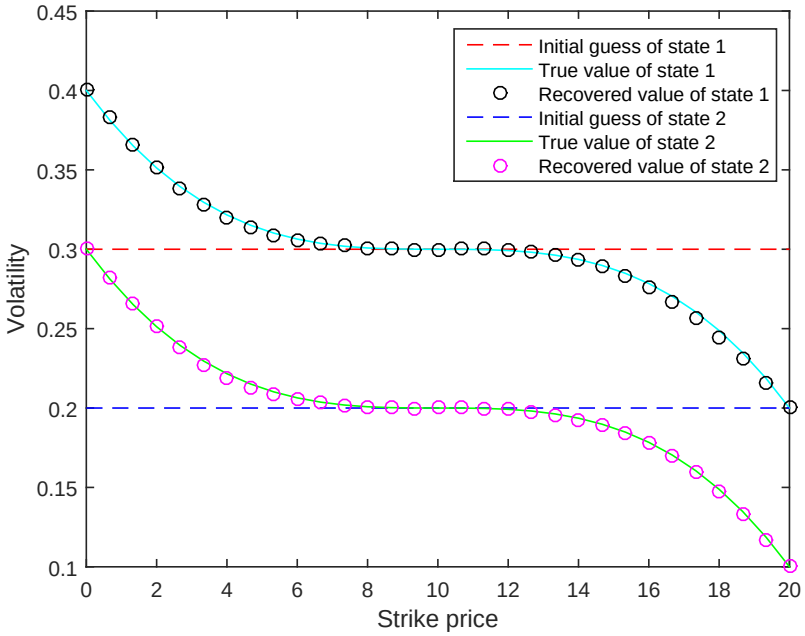

Figure 11.3: Recovery of the skew-shape volatility

Finally, our algorithm is also tested with the "skew" shape of volatility functions, because the graph for the volatility could be downward sloping for some markets [229], such as equity options. Hence, the volatility functions are selected as

$$\sigma_1(S) = 0.3 - \frac{(S-10)^3}{10000}, \quad \sigma_2(S) = 0.2 - \frac{(S-10)^3}{10000}, \tag{11.31}$$

and the results are given in Figure 11.3. Again, it is not difficult to find that the two skew volatility functions are also successfully recovered with the two flat initial guesses and the errors are in the order of 10^{-4}.

By testing the three typical kinds of volatility functions with different characteristics, we are confident to draw the conclusion that our algorithm could provide good recovery results for different shapes of volatility curves and it has the potential to be applied in real markets.

11.4.2 Stability test

Apart from the accuracy, another important factor associated with a newly derived numerical algorithm is its stability since there always exists noise in market prices. As a result, in order to demonstrate the stability of our algorithm, a white noise is added to the "true"

volatility functions, and the procedure will be illustrated in the following. As an example, we consider the "smile" case used in the last subsection, and we further introduce two random variables, x and y, both of which follow a standard normal distribution so that the noised "volatility" functions are specified as

$$\sigma_1(S) = [0.3 + \frac{(S-10)^2}{1000}](1 + \frac{x}{15}), \quad \sigma_2(S) = [0.2 + \frac{(S-10)^2}{1000}](1 + \frac{y}{15}). \tag{11.32}$$

Then, similar to the tests conducted in the last subsection, we use the noised "volatility" functions to generate state prices, which will be used as noised market state prices and recover volatility functions with our algorithm.

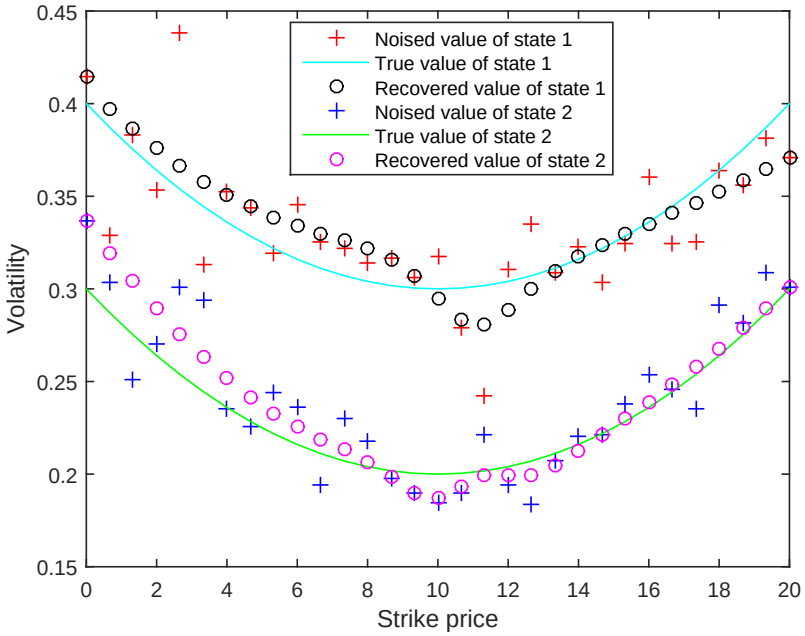

Figure 11.4: Stability test.

Depicted in Figure 11.4 are the recovery results with the generated noised state prices with initial guesses being flat lines. As expected, the recovered volatility functions from the noised state prices no longer fit very well to the un-noised "true" volatility functions as a direct result of introducing a white noise. However, it should be noted that this figure can clearly demonstrate the stability of our algorithm as the recovered volatility functions are still closely located around the un-noised "true" volatility functions.

11.4.3 Market tests

Having the accuracy and stability of the newly designed algorithm, we are now ready to test the performance our algorithm with real market data, which adds another dimension of complexity due to an additional procedure that needs to be instrumented to overcome the difficulty that there are more needed state prices than the available market prices in the calibration of a regime-switching model as discussed in Section 2 already. Such difficulty did not arise in the tests presented in the previous two subsections at all because the state prices are generated with the "true" volatility functions. In other words, there was no need to determine the market-implied state prices, C_1 and C_2, in the previous tests, whereas they now need to be recovered from the market option prices in a real empirical test. This is achieved by calibrating the standard regime switching model to find V_1 and V_2 first and then use Equation (11.3) and (11.4) to obtain C_1 and C_2 with a given market option price C^{market}.

Here, we use the market data of S&P 500 returns and options with prices quoted on 15 May 2013 and the expiry time of the options being 22 Jun 2013. This means that the underlying price is $S_0 = 1658.78$, the expiry time $T = 0.1041$ (current time is 0), the risk-free interest rate (we use the LIBOR rate as an approximation) $r = 0.0027$, and the strike price ranges from 1120 to 1800 with $N_1 = 136$. By making use of one popular global optimization algorithm, Adaptive Simulated Annealing (cf. [136, 180]), we obtain the estimated parameters as

$$\lambda_{12} = 0.2779,\ \lambda_{21} = 0.4355,\ \sigma_1 = 0.0495,\ \sigma_2 = 0.1160,\ \pi = 0.1520, \tag{11.33}$$

from which we can certainly get V_1 and V_2. In this way, we can obtain the two sets of market-implied state prices C_1 and C_2 with Equation (11.3) and (11.5).

Having obtained the market-implied state prices, the remaining work is to recover local volatility functions with our algorithm, which is similar to what we have done in numerical tests. Parameters are set to be $N_2 = 20,\ \delta = 10^-3 * S_0^2,\ \theta = 10^{-2},\ \epsilon = 10^{-9}$, and results are presented in Figure 11.5. It is clear that the level of the local volatility in State 1 is generally higher than that of State 2, and a "smile" like shape can be observed for the two recovered volatility functions that the level of the volatility is relatively higher when the options is deep in-the-money and out-of-money while it is lower when the strike price

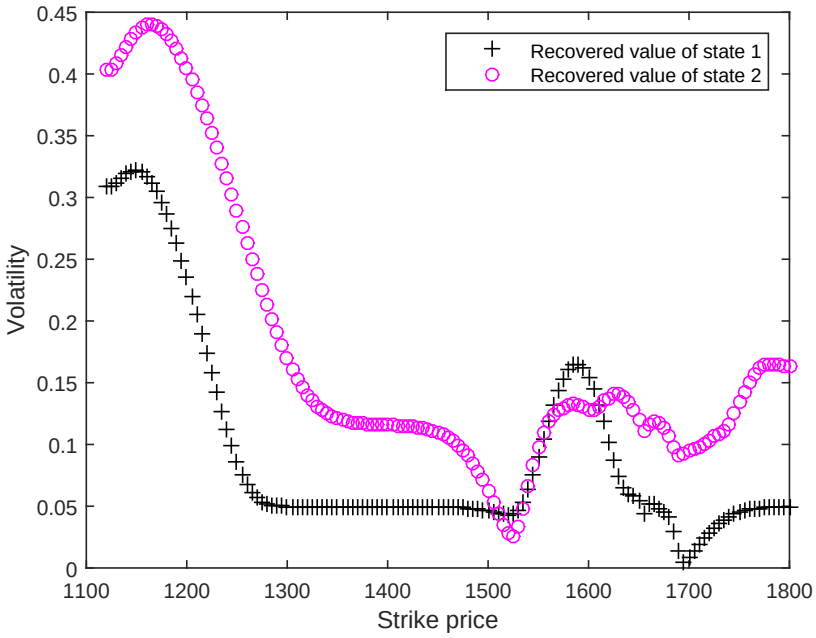

Figure 11.5: Market test.

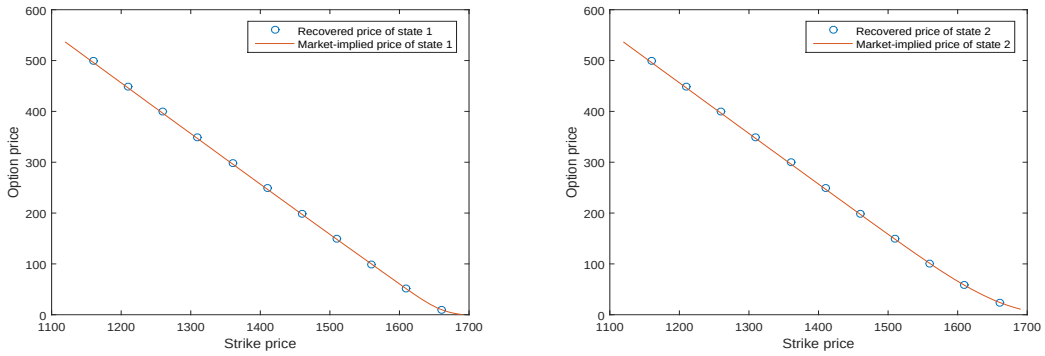

(a) State 1. (b) State 2.

Figure 11.6: Recovered price vs Market-implied price.

is close to the underlying price. To show whether we have recovered correctly recovered the two sets of market-implied state prices, we further show the option prices calculated with the recovered local volatility and those market-implied state prices in Figure 11.6. Obviously, with the maximum relative difference being 0.9%, our recovered results can certainly be regarded as accurate. From another prospective, the accuracy of our algorithm can also be demonstrated by comparing the implied volatility[2] extracted from market prices and that extracted from model prices (cf. [58]), and the results are shown in Figure 11.7. As expected, the implied volatility exhibits a smile curve, and the implied volatility

[2]Conventionally, implied volatility refers to that "implied" by the B-S model.

extracted from market prices agrees well with that extracted from model prices, with the relative difference being no larger than 0.8%. A nearly perfect replication of the volatility smile exhibits the power of adopting a modern model, such as the regime-switching model, in option pricing.

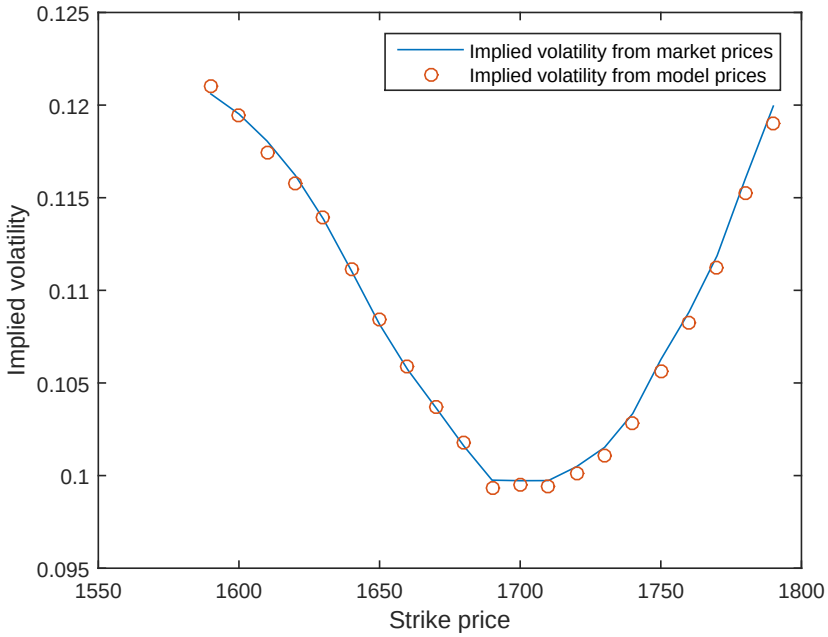

Figure 11.7: The comparison of implied volatility extracted from market prices and that from model prices.

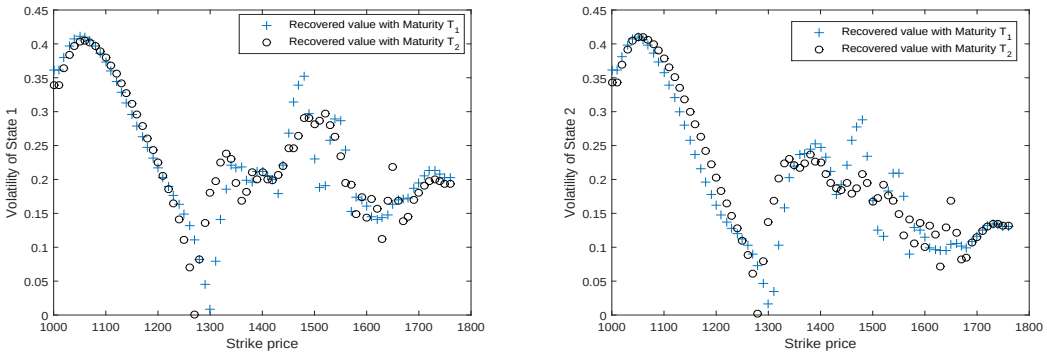

(a) State 1. (b) State 2.

Figure 11.8: Recovered volatility level with different maturities.

In order to focus on the core issue of this chapter, i.e., to propose an appropriate approach for the calibration of a local regime-switching model, we have made a simplified assumption in the illustration of the implementation of our approach that the local volatility functions is independent of time. Of course, in general, the local volatility function

should depend on not only maturities but also strike prices. Naturally, one wonders if there are cases in finance practice where our simplified assumption can be justified[3]. To address this point, we need to use market option data with two different maturities and demonstrate that the recovered local volatility functions are insignificantly different. Such an exercise was conducted on a set of one-day option data (S&P 500 returns and options) with the prices quoted on 15 April 2013 and the two expiry times of the options being 22 June 2013 and 20 July 2013, respectively.

For this case, the underlying price is $S_0 = 1552.36$, the two expiry times, T_1 and T_2, take the value of 0.1863 and 0.2630, respectively. The risk-free interest rate r is 0.0028 and the strike price ranges from 1000 to 1760 with $N_1 = 76$. Again, the first step of the calibration is to determine the market-implied state prices, C_1 and C_2, and thus we use Adaptive Simulated Annealing to obtain the estimated parameters as

$$\lambda_{12} = 0.4996,\ \lambda_{21} = 0.5010,\ \sigma_1 = 0.1826,\ \sigma_2 = 0.1222,\ \pi = 0.1222, \tag{11.34}$$

from which we can certainly obtain V_1 and V_2 as well as C_1 and C_2 through Equation (11.3) and (11.5) for each expiry time. With the market-implied state prices in hands, we are then able to recover the corresponding local volatility functions with our algorithm for different maturities, the results of which are presented in Figure 11.8. Apart from a slightly larger difference between the two recovered local volatility functions corresponding to the two maturities when the options are slightly in the money, the overall average absolute differences of the two recovered local volatility functions are very small. Specifically, the average absolute differences between the recovered volatility functions of the two maturities are 0.029 and 0.030 for State 1 and State 2 respectively. Of course, while the closeness of the local volatility functions for two different maturities found in this particular example supports that our assumption may be reasonable in some cases, this does not mean that such an assumption should always be adopted in real markets in general.

[3]Note, even there was a couple of cases in which our assumption turns out to be a reasonable assumption, it does not mean that such an assumption can suit all market situations, as there are bound to be cases where the local volatility functions need to be assumed to vary with both maturities and strike prices.

11.5 Conclusion

In this chapter, we present theoretical results on how to calibrate local regime-switching models. Although the Dupire-style formula for local regime-switching models has already been derived [85], it is shown that this formula alone can not lead to final results as all the state prices are required whereas only one market price for an option is available in real markets. As a result, a closed system for option pricing and model calibration under the classical regime-switching model is firstly proposed with the market price being the expectation of state prices, based on which one market option price is successfully split into two market-implied state prices with a special approach. Upon noticing that the direct implementation of the Dupire formula with all state prices still can not yield accurate results, the calibration problem is formed as an inverse problem, which is further transformed into an optimal control problem due to its ill-posedness. With the use of Tikhonov regularization, two necessary conditions are derived for the existence of the optimal solution, and an efficient numerical algorithm is proposed for the recovery of local volatility functions. Finally, numerical experiments with synthetic data are carried out to demonstrate the accuracy and stability of our newly proposed algorithm. Interestingly, the local volatility functions recovered with real market data exhibits a smile-shape curve.

Chapter 12

On the calibration of local regime-switching models through a Tikhonov approach

12.1 Introduction

In 1973, a breakthrough took place when Black-Scholes [19] proposed their model with the log-returns of the underlying assumed to follow a standard normal distribution. It is popular even today mainly because its simplicity with a closed-form pricing formula for European options. However, it has been pointed out by a number of authors that the classical Black-Scholes model is not able to capture the phenomenon that real market data exhibits, such as the typical skew and fat-tail property of the underlying price [188, 191]. In addition, the assumption of the constant volatility as another main drawback, which is our focus throughout this chapter, would lead to the well-known "volatility smile" [73] as well as the mis-pricing problem. All of these disadvantages have prompted the research on the modification of the Black-Scholes model.

In particular, various models have been proposed in order to incorporate the non-constant volatility, which can be divided into two categories. The first is the local volatility model proposed by Dupire [75], who assumed that the volatility be a deterministic function of the underlying price and time, and derived a so-called Dupire equation. The discrete version of the Dupire equation was implied volatility tree considered by Rubinstein [195] and Derman & Kani [67]. Contrast to the local volatility model, another kind of models

makes the volatility another random variable in addition to the underlying price, called stochastic volatility. A lot of well-known processes have been introduced in modeling the dynamic of the volatility, such as Ornstein-Uhlenbeck process used by Hull & White [127] and Cox-Ingersoll-Ross process adopted by Heston [117].

Recently, the regime-switching models have attracted plenty of attention from researchers and market practitioners since it introduces the concept of "state" in asset price modeling, which is consistent with financial markets. It is actually a stochastic volatility model since the volatility in this model is allowed to jump between different states controlled by a Markov chain. In fact, it was firstly proposed by Hamilton [103] and it was introduced to the area of derivative pricing since a lot of empirical evidence suggests that the dynamics of the underlying price are better captured by the regime-switching model [35, 86]. Specifically, option pricing under the regime-switching model has been widely studied, with European options priced in [101, 184, 244], American option priced in [26, 126], and exotic options priced in [22, 84].

In this chapter, we adopt a local regime-switching model, where the volatility could switch among different states and it could also vary as a function of the underlying price and time in each state. For simplicity, we will only consider the case of two states and this can be easily extended to the cases where there are more than two states. Our motivation originates from the fact that the classical regime-switching model with the constant volatility in each state may not provide good fitness to market option data, which is similar to the case in the Black-Scholes model.

It should be particularly emphasized that few empirical studies have been carried out on regime-switching option pricing models. Therefore, the task of calibrating local regime-switching models should be divided into two phases; in Phase I an algorithm is developed and tested with synthetic data to ensure its accuracy, and in Phase II the new algorithm is applied in real markets to show its real performance. The main reason for such a two-phase division is that in each stage, challenges one may face are quite different. While the main challenges for the Phase II are to deal with "noises" and many other specific issues associated with real data, the main two challenges in Phase I are a) the derived volatility function for each state involves all the state price variables whereas only one market price is available for model calibration; b) how to establish an appropriate algorithm to calibrate the model. In fact, as for the first challenge, one reasonable method

has recently been proposed in [115], where a new approach to properly close the system was proposed, demonstrating how to price options in real markets with classical regime-switching models. In this chapter, we will further work under their established system and show how to split one market price into two market-implied state prices. Once we have successfully obtained two market-implied state prices, we would discuss the problem of recovering the two local volatility functions, which is the second challenge and also the main focus of this chapter.

In the literature, many algorithms have been developed to recover the local volatility in the Black-Scholes model [78, 144, 163]. In a similar fashion, the calibration problem is transformed into an inverse problem of PDEs (partial differential equations) and in theory the two volatility functions could be uniquely determined given enough option prices. However, in real markets there are only a limited number of option prices with respect to some strikes and maturities. It is even worse that the inverse problem is obviously ill-posed since market option prices are observed with respect to different strike prices and maturities with a particular pair of time and underlying price, whereas the variables in the PDEs are underlying price and time. In order to alleviate these two problems, the inverse problem is formed as a minimization problem with Tikhonov Regularization [216]. Eventually, two necessary conditions are derived to obtain the optimal solution with a designed numerical algorithm. It should be noticed that the technique we adopt is distinct from that used in [115] since we calibrate the local regime-switching model directly instead of using the Dupire formula in this model [85]. Moreover, the variational derivative involved in the necessary conditions is obtained directly as the numerical solution of certain PDEs by introducing the Dirac delta function.

The rest of the chapter is organized as follows. In Section 2, how to split one market price into two market-implied state prices for an option will be briefly illustrated. In Section 3, the calibration problem will be formulated into an inverse problem, which is solved as a minimization problem with Tikhonov regularization. Two necessary conditions are also derived, with which a numerical algorithm is developed to obtain the optimal solution. In Section 4, numerical tests for our algorithm are presented, followed by some concluding remarks given in the last section.

12.2 Market-implied state prices

In this section, we will briefly illustrate the closed system for pricing options under the regime switching model proposed in [115] and describe the method to split one market price of an option into two market-implied state prices.

For regime switching models, there are different ways of adopting these models to price options. Among the proposed approaches, a common one is to assume that the market state is observable and the price of an option is the one corresponding to that particular state identified at the point when the option contact needs to be priced [244]. However, it is usually very difficult to clearly determine which state the underlying price belongs to and thus it is more reasonable to regard the state of a financial market as unobservable. Therefore, another approach is to estimate the probability of each state at the point when the option contact needs to be priced and then take the option price as the expectation of different state prices weighted by the probability of the underlying price in each state. For instance, if we denote C^{market} as the market option price with C_1 and C_2 being the two market-implied state prices, and let π represent the probability of the underlying price that stays at the regime 1, the market price is calculated with

$$C^{market} = C_1\pi + C_2(1-\pi). \tag{12.1}$$

On the other hand, when local regime switching models are taken into consideration, we need to split one market price of an option into two market-implied state prices, which implies that two equations are needed to obtain two state prices. Obviously, One equation has already been established as (12.1). The choice of another equation is free and the only requirement is that this equation should always hold when the regime-switching model degenerates to the Black-Scholes model. In [115], the authors proposed one reasonable way to construct such an equation. In the first place, model parameters (including the initial state probability) in the classical regime-switching model are estimated with only historical underlying data [142, 181], and then two state prices W_1 and W_2 under the classical regime-switching model can be calculated with those extracted model parameters. In this case, W_1 and W_2 are regarded as the good approximation for C_1 and C_2 respectively under the local regime-switching model. As a result, a relationship between them is imposed to form

as another equation

$$f(W_1, W_2, C_1, C_2) = 0. \tag{12.2}$$

Clearly, the choice of the function f is also very free. Two simplest examples are

$$\begin{aligned} (W_1 - W_2) - (C_1 - C_2) &= 0, \\ \frac{W_1}{W_2} - \frac{C_1}{C_2} &= 0, \end{aligned}$$

both of which are reasonable since when the regime-switching model degenerates to the Black-Scholes model, it is obvious that $W_1 = W_2$ and $C_1 = C_2$, which implies that they always hold.

By now, one market price could be converted into two market-implied state prices with Equation (12.1) and (12.2) derived above. Therefore, having obtained all the needed data, it is time for us to recover the two local volatility functions, which will be provided in the next section.

12.3 Calibration problem

In this section, the calibration of local regime-witching models will be transformed into an inverse problem and then a Tikhonov regularization approach is introduced to relieve the illness of the problem. Finally, two necessary conditions would be derived, with which a numerical algorithm is designed to recover the two local volatility functions.

12.3.1 An inverse problem

In this subsection, recovering the local volatility functions will be formed into an inverse problem. If we let S_t be the price process of the underlying asset, then it follows a two-state regime-switching model under the risk-neutral measure as

$$\frac{dS_t}{S_t} = rdt + \sigma_{X_t}(S, t)dW_t, \tag{12.3}$$

where r and σ_{X_t} represent the risk-free interest rate and the volatility respectively. W_t is a Brownian motion independent of a two state Markov chain X_t, which jumps between

two states

$$X_t = \begin{cases} 1, & \text{when the economy is believed to be in State 1,} \\ 2, & \text{when the economy is believed to be in State 2.} \end{cases}$$

It should be noticed that the transition between the two states follows a Poisson process as

$$P(t_{ij} > t) = e^{-\lambda_{ij} t}, i, j = 1, 2,\ i \neq j,$$

with λ_{ij} and t_{ij} being the transition rate from State i to j and the time spent in State i before transferring to State j respectively.

According to the results in [26], a system of coupled Black-Scholes equations for the option prices under the (local) regime-switching model has been derived as

$$\begin{cases} \dfrac{\partial V_1}{\partial t} + \dfrac{1}{2}\sigma_1^2 S^2 \dfrac{\partial^2 V_1}{\partial S^2} + rS\dfrac{\partial V_1}{\partial S} - rV_1 - \lambda_{12}(V_1 - V_2) = 0,\ S > 0,\ t \in [0, T], \\ V_1(S, T) = \max(S - K, 0), \\ V_1(0, t) = 0, \end{cases} \tag{12.4}$$

$$\begin{cases} \dfrac{\partial V_2}{\partial t} + \dfrac{1}{2}\sigma_2^2 S^2 \dfrac{\partial^2 V_2}{\partial S^2} + rS\dfrac{\partial V_2}{\partial S} - rV_2 - \lambda_{21}(V_2 - V_1) = 0,\ S > 0,\ t \in [0, T], \\ V_2(S, T) = \max(S - K, 0), \\ V_2(0, t) = 0, \end{cases} \tag{12.5}$$

with $V_1(S, t; K, T)$ and $V_2(S, t; K, T)$ being European call option prices for state 1 and state 2 respectively. Here, K denotes the strike price and T represents the maturity.

Recall that we have obtained two sets of market-implied state prices $V_1^*(S_0, t_0; K, T)$ and $V_2^*(S_0, t_0; K, T)$ from the set of market price $V_{market}^*(S_0, t_0; K, T)$ observed with different maturities and strike prices at time t_0. Therefore, what we need to do to recover the local volatility functions $\sigma_1(S, t)$ and $\sigma_2(S, t)$ for the two states is presented in the following inverse problem.

Problem 3. *Find the two functions $\sigma_1(S, t)$ and $\sigma_2(S, t)$ such that the solutions to the coupled PDE system (12.4)-(12.5), i.e. $V_1(S_0, t_0; K, T)$ and $V_2(S_0, t_0; K, T)$, satisfy the*

following two equations

$$\begin{aligned} V_1(S_0, t_0; K, T) &= V_1^*(S_0, t_0; K, T), \\ V_2(S_0, t_0; K, T) &= V_2^*(S_0, t_0; K, T), \end{aligned}$$

respectively for all T and K.

12.3.2 Tikhonov regularization

In this subsection, Problem 1 will be transformed into a minimization problem and Tikhonov regularization will be used to develop the numerical algorithm to find the optimal solution.

First of all, if we assume that the observations of market option prices are across a set of maturities $T_1, T_2, ..., T_N$, and for each maturity, there are M_i strike prices $K_1, K_2, ..., K_{M_i}$, then Problem 1 could certainly be converted into minimizing the following functional

$$G(\sigma_1, \sigma_2) = \sum_{i=1}^{N} \sum_{j=1}^{M_i} \{[V_1(S_0, t_0; K_j, T_i) - \bar{V}_1^{ij}]^2 + [V_2(S_0, t_0; K_j, T_i) - \bar{V}_2^{ij}]^2\}, \qquad (12.6)$$

with $\bar{V}_k^{ij} = V_k^*(S_0, t_0; K_j, T_i), k = 1, 2$. However, the problem of minimizing $G(\sigma_1, \sigma_2)$ is ill-posed since the set of market-implied state prices is discrete, which could not guarantee that σ_1 and σ_2 are uniquely determined and could also lead to unstable results that a small change in the state price could lead to a large change in the final results. As a result, this problem should be regularized to alleviate the illness of the problem. The technique we adopt is Tikhonov regularization, in which the cost functional takes the form of

$$J(\sigma_1, \sigma_2) = \frac{\delta}{2} \int_0^{+\infty} \int_0^{+\infty} (\frac{\partial \sigma_1}{\partial S})^2 + (\frac{\partial \sigma_1}{\partial t})^2 + (\frac{\partial \sigma_2}{\partial S})^2 + (\frac{\partial \sigma_2}{\partial t})^2 dS dt + G(\sigma_1, \sigma_2), \quad (12.7)$$

where δ is called the Tikhonov regularization parameter. Therefore, by minimizing the functional $J(\sigma_1, \sigma_2)$, we want to find two local volatility functions $\sigma_1(S, t)$ and $\sigma_2(S, t)$ such that $G(\sigma_1, \sigma_2)$ equals to zero. To solve the regularized minimization problem, two necessary conditions are derived for the existence of the optimal solution. To be more specific, for a perturbation function h defined as $\delta(S - X)\delta(t - \tau)$, $\sigma_1(\cdot, \cdot)$ and $\sigma_2(\cdot, \cdot)$ are the optimal solution if $J(\sigma_1 + \lambda h, \sigma_2)$ and $J(\sigma_1, \sigma_2 + \lambda h)$ reach their minimum when $\lambda = 0$.

Hence, we could obtain

$$\frac{d}{d\lambda}J(\sigma_1+\lambda h,\sigma_2)|_{\lambda=0}=0,\quad \frac{d}{d\lambda}J(\sigma_1,\sigma_2+\lambda h)|_{\lambda=0}=0, \tag{12.8}$$

which could be further calculated as

$$\delta(\frac{\partial^2\sigma_1}{\partial X^2}+\frac{\partial^2\sigma_1}{\partial\tau^2})-[V_1(S_0,t_0;K_j,T_i)-\bar{V}_1^{ij}]\xi_1(S_0,t_0;X,\tau)+[V_2(S_0,t_0;K_j,T_i)-\bar{V}_2^{ij}]\xi_2(S_0,t_0;X,\tau)=0, \tag{12.9}$$

$$\delta(\frac{\partial^2\sigma_2}{\partial X^2}+\frac{\partial^2\sigma_2}{\partial\tau^2})-[V_1(S_0,t_0;K_j,T_i)-\bar{V}_1^{ij}]\eta_1(S_0,t_0;X,\tau)+[V_2(S_0,t_0;K_j,T_i)-\bar{V}_2^{ij}]\eta_2(S_0,t_0;X,\tau)=0, \tag{12.10}$$

with the four variational derivatives defined as

$$\begin{aligned}\xi_k(S,t;X,\tau) &= \frac{dV_k(S,t;K_j,T_i,\sigma_1+\lambda h,\sigma_2)}{d\lambda}|_{\lambda=0},\\ \eta_k(S,t;X,\tau) &= \frac{dV_k(S,t;K_j,T_i,\sigma_1,\sigma_2+\lambda h)}{d\lambda}|_{\lambda=0},\end{aligned}$$

for $k=1,2$. To work out the two necessary condition (12.9) and (12.10), it is clear that we should calculate these variational derivatives. From the definition of $\xi_k, k=1,2$, it is not difficult to find that they satisfy the coupled PDE system as

$$\begin{cases}\frac{\partial\xi_1}{\partial t}+\frac{1}{2}\sigma_1^2S^2\frac{\partial^2\xi_1}{\partial S^2}+rS\frac{\partial\xi_1}{\partial S}-r\xi_1-\lambda_{12}(\xi_1-\xi_2)=-\delta(S-X)\delta(t-\tau)\sigma_1K^2\frac{\partial^2V_1}{\partial S^2},\\ \frac{\partial\xi_2}{\partial t}+\frac{1}{2}\sigma_2^2S^2\frac{\partial^2\xi_2}{\partial S^2}+rS\frac{\partial\xi_2}{\partial S}-r\xi_2-\lambda_{21}(\xi_2-\xi_1)=0.\end{cases} \tag{12.11}$$

Similarly, $\eta_k, k=1,2$ are also the solution to the following coupled PDE system

$$\begin{cases}\frac{\partial\eta_1}{\partial t}+\frac{1}{2}\sigma_1^2S^2\frac{\partial^2\eta_1}{\partial S^2}+rS\frac{\partial\eta_1}{\partial S}-r\eta_1-\lambda_{12}(\eta_1-\eta_2)=0,\\ \frac{\partial\eta_2}{\partial t}+\frac{1}{2}\sigma_2^2S^2\frac{\partial^2\eta_2}{\partial S^2}+rS\frac{\partial\eta_2}{\partial S}-r\eta_2-\lambda_{21}(\eta_2-\eta_1)=-\delta(S-X)\delta(t-\tau)\sigma_2K^2\frac{\partial^2V_2}{\partial S^2}.\end{cases} \tag{12.12}$$

It should be noted that the terminal and boundary conditions for the two PDE systems are homogeneous. To explain this, we would take ξ_1 as an example without loss of generality. According to the definition of ξ_1, it represents the variation of the option price at time t with the underlying price, strike price and the maturity being S, K_j and T_i respectively when σ_1 varies at the point (X,τ). Therefore, considering the terminal and boundary

conditions for the value of the option that it will not change for either of the following three cases, i.e. $t = T$, $S = 0$ and $S = +\infty$, it is easy to draw the conclusion that the variation derivatives satisfy homogeneous terminal and boundary conditions.

Combining the PDE systems (12.4)-(12.5), (12.11) and (12.12) with the two necessary conditions (12.9)-(12.10), we have now established a system, with which the optimal solution could be obtained. Of course, the task has not been finished yet since a numerical algorithm is still needed to solve such a system, which will be presented in the next subsection.

12.3.3 Numerical algorithm

In this subsection, a numerical algorithm is designed to minimize the functional $J(\sigma_1, \sigma_2)$ shown in the last subsection, which could contribute to the recovery of the two local volatility functions.

Before the presentation of the discrete scheme, the operating domain should be firstly introduced, which is a truncated one defined as

$$\tau \in [0, T_{max}], \quad S \in [0, 2S_0], \tag{12.13}$$

where S_0 represents the underlying price at the current time t_0, and T_{max} denotes the maximum time to maturity for the observed option data. Moreover, it should be pointed out that the domain is discretized uniformly in the time direction, while the discretization in the space direction is non-uniform. With a selected grid $\{(S_n, t_m), n = 1, 2, ..., N_1 + 1, m = 1, 2, ..., N_2 + 1\}$ for the operating domain $[0, 2S_0] \times [0, T_{max}]$ (dt is used as the time step size and dS_n acts as the distance between S_n and S_{n+1}), and the functions after l-th step iteration denoted as $\bar{\sigma}_{k,l}, V_{k,l}, \xi_{k,l}, \eta_{k,l}, k = 1, 2$, the iteration procedure is illustrated in the following.

1. Let $j = 0$. A tolerance ϵ is chosen to control the iteration. Also, initial guesses for the two volatility functions $\sigma_{i,0}, i = 1, 2$ need to be chosen.

2. With the two local volatility functions $\sigma_{k,l}, k = 1, 2$, two sets of state prices $V_{k,l}(S, t), k = 1, 2$ can be calculated through coupled PDEs (12.4)-(12.5) with an implicit discretiza-

tion as

$$\frac{V_{1,l}^{n,m+1}-V_{1,l}^{n,m}}{dt}+(\sigma_{1,l}^{n,m+1})^2(S_n)^2[\frac{V_{1,l}^{n+1,m+1}}{(dS_n+dS_{n-1})dS_n}-\frac{V_{1,l}^{n,m+1}}{dS_ndS_{n-1}}+\frac{V_{1,l}^{n-1,m+1}}{(dS_n+dS_{n-1})dS_{n-1}}]$$
$$+rS_n[-\frac{dS_nV_{1,l}^{n+1,m+1}}{(dS_n+dS_{n-1})dS_{n-1}}+\frac{(dS_n-dS_{n-1})V_{1,l}^{n,m+1}}{dS_{n-1}dS_n}+\frac{dS_{n-1}V_{1,l}^{n-1,m+1}}{(dS_n+dS_{n-1})dS_n}]$$
$$-rV_{1,l}^{n,m+1}-\lambda_{12}V_{1,l}^{n,m+1}+\lambda_{12}V_{2,l}^{n,m+1}=0,$$

and

$$\frac{V_{2,l}^{n,m+1}-V_{2,l}^{n,m}}{dt}+(\sigma_{2,l}^{n,m+1})^2(S_n)^2[\frac{V_{2,l}^{n+1,m+1}}{(dS_n+dS_{n-1})dS_n}-\frac{V_{2,l}^{n,m+1}}{dS_ndS_{n-1}}+\frac{V_{2,l}^{n-1,m+1}}{(dS_n+dS_{n-1})dS_{n-1}}]$$
$$+rS_n[-\frac{dS_nV_{2,l}^{n+1,m+1}}{(dS_n+dS_{n-1})dS_{n-1}}+\frac{(dS_n-dS_{n-1})V_{2,l}^{n,m+1}}{dS_{n-1}dS_n}+\frac{dS_{n-1}V_{2,l}^{n-1,m+1}}{(dS_n+dS_{n-1})dS_n}]$$
$$-rV_{2,l}^{n,m+1}-\lambda_{21}V_{2,l}^{n,m+1}+\lambda_{21}V_{1,l}^{n,m+1}=0,$$

If $G(\sigma_1,\sigma_2)<\epsilon$, then stop the iteration and regard $\sigma_{k,l},k=1,2$ as the recovered volatility functions. Otherwise, proceed to the next step.

3. With $\sigma_{k,l},k=1,2$ and $V_{k,l}(S,t),k=1,2$, $\xi_k,k=1,2$ and $\eta_k,k=1,2$ could be obtained simultaneously through the implicit discretization of the two PDE systems (12.11) and (12.12) respectively. The numerical scheme is omitted since it is similar to what have been presented in Step 2. It should be noted that what we need are $\xi_k(S_0,t_0;S_n,t_m)$ and $\eta_k(S_0,t_0;S_n,t_m)$, which require that the two PDE systems (12.11) and (12.12) should be solved for every n and m. It should also be remarked that the Dirac delta function is approximated by the standard normal density function.

4. With all the needed information obtained in Step 2 and 3, we are now ready to derive the updated $\sigma_{k,l+1},k=1,2$. In particular, a "false" time θ is introduced in solving the two equations (12.9)-(12.10) and the algorithm is presented as

$$\begin{aligned}\frac{\sigma_{1,l+1}^{n,m}-\sigma_{1,l}^{n,m}}{\theta} &+ W_{1,l}^{n,m}-\delta\frac{\sigma_{1,l}^{n,m+1}-2\sigma_{1,l}^{n,m}+\sigma_{1,l}^{n,m-1}}{(dt)^2}\\ &- 2\delta[\frac{\sigma_{1,l}^{n+1,m}}{(dS_n+dS_{n-1})dS_n}-\frac{\sigma_{1,l}^{n,m}}{dS_ndS_{n-1}}+\frac{\sigma_{1,l}^{n-1,m}}{(dS_n+dS_{n-1})dS_{n-1}}]=0,\end{aligned}$$

$$\begin{aligned}\frac{\sigma_{2,l+1}^{n,m}-\sigma_{2,l}^{n,m}}{\theta} &+ W_{2,l}^{n,m}-\delta\frac{\sigma_{2,l}^{n,m+1}-2\sigma_{2,l}^{n,m}+\sigma_{2,l}^{n,m-1}}{(dt)^2}\\ &- 2\delta[\frac{\sigma_{2,l}^{n+1,m}}{(dS_n+dS_{n-1})dS_n}-\frac{\sigma_{2,l}^{n,m}}{dS_ndS_{n-1}}+\frac{\sigma_{2,l}^{n-1,m}}{(dS_n+dS_{n-1})dS_{n-1}}]=0,\end{aligned}$$

with $W_{k,l}^{n,m}, k=1,2$ defined as

$$\begin{aligned}W_{1,l}^{n,m} &= \sum_{i=1}^{N}\sum_{j=1}^{M_i}\{[V_1(S_0,t_0;K_j,T_i)-\bar{V}_1^{ij}]\xi_1(S_0,t_0;S_n,t_m)\\ &+ [V_2(S_0,t_0;K_j,T_i)-\bar{V}_2^{ij}]\xi_2(S_0,t_0;S_n,t_m)\},\\ W_{2,l}^{n,m} &= \sum_{i=1}^{N}\sum_{j=1}^{M_i}\{[V_1(S_0,t_0;K_j,T_i)-\bar{V}_1^{ij}]\eta_1(S_0,t_0;S_n,t_m)\\ &+ [V_2(S_0,t_0;K_j,T_i)-\bar{V}_2^{ij}]\eta_2(S_0,t_0;S_n,t_m)\}.\end{aligned}$$

Then, let $j=j+1$ and go back to Step 2.

For any proposed algorithm, it always needs to be tested, in order to provide convincing evidence for the robustness of the algorithm. Such a test is presented in the next section.

12.4 Numerical tests

In this section, numerical experiments will be carried out to test the designed algorithm in the last section. It should be remarked that the two sets of market-implied state prices will be generated with "true" volatility functions $\sigma_k^*, k=1,2$ so that the accuracy and efficiency of the algorithm could be clearly exhibited.

In particular, model parameters in our test are

$$\begin{aligned}S_0 &= 10,\ t_0=0,\ r=0.05,\ T_{max}=0.5,\ \lambda_{12}=0.1,\ \lambda_{21}=0.2,\ N_1=78,\ N_2=50,\\ \delta &= 0.01,\ \theta=10^{-4},\end{aligned}$$

and the "true" volatility functions[1] are assumed to be

$$\sigma_1=1/S,\quad \sigma_2=2/S. \tag{12.14}$$

[1]For simplicity, the test is conducted based on the assumption that the volatility functions are independent of time. But, it should be pointed out that although our algorithm is also suitable for the case where the volatility functions depend on both of the underlying price and time, we believe the test conducted here is enough to prove the accuracy of our algorithm.

Although two specific forms of $\sigma_1(S)$ and $\sigma_2(S)$ are given in (12.14), one should not be confused with the test purpose here and the real objectives in reality. For the former, we pre-choose the specific forms of $\sigma_1(S)$ and $\sigma_2(S)$ and then use them to generate data, with which we perform the algorithm proposed here and then verify the results against the given functional form, in order to show how accurately our algorithm can "recover" the true volatility functions in a local regime switching model. Of course, for the latter, in reality we don't know the specific forms of these volatility functions; determining them through the proposed calibration procedure is what needs to be achieved if one decides to adopt a local regime switching model.

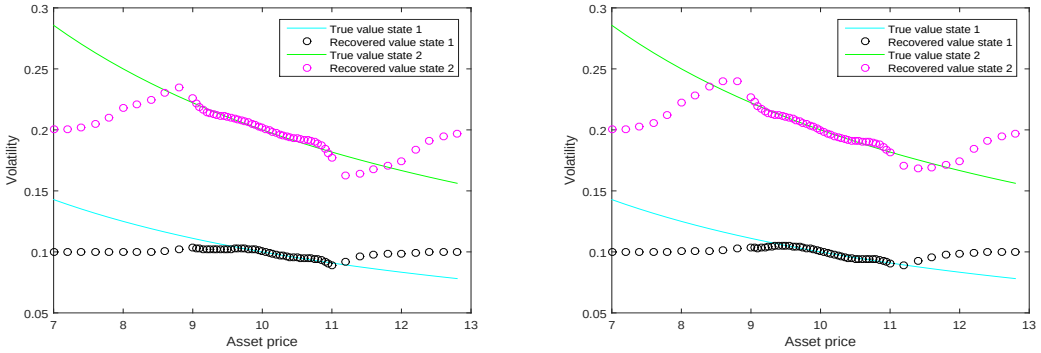

(a) Recovery with 5 pairs of two state prices. (b) Recovery with 20 pairs of two state prices.

Figure 12.1: Recovering the two local volatility functions with 100 steps.

The results of recovery after 100 iteration steps are presented in Figure 12.1. Specifically, in Figure 12.1(a), five pairs of two state prices with respect to one maturity $T = 0.5$ and five strike prices $K = \{8, 9, 10, 11, 12\}$ are chosen to recover the two volatility functions. It is clear that the two volatility functions are recovered successfully in the $S \in [9, 11]$ with a small deviation from the true volatility functions. On the other hand, what is presented in Figure 12.1(b) are the results of recovered two volatility functions with twenty pairs of two state prices across two maturities $T = \{0.25, 0.5\}$ and ten strike prices $K = \{8, 8.5, 9, ..., 11.5, 12\}$. A similar pattern could be found that the results are also quite satisfactory when the underlying asset price is between 9 and 11, although the recovery outside this region is poor. To compare the two cases, it is not difficult to find that with more observed market option prices, the two volatility functions can be better recovered with same iteration steps, which can be seen from two parts; One is that the average absolute deviation of the recovered volatility from the true volatility in Figure 12.1(a) is $2.1 * 10^{-3}$, compared with only $1.3 * 10^{-3}$ in Figure 12.1(b), another is that the average

absolute bias between the recovered price and the true price for 5 and 20 pairs of observed state prices is $3.0 * 10^{-3}$ and $1.1 * 10^{-3}$ respectively. It is also interesting to notice that when the asset price is far away from the central point 10, the recovered volatility keeps unchanged to the initial guess within 100-step iteration. Naturally, a question arises that whether such a phenomenon is caused by insufficient steps used in the iteration. This prompts us to do the iteration for 2000 steps, the results of which are presented in Figure 12.2.

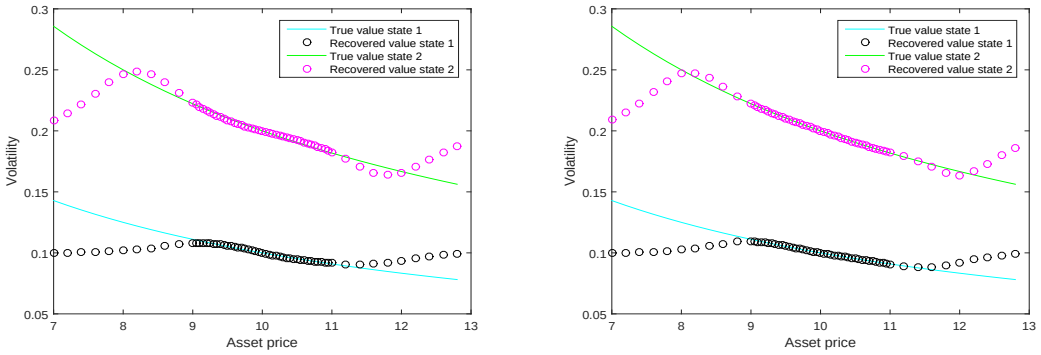

(a) Recovery with 5 pairs of two state prices. (b) Recovery with 20 pairs of two state prices.

Figure 12.2: Recovering the two local volatility functions with 2000 steps.

As expected, the two volatility functions are better recovered after 2000-step iteration than those recovered after 100 steps with the average deviation between the recovered volatility and the true volatility being $9.2 * 10^{-4}$ in figure 12.2(a) and $1.9 * 10^{-4}$ in figure 12.2(b) for 5 and 20 observations respectively. It is also obvious that more market observations could contribute to more accurate recovered results since the average deviation of 20 pairs of state prices is almost 9 times less than that of 5 pairs. Moreover, we could again find that the recovered volatility still sticks to the initial guess after 2000 steps when the asset price is far away from the central point ($S = 10$), which is consistent with our expectation since values of the volatility functions at these regions have little influence on the two state prices evaluated at $S = 10$.

12.5 Conclusion

In this chapter, the calibration of local regime-switching models is mainly concerned. With a method introduced to split one market into two market-implied state prices, the recovery of the two local volatility functions are formed as an inverse problem, which is solved as

a minimization problem. Moreover, a Tikhonov regularization approach is adopted to alleviate the illness of the problem, with which two necessary conditions are obtained. A numerical algorithm is also designed to conduct the calibration problem. Numerical tests show that our algorithm could successfully recover the two local volatility functions and it certainly has the potential to be applied in real markets.

Chapter 13

A brief summary

In this thesis, we work on three different areas in financial mathematics, i.e., option pricing models, different solution techniques, and model calibration problems, and the results are presented in three parts, respectively. In Part 1, we derive a closed-form pricing formula for European option prices under a skew Brownian motion and a modified Black-Scholes formula when the underlying price is bounded, while a new stochastic volatility model with regime-switching is proposed with an analytical approximation formula. In Part 2, a closed-form approximation formula for the price of European options with fixed-amount dividends is derived under the Black-Scholes model, and a closed-form pricing formula for European options in series form is obtained under the Heston model with the minimal entropy martingale measure. American option pricing is also considered here, and a new integral equation possessing some advantages over the existing ones is presented, followed by a newly designed numerical method for some practical purposes. In Part 3, we propose alternative forms of the existing models that not only presents the essential advantage, i.e., analytical tractability, of the original form, but also confirms a better performance when models are calibrated with real market data through some global optimization algorithms, and new algorithms to calibrate local regime-switching models are also developed.

Chapter 14

Conclusion

In this thesis, we focus on dealing with three different tasks associated with option pricing. In particular, the first task is finding analytical formulae for European option prices under different models. The second task is to solve option pricing problems with different solution techniques. The last task is related to the model calibration as any mathematical model need to be calibrated with model parameters determined with market data before they can be applied in real markets. The three tasks are dealt with in three different parts, respectively.

Different option pricing models with analytical formula for European option prices are mainly considered in the first part. As the Black-Scholes model fails to capture some characteristics of the underlying returns, one popular way to modify the Black-Scholes model is to replace the standard Brownian motion with other stochastic processes. What we choose here is a special kind of skew Brownian motions, which is able to capture the non-normal property of the distribution of log-returns. Upon identifying two errors in a key reference in this area, we introduced a new equivalent martingale measure named "endogenous risk neutral measure", based on which the analytical tractability of the problem is preserved and a new closed-form pricing formula is obtained. Another popular way is to introduce stochastic volatility into pricing models. As a result, we propose a new structural model with the constant volatility of volatility in the original Heston model allowed to change randomly following a Markov chain. Under this model, an analytical pricing formula for short-tenor European options is presented, which is fast and easy to implement with only normal distribution function involved. Empirical results demonstrate that our model significantly outperforms the Heston model for the tested case, which suggests that the new

model has a great potential to be used as an alternative to the Heston model for short-tenor options. On the other hand, being different from the two structural models discussed above, we propose that the underlying log-price follows a truncated normal distribution, which belongs to the category of non-structural models, as it only specifies the probability density function of the underlying at maturity conditional upon the filtration at the current time, and thus it can provide. more flexibility so that different characteristics of the asset returns could be captured. This assumption is able to describe the phenomenon that there should be reasonable bounds for the underlying price in a certain period. We then derive a closed-form pricing formula for European call options.

The second part of this thesis uses different solution techniques for option pricing problems. In specific, we firstly derive a closed-form approximation formula for the price of European options with fixed-amount dividends. This formula could certainly facilitate the application in real markets since no matter how many times the underlying pay its dividends before the expiry of the option, the formula is always the sum of one-dimensional integrals, the calculation of which can be rather rapid. Then, we present a closed-form pricing formula for European options in the Heston stochastic volatility model under the minimal entropy martingale measure with the series solution technique. A great advantage of our newly-derived pricing formula is that the radius of convergence for the solution can be proved theoretically. We also provide a slightly modified formula, which is constructed with a set of different formulae for different time range, for European options under the Heston model with the minimal entropy martingale measure such that it will converge on the entire time horizon of a European option contact. Afterwards, the pricing problem of American options is considered, and a novel approach is employed to find a new integral equation governing the American option price as well as the optimal exercise boundary. By making the unknown free boundary as a new variable replacing the time to expiry, the original PDE system with a free boundary is successfully transformed into a fixed boundary problem with a nonlinear PDE, which further yields a new integral equation involving only a one-dimensional integral. On the other hand, it is usually difficult to analytically price options under most models, and numerical methods must be resorted to in these cases. Therefore, the final issue of this part is devoted to proposing a new combined Monte-Carlo and the ADI method that is advantageous than classical numerical approaches in dealing with the situation where option traders are particularly interested in the influence of a

small change of variables in a certain region on option prices, while they are indifferent to option prices outside this region. The superiority of this newly proposed numerical approach is further shown by comparing the computational time of our approach, purely Monte Carlo method and purely ADI method cost to evaluate a same set of option prices on the interested domain.

The third part of this thesis presents two different issues associated with model calibration as any mathematical models need to be calibrated before they can be applied in real markets. It should be pointed out that the calibration of a model in reality is so complicated that model parameters always need to be determined numerically with an optimization algorithm, and in this case one would never be able to obtain the "optimized" set of parameters, but probably would have to settle near it. Thus, different forms of a same model can provide different results, which is the first issue of this part. In order to demonstrate this point, we set up an alternative form of the Heston model, and our empirical results confirm that our form generally outperforms the original Heston version for the case tested so far and thus we could reach the conclusion that a different form may be able to offer certain advantages in parameter determination and model calibration. With confidence of this point, we further propose an alternative form of the correlated Stein-Stein model for option pricing and model calibration, and our results show that our form generally outperforms the original Stein-Stein form, and thus it could be used as an alternative to the original Stein-Stein form for some markets.

Finally, we discuss the problem of calibrating local regime-switching models, which is the second issue of this part. In order to recover the two local volatility functions, we propose a "closed" system for pricing options under the classical regime-switching model, where the market price is the expectation of state prices. Under this newly proposed system, one market price is split into two market-implied state prices, based on which recovering the volatility functions are transformed into an optimal control problem. By applying a Tikhonov regularization approach, we design two new efficient numerical algorithms to obtain the local volatility functions according to two different methods to deal with variational derivatives; one is based on the Dupire formula in the local regime switching models, and another is to obtain the variational derivative directly as the numerical solution of certain PDEs by introducing the Dirac delta function. Moreover, different shapes of volatility curves are successfully recovered with both of our algorithms in the

numerical tests, which implies that they have the potential to be applied in real markets.

Appendix A

Proof for Chapter 2

Before we calculate the Greeks, let us first derive a useful formula which is of significance in obtaining the Greeks. It is easy to derive the follow two equations from the expression of $M_1(b_1)$ and $M_2(b_2)$:

$$S_t \frac{\partial M_1(b_1)}{\partial b_1} = -S_t e^{-g(m)} L_1(b_1, m), \tag{A.1}$$

$$K e^{-r(T-t)} \frac{\partial M_2(b_2)}{\partial b_2} = -K e^{-r(T-t)} L_2(b_2, m). \tag{A.2}$$

Then we have

$$\begin{aligned}
(A.1) &= S_t e^{-g(m)} (\phi(b_1)\Phi[sgn(\delta)\frac{\delta[\sigma\sqrt{T-t}b_1 + (T-t)\sigma^2] + m}{\sigma\sqrt{(T-t)(1-\delta^2)}}] \\
&+ e^{-2m\delta}\phi(\frac{\sigma\sqrt{T-t}b_1 + 2m\delta}{\sigma\sqrt{T-t}})\Phi[sgn(\delta)\frac{\delta[\sigma\sqrt{T-t}b_1 + (T-t)\sigma^2 + 2m\delta] - m}{\sigma\sqrt{(T-t)(1-\delta^2)}}]), \\
&= S_t e^{-g(m)+\sigma\sqrt{t-T}b_2 - 0.5*\sigma^2(T-t)} (\phi(b_2)\Phi[sgn(\delta)\frac{\delta\sigma\sqrt{T-t}b_2 + m}{\sigma\sqrt{(T-t)(1-\delta^2)}}] \\
&+ \phi(\frac{\sigma\sqrt{T-t}b_2 + 2m\delta}{\sigma\sqrt{T-t}})\Phi[sgn(\delta)\frac{\delta[\sigma\sqrt{T-t}b_2 + 2m\delta] - m}{\sigma\sqrt{(T-t)(1-\delta^2)}}]), \\
&= K e^{-r(T-t)} L_2(b_2, m).
\end{aligned} \tag{A.3}$$

As a result,

$$S_t \frac{\partial M_1(b_1)}{\partial b_1} = K e^{-r(T-t)} \frac{\partial M_2(b_2)}{\partial b_2}. \tag{A.4}$$

Now, we can calculate the Greeks with Equation (A.4).

(1) $\Delta_c = \dfrac{\partial C}{\partial S}$.

$$\begin{aligned}
\Delta_c &= M_1(b_1) + S\frac{\partial M_1(b_1)}{\partial S} - Ke^{-r(T-t)}\frac{\partial M_2(b_2)}{\partial S}, \\
&= M_1(b_1) + S\frac{\partial M_1(b_1)}{\partial b_1}\frac{\partial b_1}{\partial S} - Ke^{-r(T-t)}\frac{\partial M_2(b_2)}{\partial b_2}\frac{\partial b_2}{\partial S}, \\
&= M_1(b_1). \qquad (A.5)
\end{aligned}$$

The last step results form the equality $\dfrac{\partial b_1}{\partial S} = \dfrac{\partial b_2}{\partial S}$.

(2) $\Gamma_c = \dfrac{\partial^2 C}{\partial S^2}$.

$$\begin{aligned}
\Gamma_c &= \frac{\partial M_1(b_1)}{\partial b_1}\frac{\partial b_1}{\partial S}, \\
&= \frac{e^{-g(m)}L_1(b_1, m)}{S\sigma\sqrt{T-t}}. \qquad (A.6)
\end{aligned}$$

(3) $K_c = \dfrac{\partial C}{\partial K}$.

$$\begin{aligned}
K_c &= -e^{-r(T-t)}M_2(b_2) + S\frac{\partial M_1(b_1)}{\partial K} - Ke^{-r(T-t)}\frac{\partial M_2(b_2)}{\partial K}, \\
&= -e^{-r(T-t)}M_2(b_2) + S\frac{\partial M_1(b_1)}{\partial b_1}\frac{\partial b_1}{\partial K} - Ke^{-r(T-t)}\frac{\partial M_2(b_2)}{\partial b_2}\frac{\partial b_2}{\partial K}, \\
&= -e^{-r(T-t)}M_2(b_2). \qquad (A.7)
\end{aligned}$$

The last step results form the equality $\dfrac{\partial b_1}{\partial K} = \dfrac{\partial b_2}{\partial K}$.

(4) $R_c = \dfrac{\partial C}{\partial r}$.

$$\begin{aligned}
R_c &= K(T-t)e^{-r(T-t)}M_2(b_2) + S\frac{\partial M_1(b_1)}{\partial r} - Ke^{-r(T-t)}\frac{\partial M_2(b_2)}{\partial r}, \\
&= K(T-t)e^{-r(T-t)}M_2(b_2) + S\frac{\partial M_1(b_1)}{\partial b_1}\frac{\partial b_1}{\partial r} - Ke^{-r(T-t)}\frac{\partial M_2(b_2)}{\partial b_2}\frac{\partial b_2}{\partial r}, \\
&= K(T-t)e^{-r(T-t)}M_2(b_2). \qquad (A.8)
\end{aligned}$$

The last step results form the equality $\dfrac{\partial b_1}{\partial r} = \dfrac{\partial b_2}{\partial r}$.

(5) $\Omega_c = \dfrac{\partial C}{\partial \delta}$.

$$\begin{aligned}
\Omega_c &= S\frac{\partial M_1(b_1)}{\partial b_1}\frac{\partial b_1}{\partial \delta} + S\int_{b_1}^{\infty} e^{-g(m)}\frac{\partial L_1(x,m)}{\partial \delta}dx + S\int_{b_1}^{\infty}\frac{e^{-g(m)}}{\partial \delta}L_1(x,m)dx \\
&- Ke^{-r(T-t)}\frac{\partial M_2(b_2)}{\partial b_2}\frac{\partial b_2}{\partial \delta} - Ke^{-r(T-t)}\int_{b_2}^{\infty}\frac{\partial L_2(x,m)}{\partial \delta}dx, \\
&= SI_1 - SI_3 - Ke^{-r(T-t)}I_2. \qquad \text{(A.9)}
\end{aligned}$$

The last step results form the equality $\dfrac{\partial b_1}{\partial \delta} = \dfrac{\partial b_2}{\partial \delta}$.

Appendix B

Proof for Chapter 7

B.1 Proof for boundary conditions associated with optimal exercise boundary

In order to derive the two identities, i.e., (7.6) and (7.7), we should use the two free boundary conditions in System (7.4), which are specified as

$$p(x,\tau)|_{x=b(\tau)} = 1 - e^{b(\tau)}, \tag{B.1}$$

and

$$\frac{\partial p}{\partial x}|_{x=b(\tau)} = -e^{b(\tau)}. \tag{B.2}$$

Specifically, if we differentiate Equation (B.1) with respect to τ, we can obtain

$$\frac{\partial p}{\partial x}|_{x=b} \cdot \frac{\partial b}{\partial \tau} + \frac{\partial p}{\partial \tau}|_{x=b} = -e^b \frac{\partial b}{\partial \tau}.$$

Substituting Equation (B.2) into above equation can yield Equation (7.6). On the other hand, if we make $x = b$ in the PDE of System (7.4), it is very straightforward to obtain

$$\frac{\partial p}{\partial \tau}|_{x=b} = \frac{\partial^2 p}{\partial x^2}|_{x=b} + (k-1)\frac{\partial p}{\partial x}|_{x=b} - kp|_{x=b} = 0,$$

which can be further simplified as

$$\frac{\partial^2 p}{\partial x^2}|_{x=b} = k - e^b. \tag{B.3}$$

In addition, differentiating Equation (B.2) with respect to τ can result in

$$\frac{\partial^2 p}{\partial x^2}|_{x=b} \cdot \frac{\partial b}{\partial \tau} + \frac{\partial^2 p}{\partial x \partial \tau}|_{x=b} = -e^b \frac{\partial b}{\partial \tau}. \tag{B.4}$$

We can surely arrive at Equation (7.7) if we combine Equation (B.3) and (B.4) together. This has completed the proof.

B.2 Proof for the boundary condition at infinity

From the equality $\lim_{x \to +\infty} p(x, \tau) = 0, \ \forall \tau > 0$, it is not difficult to show that for any $\tau_0 > 0$ and $\delta > 0$, the following equation should hold

$$\lim_{x \to +\infty} [p(x, \tau_0 + \delta) - p(x, \tau_0)] = 0, \tag{B.5}$$

which further yields

$$\lim_{x \to +\infty} |\frac{p(x, \tau_0 + \delta) - p(x, \tau_0)}{\delta}| = 0. \tag{B.6}$$

This implies that for any $\epsilon > 0$, there exists $M > 0$ such that when $x > M$, we have

$$|\frac{p(x, \tau_0 + \delta) - p(x, \tau_0)}{\delta}| < \frac{\epsilon}{2}. \tag{B.7}$$

Therefore, taking the limit on both sides of Equation (B.7) leads to

$$\lim_{\delta \to 0} |\frac{p(x, \tau_0 + \delta) - p(x, \tau_0)}{\delta}| \leq \frac{\epsilon}{2} < \epsilon, \tag{B.8}$$

which can be simplified as

$$|\frac{\partial p}{\partial \tau}|_{\tau=\tau_0}| < \epsilon. \tag{B.9}$$

As a result,

$$\lim_{x \to +\infty} \frac{\partial p}{\partial \tau}|_{\tau=\tau_0} = 0. \tag{B.10}$$

Considering the fact that τ_0 can take any value, we have thus finally reached the conclusion that

$$\lim_{x \to +\infty} \frac{\partial p}{\partial \tau} = 0. \tag{B.11}$$

Appendix C

Proof for Chapter 9

Here we give the details in deriving the analytic pricing formula. Setting the coefficients of $v^{2\alpha}$ to be zero since Equation (9.11) should hold for any v, we can obtain two ordinary differential equations (ODE) as follows.

$$\begin{aligned}\frac{\partial D}{\partial \tau} &= 2\alpha^2\sigma^2 D^2 + 2\alpha(b_j + \lambda_1 + i\phi\rho\sigma)D + u_j i\phi - \frac{1}{2}\phi^2,\\ \frac{\partial C}{\partial \tau} &= \alpha[(2\alpha-1)\sigma^2 + 2\lambda_2]D + ri\phi,\end{aligned}$$

where $D(0;\phi) = 0$ and $C(0;\phi) = 0$. Let $A = 2\alpha^2\sigma^2$, $B = 2\alpha(b_j + \lambda_1 + i\phi\rho\sigma)$ and $M = u_j i\phi - \frac{1}{2}\phi^2$. So the first ODE can be simplified as

$$\frac{\partial D}{\partial \tau} = AD^2 + BD + M, \tag{C.1}$$

which is exactly the Riccati Equation. Now by applying the transformation $D = \dfrac{y'}{-Ay}$, the following is obtained

$$y'' - By' + AMy = 0, \tag{C.2}$$

with initial condition $y'(0) = 0$. Equation (C.2) is obviously a second-order linear ODE, which has a general solution with the form

$$y = C_1 e^{d^+\tau} + C_2 e^{d^-\tau}, \tag{C.3}$$

where d^+ and d^- are two roots of $d^2 - Bd + AM = 0$. Applying the initial condition of D yields

$$\frac{C_1}{C_2} = -\frac{d^-}{d^+},$$

and as a result, D can be derived as

$$\begin{aligned} D &= -\frac{1}{A} \cdot \frac{C_1 d^+ e^{d^+\tau} + C_2 d^- e^{d^-\tau}}{C_1 e^{d^+\tau} + C_2 e^{d^-\tau}}, \\ &= -\frac{1}{A} \cdot \frac{-d^- e^{d^+\tau} + d^- e^{d^-\tau}}{-\frac{d^-}{d^+} e^{d^+\tau} + e^{d^-\tau}}, \\ &= \frac{d - 2\alpha(b_j + \lambda_1 + i\phi\rho\sigma)}{4\alpha^2\sigma^2} \cdot \frac{1 - e^{d\tau}}{1 - ge^{d\tau}}. \end{aligned}$$

Therefore, once the expression of $D(\tau;\phi)$ is obtained, it is straightforward to derive $C(\tau;\phi)$ as

$$\begin{aligned} C &= \int_0^\tau \alpha[(2\alpha - 1)\sigma^2 + 2\lambda_2]D(t;\phi) + ri\phi dt, \\ &= ri\phi\tau + \frac{\alpha(2\alpha - 1)\sigma^2}{4\alpha^2\sigma^2} p(\tau;\phi). \end{aligned}$$

Now we have derived $C(\tau;\phi)$ and $D(\tau;\phi)$ so that f_j is known to us by now, which can be used to get P_j according to the relationship between probability distribution function and the characteristic function of a random variable [222]. Thus the option pricing formula is obtained.

Appendix D

Proof for Chapter 10

D.1 Proof for the sign of A and B

In Section 10.2.4, we set $A = \frac{\lambda_1}{4\lambda_2} + \frac{1}{2\sqrt{-k}}$ and $B = \frac{\lambda_1}{4\lambda_2} - \frac{1}{2\sqrt{-k}}$. Here we will prove that $A > 0, B < 0$.

1) $\lambda_1 > 0$. So we can get $B < 0$ immediately. Now if we assume $A \leq 0$, then

$$\frac{\lambda_1}{4\lambda_2} + \frac{1}{2\sqrt{-k}} \leq 0,$$

from which we can known

$$\lambda_1 \geq -\frac{2\lambda_2}{\sqrt{-k}} > 0.$$

Therefore, after some simplifications,

$$0 \geq -2\lambda_2(1-\alpha)\sigma^2, \tag{D.1}$$

which contradicts with the fact that $\lambda_2 < 0$. As a result, the assumption is not true and we have $A > 0$.

2) $\lambda_1 < 0$. Now we have $A > 0$ from $\lambda_1 < 0$. If we assume $B \geq 0$, then

$$\frac{\lambda_1}{4\lambda_2} + \frac{1}{2\sqrt{-k}} \geq 0,$$

which implies

$$-\lambda_1 \geq -\frac{2\lambda_2}{\sqrt{-k}} > 0.$$

And then we can have

$$\lambda_1^2 \geq -\frac{4\lambda_2^2}{k} > 0,$$

which again can be simplified to

$$0 \geq -2\lambda_2(1-\alpha)\sigma^2. \tag{D.2}$$

As a result, Inequality (*D.2*) contradicts with $\lambda_2 < 0$, which means that the assumption is incorrect and we obtain $B < 0$.

Combining the situations we consider, we have $A > 0, B < 0$ for all possible values of λ_1. This has complete the proof.

D.2 Proof for the pricing formula

According to the martingale pricing theory which tells us that $e^{-rt}U(S,v,t)$ should be a martingale when we seek the risk-neutral price, $U(S,v,t)$ should satisfy the following partial differential equation.

$$\begin{aligned} \frac{1}{2}v^{2\alpha}S^2\frac{\partial^2 U}{\partial S^2} &+ \rho\sigma v S\frac{\partial^2 U}{\partial v \partial S} + \frac{1}{2}\sigma^2 v^{2-2\alpha}\frac{\partial^2 U}{\partial v^2} + rS\frac{\partial U}{\partial S}, \\ &+ [\frac{1}{2}(1-\alpha)\sigma^2 v^{1-2\alpha} + \lambda_1 v^{1-\alpha} + \lambda_2 v]\frac{\partial U}{\partial v} - rU + \frac{\partial U}{\partial t} = 0, \end{aligned} \tag{D.3}$$

with the terminal and boundary conditions

$$\begin{aligned} U(S,v,T) &= \max(S-K,0), \\ U(0,v,t) &= 0, \\ \lim_{S\to\infty}\frac{U(S,v,t)}{S} &= 1. \end{aligned}$$

Now we assume the solution is of the form

$$U(S,v,t) = SP_1 - Ke^{-r(T-t)}P_2, \tag{D.4}$$

which is exactly in the same form as that of the B-S formula. By substituting (*D.4*) into the Equation (*D.3*) along with the transform $x = \ln(S)$, we can obtain the partial

differential equations that P_1 and P_2 must satisfy:

$$\begin{aligned}\frac{1}{2}v^{2\alpha}\frac{\partial^2 P_j}{\partial x^2} &+ \rho\sigma v\frac{\partial^2 P_j}{\partial v\partial x} + \frac{1}{2}\sigma^2 v^{2-2\alpha}\frac{\partial^2 P_j}{\partial v^2} + (r+a_j v)\frac{\partial P_j}{\partial x},\\ &+ [\frac{1}{2}(1-\alpha)\sigma^2 v^{1-2\alpha} + \lambda_1 v^{1-\alpha} + \lambda_2 v + b_j v]\frac{\partial P_j}{\partial v} + \frac{\partial P_j}{\partial t} = 0, \end{aligned} \tag{D.5}$$

where $j = \{1,2\}$ and the boundary condition becomes $P_j[x,v,t;\ln(K)] = 1_{\{x\geq\ln(K)\}}$. Actually, Equation (*D*.5) can be transformed to two different dynamics of x_t and v_t with Feynman-Kac formula [208],

$$\begin{aligned} dx &= (r+a_j v)dt + v^{\alpha}dW_t,\\ dv &= [\frac{1}{2}(1-\alpha)\sigma^2 v^{1-2\alpha} + \lambda_1 v^{1-\alpha} + \lambda_2 v + b_j v]dt + \sigma v^{1-\alpha}dB_t, \end{aligned} \tag{D.6}$$

and thus it is not difficult to interpret that P_1 and P_2 represent the probability of exercising the option at maturity under different measures, respectively. Therefore, we can obtain

$$P_j[x,v,t;\ln(K)] = P[x_T \geq \ln(K)] \mid x_t = x, v_t = v]. \tag{D.7}$$

Let

$$f_j(x,v,t;\phi) = E[e^{i\phi x_T} \mid x_t = x, v_t = v], \tag{D.8}$$

from which we can deduce that for any $s < t$,

$$\begin{aligned} E\{f_j(x,v,t;\phi) \mid x_s, v_s\} &= E\{E[e^{i\phi x_T} \mid x_s, v_s] \mid x_t, v_t\},\\ &= E[e^{i\phi x_T} \mid x_s, v_s],\\ &= f_j(x,v,s;\phi). \end{aligned}$$

Thus, f_j is a martingale, according to which we can obtain

$$\begin{aligned}\frac{1}{2}v^{2\alpha}\frac{\partial^2 f_j}{\partial x^2} &+ \rho\sigma v\frac{\partial^2 f_j}{\partial v\partial x} + \frac{1}{2}\sigma^2 v^{2-2\alpha}\frac{\partial^2 f_j}{\partial v^2} + (r+a_j v)\frac{\partial f_j}{\partial x},\\ &+ [\frac{1}{2}(1-\alpha)\sigma^2 v^{1-2\alpha} + \lambda_1 v^{1-\alpha} + \lambda_2 v + b_j v]\frac{\partial f_j}{\partial v} + \frac{\partial f_j}{\partial t} = 0, \end{aligned} \tag{D.9}$$

with the dynamics (*D*.6) by applying the Itô lemma. On the other hand, from Equation (*D*.8) we can easily work out the new terminal condition

$$f_j[x, v, T; \phi] = e^{i\phi x_T}, \tag{D.10}$$

by setting $t = T$.

Now we assume that the solution to the PDE (*D*.9) takes the form of

$$f_j = e^{C(T-t;\phi)+D(T-t;\phi)v^{2\alpha}+E(T-t;\phi)v^{\alpha}+i\phi x}, \tag{D.11}$$

and then substitute it into the PDE (*D*.9). After some calculations and simplifications, the following equation needs to be satisfied

$$\begin{aligned}
[\frac{\partial D}{\partial t} &+ 2\alpha^2\sigma^2 D^2 + 2\alpha(i\phi\rho\sigma + b_j + \lambda_2)D + a_j i\phi - \frac{1}{2}\phi^2]v^{2\alpha} \\
&+ [\frac{\partial E}{\partial t} + \alpha(2\alpha^2\sigma^2 D + i\phi\rho\sigma + b_j + \lambda_2)E + 2\alpha\lambda_1 D]v^{\alpha} \\
&+ [\frac{\partial E}{\partial t} + \frac{1}{2}\alpha^2\sigma^2 E^2 + \alpha^2\sigma^2 D + \alpha\lambda_1 E + ri\phi] = 0.
\end{aligned} \tag{D.12}$$

With the fact that v is an arbitrary variable, the satisfaction of Equation (*D*.12) is equivalent to the satisfaction of the following three ordinary differential equations

$$\frac{\partial D}{\partial \tau} = 2\alpha^2\sigma^2 D^2 + 2\alpha(i\phi\rho\sigma + b_j + \lambda_2)D + a_j i\phi - \frac{1}{2}\phi^2, \tag{D.13}$$

$$\frac{\partial E}{\partial \tau} = \alpha(2\alpha^2\sigma^2 D + i\phi\rho\sigma + b_j + \lambda_2)E + 2\alpha\lambda_1 D, \tag{D.14}$$

$$\frac{\partial C}{\partial \tau} = \frac{1}{2}\alpha^2\sigma^2 E^2 + \alpha^2\sigma^2 D + \alpha\lambda_1 E + ri\phi, \tag{D.15}$$

where C(0)=D(0)=E(0)=0 and $\tau = T - t$.

Now if we let $A = 2\alpha^2\sigma^2, B = 2\alpha(i\phi\rho\sigma + b_j + \lambda_2), M = a_j i\phi - \frac{1}{2}\phi^2$, (*D*.13) can be further simplified to

$$\frac{\partial D}{\partial \tau} = AD^2 + BD + M, \tag{D.16}$$

which is exactly a Riccati Equation. By applying the transform $D = \dfrac{y'}{-Ay}$ to Equation (*D*.16), we obtain

$$\frac{d^2 y}{d\tau^2} - B\frac{dy}{d\tau} + AMy = 0,$$

with its corresponding boundary condition

$$\frac{dy}{d\tau} \mid_{\tau=0} = 0. \tag{D.17}$$

The general solution of this newly derived ODE can be easily worked out as

$$y = C_1 e^{d^+\tau} + C_2 e^{d^-\tau},$$

where d^+ and d^- are the two roots of the quadratic equation

$$d^2 - Bd + AM = 0,$$

with

$$d^+ = \frac{B + \sqrt{B^2 - 4AM}}{2}, \quad d^- = \frac{B - \sqrt{B^2 - 4AM}}{2}.$$

Furthermore, by making use of the boundary condition (*D*.17), we can obtain $\frac{C_1}{C_2} = -\frac{d^-}{d^+}$. Therefore, $D(\tau;\phi)$ can be finally worked out as

$$\begin{aligned} D(\tau;\phi) &= -\frac{1}{A}\frac{C_1 d^+ e^{d^+\tau} + C_2 d^- e^{d^-\tau}}{C_1 e^{d^+\tau} + C_2 e^{d^-\tau}}, \\ &= -\frac{1}{A}\frac{-d^- e^{d^+\tau} + d^- e^{d^-\tau}}{-\frac{d^-}{d^+} e^{d^+\tau} + e^{d^-}}, \\ &= \frac{d - 2\alpha(b_j + \lambda_2 + i\phi\rho\sigma)}{4\alpha^2\sigma^2}\left(\frac{1 - e^{d\tau}}{1 - ge^{d\tau}}\right). \end{aligned}$$

After Equation (*D*.13) is solved, we now turn to Equation (*D*.14), which is nothing but a first-order linear non-homogeneous ODE with variable coefficients. To obtain a general solution, we set

$$G_1(\tau) = 2\alpha^2\sigma^2 D(\tau;\phi) + \alpha b_j + \alpha\lambda_2 + i\alpha\phi\rho\sigma, \quad G_2(\tau) = 2\alpha\lambda_1 D(\tau;\phi).$$

The solution to (*D*.14) can then be derived as

$$\begin{aligned} E(\tau;\phi) &= e^{\int_0^\tau G_1(t)dt} \int_0^\tau G_2(t) e^{-\int_0^t G_1(s)ds} dt, \\ &= e^{p(\tau)} \int_0^\tau 2\alpha\lambda_1 D(t;\phi) e^{-p(t)} dt. \end{aligned}$$

Since $D(\tau;\phi)$ and $E(\tau;\phi)$ are known by now, the derivation of $C(\tau;\phi)$ is quite straightforward because it can be obtained simply by integrating on both sides of Equation (D.15) and applying the boundary condition. This has completed the proof.

Bibliography

[1] Daily treasury bill rates data. http://www.treasury.gov/resource-center/data-chart-center/interest-rates/Pages/TextView.aspx?data=billrates.

[2] Chris J Adcock and Karl Shutes. Portfolio selection based on the multivariate skew normal distribution. *Financial Modelling*, pages 167–177, 2001.

[3] Yacine Aı, Robert Kimmel, et al. Maximum likelihood estimation of stochastic volatility models. *Journal of Financial Economics*, 83(2):413–452, 2007.

[4] Walter Allegretto, Yanping Lin, and Hongtao Yang. A fast and highly accurate numerical method for the evaluation of American options. *Dynamics of Continuous Discrete and Impulsive Systems Series B*, 8:127–138, 2001.

[5] Joao Amaro de Matos, Rui Dilao, and Bruno Ferreira. The exact value for European options on a stock paying a discrete dividend. 2006.

[6] Torben G Andersen, Hyung-Jin Chung, and Bent E Sørensen. Efficient method of moments estimation of a stochastic volatility model: A monte carlo study. *Journal of Econometrics*, 91(1):61–87, 1999.

[7] Jonathan Aquan-Assee. Boundary conditions for mean-reverting square root process. *University of Waterloo*, 2009.

[8] Adelchi Azzalini. A class of distributions which includes the normal ones. *Scandinavian Journal of Jtatistics*, pages 171–178, 1985.

[9] Louis Bachelier. *Théorie de la spéculation.* Gauthier-Villars, 1900.

[10] Pratibha Bajpai and Manoj Kumar. Genetic algorithm–an approach to solve global optimization problems. *Indian Journal of Computer Science and Engineering*, 1(3): 199–206, 2010.

[11] Gurdip Bakshi, Charles Cao, and Zhiwu Chen. Empirical performance of alternative option pricing models. *The Journal of Finance*, 52(5):2003–2049, 1997.

[12] Gurdip Bakshi, Nengjiu Ju, and Hui Ou-Yang. Estimation of continuous-time models with an application to equity volatility dynamics. *Journal of Financial Economics*, 82(1):227–249, 2006.

[13] David S Bates. Post-'87 crash fears in the S&P 500 futures option market. *Journal of Econometrics*, 94(1):181–238, 2000.

[14] Stan Beckers. Variances of security price returns based on high, low, and closing prices. *Journal of Business*, pages 97–112, 1983.

[15] Fabio Bellini and Marco Frittelli. On the existence of minimax martingale measures. *Mathematical Finance*, 12(1):1–21, 2002.

[16] Carl M Bender and Steven A Orszag. *Advanced Mathematical Methods for Scientists and Engineers I*. Springer Science & Business Media, 1999.

[17] Mitchell A Benjamin, Harris O Hinnant, Thomas T Shigeno, and David N Olmstead. Multi-sensor fusion, October 16 2007. US Patent 7,283,904.

[18] Chen Bin. Calibration of the Heston model with application in derivative pricing and hedging. *Master's thesis, Department of Mathematics, Technical University of Delft, Delft, The Netherlands*, 2007.

[19] Fischer Black and Myron Scholes. The pricing of options and corporate liabilities. *The Journal of Political Economy*, pages 637–654, 1973.

[20] Nicolas PB Bollen. Valuing options in regime-switching models. *The Journal of Derivatives*, 6(1):38–49, 1998.

[21] Ilia Bouchouev and Victor Isakov. The inverse problem of option pricing. *Inverse Problems*, 13(5):L11, 1997.

[22] Phelim Boyle and Thangaraj Draviam. Pricing exotic options under regime switching. *Insurance: Mathematics and Economics*, 40(2):267–282, 2007.

[23] Phelim Boyle, Mark Broadie, and Paul Glasserman. Monte Carlo methods for security pricing. *Journal of Economic Dynamics and Control*, 21(8):1267–1321, 1997.

[24] Michael J Brennan and Eduardo S Schwartz. Finite difference methods and jump processes arising in the pricing of contingent claims: A synthesis. *Journal of Financial and Quantitative Analysis*, 13(03):461–474, 1978.

[25] Peter W Buchen and Michael Kelly. The maximum entropy distribution of an asset inferred from option prices. *Journal of Financial and Quantitative Analysis*, 31(01): 143–159, 1996.

[26] John Buffington and Robert J Elliott. American options with regime switching. *International Journal of Theoretical and Applied Finance*, 5(05):497–514, 2002.

[27] Hans Bühler. Volatility markets. consistent modeling, hedging and practical implementation. *PhD Disseration, Technical University Berlin*, 2006.

[28] Peter Carr. Randomization and the American put. *Review of Financial Studies*, 11 (3):597–626, 1998.

[29] Peter Carr, Hélyette Geman, Dilip B Madan, and Marc Yor. The fine structure of asset returns: An empirical investigation*. *The Journal of Business*, 75(2):305–333, 2002.

[30] Kalok C Chan, G Andrew Karolyi, Francis A Longstaff, and Anthony B Sanders. An empirical comparison of alternative models of the short-term interest rate. *The Journal of Finance*, 47(3):1209–1227, 1992.

[31] S Chen, BL Luk, and Y Liu. Application of adaptive simulated annealing to blind channel identification with hoc fitting. *Electronics Letters*, 34(3):234–235, 1998.

[32] Sheng Chen and Bing Lam Luk. Adaptive simulated annealing for optimization in signal processing applications. *Signal Processing*, 79(1):117–128, 1999.

[33] Xinfu Chen and John Chadam. A mathematical analysis of the optimal exercise boundary for American put options. *SIAM Journal on Mathematical Analysis*, 38 (5):1613–1641, 2007.

[34] Xinfu Chen, Huibin Cheng, and John Chadam. Nonconvexity of the optimal exercise boundary for an American put option on a dividend-paying asset. *Mathematical Finance*, 23(1):169–185, 2013.

[35] Mikhail Chernov, A Ronald Gallant, Eric Ghysels, and George Tauchen. Alternative models for stock price dynamics. *Journal of Econometrics*, 116(1):225–257, 2003.

[36] Carl Chiarella, Mark Craddock, Nadima El-Hassan, et al. The calibration of stock option pricing models using inverse problem methodology. *QFRQ Research Papers, UTS Sydney*, 2000.

[37] Carl Chiarella, Andrew Ziogas, and Adam Kucera. *A survey of the integral representation of American option prices*. University of Technology Sydney, 2004.

[38] Sun-Yong Choi, Jean-Pierre Fouque, and Jeong-Hoon Kim. Option pricing under hybrid stochastic and local volatility. *Quantitative Finance*, 13(8):1157–1165, 2013.

[39] Peter Christoffersen and Kris Jacobs. Which garch model for option valuation? *Management Science*, 50(9):1204–1221, 2004.

[40] Peter Christoffersen and Kris Jacobs. The importance of the loss function in option valuation. *Journal of Financial Economics*, 72(2):291–318, 2004.

[41] Peter Christoffersen, Kris Jacobs, and Karim Mimouni. An empirical comparison of affine and non-affine models for equity index options. *Manuscript, Springer*, 2006.

[42] Peter Christoffersen, Kris Jacobs, and Karim Mimouni. Models for S&P 500 dynamics: evidence from realized volatility, daily returns, and option prices. *CREATES Research Paper*, (2007-37), 2007.

[43] Peter Christoffersen, Steven Heston, and Kris Jacobs. The shape and term structure of the index option smirk: Why multifactor stochastic volatility models work so well. *Management Science*, 55(12):1914–1932, 2009.

[44] San-Lin Chung and Mark Shackleton. The simplest American and real option approximations: Geske–johnson interpolation in maturity and yield. *Applied Economics Letters*, 10(11):709–716, 2003.

[45] Thomas F Coleman, Yuying Li, and Arun Verma. Reconstructing the unknown local volatility function. In *Quantitative Analysis in Financial Markets: Collected Papers of the New York University Mathematical Finance Seminar*, volume 2, page 192, 2001.

[46] David A Coley. *An introduction to genetic algorithms for scientists and engineers*, volume 1655. World scientific Singapore, 1999.

[47] Rama Cont and Sana Ben Hamida. Recovering volatility from option prices by evolutionary optimization. 2004.

[48] Rama Cont and Peter Tankov. Calibration of jump-diffusion option pricing models: a robust non-parametric approach. 2002.

[49] Rama Cont and Peter Tankov. Retrieving lévy processes from option prices: Regularization of an ill-posed inverse problem. *SIAM Journal on Control and Optimization*, 45(1):1–25, 2006.

[50] Rama Cont and Ekaterina Voltchkova. A finite difference scheme for option pricing in jump diffusion and exponential Lévy models. *SIAM Journal on Numerical Analysis*, 43(4):1596–1626, 2005.

[51] TRA Corns and SE Satchell. Skew Brownian motion and pricing European options. *The European Journal of Finance*, 13(6):523–544, 2007.

[52] Charles Corrado. The hidden martingale restriction in Gram-Charlier option prices. *Journal of Futures Markets*, 27(6):517–534, 2007.

[53] Charles J Corrado and Tie Su. Skewness and kurtosis in S&P 500 index returns implied by option prices. *Journal of Financial Research*, 19(2):175–192, 1996.

[54] John C Cox, Stephen A Ross, and Mark Rubinstein. Option pricing: A simplified approach. *Journal of Financial Economics*, 7(3):229–263, 1979.

[55] Ian JD Craig and Alfred D Sneyd. An alternating-direction implicit scheme for parabolic equations with mixed derivatives. *Computers & Mathematics with Applications*, 16(4):341–350, 1988.

[56] S Crépey. Calibration of the local volatility in a trinomial tree using Tikhonov regularization. *Inverse Problems*, 19(1):91, 2002.

[57] Stephane Crepey. Calibration of the local volatility in a generalized Black–Scholes model using Tikhonov regularization. *SIAM Journal on Mathematical Analysis*, 34 (5):1183–1206, 2003.

[58] Min Dai, Ling Tang, and Xingye Yue. Calibration of stochastic volatility models: A tikhonov regularization approach. *Journal of Economic Dynamics and Control*, 64: 66–81, 2016.

[59] Tian-Shyr Dai. Efficient option pricing on stocks paying discrete or path-dependent dividends with the stair tree. *Quantitative Finance*, 9(7):827–838, 2009.

[60] Tian-Shyr Dai and Yuh-Dauh Lyuu. An accurate approximate analytical formula for stock options with known dividends. In *NTU International Conference on Finance*, 2006.

[61] Robert C Dalang, Andrew Morton, and Walter Willinger. Equivalent martingale measures and no-arbitrage in stochastic securities market models. *Stochastics: An International Journal of Probability and Stochastic Processes*, 29(2):185–201, 1990.

[62] Alexander David and Pietro Veronesi. Option prices with uncertain fundamentals. *Olin School of Business Working Paper*, pages 07–001, 2002.

[63] A De Cezaro, O Scherzer, and JP Zubelli. Convex regularization of local volatility models from option prices: convergence analysis and rates. *Nonlinear Analysis: Theory, Methods & Applications*, 75(4):2398–2415, 2012.

[64] Sybren Ruurds De Groot and Peter Mazur. *Non-equilibrium thermodynamics*. Courier Corporation, 2013.

[65] Marc Decamps, Ann De Schepper, and Marc Goovaerts. Applications of δ-function perturbation to the pricing of derivative securities. *Physica A: Statistical Mechanics and its Applications*, 342(3):677–692, 2004.

[66] Freddy Delbaen, Peter Grandits, Thorsten Rheinländer, Dominick Samperi, Martin Schweizer, and Christophe Stricker. Exponential hedging and entropic penalties. *Mathematical finance*, 12(2):99–123, 2002.

[67] E Derman and I Kani. Riding on a smile. *Risk*, 7(1):32–39, 1994.

[68] Emanuel Derman, Iraj Kani, and Joseph Z Zou. The local volatility surface: Unlocking the information in index option prices. *Financial Analysts Journal*, 52(4): 25–36, 1996.

[69] John W Dettman. *Applied complex variables*. Courier Corporation, 2012.

[70] Oshmita Dey and Debjani Chakraborty. A single period inventory model with a truncated normally distributed fuzzy random variable demand. *International Journal of Systems Science*, 43(3):518–525, 2012.

[71] Jim Douglas and Henry H Rachford. On the numerical solution of heat conduction problems in two and three space variables. *Transactions of the American Mathematical Society*, 82(2):421–439, 1956.

[72] Gabriel G Drimus. Options on realized variance by transform methods: a non-affine stochastic volatility model. *Quantitative Finance*, 12(11):1679–1694, 2012.

[73] Bernard Dumas, Jeff Fleming, and Robert E Whaley. Implied volatility functions: Empirical tests. *The Journal of Finance*, 53(6):2059–2106, 1998.

[74] Bruno Dupire. *Pricing and hedging with smiles*. Mathematics of Derivative Securities. Dempster and Pliska eds., Cambridge Uni. Press, 1997.

[75] Bruno Dupire et al. Pricing with a smile. *Risk*, 7(1):18–20, 1994.

[76] Kabir K Dutta and David F Babbel. Extracting probabilistic information from the prices of interest rate options: Tests of distributional assumptions*. *The Journal of Business*, 78(3):841–870, 2005.

[77] Ernst Eberlein. Application of generalized hyperbolic Lévy motions to finance. In *Lévy processes*, pages 319–336. Springer, 2001.

[78] Herbert Egger and Heinz W Engl. Tikhonov regularization applied to the inverse problem of option pricing: convergence analysis and rates. *Inverse Problems*, 21(3): 1027, 2005.

[79] Erik Ekström, Per Lötstedt, and Johan Tysk. Boundary values and finite difference methods for the single factor term structure equation. *Applied Mathematical Finance*, 16(3):253–259, 2009.

[80] Martin Eling, Simone Farinelli, Damiano Rossello, and Luisa Tibiletti. Skewness in hedge funds returns: classical skewness coefficients vs azzalini's skewness parameter. *International Journal of Managerial Finance*, 6(4):290–304, 2010.

[81] Robert J Elliott and Guang-Hua Lian. Pricing variance and volatility swaps in a stochastic volatility model with regime switching: discrete observations case. *Quantitative Finance*, 13(5):687–698, 2013.

[82] Robert J Elliott, Tak Kuen Siu, and Leunglung Chan. Pricing volatility swaps under heston's stochastic volatility model with regime switching. *Applied Mathematical Finance*, 14(1):41–62, 2007.

[83] Robert J Elliott, Lakhdar Aggoun, and John B Moore. *Hidden Markov models: estimation and control*, volume 29. Springer Science & Business Media, 2008.

[84] Robert J Elliott, Tak Kuen Siu, and Leunglung Chan. On pricing barrier options with regime switching. *Journal of Computational and Applied Mathematics*, 256: 196–210, 2014.

[85] Robert J Elliott, Leunglung Chan, and Tak Kuen Siu. A Dupire equation for a regime-switching model. *International Journal of Theoretical and Applied Finance*, 18(04):1550023, 2015.

[86] Bjørn Eraker. Do stock prices and volatility jump? Reconciling evidence from spot and option prices. *The Journal of Finance*, 59(3):1367–1404, 2004.

[87] Frank J Fabozzi, Radu Tunaru, and George Albota. Estimating risk-neutral density with parametric models in interest rate markets. *Quantitative Finance*, 9(1):55–70, 2009.

[88] Matthias R Fengler, Wolfgang K Härdle, and Christophe Villa. The dynamics of implied volatilities: A common principal components approach. *Review of Derivatives Research*, 6(3):179–202, 2003.

[89] Avner Friedman. *Partial differential equations of parabolic type*. Courier Corporation, 2013.

[90] Volf Frishling. A discrete question. *Risk*, 15(1):115–116, 2002.

[91] Marco Frittelli. The minimal entropy martingale measure and the valuation problem in incomplete markets. *Mathematical finance*, 10(1):39–52, 2000.

[92] Alexander Gairat and Vadim Shcherbakov. Density of skew Brownian motion and its functionals with application in finance. *arXiv preprint arXiv:1407.1715*, 2014.

[93] CW Gardiner. *Stochastic methods*. Springer-Verlag, Berlin–Heidelberg–New York–Tokyo, 1985.

[94] Jim Gatheral. *The volatility surface: a practitioner's guide*, volume 357. John Wiley & Sons, 2011.

[95] Robert Geske and Herb E Johnson. The American put option valued analytically. *The Journal of Finance*, 39(5):1511–1524, 1984.

[96] J Gil-Pelaez. Note on the inversion theorem. *Biometrika*, 38(3-4):481–482, 1951.

[97] Ricardo Gimeno and Juan M Nave. A genetic algorithm estimation of the term structure of interest rates. *Computational Statistics & Data Analysis*, 53(6):2236–2250, 2009.

[98] Stéphane Goutte. Pricing and hedging in stochastic volatility regime switching models. *Journal of Mathematical Finance*, 3(01):70, 2013.

[99] Bruce K Grace. Black-Scholes option pricing via genetic algorithms. *Applied Economics Letters*, 7(2):129–132, 2000.

[100] Weiyu Guo and Tie Su. Option put-call parity relations when the underlying security pays dividends. *International Journal of Business and Economics*, 5(3):225–230, 2006.

[101] Xin Guo. Information and option pricings. *Quantitive Finance*, 1(1):38–44, 2001.

[102] Patrick S Hagan, Deep Kumar, Andrew S Lesniewski, and Diana E Woodward. Managing smile risk. *70+ DVDs FOR SALE & EXCHANGE*, page 249, 2002.

[103] James D Hamilton. A new approach to the economic analysis of nonstationary time series and the business cycle. *Econometrica: Journal of the Econometric Society*, pages 357–384, 1989.

[104] James D Hamilton. Analysis of time series subject to changes in regime. *Journal of Econometrics*, 45(1):39–70, 1990.

[105] Martin Hanke and Elisabeth Rösler. Computation of local volatilities from regularized Dupire equations. *International Journal of Theoretical and Applied Finance*, 8 (02):207–221, 2005.

[106] J Michael Harrison and David M Kreps. Martingales and arbitrage in multiperiod securities markets. *Journal of Economic Theory*, 20(3):381–408, 1979.

[107] J Michael Harrison and Stanley R Pliska. Martingales and stochastic integrals in the theory of continuous trading. *Stochastic Processes and Their Applications*, 11 (3):215–260, 1981.

[108] John Michael Harrison and Lawrence A Shepp. On skew Brownian motion. *The Annals of Probability*, pages 309–313, 1981.

[109] Md Zobaer Hasan, Anton Abdulbasah Kamil, Adli Mustafa, and Md Azizul Baten. Stochastic frontier model approach for measuring stock market efficiency with different distributions. *PloS one*, 7(5):e37047, 2012.

[110] Espen Gaarder Haug. *The complete guide to option pricing formulas*. McGraw-Hill Companies, 2007.

[111] Xin-Jiang He and Song-Ping Zhu. An analytical approximation formula for European option pricing under a new stochastic volatility model with regime-switching. *Journal of Economic Dynamics and Control*, 71:77–85, 2016.

[112] Xin-Jiang He and Song-Ping Zhu. On the calibration of local regime-switching models through a Tikhonov approach. *Operations Research (submitted)*, 2016.

[113] Xin-Jiang He and Song-Ping Zhu. An alternative form used to calibrate the Heston option pricing model. *Computers & Mathematics with Applications*, 71(9):1831–1842, 2016.

[114] Xin-Jiang He and Song-Ping Zhu. Pricing European options with stochastic volatility under the minimal entropy martingale measure. *European Journal of Applied Mathematics*, 27(2):233–247, 2016.

[115] Xin-Jiang He and Song-Ping Zhu. How should a local regime-switching model be calibrated? *Journal of Economic Dynamics and Control*, 78:149–163, 2017.

[116] Xin-Jiang He and Song-Ping Zhu. An alternative form to calibrate the correlated Stein-Stein option pricing model. *Decisions in Economics and Finance (submitted)*, 2017.

[117] Steven L Heston. A closed-form solution for options with stochastic volatility with applications to bond and currency options. *Review of Financial Studies*, 6(2):327–343, 1993.

[118] David Hobson. Stochastic volatility models, correlation, and the q-optimal measure. *Mathematical Finance*, 14(4):537–556, 2004.

[119] Alexandre Hocquard, Nicolas Papageorgiou, and Bruno Remillard. The payoff distribution model: an application to dynamic portfolio insurance. *Quantitative Finance*, (ahead-of-print):1–14, 2012.

[120] Bernd Hofmann and Romy Krämer. On maximum entropy regularization for a specific inverse problem of option pricing. *Journal of Inverse and Ill-posed Problems jiip*, 13(1):41–63, 2005.

[121] Anthony D Holmes and Hongtao Yang. A front-fixing finite element method for the valuation of American options. *SIAM Journal on Scientific Computing*, 30(4): 2158–2180, 2008.

[122] Yiu-Chung Hon and Xian-Zhong Mao. A radial basis function method for solving options pricing models. *Journal of Financial Engineering*, 8:31–50, 1999.

[123] Sam Howison. Matched asymptotic expansions in financial engineering. *Journal of Engineering Mathematics*, 53(3-4):385–406, 2005.

[124] Jacqueline Huang and Jong-Shi Pang. Option pricing and linear complementarity. Technical report, Cornell University, 2003.

[125] Jing-zhi Huang, Marti G Subrahmanyam, and G George Yu. Pricing and hedging American options: a recursive integration method. *Review of Financial Studies*, 9 (1):277–300, 1996.

[126] Yunqing Huang, Peter A Forsyth, and George Labahn. Methods for pricing American options under regime switching. *SIAM Journal on Scientific Computing*, 33(5):2144–2168, 2011.

[127] John Hull and Alan White. The pricing of options on assets with stochastic volatilities. *The Journal of Finance*, 42(2):281–300, 1987.

[128] John Hull and Alan White. Valuing derivative securities using the explicit finite difference method. *Journal of Financial and Quantitative Analysis*, 25(01):87–100, 1990.

[129] John C Hull. *Options, futures, and other derivatives*. Pearson Education India, 2006.

[130] Willem Hundsdorfer and Jan G Verwer. *Numerical solution of time-dependent advection-diffusion-reaction equations*, volume 33. Springer Science & Business Media, 2013.

[131] A Stan Hurn, Kenneth A Lindsay, and Andrew J McClelland. Estimating the parameters of stochastic volatility models using option price data. *Journal of Business & Economic Statistics*, 33(4):579–594, 2015.

[132] Soosung Hwang, S Stachell, and PL Valls Pereira. How persistent is volatility? An answer with stochastic volatility models with Markov regime switching state equations. *Journal of Business Finance & Accounting*, 34:1002–1024, 2007.

[133] Aytaç Ilhan, Mattias Jonsson, and Ronnie Sircar. Optimal investment with derivative securities. *Finance and Stochastics*, 9(4):585–595, 2005.

[134] Lester Ingber. Home page of lester ingber. *https://www.ingber.com*.

[135] Lester Ingber. Very fast simulated re-annealing. *Mathematical and computer modelling*, 12(8):967–973, 1989.

[136] Lester Ingber. High-resolution path-integral development of financial options. *Physica A: Statistical Mechanics and its Applications*, 283(3):529–558, 2000.

[137] Lester Ingber et al. Adaptive simulated annealing (ASA): Lessons learned. *Control and Cybernetics*, 25:33–54, 1996.

[138] KJ In't Hout and S Foulon. ADI finite difference schemes for option pricing in the Heston model with correlation. *Int. J. Numer. Anal. Model*, 7(2):303–320, 2010.

[139] Kiyosi Itô and HP McKean Jr. Diffusion processes and their sample paths, 1965.

[140] Eric Jacquier, Nicholas G Polson, and Peter E Rossi. Bayesian analysis of stochastic volatility models with fat-tails and correlated errors. *Journal of Econometrics*, 122 (1):185–212, 2004.

[141] Farshid Jamshidian. An analysis of American options. *Review of Futures Markets*, 11(1):72–80, 1992.

[142] Joanna Janczura and Rafał Weron. Efficient estimation of Markov regime-switching models: An application to electricity spot prices. *AStA Advances in Statistical Analysis*, 96(3):385–407, 2012.

[143] Robert Jarrow and Andrew Rudd. Approximate option valuation for arbitrary stochastic processes. *Journal of Financial Economics*, 10(3):347–369, 1982.

[144] Lishang Jiang, Qihong Chen, Lijun Wang, Jin E Zhang, et al. A new well-posed algorithm to recover implied local volatility. *Quantitative Finance*, 3(6):451–457, 2003.

[145] Michael S Johannes and Nick Polson. MCMC methods for continuous-time financial econometrics. *Available at SSRN 480461*, 2003.

[146] Herb Johnson. Option pricing when the variance rate is changing. *Working Paper, University of California, Los Angeles*, 1979.

[147] Herb Johnson and David Shanno. Option pricing when the variance is changing. *Journal of Financial and Quantitative Analysis*, 22(02):143–151, 1987.

[148] Eric Jondeau, Ser-Huang Poon, and Michael Rockinger. *Financial modeling under non-Gaussian distributions*. Springer Science & Business Media, 2007.

[149] Gareth Jones. Genetic and evolutionary algorithms. *Encyclopedia of Computational Chemistry. John Wiley and Sons*, pages 323–330, 1998.

[150] Andreas Kaeck and Carol Alexander. Vix dynamics with stochastic volatility of volatility. *ICMA Centre, Henley Business School, University of Reading, UK*, 2010.

[151] Madhu Kalimipalli and Raul Susmel. Regime-switching stochastic volatility and short-term interest rates. *Journal of Empirical Finance*, 11(3):309–329, 2004.

[152] Roel Kamp. Local volatility modelling. 2009.

[153] Dongcheol Kim and Stanley J Kon. Structural change and time dependence in models of stock returns. *Journal of Empirical Finance*, 6(3):283–308, 1999.

[154] In Joon Kim. The analytic valuation of American options. *Review of Financial Studies*, 3(4):547–572, 1990.

[155] Scott Kirkpatrick, C Daniel Gelatt, Mario P Vecchi, et al. Optimization by simmulated annealing. *Science*, 220(4598):671–680, 1983.

[156] John Knight and Stephen Satchell. Pricing derivatives written on assets with arbitrary skewness and kurtosis. *Return Distributions in Finance*, pages 252–275, 2001.

[157] Dessislava Koleva and Elisa Nicolato. Option pricing under Heston and 3/2 stochastic volatility models: an approximation to the fast fourier transform. 2012.

[158] Steven G Kou. A jump-diffusion model for option pricing. *Management Science*, 48 (8):1086–1101, 2002.

[159] Minas D Koulisianis and Theodore S Papatheodorou. Pricing of American options using linear complementarity formulation: methods and their evaluation. *Neural, Parallel & Scientific Computations*, 11(4):423–444, 2003.

[160] Joshua Krausz. Option parameter analysis and market efficiency tests: a simultaneous solution approach. *Applied Economics*, 17(5):885–896, 1985.

[161] Noureddine Krichene. *Islamic Capital Markets: Theory and Practice*. John Wiley & Sons, 2012.

[162] Yue-Kuen Kwok. *Mathematical models of financial derivatives*. Springer Science & Business Media, 2008.

[163] Ronald Lagnado and Stanley Osher. A technique for calibrating derivative security pricing models: numerical solution of an inverse problem. *Journal of Computational Finance*, 1(1):13–25, 1997.

[164] Jean Paul Laurent and Huyên Pham. Dynamic programming and mean-variance hedging. *Finance and Stochastics*, 3(1):83–110, 1999.

[165] Anh Le. Separating the components of default risk: A derivative-based approach. *The Quarterly Journal of Finance*, 2014.

[166] Antoine Lejay et al. On the constructions of the skew Brownian motion. *Probab. Surv*, 3:413–466, 2006.

[167] Sergei Levendorskiĭ. Efficient pricing and reliable calibration in the Heston model. *International Journal of Theoretical and Applied Finance*, 15(07):1250050, 2012.

[168] Alan L Lewis. Option valuation under stochastic volatility. *Option Valuation under Stochastic Volatility*, 2000.

[169] Kian Guan Lim and Da Zhi. Pricing options using implied trees: Evidence from FTSE-100 options. *Journal of Futures Markets*, 22(7):601–626, 2002.

[170] Francis A Longstaff. Option pricing and the martingale restriction. *Review of Financial Studies*, 8(4):1091–1124, 1995.

[171] Francis A Longstaff and Eduardo S Schwartz. Valuing American options by simulation: a simple least-squares approach. *Review of Financial Studies*, 14(1):113–147, 2001.

[172] Dilip B Madan and Frank Milne. Contingent claims valued and hedged by pricing and investing in a basis. *Mathematical Finance*, 4(3):223–245, 1994.

[173] Dilip B Madan, Peter P Carr, and Eric C Chang. The variance gamma process and option pricing. *European Finance Review*, 2(1):79–105, 1998.

[174] James B McDonald and Richard M Bookstaber. Option pricing for generalized distributions. *Communications in Statistics-Theory and Methods*, 20(12):4053–4068, 1991.

[175] Henry P McKean. Appendix: A free boundary problem for the heat equation arising from a problem in mathematical economics. *Sloan Management Review*, 6(2):32, 1965.

[176] Alexey Medvedev and Olivier Scaillet. Pricing American options under stochastic volatility and stochastic interest rates. *Journal of Financial Economics*, 98(1):145–159, 2010.

[177] Robert C Merton. Theory of rational option pricing. *Bell Journal of Economics and Management Science*, 4:141–183, 1973.

[178] Robert C Merton. Option pricing when underlying stock returns are discontinuous. *Journal of Financial Economics*, 3(1):125–144, 1976.

[179] Robert C Merton, Michael J Brennan, and Eduardo S Schwartz. The valuation of American put options. *The Journal of Finance*, 32(2):449–462, 1977.

[180] Sergei Mikhailov and Ulrich Nögel. *Hestons stochastic volatility model: Implementation, calibration and some extensions.* John Wiley and Sons, 2004.

[181] Sovan Mitra and Paresh Date. Regime switching volatility calibration by the Baum–Welch method. *Journal of Computational and Applied Mathematics*, 234(12):3243–3260, 2010.

[182] Thibaut Moyaert and Mikael Petitjean. The performance of popular stochastic volatility option pricing models during the subprime crisis. *Applied Financial Economics*, 21(14):1059–1068, 2011.

[183] Marek Musiela and Marek Rutkowski. *Martingale methods in financial modelling*, volume 36. Springer Science & Business Media, 2006.

[184] Vasanttilak Naik. Option valuation and hedging strategies with jumps in the volatility of asset returns. *The Journal of Finance*, 48(5):1969–1984, 1993.

[185] Ciprian Necula. Option pricing in a fractional Brownian motion environment. *Available at SSRN 1286833*, 2002.

[186] Wayne Nilsen and Hasanjan Sayit. No arbitrage in markets with bounces and sinks. *Int. Rev. Appld. Financ. Issues Econ*, 3(4):696–699, 2011.

[187] R Norgaard and T Killeen. Expected utility and the truncated normal distribution. *Management Science*, 26(9):901–909, 1980.

[188] Amado Peiro. Skewness in financial returns. *Journal of Banking & Finance*, 23(6): 847–862, 1999.

[189] Jamol Pender. The truncated normal distribution: Applications to queues with impatient customers. *Operations Research Letters*, 43(1):40–45, 2015.

[190] George C Philippatos and Charles J Wilson. Entropy, market risk, and the selection of efficient portfolios. *Applied Economics*, 4(3):209–220, 1972.

[191] Svetlozar T Rachev, Christian Menn, and Frank J Fabozzi. *Fat-tailed and skewed asset return distributions: implications for risk management, portfolio selection, and option pricing*, volume 139. John Wiley & Sons, 2005.

[192] Riccardo Rebonato. *Volatility and correlation: the perfect hedger and the fox*. John Wiley & Sons, 2005.

[193] Damiano Rossello. Arbitrage in skew Brownian motion models. *Insurance: Mathematics and Economics*, 50(1):50–56, 2012.

[194] Mark Rubinstein. Nonparametric tests of alternative option pricing models using all reported trades and quotes on the 30 most active cboe option classes from august 23, 1976 through august 31, 1978. *The Journal of Finance*, 40(2):455–480, 1985.

[195] Mark Rubinstein. Implied binomial trees. *The Journal of Finance*, 49(3):771–818, 1994.

[196] Tina Hviid Rydberg. The normal inverse Gaussian Lévy process: simulation and approximation. *Communications in Statistics. Stochastic Models*, 13(4):887–910, 1997.

[197] Robert Savickas. A simple option-pricing formula. *Financial Review*, 37(2):207–226, 2002.

[198] Rainer Schöbel and Jianwei Zhu. Stochastic volatility with an Ornstein–Uhlenbeck process: an extension. *European Finance Review*, 3(1):23–46, 1999.

[199] Eduardo S Schwartz. The valuation of warrants: implementing a new approach. *Journal of Financial Economics*, 4(1):79–93, 1977.

[200] Eduardo S Schwartz and Walter N Torous. Prepayment and the valuation of mortgage-backed securities. *The Journal of Finance*, 44(2):375–392, 1989.

[201] Martin Schweizer. On the minimal martingale measure and the möllmer-schweizer decomposition. *Stochastic Analysis and Applications*, 13(5):573–599, 1995.

[202] Martin Schweizer. Approximation pricing and the variance-optimal martingale measure. *The Annals of Probability*, 24(1):206–236, 1996.

[203] Martin Schweizer. A minimality property of the minimal martingale measure. *Statistics & Probability Letters*, 42(1):27–31, 1999.

[204] Louis O Scott. Option pricing when the variance changes randomly: Theory, estimation, and an application. *Journal of Financial and Quantitative analysis*, 22(04): 419–438, 1987.

[205] Louis O Scott. Pricing stock options in a jump-diffusion model with stochastic volatility and interest rates: Applications of Fourier inversion methods. *Mathematical Finance*, 7(4):413–426, 1997.

[206] Slimane Sefiane and Mohamed Benbouziane. Portfolio selection using genetic algorithm. 2012.

[207] Bruce J Sherrick, Philip Garcia, and Viswanath Tirupattur. Recovering probabilistic information from option markets: Tests of distributional assumptions. *Journal of Futures Markets*, 16(5):545–560, 1996.

[208] Steven E Shreve. *Stochastic calculus for finance II: Continuous-time models*, volume 11. Springer Science & Business Media, 2004.

[209] Jinghong Shu and Jin E Zhang. Pricing S&P 500 index options under stochastic volatility with the indirect inference method. *Journal of Derivatives Accounting*, 1 (2):1–16, 2004.

[210] Tak Kuen Siu, Hailiang Yang, and John W Lau. Pricing currency options under two-factor Markov-modulated stochastic volatility models. *Insurance: Mathematics and Economics*, 43(3):295–302, 2008.

[211] Courtney Smith. *Option strategies: profit-making techniques for stock, stock index, and commodity options*, volume 362. John Wiley & Sons, 2008.

[212] Mike EC P So, Kin Lam, and Wai Keung Li. A stochastic volatility model with Markov switching. *Journal of Business & Economic Statistics*, 16(2):244–253, 1998.

[213] Elias M Stein and Jeremy C Stein. Stock price distributions with stochastic volatility: an analytic approach. *Review of Financial Studies*, 4(4):727–752, 1991.

[214] Sasha F Stoikov. Pricing options from the point of view of a trader. *International Journal of Theoretical and Applied Finance*, 9(08):1245–1266, 2006.

[215] Harold Szu and Ralph Hartley. Fast simulated annealing. *Physics Letters A*, 122 (3-4):157–162, 1987.

[216] Andreĭ Nikolaevich Tikhonov, AV Goncharsky, VV Stepanov, and Anatoly G Yagola. *Numerical methods for the solution of ill-posed problems*, volume 328. Springer Science & Business Media, 2013.

[217] Anthonie W Van der Stoep, Lech A Grzelak, and Cornelis W Oosterlee. The Heston stochastic-local volatility model: efficient Monte Carlo simulation. *International Journal of Theoretical and Applied Finance*, 17(07):1450045, 2014.

[218] Raluca Vernic. Multivariate skew-normal distributions with applications in insurance. *Insurance: Mathematics and Economics*, 38(2):413–426, 2006.

[219] Minh T Vo. Regime-switching stochastic volatility: evidence from the crude oil market. *Energy Economics*, 31(5):779–788, 2009.

[220] Curtis R Vogel. *Computational methods for inverse problems*, volume 23. Siam, 2002.

[221] S Wang, XQ Yang, and KL Teo. Power penalty method for a linear complementarity problem arising from American option valuation. *Journal of Optimization Theory and Applications*, 129(2):227–254, 2006.

[222] JG Wendel et al. The non-absolute convergence of gil-pelaez'inversion integral. *The Annals of Mathematical Statistics*, 32(1):338–339, 1961.

[223] A Elizabeth Whalley, Paul Wilmott, et al. An asymptotic analysis of an optimal hedging model for option pricing with transaction costs. *Mathematical Finance*, 7 (3):307–324, 1997.

[224] James B Wiggins. Option values under stochastic volatility: Theory and empirical estimates. *Journal of Financial Economics*, 19(2):351–372, 1987.

[225] Walter Willinger, Murad S Taqqu, and Vadim Teverovsky. Stock market prices and long-range dependence. *Finance and Stochastics*, 3(1):1–13, 1999.

[226] Paul Wilmott, Jeff Dewynne, and Sam Howison. *Option pricing: mathematical models and computation*. Oxford financial press, 1993.

[227] Lixin Wu and Yue-Kuen Kwok. A front-fixing finite difference method for the valuation of American options. *Journal of Financial Engineering*, 6(2):83–97, 1997.

[228] J Xia and JA Yan. The utility maximization approach to a martingale measure constructed via esscher transform. *Preprint*, 2000.

[229] Yuhang Xing, Xiaoyan Zhang, and Rui Zhao. What does the individual option volatility smirk tell us about future equity returns? 2010.

[230] Jerome Yen and Kin Keung Lai. *Emerging Financial Derivatives: Understanding Exotic Options and Structured Products*. Routledge, 2014.

[231] Jun Yu. On leverage in a stochastic volatility model. *Journal of Econometrics*, 127 (2):165–178, 2005.

[232] Song-Ping Zhu. An exact and explicit solution for the valuation of American put options. *Quantitative Finance*, 6(3):229–242, 2006.

[233] Song-Ping Zhu. A new analytical approximation formula for the optimal exercise boundary of American put options. *International Journal of Theoretical and Applied Finance*, 9(07):1141–1177, 2006.

[234] Song-Ping Zhu and Wen-Ting Chen. A new analytical approximation for European puts with stochastic volatility. *Applied Mathematics Letters*, 23(6):687–692, 2010.

[235] Song-Ping Zhu and Wen-Ting Chen. A predictor–corrector scheme based on the ADI method for pricing american puts with stochastic volatility. *Computers & Mathematics with Applications*, 62(1):1–26, 2011.

[236] Song-Ping Zhu and Wen-Ting Chen. An inverse finite element method for pricing American options. *Journal of Economic Dynamics and Control*, 37(1):231–250, 2013.

[237] Song-Ping Zhu and William J Francis. A comparative study of two analytical-approximation formulae and the binomial method for the optimal exercise boundary of american put options. 2004.

[238] Song-Ping Zhu and Xin-Jiang He. An accurate approximation formula for pricing European options with discrete dividend payments. *IMA Journal of Management Mathematics (accepted)*, 2016.

[239] Song-Ping Zhu and Xin-Jiang He. On the convergence of He and Zhu's new series solution for pricing options with the Heston model. *Acta Mathematica Universitatis Comenianae (accepted)*, 2017.

[240] Song-Ping Zhu and Xin-Jiang He. A hybrid computational approach for option pricing. *European Journal of Applied Mathematics (submitted)*, 2017.

[241] Song-Ping Zhu and Xin-Jiang He. A modified Black-Scholes pricing formula for European options with bounded underlying prices. *Computers & Mathematics with Applications (submitted)*, 2017.

[242] Song-Ping Zhu and Xin-Jiang He. A new closed-form formula for pricing European options under a skew Brownian motion. *European Journal of Finance (accepted)*, 2017.

[243] Song-Ping Zhu and Guang-Hua Lian. An analytical formula for VIX futures and its applications. *Journal of Futures Markets*, 32(2):166–190, 2012.

[244] Song-Ping Zhu, Alexander Badran, and Xiaoping Lu. A new exact solution for pricing European options in a two-state regime-switching economy. *Computers & Mathematics with Applications*, 64(8):2744–2755, 2012.

[245] Song-Ping Zhu, Xin-Jiang He, and Xiao-Ping Lu. A new integral equation for American put options. *Quantitative Finance (accepted)*, 2017.

List of Publication

- S.-P. Zhu, X.-J. He and X.-P. Lu. A new integral equation for American put options. *Quantitative Finance (accepted)*, 2017.

- S.-P. Zhu and X.-J. He. A new closed-form formula for pricing European options under a skew Brownian motion. *European Journal of Finance (accepted)*, 2017.

- X.-J. He and S.-P. Zhu. How should a local regime-switching model be calibrated? *Journal of Economic Dynamics and ControL*, 78: 149-163, 2017.

- S.-P. Zhu and X.-J. He. On the convergence of He and Zhu's new series solution for pricing options with the Heston model. *Acta Mathematica Universitatis Comenianae (accepted)*, 2017.

- X.-J. He and S.-P. Zhu. An analytical approximation formula for European option pricing under a new stochastic volatility model with regime-switching. *Journal of Economic Dynamics and Control* 71: 77-85, 2016.

- X.-J. He and S.-P. Zhu. Pricing European options with stochastic volatility under the minimal entropy martingale measure. *European Journal of Applied Mathematics*, 27(2): 233-247, 2016.

- X.-J. He and S.-P. Zhu. An alternative form used to calibrate the Heston option pricing model. *Computers & Mathematics with Applications*, 71(9): 1831-1842, 2016.

- S.-P. Zhu and X.-J. He. An accurate approximation formula for pricing European options with discrete dividend payments. *IMA Journal of Management Mathematics (accepted)*, doi: 10.1093/imaman/dpw020, 2016.

- S.-P. Zhu, X.-J. He. A hybrid computational approach for option pricing. *European Journal of Applied Mathematics (submitted)*, 2017.

- X.-J. He and S.-P. Zhu. An alternative form to calibrate the correlated Stein-Stein option pricing model. *Decisions in Economics and Finance (submitted)*, 2017.

- S.-P. Zhu and X.-J. He. A modified Black-Scholes pricing formula for European options with bounded underlying prices. *Computers & Mathematics with Applications (submitted)*, 2016.

- X.-J. He and S.-P. Zhu. On the calibration of local regime-switching models through a Tikhonov approach. *Operations Research (submitted)*, 2016.